



THE UNIVERSITY OF
WAIKATO
Te Whare Wānanga o Waikato

Research Commons

<http://waikato.researchgateway.ac.nz/>

Research Commons at the University of Waikato

Copyright Statement:

The digital copy of this thesis is protected by the Copyright Act 1994 (New Zealand).

The thesis may be consulted by you, provided you comply with the provisions of the Act and the following conditions of use:

- Any use you make of these documents or images must be for research or private study purposes only, and you may not make them available to any other person.
- Authors control the copyright of their thesis. You will recognise the author's right to be identified as the author of the thesis, and due acknowledgement will be made to the author where appropriate.
- You will obtain the author's permission before publishing any material from the thesis.

Bioactive Chemicals of Importance in Endophyte- Infected Grasses

**A thesis submitted in fulfilment of the requirements
for the degree of Doctor of Philosophy at
The University of Waikato**

**by
Jacob Vadakkal Babu**



**The
University
of Waikato**

*Te Whare Wānanga
o Waikato*

2008

Abstract

Janthitrems are believed to be involved in the observed sporadic cases of AR37-infected perennial ryegrass staggers. Investigations into the role of janthitrems in perennial ryegrass staggers are difficult as isolation of the compounds from the ryegrass is hindered by the inherent instability of these compounds. Therefore attempts were made to isolate janthitrems from an alternative source, allowing these janthitrem analogues to be used as surrogates for endophyte produced janthitrems.

Analysis of a series of *Penicillium janthinellum* cultures revealed the presence of janthitrems in a number of strains, including janthitrem B, janthitrem C and two novel janthitrem compounds. Detailed one- and two-dimensional NMR and mass spectral techniques identified the two novel compounds as 11,12-epoxyjanthitrems B and C, which were subsequently given the trivial names janthitrems A and D, respectively. Janthitrems B and C were isolated and identified by NMR and revisions of some previously reported chemical shift assignments were proposed. In addition to the janthitrems, penitrems were also identified in two strains of *P. janthinellum*.

The isolated janthitrem B was utilised for the development of efficient extraction procedures, and for the determination of ideal storage conditions for janthitrem compounds. A method for the extraction and isolation of janthitrem B from a *P. janthinellum* culture was developed and optimised to yield 6 mg of janthitrem B from 900 mL of fungal culture in two days. Stability studies of janthitrem B indicated the ideal storage condition which minimised degradation was dry at -80°C where only 7% sample loss was observed over 300 days.

Bioactivity studies of janthitrems A and B found these compounds to be tremorgenic to mice, with janthitrem A (an epoxyjanthitrem) inducing more severe tremors than janthitrem B. Insect testing also showed that both janthitrems A and B displayed anti-insect activity to porina larvae. Since the epoxyjanthitrems, which are associated with AR37 endophyte-infected ryegrass, were also shown to be tremorgenic and to display anti-insect activity, the insect resistance and the sporadic cases of ryegrass staggers displayed by AR37 may be related to the presence of epoxyjanthitrem compounds.

LC–UV–MS analysis of janthitrems A–D, penitrems A–F, lolitrem B, paspalinine, paxilline and terpendole C found these indole–diterpenoids to be more sensitive by analysis using an APCI source as opposed to an ESI source. APCI negative ion LC–UV–MS required source induced dissociation in combination with increased collision energy to suppress an acetate adduct peak, sourced from the acetic acid buffer. Negative ion MS^2 and MS^3 data produced more informative fragments compared to the conventional positive ion MS^2 and MS^3 data. The availability of both positive and negative ion LC–UV–MS methodologies will allow future endophyte products to be more thoroughly screened for different classes of secondary metabolites.

Extracts of mouldy walnuts were analysed for the presence of tremorgenic mycotoxins after a dog was found to exhibit symptoms characteristic of tremorgenic mycotoxicosis. LC–UV–MS analysis of the mouldy walnuts identified the tremorgenic mycotoxins penitrems A–F, thus confirming the veterinarian’s tentative diagnosis of canine tremorgenic mycotoxicosis — the first reported case in New Zealand.

Acknowledgements

I would like to express my sincere appreciation and thanks first and foremost to my supervisors, Professor Alistair Wilkins (The University of Waikato), Dr. Christopher Miles (AgResearch) and Dr. Sarah Finch (AgResearch) for their invaluable support, advice, guidance and patience throughout the course of this project.

Thanks to AgResearch for their help and support during my PhD and to the toxinology group, in particular Allan Hawkes, for making my time at AgResearch an enjoyable and memorable experience and Dr Jared Loader for proofreading my thesis. In addition I would also like to thank Wendy Jackson (The University of Waikato) for help with the LC–UV–MS instrument and Pat Gread (The University of Waikato) for running high resolution mass spectrometry samples.

Thanks must also be extended to Dr. Margaret di Menna (AgResearch) for growth and identification of fungal cultures, Sharon Sayer (AgResearch) for growing fungal cultures, Karl Fraser (AgResearch) and Dr. Geoff Lane (AgResearch) for running samples on the LC–UV–MS and for their advice and assistance with LC–UV–MS analyses, Ric Broadhurst for the care of the animals used in the small animal trial, Dr. Alison Popay for running and supervising the insect trial and to Professor Satoshi Omura and Professor Hiroshi Tomoda for supplying a sample of terpendole C.

The Technology Industry Fellowship (TIF) provided by Technology New Zealand and The University of Waikato via UNILINK is also gratefully acknowledged, their financial help was invaluable.

Finally I would like to thank my Mum and Dad for their support and encouragement, and in particular my sister, Kavitha, whose proofreading and computer skills were employed fulltime.

Table of Contents

	Page
Abstract	<i>i</i>
Acknowledgements	<i>iii</i>
List of Figures	<i>x</i>
List of Tables	<i>xviii</i>
Abbreviations	<i>xx</i>
Chapter One	
Introduction	1
1.1	Perennial Ryegrass Staggers 1
1.2	History of Ryegrass Staggers 2
	<i>1.2.1 The Advantages and Disadvantages of Endophyte-Infected Perennial Ryegrass 6</i>
	<i>1.2.2 Options for Control of Ryegrass Staggers 7</i>
1.3	Toxicoses Associated with Grasses Infected with Endophytic Fungi 8
	<i>1.3.1 Ryegrass Staggers 8</i>
	<i>1.3.2 Tall Fescue Toxicosis 8</i>
	<i>1.3.3 Sleepygrass Toxicosis 11</i>
	<i>1.3.4 Drunken Horse Grass 12</i>
1.4	Indole–Diterpenoids 13
	<i>1.4.1 Penitrems 14</i>
	<i>1.4.2 Lolitrems 19</i>
	<i>1.4.3 Paspaline 22</i>
	<i>1.4.4 Paxilline 24</i>
	<i>1.4.5 Terpendoles 26</i>
	<i>1.4.6 Sulpinines 28</i>
	<i>1.4.7 Shearinines 29</i>
	<i>1.4.8 Emindoles 31</i>
	<i>1.4.9 Aflatrems 32</i>
	<i>1.4.10 Janthitrems 33</i>
1.5	Biosynthetic Studies 36
1.6	Mode of Action of Tremorgenic Mycotoxins 38

1.7	Novel Endophyte Technology	40
1.8	Scope of the Present Study	41
Chapter Two	Isolation and Structure Elucidation of Janthitrems	44
2.1	Screening of Cultures	44
	2.1.1 <i>Introduction</i>	44
	2.1.2 <i>LC–UV–MS Analysis of Culture Extracts</i>	46
2.2	Isolation of Janthitrem A and Janthitrem B	50
	2.2.1 <i>Extraction and Isolation of Janthitrem A and Janthitrem B</i>	50
	2.2.2 <i>Analysis of Janthitrem Compounds</i>	53
2.3	Isolation of Janthitrem C and Janthitrem D	57
	2.3.1 <i>Extraction and Isolation of Janthitrem C and Janthitrem D</i>	57
	2.3.2 <i>Analysis of Janthitrem Compounds</i>	60
2.4	Janthitrem B Stability Investigations	65
	2.4.1 <i>Introduction</i>	65
	2.4.2 <i>Stability Investigation Conditions</i>	65
	2.4.3 <i>Results of the Stability Investigation</i>	66
	2.4.4 <i>Summary of Findings</i>	68
Chapter Three	NMR Analysis of Janthitrems A, B, C and D	69
3.1	Introduction	69
3.2	Janthitrem B NMR Discussion	71
	3.2.1 <i>¹H, ¹³C, DEPT-135, COSY and TOCSY NMR Spectra of Janthitrem B</i>	71
	3.2.2 <i>g-HSQC and g-HMBC NMR Spectra of Janthitrem B</i>	78
	3.2.3 <i>NOESY NMR Spectrum of Janthitrem B</i>	82
	3.2.4 <i>Summary; Janthitrem B NMR Assignments</i>	92
3.3	Janthitrem A NMR Discussion	92
	3.3.1 <i>¹H, ¹³C, DEPT-135, COSY and TOCSY NMR Spectra of Janthitrem A</i>	93
	3.3.2 <i>g-HSQC and g-HMBC NMR Spectra of Janthitrem A</i>	99
	3.3.3 <i>NOESY NMR Spectrum of Janthitrem A</i>	100
	3.3.4 <i>Summary; Janthitrem A NMR Assignments</i>	107
3.4	Janthitrem C NMR Discussion	107

3.4.1	<i>¹H, ¹³C, DEPT-135, COSY and TOCSY NMR Spectra of Janthitrem C</i>	108
3.4.2	<i>g-HSQC and g-HMBC NMR Spectra of Janthitrem C</i>	117
3.4.3	<i>Summary; Janthitrem C NMR Assignments</i>	117
3.5	Janthitrem D NMR Discussion	118
3.5.1	<i>¹H, ¹³C, DEPT-135, COSY and TOCSY NMR Spectra of Janthitrem D</i>	119
3.5.2	<i>g-HSQC and g-HMBC NMR Spectra of Janthitrem D</i>	125
3.5.3	<i>NOESY NMR Spectrum of Janthitrem D</i>	126
3.5.4	<i>Summary; Janthitrem D NMR Assignments</i>	133
Chapter Four	LC–UV–MS Analysis of Indole–Diterpenoids	134
4.1	Introduction	134
4.2	Comparison of an APCI and ESI Source in an LC–UV–MS System	135
4.3	APCI Vapourisation Temperature	139
4.4	LC–UV–MS APCI and ESI Positive Ion Modes	143
4.4.1	<i>Fragmentation of Janthitrems</i>	143
4.4.2	<i>Fragmentation of Penitrems</i>	151
4.4.3	<i>Fragmentation of Lolitrem B</i>	159
4.4.4	<i>Fragmentation of Paxilline</i>	162
4.4.5	<i>Fragmentation of Terpendole C</i>	163
4.4.6	<i>Fragmentation of Paspalinine</i>	165
4.5	LC–UV–MS APCI Negative Ion Mode	167
4.5.1	<i>Fragmentation of Janthitrems</i>	171
4.5.2	<i>Fragmentation of Penitrems</i>	177
4.5.3	<i>Fragmentation of Lolitrem B</i>	185
4.5.4	<i>Fragmentation of Paxilline</i>	187
4.5.5	<i>Fragmentation of Terpendole C</i>	189
4.5.6	<i>Fragmentation of Paspalinine</i>	190
4.5.7	<i>Summary of Findings</i>	191
Chapter Five	<i>In vivo</i> Effects of the Isolated Indole–Diterpenoid Compounds	193
5.1	Assessment of Tremorgenicity, Heart Rate, Blood Pressure and Motor Control of Mice Dosed with Janthitrems A and B	193
5.1.1	<i>Introduction</i>	193

5.1.2	<i>Tremorgen Bioassay</i>	195
5.1.3	<i>Effect of the Test Compounds on the Heart Rate of the Mice</i>	197
5.1.4	<i>Effect of the Test Compounds on the Systolic Pressure of the Mice</i>	198
5.1.5	<i>Effect of the Test Compounds on the Diastolic Pressure of the Mice</i>	199
5.1.6	<i>Effect of the Test Compounds on the Motor Control of the Mice</i>	199
5.1.7	<i>Summary of Findings</i>	202
5.2	Insect testing of Janthitrem A and Janthitrem B	206
5.2.1	<i>Introduction</i>	206
5.2.2	<i>Stability of the Test Mycotoxins Janthitrem A, Janthitrem B and Paxilline in the Diets Prepared for the Insect Bioassay</i>	208
5.2.3	<i>Preparation of the Diets for the Insect Bioassay</i>	209
5.2.4	<i>Insect Bioassay</i>	210
5.2.5	<i>Summary of Findings</i>	214
Chapter Six	Analysis of Mouldy Walnuts	215
6.1	Introduction	215
6.2	Identification of the Fungus from the Mouldy Walnuts	217
6.3	LC–UV–MS Analysis of the Mouldy Walnuts and <i>P. crustosum</i> Extracts	219
6.3.1	<i>LC–UV–MS Method Validation</i>	219
6.3.2	<i>LC–UV–MS Identification of the Penitrems and Roquefortine C in the Mouldy Walnuts and <i>P. crustosum</i> Extracts</i>	222
6.3.3	<i>LC–UV–MS Quantitation of Penitrems in Mouldy Walnuts and <i>P. crustosum</i> Extracts</i>	226
6.3.4	<i>LC–UV–MS Identification of Additional Metabolites Detected in the Mouldy Walnuts and <i>P. crustosum</i> Extracts</i>	228
6.4	Summary of Findings	229
Chapter Seven	Summary and Conclusions	230
7.1	Screening of Cultures	230
7.2	Isolation and Structure Elucidation of Janthitrems A and B	230
7.3	Isolation and Structure Elucidation of Janthitrems C and D	232
7.4	Janthitrems Structural Inter-Relationship	233

7.5	Stability of Janthitrem B	235
7.6	Bioactivity of Janthitrems	235
	7.6.1 <i>Mice Testing</i>	235
	7.6.2 <i>Insect Testing</i>	237
7.7	LC–UV–MS Investigations	237
	7.7.1 <i>APCI vs. ESI</i>	237
	7.7.2 <i>Positive Ion Analysis</i>	238
	7.7.3 <i>Negative Ion Analysis</i>	238
7.8	Mouldy Walnuts Investigation	239
7.9	Conclusion	240
7.10	Future Work	241
Chapter Eight	Experimental	242
8.1	Screening of Cultures	242
	8.1.1 <i>Culturing</i>	242
	8.1.2 <i>Extraction</i>	242
	8.1.3 <i>LC –UV –MS</i>	243
8.2	Isolation of Janthitrem A and Janthitrem B	244
	8.2.1 <i>Culturing</i>	244
	8.2.2 <i>Extraction</i>	244
	8.2.3 <i>Flash Column Chromatography</i>	244
	8.2.4 <i>TLC</i>	245
	8.2.5 <i>Analytical HPLC</i>	245
	8.2.6 <i>De-fatting of Samples</i>	245
	8.2.7 <i>Flash Column Chromatography 2</i>	246
	8.2.8 <i>Solid Phase Extraction</i>	246
	8.2.9 <i>Semi-preparative HPLC</i>	246
	8.2.10 <i>HRMS</i>	247
	8.2.11 <i>NMR</i>	247
	8.2.12 <i>Molecular Modelling</i>	247
8.3	Isolation of Janthitrem C and Janthitrem D	248
	8.3.1 <i>De-fatting of Samples</i>	248
	8.3.2 <i>Flash Column Chromatography</i>	248

8.3.3	<i>TLC</i>	248
8.3.4	<i>NMR</i>	249
8.4	Stability Trial	249
8.5	LC–UV–MS Analysis	251
8.5.1	<i>APCI vs. ESI</i>	251
8.5.2	<i>APCI Vapouriser Temperatures</i>	252
8.5.3	<i>Positive Ion Analyses</i>	252
8.5.4	<i>Negative Ion Analyses</i>	252
8.6	Assessment of Tremorgenicity, Heart Rate, Blood Pressure and Motor Control on Mice Dosed with Janthitrems A and B	253
8.6.1	<i>Mouse Bioassay</i>	253
8.6.2	<i>Tremor Score</i>	254
8.6.3	<i>Blood Pressure and Heart Rate</i>	254
8.6.4	<i>Motor Control</i>	255
8.7	Insect Testing	256
8.7.1	<i>Stability of the Test Mycotoxins</i>	256
8.7.2	<i>Diets Prepared with the Inclusion of the Test Mycotoxins</i>	257
8.7.3	<i>Diets Prepared with the Inclusion of Endophyte-Free and AR37-Infected Ryegrass</i>	257
8.7.4	<i>Insect Bioassay Trial</i>	258
8.8	Analysis of Mouldy Walnuts	259
8.8.1	<i>Culturing and Isolation of Fungus from the Mouldy Walnuts</i>	259
8.8.2	<i>Toxin Extraction</i>	260
8.8.3	<i>LC–UV–MS Analysis</i>	260
8.8.4	<i>LC–UV–MS Method Validation</i>	261
	References	262
	Appendix	277
Appendix 1	Published account of mouldy walnuts investigation.	278
Appendix 2	Poster presented at the 6th International Symposium on Fungal Endophytes of Grasses, 2007.	281

List of Figures

	Page
1.1 A sheep affected by ryegrass staggers.	2
1.2 Comparison of endophyte-free perennial ryegrass (left) to endophyte-infected perennial ryegrass (right). The damage to the endophyte-free ryegrass was inflicted by the Argentine stem weevil. Photo courtesy of AgResearch, Ruakura.	5
1.3 Argentine stem weevil. Photo courtesy of AgResearch, Ruakura.	5
1.4 Peramine.	6
1.5 Comparison of (a) endophyte-infected and (b) endophyte-free grass, (Schardl et al., 2007).	6
1.6 Ergovaline.	10
1.7 Structures of loline, <i>N</i> -formylloline, <i>N</i> -acetylloline, <i>N</i> -methylloline, norloline, <i>N</i> -acetylnorloline and <i>N</i> -formylloline.	11
1.8 Lysergic acid amide.	12
1.9 Structures of penitrems A–F.	14
1.10 Structures of penitrem G, secopenitrem B, 10-oxo-11,33-dihydropenitrem B and 6-bromopenitrem E.	16
1.11 Structures of pennigritrem, penitremones A–C and thomitrems A and E.	18
1.12 Structure of lolitrem B.	19
1.13 Structures of lolitrems A, E, F, G, H, J, K, L, M and N.	20
1.14 Structures of lolilline, lolitriol, lolicines A and B, and 31- <i>epi</i> -lolitrems F and N.	21
1.15 Structures of paspaline, paspaline B, paspalicine, 14 α -hydroxypaspalinine, paspalinine and paspalitrems A, B and C.	23
1.16 Structures of paxilline, 13-desoxypaxilline, paxilline-27- <i>O</i> -acetate, 7-hydroxy-13-desoxypaxilline, PCM5', PCM6 and paxinorol.	25
1.17 Structure of 21-isopentenylpaxilline.	26
1.18 Structures of terpendoles A–M.	27
1.19 Structures of sulphinines A–C.	29
1.20 Structures of shearinines A–K.	30
1.21 Structures of emindoles SA, SB, DA and DB.	31

1.22	Structures of emindoles PA, PB and PC and emeniveol.	32
1.23	Aflatrem.	33
1.24	Structures of janthitrems B and C.	34
1.25	Structures of janthitrems E–G.	34
1.26	10- <i>epi</i> -11,12-epoxyjanthitrem G.	36
1.27	Proposed biosynthetic pathway for the early stages of indole–diterpenoid biosynthesis.	37
2.1	Screening of <i>P. janthinellum</i> cultures.	45
2.2	LC–MS chromatograms of E1 and E2 and penitrem A standard. Values of m/z for $[M+H]^+$ are given above their corresponding peaks.	49
2.3	The isolation of janthitrem A and janthitrem B.	52
2.4	Full scan mass spectrum of the minor later-eluting peak. Values of m/z for major ions observed are given.	53
2.5	Full scan mass spectrum of the major early-eluting peak. Values of m/z for major ions observed are given.	54
2.6	Normalised UV absorbance spectra of minor (red) and major (black) peaks.	54
2.7	Structures of janthitrem B and 11,12-epoxyjanthitrem B.	56
2.8	Isolation of janthitrem C and janthitrem D.	59
2.9	Full scan mass spectrum of fractions 14–18. Values of m/z for major ions observed are given.	60
2.10	Full scan mass spectrum of fractions 10–13. Values of m/z for major ions observed are given.	61
2.11	Normalised UV absorbance spectra of fractions 14–18 (red) and fractions 10–13 (black).	61
2.12	Structures of janthitrem C and 11,12-epoxyjanthitrem C.	63
2.13	Graph displaying stability properties of tested conditions.	67
3.1	Numbered structures for janthitrems A–D, penitrem A and shearinine D.	70
3.2	The COSY NMR spectrum of janthitrem B.	75
3.3	The TOCSY NMR spectrum of janthitrem B.	75
3.4	The g-HSQC NMR spectrum of janthitrem B.	79
3.5	The g-HMBC NMR spectrum of janthitrem B.	79
3.6	Selected g-HMBC correlations observed for H-37 and H-39 of janthitrem B.	80

3.7	Selected g-HMBC correlations observed for H-38 and H-40 of janthitrem B.	80
3.8	The NOESY NMR spectrum of janthitrem B.	83
3.9	NOESY correlations observed for H-37 (black), H-38 (green), H-39 (red) and H-40 (blue) of janthitrem B.	84
3.10	NOESY correlations observed for H-5 α (black) and H-5 β (blue) of janthitrem B.	85
3.11	NOESY correlations observed for H-6 α (black) and H-6 β (blue) of janthitrem B.	86
3.12	NOESY correlations observed for H-14 α (black) and H-14 β (blue) of janthitrem B.	87
3.13	NOESY correlations observed for H-15 α (black) and H-15 β (blue) of janthitrem B.	87
3.14	NOESY correlations observed for H-17 α (black) and H-17 β (blue) of janthitrem B.	88
3.15	NOESY correlations observed for H-29E and H-29Z of janthitrem B.	89
3.16	NOESY correlations observed for H-20 (blue) and H-23 (red) of janthitrem B.	90
3.17	NOESY correlations observed for H-5 α (black) and H-5 β (blue) of janthitrem A.	102
3.18	NOESY correlations observed for H-6 α (black) and H-6 β (blue) of janthitrem A.	102
3.19	NOESY correlations observed for H-14 α (black) and H-14 β (blue) of janthitrem A.	103
3.20	NOESY correlations observed for H-15 α (black) and H-15 β (blue) of janthitrem A.	104
3.21	NOESY correlations observed for H-17 α (black) and H-17 β (blue) of janthitrem A.	104
3.22	NOESY correlations observed for H-29E and H-29Z of janthitrem A.	105
3.23	NOESY correlations observed for H-37 (black), H-38 (green), H-39 (red) and H-40 (blue) of janthitrem D.	126
3.24	NOESY correlations observed for H-5 α (black) and H-5 β (blue) of janthitrem D.	127
3.25	NOESY correlations observed for H-6 α (black) and H-6 β (blue) of janthitrem D.	128
3.26	NOESY correlations observed for H-14 α (black) and H-14 β (blue) of janthitrem D.	129

3.27	NOESY correlations observed for H-15 α (black) and H-15 β (blue) of janthitrem D.	129
3.28	NOESY correlations observed for H-17 α (black) and H-17 β (blue) of janthitrem D.	130
3.29	NOESY correlations observed for H-30 α (black) and H-30 β (blue) of janthitrem D.	131
3.30	NOESY correlations observed for H-29E and H-29Z of janthitrem D.	132
4.1	LC–UV–MS spectrum of penitrem A (ESI) at 233 nm (upper profile) and m/z 634, [M+H] ⁺ (lower profile).	138
4.2	LC–UV–MS spectrum of penitrem A (APCI) at 233 nm (upper profile) and m/z 634, [M+H] ⁺ (lower profile).	138
4.3	250°C APCI mass spectrum. Values of m/z for major ions observed are given.	139
4.4	300°C APCI mass spectrum. Values of m/z for major ions observed are given.	139
4.5	350°C APCI spectrum. Values of m/z for major ions observed are given.	140
4.6	400°C APCI spectrum. Values of m/z for major ions observed are given.	141
4.7	450°C APCI spectrum. Values of m/z for major ions observed are given.	142
4.8	Loss of acetone in janthitrems A–D.	144
4.9	Fragmentation of janthitrem A in positive ion MS ² and MS ³ spectra.	145
4.10	Fragmentation of janthitrem B in positive ion MS ² and MS ³ spectra (ESI).	146
4.11	Fragmentation of janthitrem B in positive ion MS ² and MS ³ spectra (APCI).	147
4.12	Retro Diels–Alder rearrangement of janthitrem B involving formation of an enol group which equilibrates to the corresponding aldehyde form.	147
4.13	Fragmentation of janthitrem C in positive ion MS ² and MS ³ spectra (ESI).	149
4.14	Fragmentation of janthitrem C in positive ion MS ² and MS ³ spectra (APCI).	149
4.15	Fragmentation of janthitrem D in positive ion MS ² and MS ³ spectra.	150
4.16	Structures of penitrems A–F.	153

4.17	Fragmentation of penitrems A and E in positive ion MS ² , MS ³ and MS ⁴ spectra.	155
4.18	Fragmentation of penitrems B and F in positive ion MS ² , MS ³ and MS ⁴ spectra.	157
4.19	Fragmentation of penitrems C and D in positive ion MS ² , MS ³ and MS ⁴ spectra.	159
4.20	Fragmentation of lolitrem B in positive ion MS ² and MS ³ spectra (ESI).	160
4.21	Fragmentation of lolitrem B in positive ion MS ² and MS ³ spectra (APCI).	161
4.22	Fragmentation of paxilline in positive ion MS ² and MS ³ spectra (ESI).	162
4.23	Fragmentation of paxilline in positive ion MS ² and MS ³ spectra (APCI).	163
4.24	Fragmentation of terpendole C in positive ion MS ² and MS ³ spectra (ESI).	164
4.25	Fragmentation of terpendole C in positive ion MS ² and MS ³ spectra (APCI).	165
4.26	Fragmentation of paspalinine in positive ion MS ² and MS ³ spectra (ESI).	166
4.27	Fragmentation of paspalinine in positive ion MS ² and MS ³ spectra (APCI).	167
4.28	Full scan negative ion spectrum of janthitrem B.	169
4.29	Full scan negative ion spectrum of terpendole C.	169
4.30	Full scan negative ion spectrum of janthitrem B with SID.	170
4.31	Full scan negative ion spectrum of terpendole C with SID.	170
4.32	Ions generated through loss of acetone from janthitrems A–D.	171
4.33	Janthitrem A full scan negative ion mass spectrum.	172
4.34	Janthitrem A negative ion MS ² spectrum (<i>m/z</i> 600).	172
4.35	Janthitrem A negative ion MS ³ spectrum (<i>m/z</i> 600 → <i>m/z</i> 582).	172
4.36	Fragmentation of janthitrem A in negative ion MS ² and MS ³ spectra.	173
4.37	Janthitrem B full scan negative ion mass spectrum.	173
4.38	Janthitrem B negative ion MS ² spectrum (<i>m/z</i> 584).	174
4.39	Janthitrem B negative ion MS ³ spectrum (<i>m/z</i> 584 → <i>m/z</i> 526).	174
4.40	Fragmentation of janthitrem B in negative ion MS ² and MS ³ spectra.	175

4.41	Retro Diels–Alder rearrangement of janthirem B involving formation of an enol group which equilibrates to the corresponding aldehyde form.	175
4.42	Fragmentation of janthirem C in negative ion MS ² and MS ³ spectra.	176
4.43	Fragmentation of janthirem D in negative ion MS ² and MS ³ spectra.	177
4.44	Penitrem A full scan negative ion mass spectrum.	179
4.45	Penitrem A negative ion MS ² spectrum (<i>m/z</i> 632).	179
4.46	Penitrem A negative ion MS ³ spectrum (<i>m/z</i> 632 → <i>m/z</i> 546).	179
4.47	Fragmentation of penitrems A and E in negative ion MS ² and MS ³ spectra.	180
4.48	Penitrem C full scan negative ion mass spectrum.	181
4.49	Penitrem C negative ion MS ² spectrum (<i>m/z</i> 600).	181
4.50	Penitrem C negative ion MS ³ spectrum (<i>m/z</i> 600 → <i>m/z</i> 514).	181
4.51	Fragmentation of penitrems C and D in negative ion MS ² and MS ³ spectra.	182
4.52	Penitrem F full scan negative ion mass spectrum.	183
4.53	Penitrem F negative ion MS ² spectrum (<i>m/z</i> 616).	183
4.54	Penitrem F negative ion MS ³ spectrum (<i>m/z</i> 616 → <i>m/z</i> 486).	183
4.55	Fragmentation of penitrems B and F in negative ion MS ² and MS ³ spectra.	184
4.56	Lolitrem B full scan negative ion mass spectrum.	185
4.57	Lolitrem B negative ion MS ² spectrum (<i>m/z</i> 684).	185
4.58	Lolitrem B negative ion MS ³ spectrum (<i>m/z</i> 684 → <i>m/z</i> 470).	186
4.59	Fragmentation of lolitrem B in negative ion MS ² and MS ³ spectra.	187
4.60	Fragmentation of paxilline in negative ion MS ² and MS ³ spectra.	188
4.61	Fragmentation of terpendole C in negative ion MS ² and MS ³ spectra.	189
4.62	Fragmentation of paspalinine in negative ion MS ² and MS ³ spectra.	191
5.1	The rotamex 4 rotarod.	194
5.2	The BP-2000 blood pressure and heart rate measurement instrument.	195

5.3	Mean tremor score vs time post-injection for mice dosed i.p. with janthitrem A (n = 4), janthitrem B (n = 4) and their respective controls (n = 4).	196
5.4	Mean heart rate vs time post-injection for mice dosed i.p. with janthitrem A (n = 4), janthitrem B (n = 4) and their respective controls (n = 4).	197
5.5	Mean systolic pressure vs time post-injection for mice dosed i.p. with janthitrem A (n = 4), janthitrem B (n = 4) and their respective controls (n = 4).	198
5.6	Mean diastolic pressure vs time post-injection for mice dosed i.p. with janthitrem A (n = 4), janthitrem B (n = 4) and their respective controls (n = 4).	199
5.7	Mean rotarod score vs time post-injection for mice dosed i.p. with janthitrem A (n = 4), janthitrem B (n = 4) and their respective controls (n = 4).	200
5.8	Mean rotarod scores expressed as a percentage of the score at t = 0 vs time post-injection for mice dosed i.p. with janthitrem A (n=4), janthitrem B (n=4) and their respective controls (n=4).	201
5.9	Structures of lolitrem B, janthitrem A, janthitrem B, paspalinine, terpendole C, paxilline and lolilline.	203
5.10	Comparison of mean tremor scores vs time post-injection for mice dosed i.p. with janthitrem A (n = 4), janthitrem B (n = 4), lolitrem B (Munday-Finch, 1997) and paxilline (Munday-Finch, 1997).	204
5.11	Porina (<i>Wiseana cervinata</i>) larva. Photo courtesy of AgResearch, Ruakura.	207
5.12	a) Transfer of the prepared diet with the test mycotoxin into a petri dish and b) allowing the prepared diets for each treatment to cool.	209
5.13	Specimen containers placed in a controlled environment room.	211
5.14	Percentage of diet eaten by the porina for each treatment.	213
6.1	The collected mouldy walnuts.	217
6.2	a) Extraction of the fungus. b) Inoculation of the media with the fungus. c) The inoculated culture flasks. d) Incubation of the cultures.	218
6.3	Calibration curve for five penitrem A standards obtained from the mass spectrometer (using an APCI source). The error bars representing the relative standard deviation are too small to be visible.	220
6.4	Calibration curve for five penitrem A standards obtained from the PDA (at 296 nm). The error bars representing the relative standard deviation are too small to be visible.	220

6.5	LC–MS chromatogram of <i>P. crustosum</i> . Values of m/z for $[M+H]^+$ are given above their corresponding peaks.	222
6.6	LC–MS chromatogram of the mouldy walnut extract. Values of m/z for $[M+H]^+$ are given above their corresponding peaks.	223
6.7	Full scan of penitrem A peak from <i>P. crustosum</i> . Values of m/z for major ions observed are given.	224
6.8	MS ² (m/z 634) spectrum of penitrem A peak from <i>P. crustosum</i> . Values of m/z for major ions observed are given.	224
6.9	MS ³ (m/z 634→558) spectrum of penitrem A peak from <i>P. crustosum</i> . Values of m/z for major ions observed are given.	224
6.10	UV absorbance spectrum of penitrem A.	225
7.1	The structural inter-relationship between the janthitrems.	234
7.2	Structure of janthitrems A–G.	234

List of Tables

	Page
2.1 Penitrems and janthitrems detected in each strain of <i>P. janthinellum</i> .	48
2.2 ^{13}C NMR resonances observed for janthitrem B and the unknown janthitrem analogue and published assignments for penitrem A ^a (δ).	56
2.3 ^{13}C NMR resonances observed for janthitrem A, janthitrem C and the unknown janthitrem analogue (δ).	62
2.4 Conditions used to monitor the stability of janthitrem B.	66
2.5 Test conditions ranked based on percentage of janthitrem B degraded. Unless otherwise stated, samples were stored at room temperature (20°C).	68
3.1 ^1H and ^{13}C NMR assignments established for janthitrems A and B and published assignments for penitrem A ^a (δ).	73
3.2 COSY NMR correlations observed for janthitrem B (δ).	76
3.3 TOCSY NMR correlations observed for janthitrem B (δ).	77
3.4 Long-range ^{13}C - ^1H NMR correlations observed in the g-HMBC NMR spectrum of janthitrem B (δ).	81
3.5 NOESY NMR correlations observed for janthitrem B (δ).	90
3.6 COSY NMR correlations observed for janthitrem A (δ).	97
3.7 TOCSY NMR correlations observed for janthitrem A (δ).	98
3.8 Long-range ^{13}C - ^1H NMR correlations observed in the g-HMBC NMR spectrum of janthitrem A (δ).	100
3.9 NOESY NMR correlations observed for janthitrem A (δ).	106
3.10 ^1H and ^{13}C NMR assignments established for janthitrem C and published assignments for janthitrem C ^a (δ).	109
3.11 COSY NMR correlations observed for janthitrem C (δ).	115
3.12 TOCSY NMR correlations observed for janthitrem C (δ).	116
3.13 Long-range ^{13}C - ^1H NMR correlations observed in the g-HMBC NMR spectrum of janthitrem C (δ).	117
3.14 ^1H and ^{13}C NMR assignments established for janthitrem D (δ).	120
3.15 COSY NMR correlations observed for janthitrem D (δ).	123
3.16 TOCSY NMR correlations observed for janthitrem D (δ).	124

3.17	Long-range ^{13}C - ^1H NMR correlations observed in the HMBC NMR spectrum of janthitrem D (δ).	125
3.18	NOESY NMR correlations observed for janthitrem D.	132
4.1	% UV versus APCI or ESI $[\text{M}+\text{H}]^+$ peak area responses.	137
4.2	Ions observed in MS spectra of penitrems A–F under positive ion conditions.	153
4.3	Ions observed in full scan, MS^2 and MS^3 spectra of penitrems A–F under negative ion conditions.	178
5.1	Tremorgenic activity of the tested janthitrems.	202
5.2	Mycotoxin recovered (as a percentage of that added) from diets at time zero and after 24 hours.	208
5.3	Prepared bioassay diets with the test mycotoxin/ryegrass.	210
5.4	Results of the insect bioassay.	212
6.1	Comparison of the reference concentration and the average experimental concentration for penitrem A.	222
6.2	Comparison of penitrem production in the mouldy walnuts and <i>P. crustosum</i> extracts.	227
8.1	Conditions used to monitor the stability of janthitrem B.	249
8.2	The visual rating scale for tremor assessment.	254

Abbreviations

α	alpha (lower face)
β	beta (upper face)
$^{\circ}\text{C}$	degrees Celsius
δ	delta
>	greater than
<	less than
%	percent
1J	one bond NMR coupling constant
2J	two bond NMR coupling constant
3J	three bond NMR coupling constant
4J	four bond NMR coupling constant
APCI	atmospheric pressure chemical ionisation
bpm	beats per minute
<i>ca.</i>	approximately
calc.	calculated
CDCl_3	deuteriochloroform
CE	collision energy
CIP	Cahn–Ingold–Prelog
COSY	correlated spectroscopy
cv.	cultivated variety
dd	doublet of doublets
DEPT	distortionless enhancement by polarisation transfer
DMSO	dimethylsulphoxide
<i>E</i>	<i>entgegen</i>
e.g.	for example
ESI	electrospray ionisation

et al.	and others
GABA	γ -aminobutyric acid
GGDP	geranylgeranyl diphosphate
g-HMBC	gradient selected heteronuclear multiple bond correlation
g-HSQC	gradient selected heteronuclear single quantum coherence
HPLC	high performance liquid chromatography
HRMS	high resolution mass spectrometry
Hz	Hertz
i.e.	as in
i.p.	intraperitoneally
i.v.	intravenous
kg	kilogram
L	litre
LC	liquid chromatography
LC-MS	liquid chromatography mass spectrometry
LC-UV-MS	liquid chromatography ultra-violet mass spectrometry
LSD	lysergic acid diethylamide
mL	millilitre
μ L	microlitre
μ g	microgram
μ m	micrometer
mg	milligram
$[M-H]^-$	molecular ion (negative ion detection)
$[M+H]^+$	molecular ion (positive ion detection)
m/z	mass/charge ratio
Me	methyl
MHz	mega Hertz

min	minutes
ms	millisecond
MS	mass spectrometry
nm	nanometer
NMR	nuclear magnetic resonance
NOE	nuclear Overhauser effect
NOESY	nuclear Overhauser effect spectroscopy
<i>p</i>	probability
PDA	photodiode array
PDD	Plant Diseases Division
ppm	parts per million
q	quartet
RDA	retro Diels–Alder
rpm	revolutions per minute
RSD	relative standard deviation
s	singlet
sec	seconds
SID	source-induced dissociation
sp	species
t	triplet
TLC	thin layer chromatography
TOCSY	total correlation spectroscopy
UV	ultra-violet
V	volts
v/v	volume per volume
XHCOR	X–H correlated
Z	<i>zusammen</i>

Bioactive Chemicals of Importance in Endophyte- Infected Grasses

**A thesis submitted in fulfilment of the requirements
for the degree of Doctor of Philosophy at
The University of Waikato**

**by
Jacob Vadakkal Babu**



**The
University
of Waikato**

*Te Whare Wānanga
o Waikato*

2008

Abstract

Janthitremes are believed to be involved in the observed sporadic cases of AR37-infected perennial ryegrass staggers. Investigations into the role of janthitremes in perennial ryegrass staggers are difficult as isolation of the compounds from the ryegrass is hindered by the inherent instability of these compounds. Therefore attempts were made to isolate janthitremes from an alternative source, allowing these janthitrem analogues to be used as surrogates for endophyte produced janthitremes.

Analysis of a series of *Penicillium janthinellum* cultures revealed the presence of janthitremes in a number of strains, including janthitrem B, janthitrem C and two novel janthitrem compounds. Detailed one- and two-dimensional NMR and mass spectral techniques identified the two novel compounds as 11,12-epoxyjanthitremes B and C, which were subsequently given the trivial names janthitremes A and D, respectively. Janthitremes B and C were isolated and identified by NMR and revisions of some previously reported chemical shift assignments were proposed. In addition to the janthitremes, penitremes were also identified in two strains of *P. janthinellum*.

The isolated janthitrem B was utilised for the development of efficient extraction procedures, and for the determination of ideal storage conditions for janthitrem compounds. A method for the extraction and isolation of janthitrem B from a *P. janthinellum* culture was developed and optimised to yield 6 mg of janthitrem B from 900 mL of fungal culture in two days. Stability studies of janthitrem B indicated the ideal storage condition which minimised degradation was dry at -80°C where only 7% sample loss was observed over 300 days.

Bioactivity studies of janthitrems A and B found these compounds to be tremorgenic to mice, with janthitrem A (an epoxyjanthitrem) inducing more severe tremors than janthitrem B. Insect testing also showed that both janthitrems A and B displayed anti-insect activity to porina larvae. Since the epoxyjanthitrems, which are associated with AR37 endophyte-infected ryegrass, were also shown to be tremorgenic and to display anti-insect activity, the insect resistance and the sporadic cases of ryegrass staggers displayed by AR37 may be related to the presence of epoxyjanthitrem compounds.

LC–UV–MS analysis of janthitrems A–D, penitrems A–F, lolitrem B, paspalinine, paxilline and terpendole C found these indole–diterpenoids to be more sensitive by analysis using an APCI source as opposed to an ESI source. APCI negative ion LC–UV–MS required source induced dissociation in combination with increased collision energy to suppress an acetate adduct peak, sourced from the acetic acid buffer. Negative ion MS^2 and MS^3 data produced more informative fragments compared to the conventional positive ion MS^2 and MS^3 data. The availability of both positive and negative ion LC–UV–MS methodologies will allow future endophyte products to be more thoroughly screened for different classes of secondary metabolites.

Extracts of mouldy walnuts were analysed for the presence of tremorgenic mycotoxins after a dog was found to exhibit symptoms characteristic of tremorgenic mycotoxicosis. LC–UV–MS analysis of the mouldy walnuts identified the tremorgenic mycotoxins penitrems A–F, thus confirming the veterinarian’s tentative diagnosis of canine tremorgenic mycotoxicosis — the first reported case in New Zealand.

Acknowledgements

I would like to express my sincere appreciation and thanks first and foremost to my supervisors, Professor Alistair Wilkins (The University of Waikato), Dr. Christopher Miles (AgResearch) and Dr. Sarah Finch (AgResearch) for their invaluable support, advice, guidance and patience throughout the course of this project.

Thanks to AgResearch for their help and support during my PhD and to the toxinology group, in particular Allan Hawkes, for making my time at AgResearch an enjoyable and memorable experience and Dr Jared Loader for proofreading my thesis. In addition I would also like to thank Wendy Jackson (The University of Waikato) for help with the LC–UV–MS instrument and Pat Gread (The University of Waikato) for running high resolution mass spectrometry samples.

Thanks must also be extended to Dr. Margaret di Menna (AgResearch) for growth and identification of fungal cultures, Sharon Sayer (AgResearch) for growing fungal cultures, Karl Fraser (AgResearch) and Dr. Geoff Lane (AgResearch) for running samples on the LC–UV–MS and for their advice and assistance with LC–UV–MS analyses, Ric Broadhurst for the care of the animals used in the small animal trial, Dr. Alison Popay for running and supervising the insect trial and to Professor Satoshi Omura and Professor Hiroshi Tomoda for supplying a sample of terpendole C.

The Technology Industry Fellowship (TIF) provided by Technology New Zealand and The University of Waikato via UNILINK is also gratefully acknowledged, their financial help was invaluable.

Finally I would like to thank my Mum and Dad for their support and encouragement, and in particular my sister, Kavitha, whose proofreading and computer skills were employed fulltime.

Table of Contents

	Page
Abstract	<i>i</i>
Acknowledgements	<i>iii</i>
List of Figures	<i>x</i>
List of Tables	<i>xviii</i>
Abbreviations	<i>xx</i>
Chapter One	
Introduction	1
1.1	Perennial Ryegrass Staggers 1
1.2	History of Ryegrass Staggers 2
	<i>1.2.1 The Advantages and Disadvantages of Endophyte-Infected Perennial Ryegrass 6</i>
	<i>1.2.2 Options for Control of Ryegrass Staggers 7</i>
1.3	Toxicoses Associated with Grasses Infected with Endophytic Fungi 8
	<i>1.3.1 Ryegrass Staggers 8</i>
	<i>1.3.2 Tall Fescue Toxicosis 8</i>
	<i>1.3.3 Sleepygrass Toxicosis 11</i>
	<i>1.3.4 Drunken Horse Grass 12</i>
1.4	Indole–Diterpenoids 13
	<i>1.4.1 Penitrems 14</i>
	<i>1.4.2 Lolitrems 19</i>
	<i>1.4.3 Paspaline 22</i>
	<i>1.4.4 Paxilline 24</i>
	<i>1.4.5 Terpendoles 26</i>
	<i>1.4.6 Sulpinines 28</i>
	<i>1.4.7 Shearinines 29</i>
	<i>1.4.8 Emindoles 31</i>
	<i>1.4.9 Aflatrems 32</i>
	<i>1.4.10 Janthitrems 33</i>
1.5	Biosynthetic Studies 36
1.6	Mode of Action of Tremorgenic Mycotoxins 38

1.7	Novel Endophyte Technology	40
1.8	Scope of the Present Study	41
Chapter Two	Isolation and Structure Elucidation of Janthitrem	44
2.1	Screening of Cultures	44
	2.1.1 <i>Introduction</i>	44
	2.1.2 <i>LC–UV–MS Analysis of Culture Extracts</i>	46
2.2	Isolation of Janthitrem A and Janthitrem B	50
	2.2.1 <i>Extraction and Isolation of Janthitrem A and Janthitrem B</i>	50
	2.2.2 <i>Analysis of Janthitrem Compounds</i>	53
2.3	Isolation of Janthitrem C and Janthitrem D	57
	2.3.1 <i>Extraction and Isolation of Janthitrem C and Janthitrem D</i>	57
	2.3.2 <i>Analysis of Janthitrem Compounds</i>	60
2.4	Janthitrem B Stability Investigations	65
	2.4.1 <i>Introduction</i>	65
	2.4.2 <i>Stability Investigation Conditions</i>	65
	2.4.3 <i>Results of the Stability Investigation</i>	66
	2.4.4 <i>Summary of Findings</i>	68
Chapter Three	NMR Analysis of Janthitrem A, B, C and D	69
3.1	Introduction	69
3.2	Janthitrem B NMR Discussion	71
	3.2.1 <i>¹H, ¹³C, DEPT-135, COSY and TOCSY NMR Spectra of Janthitrem B</i>	71
	3.2.2 <i>g-HSQC and g-HMBC NMR Spectra of Janthitrem B</i>	78
	3.2.3 <i>NOESY NMR Spectrum of Janthitrem B</i>	82
	3.2.4 <i>Summary; Janthitrem B NMR Assignments</i>	92
3.3	Janthitrem A NMR Discussion	92
	3.3.1 <i>¹H, ¹³C, DEPT-135, COSY and TOCSY NMR Spectra of Janthitrem A</i>	93
	3.3.2 <i>g-HSQC and g-HMBC NMR Spectra of Janthitrem A</i>	99
	3.3.3 <i>NOESY NMR Spectrum of Janthitrem A</i>	100
	3.3.4 <i>Summary; Janthitrem A NMR Assignments</i>	107
3.4	Janthitrem C NMR Discussion	107

3.4.1	<i>¹H, ¹³C, DEPT-135, COSY and TOCSY NMR Spectra of Janthitrem C</i>	108
3.4.2	<i>g-HSQC and g-HMBC NMR Spectra of Janthitrem C</i>	117
3.4.3	<i>Summary; Janthitrem C NMR Assignments</i>	117
3.5	Janthitrem D NMR Discussion	118
3.5.1	<i>¹H, ¹³C, DEPT-135, COSY and TOCSY NMR Spectra of Janthitrem D</i>	119
3.5.2	<i>g-HSQC and g-HMBC NMR Spectra of Janthitrem D</i>	125
3.5.3	<i>NOESY NMR Spectrum of Janthitrem D</i>	126
3.5.4	<i>Summary; Janthitrem D NMR Assignments</i>	133
Chapter Four	LC–UV–MS Analysis of Indole–Diterpenoids	134
4.1	Introduction	134
4.2	Comparison of an APCI and ESI Source in an LC–UV–MS System	135
4.3	APCI Vapourisation Temperature	139
4.4	LC–UV–MS APCI and ESI Positive Ion Modes	143
4.4.1	<i>Fragmentation of Janthitrems</i>	143
4.4.2	<i>Fragmentation of Penitrems</i>	151
4.4.3	<i>Fragmentation of Lolitrem B</i>	159
4.4.4	<i>Fragmentation of Paxilline</i>	162
4.4.5	<i>Fragmentation of Terpendole C</i>	163
4.4.6	<i>Fragmentation of Paspalinine</i>	165
4.5	LC–UV–MS APCI Negative Ion Mode	167
4.5.1	<i>Fragmentation of Janthitrems</i>	171
4.5.2	<i>Fragmentation of Penitrems</i>	177
4.5.3	<i>Fragmentation of Lolitrem B</i>	185
4.5.4	<i>Fragmentation of Paxilline</i>	187
4.5.5	<i>Fragmentation of Terpendole C</i>	189
4.5.6	<i>Fragmentation of Paspalinine</i>	190
4.5.7	<i>Summary of Findings</i>	191
Chapter Five	<i>In vivo</i> Effects of the Isolated Indole–Diterpenoid Compounds	193
5.1	Assessment of Tremorgenicity, Heart Rate, Blood Pressure and Motor Control of Mice Dosed with Janthitrems A and B	193
5.1.1	<i>Introduction</i>	193

5.1.2	<i>Tremorgen Bioassay</i>	195
5.1.3	<i>Effect of the Test Compounds on the Heart Rate of the Mice</i>	197
5.1.4	<i>Effect of the Test Compounds on the Systolic Pressure of the Mice</i>	198
5.1.5	<i>Effect of the Test Compounds on the Diastolic Pressure of the Mice</i>	199
5.1.6	<i>Effect of the Test Compounds on the Motor Control of the Mice</i>	199
5.1.7	<i>Summary of Findings</i>	202
5.2	Insect testing of Janthitrem A and Janthitrem B	206
5.2.1	<i>Introduction</i>	206
5.2.2	<i>Stability of the Test Mycotoxins Janthitrem A, Janthitrem B and Paxilline in the Diets Prepared for the Insect Bioassay</i>	208
5.2.3	<i>Preparation of the Diets for the Insect Bioassay</i>	209
5.2.4	<i>Insect Bioassay</i>	210
5.2.5	<i>Summary of Findings</i>	214
Chapter Six	Analysis of Mouldy Walnuts	215
6.1	Introduction	215
6.2	Identification of the Fungus from the Mouldy Walnuts	217
6.3	LC–UV–MS Analysis of the Mouldy Walnuts and <i>P. crustosum</i> Extracts	219
6.3.1	<i>LC–UV–MS Method Validation</i>	219
6.3.2	<i>LC–UV–MS Identification of the Penitrems and Roquefortine C in the Mouldy Walnuts and <i>P. crustosum</i> Extracts</i>	222
6.3.3	<i>LC–UV–MS Quantitation of Penitrems in Mouldy Walnuts and <i>P. crustosum</i> Extracts</i>	226
6.3.4	<i>LC–UV–MS Identification of Additional Metabolites Detected in the Mouldy Walnuts and <i>P. crustosum</i> Extracts</i>	228
6.4	Summary of Findings	229
Chapter Seven	Summary and Conclusions	230
7.1	Screening of Cultures	230
7.2	Isolation and Structure Elucidation of Janthitrems A and B	230
7.3	Isolation and Structure Elucidation of Janthitrems C and D	232
7.4	Janthitrems Structural Inter-Relationship	233

7.5	Stability of Janthitrem B	235
7.6	Bioactivity of Janthitrem	235
	7.6.1 <i>Mice Testing</i>	235
	7.6.2 <i>Insect Testing</i>	237
7.7	LC–UV–MS Investigations	237
	7.7.1 <i>APCI vs. ESI</i>	237
	7.7.2 <i>Positive Ion Analysis</i>	238
	7.7.3 <i>Negative Ion Analysis</i>	238
7.8	Mouldy Walnuts Investigation	239
7.9	Conclusion	240
7.10	Future Work	241
Chapter Eight	Experimental	242
8.1	Screening of Cultures	242
	8.1.1 <i>Culturing</i>	242
	8.1.2 <i>Extraction</i>	242
	8.1.3 <i>LC –UV –MS</i>	243
8.2	Isolation of Janthitrem A and Janthitrem B	244
	8.2.1 <i>Culturing</i>	244
	8.2.2 <i>Extraction</i>	244
	8.2.3 <i>Flash Column Chromatography</i>	244
	8.2.4 <i>TLC</i>	245
	8.2.5 <i>Analytical HPLC</i>	245
	8.2.6 <i>De-fatting of Samples</i>	245
	8.2.7 <i>Flash Column Chromatography 2</i>	246
	8.2.8 <i>Solid Phase Extraction</i>	246
	8.2.9 <i>Semi-preparative HPLC</i>	246
	8.2.10 <i>HRMS</i>	247
	8.2.11 <i>NMR</i>	247
	8.2.12 <i>Molecular Modelling</i>	247
8.3	Isolation of Janthitrem C and Janthitrem D	248
	8.3.1 <i>De-fatting of Samples</i>	248
	8.3.2 <i>Flash Column Chromatography</i>	248

8.3.3	<i>TLC</i>	248
8.3.4	<i>NMR</i>	249
8.4	Stability Trial	249
8.5	LC–UV–MS Analysis	251
8.5.1	<i>APCI vs. ESI</i>	251
8.5.2	<i>APCI Vapouriser Temperatures</i>	252
8.5.3	<i>Positive Ion Analyses</i>	252
8.5.4	<i>Negative Ion Analyses</i>	252
8.6	Assessment of Tremorgenicity, Heart Rate, Blood Pressure and Motor Control on Mice Dosed with Janthitrems A and B	253
8.6.1	<i>Mouse Bioassay</i>	253
8.6.2	<i>Tremor Score</i>	254
8.6.3	<i>Blood Pressure and Heart Rate</i>	254
8.6.4	<i>Motor Control</i>	255
8.7	Insect Testing	256
8.7.1	<i>Stability of the Test Mycotoxins</i>	256
8.7.2	<i>Diets Prepared with the Inclusion of the Test Mycotoxins</i>	257
8.7.3	<i>Diets Prepared with the Inclusion of Endophyte-Free and AR37-Infected Ryegrass</i>	257
8.7.4	<i>Insect Bioassay Trial</i>	258
8.8	Analysis of Mouldy Walnuts	259
8.8.1	<i>Culturing and Isolation of Fungus from the Mouldy Walnuts</i>	259
8.8.2	<i>Toxin Extraction</i>	260
8.8.3	<i>LC–UV–MS Analysis</i>	260
8.8.4	<i>LC–UV–MS Method Validation</i>	261
	References	262
	Appendix	277
Appendix 1	Published account of mouldy walnuts investigation.	278
Appendix 2	Poster presented at the 6th International Symposium on Fungal Endophytes of Grasses, 2007.	281

List of Figures

	Page
1.1 A sheep affected by ryegrass staggers.	2
1.2 Comparison of endophyte-free perennial ryegrass (left) to endophyte-infected perennial ryegrass (right). The damage to the endophyte-free ryegrass was inflicted by the Argentine stem weevil. Photo courtesy of AgResearch, Ruakura.	5
1.3 Argentine stem weevil. Photo courtesy of AgResearch, Ruakura.	5
1.4 Peramine.	6
1.5 Comparison of (a) endophyte-infected and (b) endophyte-free grass, (Scharidl et al., 2007).	6
1.6 Ergovaline.	10
1.7 Structures of loline, <i>N</i> -formylloline, <i>N</i> -acetylloline, <i>N</i> -methylloline, norloline, <i>N</i> -acetylnorloline and <i>N</i> -formylloline.	11
1.8 Lysergic acid amide.	12
1.9 Structures of penitrems A–F.	14
1.10 Structures of penitrem G, secopenitrem B, 10-oxo-11,33-dihydropenitrem B and 6-bromopenitrem E.	16
1.11 Structures of pennigritrem, penitremones A–C and thomitrems A and E.	18
1.12 Structure of lolitrem B.	19
1.13 Structures of lolitrems A, E, F, G, H, J, K, L, M and N.	20
1.14 Structures of lolilline, lolitriol, lolicines A and B, and 31- <i>epi</i> -lolitrems F and N.	21
1.15 Structures of paspaline, paspaline B, paspalicine, 14 α -hydroxypaspalinine, paspalinine and paspalitrems A, B and C.	23
1.16 Structures of paxilline, 13-desoxypaxilline, paxilline-27- <i>O</i> -acetate, 7-hydroxy-13-desoxypaxilline, PCM5', PCM6 and paxinorol.	25
1.17 Structure of 21-isopentenylpaxilline.	26
1.18 Structures of terpendoles A–M.	27
1.19 Structures of sulphinines A–C.	29
1.20 Structures of shearinines A–K.	30
1.21 Structures of emindoles SA, SB, DA and DB.	31

1.22	Structures of emindoles PA, PB and PC and emeniveol.	32
1.23	Aflatrem.	33
1.24	Structures of janthitrems B and C.	34
1.25	Structures of janthitrems E–G.	34
1.26	10- <i>epi</i> -11,12-epoxyjanthitrem G.	36
1.27	Proposed biosynthetic pathway for the early stages of indole–diterpenoid biosynthesis.	37
2.1	Screening of <i>P. janthinellum</i> cultures.	45
2.2	LC–MS chromatograms of E1 and E2 and penitrem A standard. Values of m/z for $[M+H]^+$ are given above their corresponding peaks.	49
2.3	The isolation of janthitrem A and janthitrem B.	52
2.4	Full scan mass spectrum of the minor later-eluting peak. Values of m/z for major ions observed are given.	53
2.5	Full scan mass spectrum of the major early-eluting peak. Values of m/z for major ions observed are given.	54
2.6	Normalised UV absorbance spectra of minor (red) and major (black) peaks.	54
2.7	Structures of janthitrem B and 11,12-epoxyjanthitrem B.	56
2.8	Isolation of janthitrem C and janthitrem D.	59
2.9	Full scan mass spectrum of fractions 14–18. Values of m/z for major ions observed are given.	60
2.10	Full scan mass spectrum of fractions 10–13. Values of m/z for major ions observed are given.	61
2.11	Normalised UV absorbance spectra of fractions 14–18 (red) and fractions 10–13 (black).	61
2.12	Structures of janthitrem C and 11,12-epoxyjanthitrem C.	63
2.13	Graph displaying stability properties of tested conditions.	67
3.1	Numbered structures for janthitrems A–D, penitrem A and shearinine D.	70
3.2	The COSY NMR spectrum of janthitrem B.	75
3.3	The TOCSY NMR spectrum of janthitrem B.	75
3.4	The g-HSQC NMR spectrum of janthitrem B.	79
3.5	The g-HMBC NMR spectrum of janthitrem B.	79
3.6	Selected g-HMBC correlations observed for H-37 and H-39 of janthitrem B.	80

3.7	Selected g-HMBC correlations observed for H-38 and H-40 of janthitrem B.	80
3.8	The NOESY NMR spectrum of janthitrem B.	83
3.9	NOESY correlations observed for H-37 (black), H-38 (green), H-39 (red) and H-40 (blue) of janthitrem B.	84
3.10	NOESY correlations observed for H-5 α (black) and H-5 β (blue) of janthitrem B.	85
3.11	NOESY correlations observed for H-6 α (black) and H-6 β (blue) of janthitrem B.	86
3.12	NOESY correlations observed for H-14 α (black) and H-14 β (blue) of janthitrem B.	87
3.13	NOESY correlations observed for H-15 α (black) and H-15 β (blue) of janthitrem B.	87
3.14	NOESY correlations observed for H-17 α (black) and H-17 β (blue) of janthitrem B.	88
3.15	NOESY correlations observed for H-29E and H-29Z of janthitrem B.	89
3.16	NOESY correlations observed for H-20 (blue) and H-23 (red) of janthitrem B.	90
3.17	NOESY correlations observed for H-5 α (black) and H-5 β (blue) of janthitrem A.	102
3.18	NOESY correlations observed for H-6 α (black) and H-6 β (blue) of janthitrem A.	102
3.19	NOESY correlations observed for H-14 α (black) and H-14 β (blue) of janthitrem A.	103
3.20	NOESY correlations observed for H-15 α (black) and H-15 β (blue) of janthitrem A.	104
3.21	NOESY correlations observed for H-17 α (black) and H-17 β (blue) of janthitrem A.	104
3.22	NOESY correlations observed for H-29E and H-29Z of janthitrem A.	105
3.23	NOESY correlations observed for H-37 (black), H-38 (green), H-39 (red) and H-40 (blue) of janthitrem D.	126
3.24	NOESY correlations observed for H-5 α (black) and H-5 β (blue) of janthitrem D.	127
3.25	NOESY correlations observed for H-6 α (black) and H-6 β (blue) of janthitrem D.	128
3.26	NOESY correlations observed for H-14 α (black) and H-14 β (blue) of janthitrem D.	129

3.27	NOESY correlations observed for H-15 α (black) and H-15 β (blue) of janthitrem D.	129
3.28	NOESY correlations observed for H-17 α (black) and H-17 β (blue) of janthitrem D.	130
3.29	NOESY correlations observed for H-30 α (black) and H-30 β (blue) of janthitrem D.	131
3.30	NOESY correlations observed for H-29E and H-29Z of janthitrem D.	132
4.1	LC–UV–MS spectrum of penitrem A (ESI) at 233 nm (upper profile) and m/z 634, [M+H] ⁺ (lower profile).	138
4.2	LC–UV–MS spectrum of penitrem A (APCI) at 233 nm (upper profile) and m/z 634, [M+H] ⁺ (lower profile).	138
4.3	250°C APCI mass spectrum. Values of m/z for major ions observed are given.	139
4.4	300°C APCI mass spectrum. Values of m/z for major ions observed are given.	139
4.5	350°C APCI spectrum. Values of m/z for major ions observed are given.	140
4.6	400°C APCI spectrum. Values of m/z for major ions observed are given.	141
4.7	450°C APCI spectrum. Values of m/z for major ions observed are given.	142
4.8	Loss of acetone in janthitrems A–D.	144
4.9	Fragmentation of janthitrem A in positive ion MS ² and MS ³ spectra.	145
4.10	Fragmentation of janthitrem B in positive ion MS ² and MS ³ spectra (ESI).	146
4.11	Fragmentation of janthitrem B in positive ion MS ² and MS ³ spectra (APCI).	147
4.12	Retro Diels–Alder rearrangement of janthitrem B involving formation of an enol group which equilibrates to the corresponding aldehyde form.	147
4.13	Fragmentation of janthitrem C in positive ion MS ² and MS ³ spectra (ESI).	149
4.14	Fragmentation of janthitrem C in positive ion MS ² and MS ³ spectra (APCI).	149
4.15	Fragmentation of janthitrem D in positive ion MS ² and MS ³ spectra.	150
4.16	Structures of penitrems A–F.	153

4.17	Fragmentation of penitrems A and E in positive ion MS ² , MS ³ and MS ⁴ spectra.	155
4.18	Fragmentation of penitrems B and F in positive ion MS ² , MS ³ and MS ⁴ spectra.	157
4.19	Fragmentation of penitrems C and D in positive ion MS ² , MS ³ and MS ⁴ spectra.	159
4.20	Fragmentation of lolitrem B in positive ion MS ² and MS ³ spectra (ESI).	160
4.21	Fragmentation of lolitrem B in positive ion MS ² and MS ³ spectra (APCI).	161
4.22	Fragmentation of paxilline in positive ion MS ² and MS ³ spectra (ESI).	162
4.23	Fragmentation of paxilline in positive ion MS ² and MS ³ spectra (APCI).	163
4.24	Fragmentation of terpendole C in positive ion MS ² and MS ³ spectra (ESI).	164
4.25	Fragmentation of terpendole C in positive ion MS ² and MS ³ spectra (APCI).	165
4.26	Fragmentation of paspalinine in positive ion MS ² and MS ³ spectra (ESI).	166
4.27	Fragmentation of paspalinine in positive ion MS ² and MS ³ spectra (APCI).	167
4.28	Full scan negative ion spectrum of janthitrem B.	169
4.29	Full scan negative ion spectrum of terpendole C.	169
4.30	Full scan negative ion spectrum of janthitrem B with SID.	170
4.31	Full scan negative ion spectrum of terpendole C with SID.	170
4.32	Ions generated through loss of acetone from janthitrems A–D.	171
4.33	Janthitrem A full scan negative ion mass spectrum.	172
4.34	Janthitrem A negative ion MS ² spectrum (<i>m/z</i> 600).	172
4.35	Janthitrem A negative ion MS ³ spectrum (<i>m/z</i> 600 → <i>m/z</i> 582).	172
4.36	Fragmentation of janthitrem A in negative ion MS ² and MS ³ spectra.	173
4.37	Janthitrem B full scan negative ion mass spectrum.	173
4.38	Janthitrem B negative ion MS ² spectrum (<i>m/z</i> 584).	174
4.39	Janthitrem B negative ion MS ³ spectrum (<i>m/z</i> 584 → <i>m/z</i> 526).	174
4.40	Fragmentation of janthitrem B in negative ion MS ² and MS ³ spectra.	175

4.41	Retro Diels–Alder rearrangement of janthirem B involving formation of an enol group which equilibrates to the corresponding aldehyde form.	175
4.42	Fragmentation of janthirem C in negative ion MS ² and MS ³ spectra.	176
4.43	Fragmentation of janthirem D in negative ion MS ² and MS ³ spectra.	177
4.44	Penitrem A full scan negative ion mass spectrum.	179
4.45	Penitrem A negative ion MS ² spectrum (<i>m/z</i> 632).	179
4.46	Penitrem A negative ion MS ³ spectrum (<i>m/z</i> 632 → <i>m/z</i> 546).	179
4.47	Fragmentation of penitrems A and E in negative ion MS ² and MS ³ spectra.	180
4.48	Penitrem C full scan negative ion mass spectrum.	181
4.49	Penitrem C negative ion MS ² spectrum (<i>m/z</i> 600).	181
4.50	Penitrem C negative ion MS ³ spectrum (<i>m/z</i> 600 → <i>m/z</i> 514).	181
4.51	Fragmentation of penitrems C and D in negative ion MS ² and MS ³ spectra.	182
4.52	Penitrem F full scan negative ion mass spectrum.	183
4.53	Penitrem F negative ion MS ² spectrum (<i>m/z</i> 616).	183
4.54	Penitrem F negative ion MS ³ spectrum (<i>m/z</i> 616 → <i>m/z</i> 486).	183
4.55	Fragmentation of penitrems B and F in negative ion MS ² and MS ³ spectra.	184
4.56	Lolitrem B full scan negative ion mass spectrum.	185
4.57	Lolitrem B negative ion MS ² spectrum (<i>m/z</i> 684).	185
4.58	Lolitrem B negative ion MS ³ spectrum (<i>m/z</i> 684 → <i>m/z</i> 470).	186
4.59	Fragmentation of lolitrem B in negative ion MS ² and MS ³ spectra.	187
4.60	Fragmentation of paxilline in negative ion MS ² and MS ³ spectra.	188
4.61	Fragmentation of terpendole C in negative ion MS ² and MS ³ spectra.	189
4.62	Fragmentation of paspalinine in negative ion MS ² and MS ³ spectra.	191
5.1	The rotamex 4 rotarod.	194
5.2	The BP-2000 blood pressure and heart rate measurement instrument.	195

5.3	Mean tremor score vs time post-injection for mice dosed i.p. with janthitrem A (n = 4), janthitrem B (n = 4) and their respective controls (n = 4).	196
5.4	Mean heart rate vs time post-injection for mice dosed i.p. with janthitrem A (n = 4), janthitrem B (n = 4) and their respective controls (n = 4).	197
5.5	Mean systolic pressure vs time post-injection for mice dosed i.p. with janthitrem A (n = 4), janthitrem B (n = 4) and their respective controls (n = 4).	198
5.6	Mean diastolic pressure vs time post-injection for mice dosed i.p. with janthitrem A (n = 4), janthitrem B (n = 4) and their respective controls (n = 4).	199
5.7	Mean rotarod score vs time post-injection for mice dosed i.p. with janthitrem A (n = 4), janthitrem B (n = 4) and their respective controls (n = 4).	200
5.8	Mean rotarod scores expressed as a percentage of the score at t = 0 vs time post-injection for mice dosed i.p. with janthitrem A (n=4), janthitrem B (n=4) and their respective controls (n=4).	201
5.9	Structures of lolitrem B, janthitrem A, janthitrem B, paspalinine, terpendole C, paxilline and lolilline.	203
5.10	Comparison of mean tremor scores vs time post-injection for mice dosed i.p. with janthitrem A (n = 4), janthitrem B (n = 4), lolitrem B (Munday-Finch, 1997) and paxilline (Munday-Finch, 1997).	204
5.11	Porina (<i>Wiseana cervinata</i>) larva. Photo courtesy of AgResearch, Ruakura.	207
5.12	a) Transfer of the prepared diet with the test mycotoxin into a petri dish and b) allowing the prepared diets for each treatment to cool.	209
5.13	Specimen containers placed in a controlled environment room.	211
5.14	Percentage of diet eaten by the porina for each treatment.	213
6.1	The collected mouldy walnuts.	217
6.2	a) Extraction of the fungus. b) Inoculation of the media with the fungus. c) The inoculated culture flasks. d) Incubation of the cultures.	218
6.3	Calibration curve for five penitrem A standards obtained from the mass spectrometer (using an APCI source). The error bars representing the relative standard deviation are too small to be visible.	220
6.4	Calibration curve for five penitrem A standards obtained from the PDA (at 296 nm). The error bars representing the relative standard deviation are too small to be visible.	220

6.5	LC–MS chromatogram of <i>P. crustosum</i> . Values of m/z for $[M+H]^+$ are given above their corresponding peaks.	222
6.6	LC–MS chromatogram of the mouldy walnut extract. Values of m/z for $[M+H]^+$ are given above their corresponding peaks.	223
6.7	Full scan of penitrem A peak from <i>P. crustosum</i> . Values of m/z for major ions observed are given.	224
6.8	MS ² (m/z 634) spectrum of penitrem A peak from <i>P. crustosum</i> . Values of m/z for major ions observed are given.	224
6.9	MS ³ (m/z 634→558) spectrum of penitrem A peak from <i>P. crustosum</i> . Values of m/z for major ions observed are given.	224
6.10	UV absorbance spectrum of penitrem A.	225
7.1	The structural inter-relationship between the janthitrems.	234
7.2	Structure of janthitrems A–G.	234

List of Tables

	Page
2.1 Penitrems and janthitrems detected in each strain of <i>P. janthinellum</i> .	48
2.2 ^{13}C NMR resonances observed for janthitrem B and the unknown janthitrem analogue and published assignments for penitrem A ^a (δ).	56
2.3 ^{13}C NMR resonances observed for janthitrem A, janthitrem C and the unknown janthitrem analogue (δ).	62
2.4 Conditions used to monitor the stability of janthitrem B.	66
2.5 Test conditions ranked based on percentage of janthitrem B degraded. Unless otherwise stated, samples were stored at room temperature (20°C).	68
3.1 ^1H and ^{13}C NMR assignments established for janthitrems A and B and published assignments for penitrem A ^a (δ).	73
3.2 COSY NMR correlations observed for janthitrem B (δ).	76
3.3 TOCSY NMR correlations observed for janthitrem B (δ).	77
3.4 Long-range ^{13}C - ^1H NMR correlations observed in the g-HMBC NMR spectrum of janthitrem B (δ).	81
3.5 NOESY NMR correlations observed for janthitrem B (δ).	90
3.6 COSY NMR correlations observed for janthitrem A (δ).	97
3.7 TOCSY NMR correlations observed for janthitrem A (δ).	98
3.8 Long-range ^{13}C - ^1H NMR correlations observed in the g-HMBC NMR spectrum of janthitrem A (δ).	100
3.9 NOESY NMR correlations observed for janthitrem A (δ).	106
3.10 ^1H and ^{13}C NMR assignments established for janthitrem C and published assignments for janthitrem C ^a (δ).	109
3.11 COSY NMR correlations observed for janthitrem C (δ).	115
3.12 TOCSY NMR correlations observed for janthitrem C (δ).	116
3.13 Long-range ^{13}C - ^1H NMR correlations observed in the g-HMBC NMR spectrum of janthitrem C (δ).	117
3.14 ^1H and ^{13}C NMR assignments established for janthitrem D (δ).	120
3.15 COSY NMR correlations observed for janthitrem D (δ).	123
3.16 TOCSY NMR correlations observed for janthitrem D (δ).	124

3.17	Long-range ^{13}C - ^1H NMR correlations observed in the HMBC NMR spectrum of janthitrem D (δ).	125
3.18	NOESY NMR correlations observed for janthitrem D.	132
4.1	% UV versus APCI or ESI $[\text{M}+\text{H}]^+$ peak area responses.	137
4.2	Ions observed in MS spectra of penitrems A–F under positive ion conditions.	153
4.3	Ions observed in full scan, MS^2 and MS^3 spectra of penitrems A–F under negative ion conditions.	178
5.1	Tremorgenic activity of the tested janthitrems.	202
5.2	Mycotoxin recovered (as a percentage of that added) from diets at time zero and after 24 hours.	208
5.3	Prepared bioassay diets with the test mycotoxin/ryegrass.	210
5.4	Results of the insect bioassay.	212
6.1	Comparison of the reference concentration and the average experimental concentration for penitrem A.	222
6.2	Comparison of penitrem production in the mouldy walnuts and <i>P. crustosum</i> extracts.	227
8.1	Conditions used to monitor the stability of janthitrem B.	249
8.2	The visual rating scale for tremor assessment.	254

Abbreviations

α	alpha (lower face)
β	beta (upper face)
$^{\circ}\text{C}$	degrees Celsius
δ	delta
>	greater than
<	less than
%	percent
1J	one bond NMR coupling constant
2J	two bond NMR coupling constant
3J	three bond NMR coupling constant
4J	four bond NMR coupling constant
APCI	atmospheric pressure chemical ionisation
bpm	beats per minute
<i>ca.</i>	approximately
calc.	calculated
CDCl_3	deuteriochloroform
CE	collision energy
CIP	Cahn–Ingold–Prelog
COSY	correlated spectroscopy
cv.	cultivated variety
dd	doublet of doublets
DEPT	distortionless enhancement by polarisation transfer
DMSO	dimethylsulphoxide
<i>E</i>	<i>entgegen</i>
e.g.	for example
ESI	electrospray ionisation

et al.	and others
GABA	γ -aminobutyric acid
GGDP	geranylgeranyl diphosphate
g-HMBC	gradient selected heteronuclear multiple bond correlation
g-HSQC	gradient selected heteronuclear single quantum coherence
HPLC	high performance liquid chromatography
HRMS	high resolution mass spectrometry
Hz	Hertz
i.e.	as in
i.p.	intraperitoneally
i.v.	intravenous
kg	kilogram
L	litre
LC	liquid chromatography
LC-MS	liquid chromatography mass spectrometry
LC-UV-MS	liquid chromatography ultra-violet mass spectrometry
LSD	lysergic acid diethylamide
mL	millilitre
μ L	microlitre
μ g	microgram
μ m	micrometer
mg	milligram
$[M-H]^-$	molecular ion (negative ion detection)
$[M+H]^+$	molecular ion (positive ion detection)
m/z	mass/charge ratio
Me	methyl
MHz	mega Hertz

min	minutes
ms	millisecond
MS	mass spectrometry
nm	nanometer
NMR	nuclear magnetic resonance
NOE	nuclear Overhauser effect
NOESY	nuclear Overhauser effect spectroscopy
<i>p</i>	probability
PDA	photodiode array
PDD	Plant Diseases Division
ppm	parts per million
q	quartet
RDA	retro Diels–Alder
rpm	revolutions per minute
RSD	relative standard deviation
s	singlet
sec	seconds
SID	source-induced dissociation
sp	species
t	triplet
TLC	thin layer chromatography
TOCSY	total correlation spectroscopy
UV	ultra-violet
V	volts
v/v	volume per volume
XHCOR	X–H correlated
Z	<i>zusammen</i>

CHAPTER ONE

Introduction

1.1 Perennial Ryegrass Staggers

Perennial ryegrass staggers (hereafter referred to as ryegrass staggers) is a nervous disorder affecting animals such as sheep, cattle, horses and deer (Armstrong, 1956; Cunningham and Hartley, 1959; Galey et al., 1991; Hunt et al., 1983; Mackintosh et al., 1982; Mitchell and McCaughan, 1992; Munday et al., 1985; Odriozola et al., 1993) that graze perennial ryegrass (*Lolium perenne* L.) pastures infected with the endophyte *Neotyphodium lolii*. The disease is most prevalent in New Zealand and Australia (Armstrong, 1956; Cunningham and Hartley, 1959; di Menna et al., 1976; Fink-Gremmels and Blom, 1994; Mitchell and McCaughan, 1992; Munday et al., 1985) but has also been reported in the United Kingdom (Clegg and Watson, 1960), United States (Galey et al., 1991; Hunt et al., 1983), Argentina (Odriozola et al., 1993) and the Netherlands (Fink-Gremmels and Blom, 1994).

The name ryegrass staggers was so given due to the staggering gait of affected animals when grazing perennial ryegrass dominant pastures (Figure 1.1) (Cunningham and Hartley, 1959; Gilruth, 1906). The symptoms of ryegrass staggers include severe muscular incoordination and hypersensitivity to external stimuli such as sunlight and loud noises. These symptoms can be observed one to two weeks after initial exposure which begins as tremors of the head, neck and shoulders, progressing to head nodding and uncoordinated limb jerking. The condition (which is prevalent in autumn) is rarely fatal, however, deaths from misadventure (such as falling from a cliff) can occur.



Figure 1.1. A sheep affected by ryegrass staggers.

Perennial ryegrass staggers is estimated to cost New Zealand \$100 million a year as a result of lost animal production (AgResearch, 2005). Ryegrass staggers can cause decreased weight gain in livestock (Fletcher and Barrell, 1984) and increased time and labour for feeding, moving, shearing and drenching affected animals. Ryegrass staggers also severely impacts farm management where movement of affected animals can be a major issue.

Ryegrass staggers is caused by tremorgenic mycotoxins that are present in ryegrass plants infected with the endophytic fungus *Neotyphodium lolii* (formerly known as *Acremonium lolii*). This fungus is termed an endophyte as it is an organism which resides within the plant tissue (Cheeke, 1995). Though it was realised that fungal tremorgens were the cause of ryegrass staggers in the 1980s, it took many years of research to establish and substantiate this finding.

1.2 History of Ryegrass Staggers

A connection between the endophyte of ryegrass and animal toxicity was first investigated by Neill (1941). Sparrows, chickens, rats and mice were fed ground ryegrass seeds, but tremors were not observed (Cunningham, 1958; Neill, 1941).

This experimental observation along with the belief held by Neill that “a widely distributed fungus such as the *Lolium* endophyte could not be responsible for localised outbreaks of ryegrass staggers” (Cunningham and Hartley, 1959), subsequently led to the conclusion that the endophyte was not the cause of ryegrass staggers. Keogh (1973) made the important discovery that sheep forced to graze the base of pastures were affected by ryegrass staggers whereas sheep grazing longer pastures did not suffer the disorder. Consequently, soil-borne fungi, which would be consumed by sheep grazing short pastures, were considered as a possible cause of ryegrass staggers.

Sheep and calves orally dosed with the homogenised mycelium of *Penicillium cyclopium* (a fungus which occurs in New Zealand soils) produced symptoms similar to ryegrass staggers (di Menna et al., 1976). Clinical symptoms were also reproduced by Gallagher et al. (1977) when *Penicillium* species (isolated from perennial ryegrass pastures and the excrement of affected animals) were cultured and fed to animals. Further reports (di Menna and Mantle, 1978; Mantle et al., 1977; Mantle et al., 1978; Shreeve et al., 1978) of fungi isolated from soils producing tremorgenic toxins substantiated the finding of Gallagher et al. (1977). However, contrary to this reasoning, White et al. (1980) reported that the quantity of soil ingested by the animal was unlikely to yield sufficient tremorgens to cause ryegrass staggers. A possible explanation was that the tremorgens produced by the fungi in the soil could be absorbed by the roots of the plant and then translocated into the leaves. This theory was strengthened by experimental evidence where extracts of plants grown in sand containing *Penicillium crustosum* mycelium were found to be tremorgenic in contrast to the control plant extracts which were non-tremorgenic (White et al., 1980).

Tremorgens such as penitrem A, fumitremorgins A and B, janthitrems A–C and verruculogen were found in pastures where ryegrass staggers had been reported

(Gallagher et al., 1980a). These studies indicated that fungal tremorgens may be the cause of ryegrass staggers.

In 1981, an experimental trial to measure hogget growth on three different perennial ryegrass cultivars was carried out. During drought conditions a 100% incidence of ryegrass staggers was observed on one plot, 50% on another and no incidence on the other plot. The three plots were subsequently extensively compared which showed a strong correlation between the percentage of endophyte infection and the severity of ryegrass staggers (Fletcher and Harvey, 1981; Mortimer et al., 1982). Fletcher and Harvey (1981) reinforced this finding with the observation that the endophyte was concentrated in the base of the plant. Gallagher et al. (1981) examined the grass which had caused ryegrass staggers and identified two compounds (lolitrems A and B) which were tremorgenic to mice. A year later Gallagher et al. (1982a) showed that feeding sheep with lolitrem-containing seeds gave clinical signs that were indistinguishable from ryegrass staggers. These results indicated that lolitrems were involved in ryegrass staggers.

Further studies showed a correlation between the presence of lolitrems and endophyte infection (Gallagher et al., 1982b). Consequently, it was believed that removal of the endophyte from ryegrass would resolve the ryegrass staggers issue. However, it soon became evident that removal of the endophyte would not be the answer, as trials conducted on endophyte-free and endophyte-infected ryegrass pastures showed that endophyte-free ryegrass had little growth and severe damage (Figure 1.2) due to the larvae of the Argentine stem weevil (*Listronotus bonariensis*) (Figure 1.3) (Mortimer and di Menna, 1983; Mortimer et al., 1982).



Figure 1.2. Comparison of endophyte-free perennial ryegrass (left) to endophyte-infected perennial ryegrass (right). The damage to the endophyte-free ryegrass was inflicted by the Argentine stem weevil. Photo courtesy of AgResearch, Ruakura.

The damage to pastures by the Argentine stem weevil was estimated in 1991 to cost New Zealand \$46–200 million per year (Prestidge et al., 1991).



Figure 1.3. Argentine stem weevil. Photo courtesy of AgResearch, Ruakura.

It was subsequently shown that in addition to the tremorgens, the endophyte also produced peramine. Peramine (Figure 1.4), isolated by Rowan and Gaynor (1986), is known to be responsible for insecticidal activity. The concentration of peramine was found to be greater in the younger compared to older leaves of ryegrass tillers (Keogh et al., 1996). During seed germination, peramine moves

through to the developing seedling protecting it against insect activity until the post-germination endophyte activity starts to generate new peramine (Ball et al., 1993).

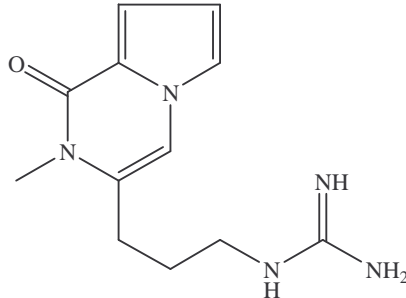


Figure 1.4. Peramine.

1.2.1 The Advantages and Disadvantages of Endophyte-Infected Perennial Ryegrass

The plant–fungus association produces a number of compounds, some of which are beneficial and some detrimental to agriculturists.

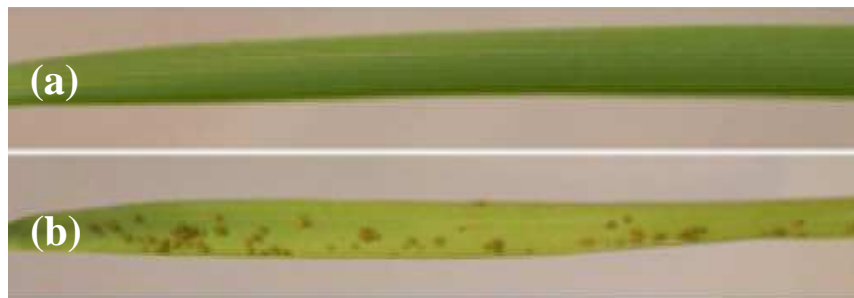


Figure 1.5. Comparison of (a) endophyte-infected and (b) endophyte-free grass, (Schardl et al., 2007).

In addition to causing ryegrass staggers, other compounds produced by the endophyte–grass association give the host plant increased survival under climatic stress, reduced insect attack, produce more herbage and persist longer in grazing pastures (Figure 1.5). For example, peramine deters feeding and egg deposition

by larval and adult Argentine stem weevil (Ball et al., 1993; Mortimer and di Menna, 1983; Prestidge and Ball, 1993; Prestidge et al., 1982).

1.2.2 Options for Control of Ryegrass Staggers

Ryegrass staggers is more prevalent in sheep, deer and horses compared to cattle as these animals graze closer to the base of the plant thereby ingesting more basal sheath material (as the tremorgens are concentrated at the base of the plant). Furthermore, outbreaks of ryegrass staggers mainly occur during summer and autumn where reduced pasture growth leads to consumption of a greater portion of the basal area of the plant. Because ryegrass staggers is a reversible condition and complete recovery of the animal is possible, moves were made to put practices in place to minimise the occurrence of ryegrass staggers. Such practices included “diluting” the amount of endophyte-infected perennial ryegrass by growing companion grass species such as white clover (*Trifolium repens*).

Grazing management can minimise ryegrass staggers by restricting consumption of the basal plant material. However, this practice is difficult when the grass is in short supply, and also when the animal is suffering from the disease as movement of the animal will be difficult. Another option is to breed animal resistance to ryegrass staggers. Ryegrass staggers is a heritable trait (Campbell, 1986) and therefore resistance to the disease can be increased by breeding from rams which are not prone to the disease.

In addition to having such practices in place, research has been carried out to resolve the endophyte-related disorders by identifying endophyte types which vary in toxin production. Research has focused on discovering and developing endophytes which produce the beneficial compounds without the detrimental ones. Such endophytes would confer resistance to insect pests such as the

Argentine stem weevil without inducing toxic effects on livestock. These endophytes (termed “novel” endophytes) aim to reduce the negative effects on stock health while maintaining the benefits.

1.3 Toxicoses Associated with Grasses Infected with Endophytic Fungi

The grass–endophyte interaction is mutualistic as both the plant and the fungus receive benefits (Scott and Schardl, 1993). The plant provides the fungus with a suitable environment and the fungus protects this environment by producing the protective chemicals i.e. mycotoxins. The grass–endophyte interaction can produce compounds which are beneficial for plant growth and persistence, however, this interaction can also produce compounds which can be deleterious to the health of the animal which graze the infected pastures. These detrimental compounds are responsible for a number of conditions such as tall fescue toxicosis (caused by tall fescue infected with the endophyte *Neotyphodium coenophialum*) and ryegrass staggers (caused by *N. lolii*).

1.3.1 Ryegrass Staggers

As discussed in Sections 1.1 and 1.2, *Neotyphodium lolii*-infected perennial ryegrass is associated with ryegrass staggers.

1.3.2 Tall Fescue Toxicosis

Tall fescue infected with the endophyte *Acremonium coenophialum* (more recently classified as *Neotyphodium coenophialum*) is a popular pasture forage and covers approximately 35 million acres in the USA and Canada (Blodgett, 2001). Its popularity is due to its ease of establishment, wide range of adaptation,

pest resistance, tolerance to abuse and good seed production (Hoveland, 1993). However, tall fescue has also been associated with poor animal performance. Beef calf gains and cow conception rates were found to be substantially lower on tall fescue compared to tall fescue–legume (i.e. tall fescue pasture diluted with legumes) (Petritz et al., 1980). The pregnancy rate of heifers on highly infected endophyte tall fescue was only 55% compared to 96% on tall fescue infected with low levels of endophyte (Schmidt, 1986). In addition, lower milk production (Seath et al., 1956) and poor animal performance (Hemken et al., 1979) in cows have also been observed. At one stage tall fescue toxicosis was estimated to cost the US beef industry \$600 million per annum (Hoveland, 1993).

Symptoms of tall fescue toxicosis include decreased serum prolactin (a hormone which is necessary for mammary development and milk production), agalactia (decreased milk production) and reproduction problems (Hemken and Bush, 1989; Hemken et al., 1984). Reproduction problems include prolonged gestation, inhibition of mammary gland development, thickened placentas and affected fertility (Meerdink, 2002). Removal of pregnant mares from affected pastures leads to improvement/elimination of symptoms depending on the time of removal (Meerdink, 2002).

Tall fescue toxicosis is also responsible for fescue foot and summer syndrome. Fescue foot, which occurs mainly in cattle, is a gangrenous condition affecting the extremities such as the feet, ears and tail (van Heeswijck and McDonald, 1992). Summer syndrome is a condition which as the name suggests occurs during summer and is associated with reduced weight gain, decreased milk production, increased respiration, excessive salivation and fever (van Heeswijck and McDonald, 1992). The compounds responsible for summer syndrome and fescue foot are the ergot alkaloids (particularly ergovaline (Figure 1.6)) which are produced by the endophyte–grass association. Ergovaline has also been found in

endophyte-infected ryegrass (Rowan and Shaw, 1987) accounting for reports of heat stress in livestock (Easton et al., 1996; Sutherland, 1984). Ergovaline may also interact with lolitrem B to exacerbate ryegrass staggers (Fletcher and Easton, 1997).

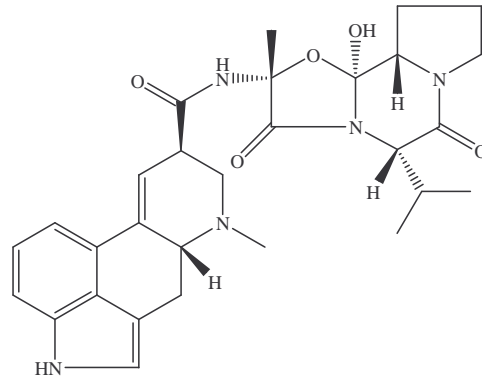


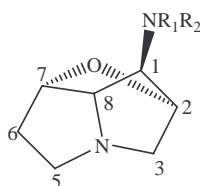
Figure 1.6. Ergovaline.

Although removal of endophytes is easy, nil endophyte fescue is not an option as the endophyte produces other compounds which provide benefits such as good pasture growth, pest resistance, tolerance to abuse and the ability to establish itself in a range of conditions. These benefits are provided by the loline alkaloids.

Lolines are alkaloids which deter insect feeding and have insecticidal properties (Bush et al., 1993; Wilkinson et al., 2000). Lolines were originally isolated from *Lolium cuneatum* Nevski (Gramineae) (Yunusov and Akramov, 1955). Lolines are saturated pyrrolizidines comprising an oxygen bridge between C-2 and C-7 (Faulkner et al., 2006; Powell and Petroski, 1992). An amino group is located at C-1 and the various types of lolines are differentiated by the substituent on this amino group.

The loline-type alkaloids (Figure 1.7) include loline, norloline, *N*-methylloline, *N*-formylloline, *N*-acetylloline, *N*-formylnorloline and *N*-acetylnorloline (Faulkner

et al., 2006; Jackson et al., 1996; Petroski et al., 1994; Powell and Petroski, 1992; Yates et al., 1990).



Loline	$R_1 = H$	$R_2 = CH_3$
<i>N</i> -Formylloline	$R_1 = CHO$	$R_2 = CH_3$
<i>N</i> -Acetylloline	$R_1 = COCH_3$	$R_2 = CH_3$
<i>N</i> -Methylloine	$R_1 = CH_3$	$R_2 = CH_3$
Norloline	$R_1 = H$	$R_2 = H$
<i>N</i> -Acetylnorloline	$R_1 = COCH_3$	$R_2 = H$
<i>N</i> -Formylnorloline	$R_1 = CHO$	$R_2 = H$

Figure 1.7. Structures of loline, *N*-formylloline *N*-acetylloline, *N*-methylloline, norloline, *N*-acetylnorloline and *N*-formylloline.

The activities of these loline compounds vary, with *N*-formylloline and *N*-acetylloline appearing to have a more significant effect in insect deterrence (Powell and Petroski, 1992). The lolines are believed to be non-toxic to mammals (Schardl et al., 2007; Tong et al., 2006).

1.3.3 *Sleepygrass Toxicosis*

Sleepygrass (*Stipa robusta*) is a perennial grass found in the rangelands of southwestern USA. As a result of consumption of grass (infected with a *Neotyphodium* species), the animal exhibits a stuporous behaviour which can last for several days. In some cases the animal may even be in a state of somnolence from which they cannot be roused (Cheeke, 1995). It was initially thought diacetone alcohol

in the plant was the soporific agent (Epstein et al., 1964). However, it is now believed that ergot alkaloids produced by the endophyte are responsible.

The principle ergot alkaloid in sleepygrass was found to be lysergic acid amide (Figure 1.8) which has a sedative effect in humans and is similar in structure to the hallucinogen LSD (lysergic acid diethylamide). Analysis of grass from a sleepygrass toxicosis-affected area found the presence of a *Neotyphodium* species (Petroski et al., 1992). The level of lysergic acid amide in the endophyte-infected grass was high enough to be consistent with this being the cause of sleepygrass poisoning.

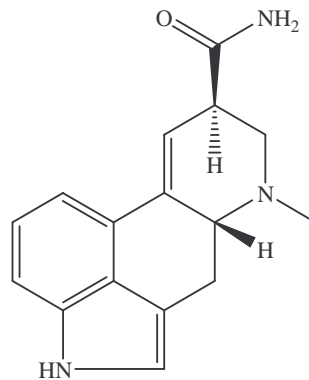


Figure 1.8. Lysergic acid amide.

1.3.4 *Drunken Horse Grass*

Drunken horse grass (*Achnatherum inebrians*) induces a condition so named due to the observed narcosis of horses grazing on pastures infected with the endophytes *Neotyphodium inebrians* and *Neotyphodium gansuense* (Wei et al., 2006). These two endophytes have been found in the seeds, leaf sheaths and peduncles of infected grass (Bruehl et al., 1994; Li et al., 2004; Wei et al., 2006). This perennial bunchgrass is predominately found on alpine and subalpine grasslands in Gansu, Xinjiang, Qinghai, Tibet and Inner Mongolia, China (Li

et al., 2008). The fungal endophytes produce the ergot alkaloids ergine (lysergic acid amide) and ergonovine (Miles et al., 1995a; 1996).

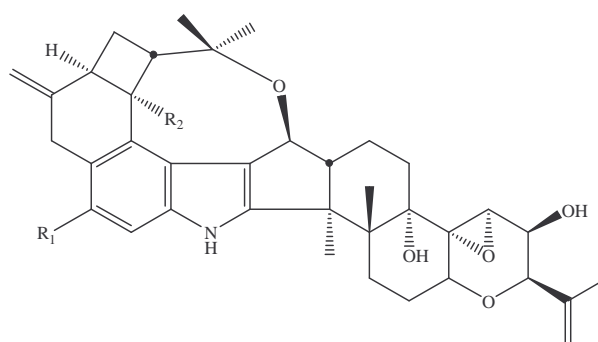
1.4 Indole–Diterpenoids

Many of the compounds responsible for toxicoses associated with endophyte-infected grasses belong to a class of compounds known as indole–diterpenoids. The indole–diterpenoids are a group of secondary metabolites (Steyn and Vleggaar, 1985) which are produced by a diverse group of fungi. Natural products known to induce tremors were rare until the discovery of fungal tremorgens.

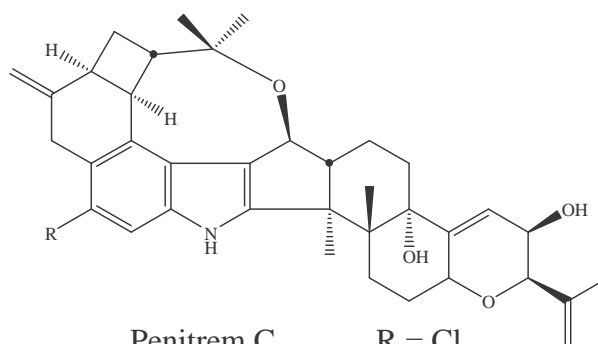
The indole–diterpenoid compounds comprise a cyclic diterpene-derived skeleton (which is derived from four isoprene units i.e. geranylgeranyl diphosphate (GGDP)) and an indole moiety (which is derived from tryptophan or a tryptophan precursor) (Laws and Mantle, 1989; Parker and Scott, 2004). The structural diversity of these metabolites is due to the different patterns of ring substitutions, different ring stereochemistry and additional prenylations (Parker and Scott, 2004). The diterpenoids have been arbitrarily classified into six groups comprising penitrems, janthitrems, lolitrems, aflatrems, paxilline and paspalinine/paspalitrems/paspaline (Steyn and Vleggaar, 1985). However, more recently new groups have been added such as the shearinines (Belofsky et al., 1995), terpendoles (Gatenby et al., 1999; Huang et al., 1995a; Huang et al., 1995b; Tomoda et al., 1995) and sulphinines (Laakso et al., 1992).

1.4.1 Penitrems

The penitrems were among one of the first classes of tremorgenic mycotoxins to be isolated. Penitrem A was first isolated in 1968 by Wilson et al. (1968) from *Penicillium cyclopium* Westling (which was later classified as *Penicillium crustosum* Thom) (Hosoe et al., 1990). The production of a tremorgenic mycotoxin by *Penicillium palitans* Westling was also reported (Ciegler, 1969) and this compound was named tremortin A (Hou et al., 1970). However, penitrem A and tremortin A were later found to be identical compounds and although the name tremortin A was reported in the literature two years prior to penitrem A, the toxin was mutually agreed to be named penitrem A. Consequently tremortins are now referred to as penitrems.



Penitrem A	$R_1 = \text{Cl}$	$R_2 = \text{OH}$
Penitrem B	$R_1 = \text{H}$	$R_2 = \text{H}$
Penitrem E	$R_1 = \text{H}$	$R_2 = \text{OH}$
Penitrem F	$R_1 = \text{Cl}$	$R_2 = \text{H}$



Penitrem C	$R = \text{Cl}$
Penitrem D	$R = \text{H}$

Figure 1.9. Structures of penitrems A–F.

Although the penitrems were first isolated in 1968 (Wilson et al., 1968), it was not until much later that the structures of penitrems A–F (Figure 1.9) were determined. The difficulty in structure elucidation was due to insufficient material, molecular complexity and instability (Aasen et al., 1969; Steyn and Vlegaar, 1985). The structures of all six penitrems were deduced through biosynthetic (which involved feeding labelled tryptophan to fungal cultures) and NMR (nuclear magnetic resonance) studies (de Jesus et al., 1981; de Jesus et al., 1983a; b).

P. crustosum is commonly used for producing penitrem A. *P. cyclopium* (Hosoe et al., 1990; Hou et al., 1971; Pitt, 1979), *Penicillium verrucosum* var. *cyclopium* (Pitt, 1979), *P. palitans* (Hou et al., 1971; Pitt, 1979) and *Penicillium puberulum* (Hou et al., 1971) have also been reported as producing penitrem A. These isolates, however, were later shown to be variants of *P. crustosum*. Penitrem A has also been isolated from *Penicillium lanoso-coeruleum* (Wells and Cole, 1977) and *Penicillium janczewskii* Zaleski (Mantle and Penn, 1989) and penitrem B has been isolated from *Aspergillus sulphureus* (Fres.) Thom and Church (Laakso et al., 1992).

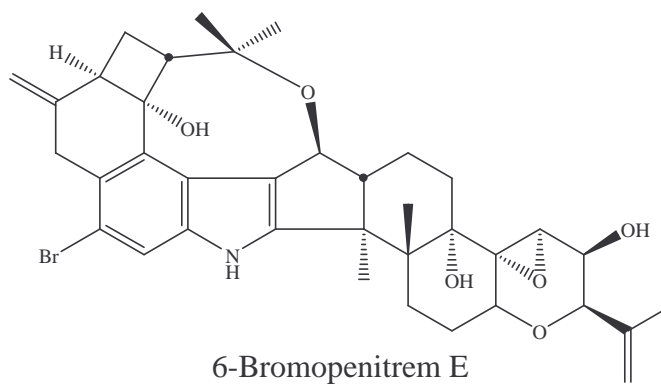
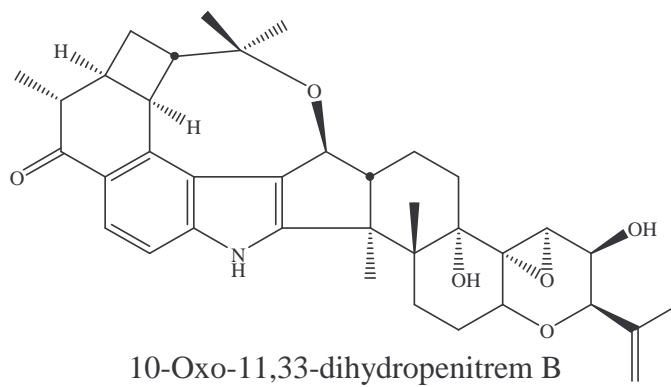
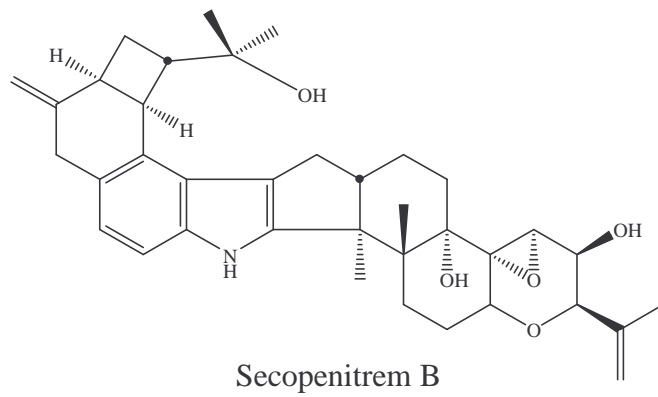
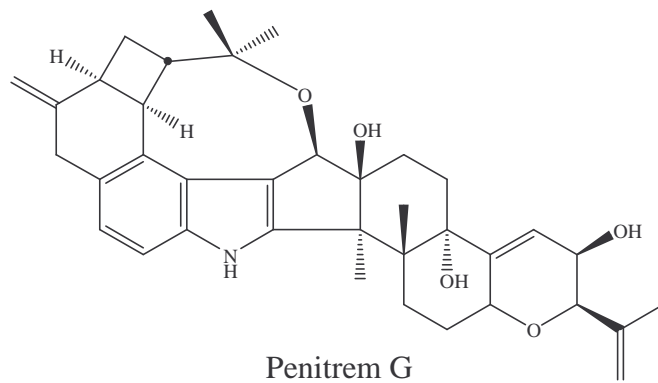


Figure 1.10. Structures of penitrem G, secopenitrem B, 10-oxo-11,33-dihydropenitrem B and 6-bromopenitrem E.

An additional penitrem, penitrem G (Figure 1.10), was more recently isolated from *P. crustosum* (Gonzalez et al., 2003). Other isolated penitrem analogues include secopenitrem B (Figure 1.10) (Laakso et al., 1992) and 10-oxo-11,33-dihydropenitrem B from *A. sulphureus* (Laakso et al., 1993) (Figure 1.10), 6-bromopenitrem E (which has a bromine atom instead of a chlorine atom at C-6 of penitrem A) isolated from *Penicillium simplicissimum* AK-40 (Hayashi et al., 1993) (Figure 1.10), pennigritrem from *Penicillium nigricans* (Figure 1.11) (Penn et al., 1992) and penitremones A–C (Figure 1.11) from a *Penicillium* species (Naik et al., 1995). Penitremone A is consistent with 10-oxo-11,33-dihydropenitrem B although the stereochemistry at C-11 of penitremone A has not been determined.

More recently two new indole–alkaloid isoprenoids 18,19-dehydrosecopenitrem A (thomitrem A) and 18,19-dehydrosecopenitrem E (thomitrem E) have been isolated from *P. crustosum* Thom (Rundberget and Wilkins, 2002a) (Figure 1.11).

Penitrems are capable of causing tremors in animals, and fungi capable of producing tremorgenic mycotoxins such as penitrems are found in agricultural products such as silage and maize (Steyn and Vleggaar, 1985). Penitrems also exhibit insecticidal activity. Penitrem A has shown activity against *Bombyx mori* (silkworm) (Hayashi, 1998; Hayashi et al., 1993), *Spodoptera frugiperda* (fall armyworm) and *Heliothis zea* (corn earworm) (Dowd et al., 1988).

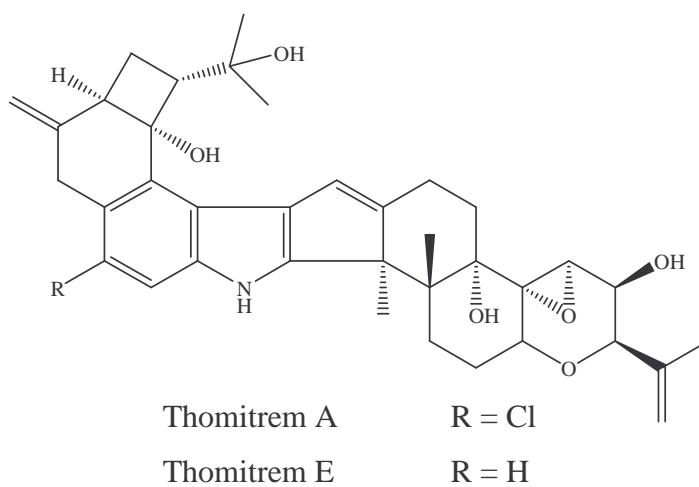
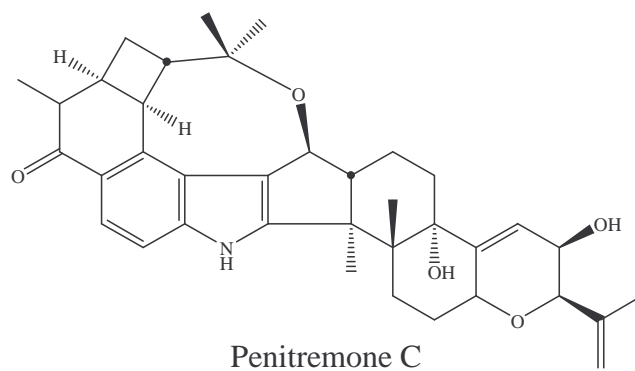
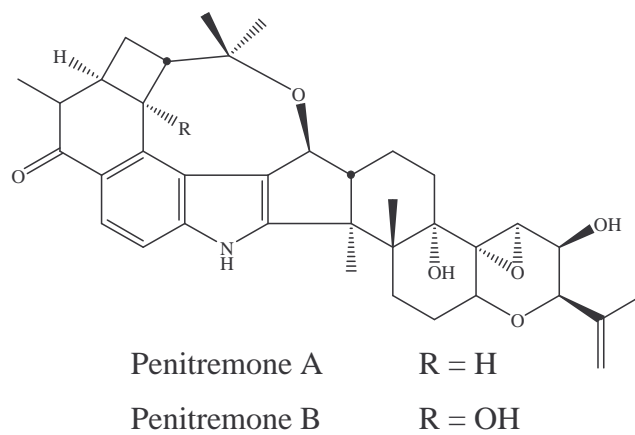
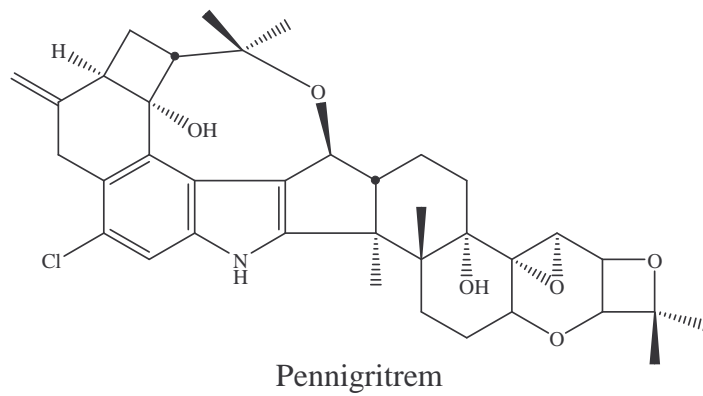


Figure 1.11. Structures of pennigritrem, penitremones A–C and thomitrem A and E.

1.4.2 Lolitrems

Compared to penitrems, lolitrems have an additional isoprene unit attached to the oxygen at the far right-hand side, at C-43. Lolitrem B (Figure 1.12) is believed to be the principal causative agent of ryegrass staggers (Berny et al., 1997; Munday-Finch et al., 1996a; Rowan, 1993). Lolitrem B was isolated in 1981 (Gallagher et al., 1981) and although the structure was determined a few years later by NMR (Gallagher et al., 1984), the stereochemistry at the A/B junction had yet to be defined. The stereochemistry was later reported by Ede et al. (1994).

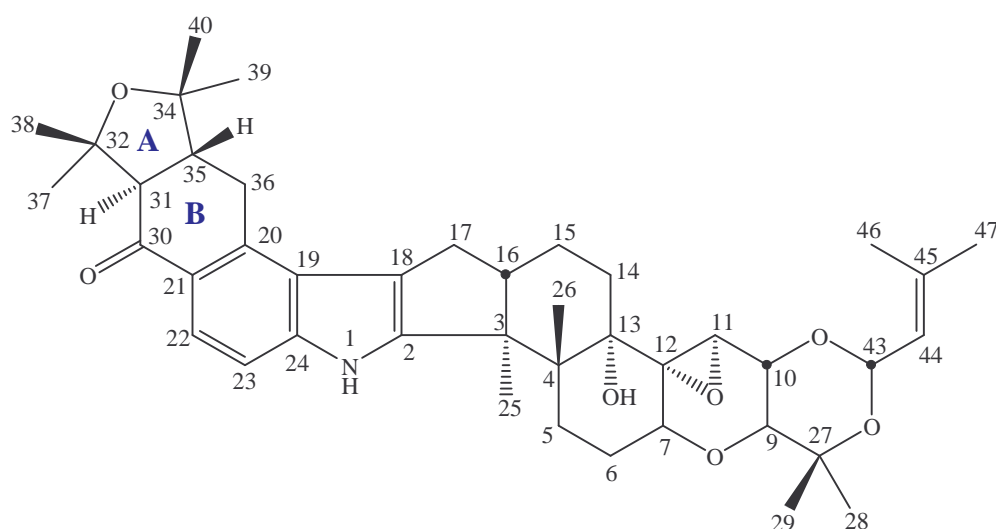


Figure 1.12. Structure of lolitrem B.

Large scale isolation of lolitrem B led to the identification of lolitrem A (Munday-Finch et al., 1995) (Figure 1.13), lolitrem E (Miles et al., 1994) (Figure 1.13) and lolitrem F (Munday-Finch et al., 1996b) (Figure 1.13). Additional identified lolitrems include lolitrems G, H, J, K, L, M and N (Figure 1.13) (Munday-Finch, 1997) as well as lolilline (Figure 1.14) (Munday-Finch et al., 1997), lolitriol, lolicine A and lolicine B and 31-*epi*-lolitrem F and 31-*epi*-lolitrem N (Munday-Finch et al., 1998) (Figure 1.14).

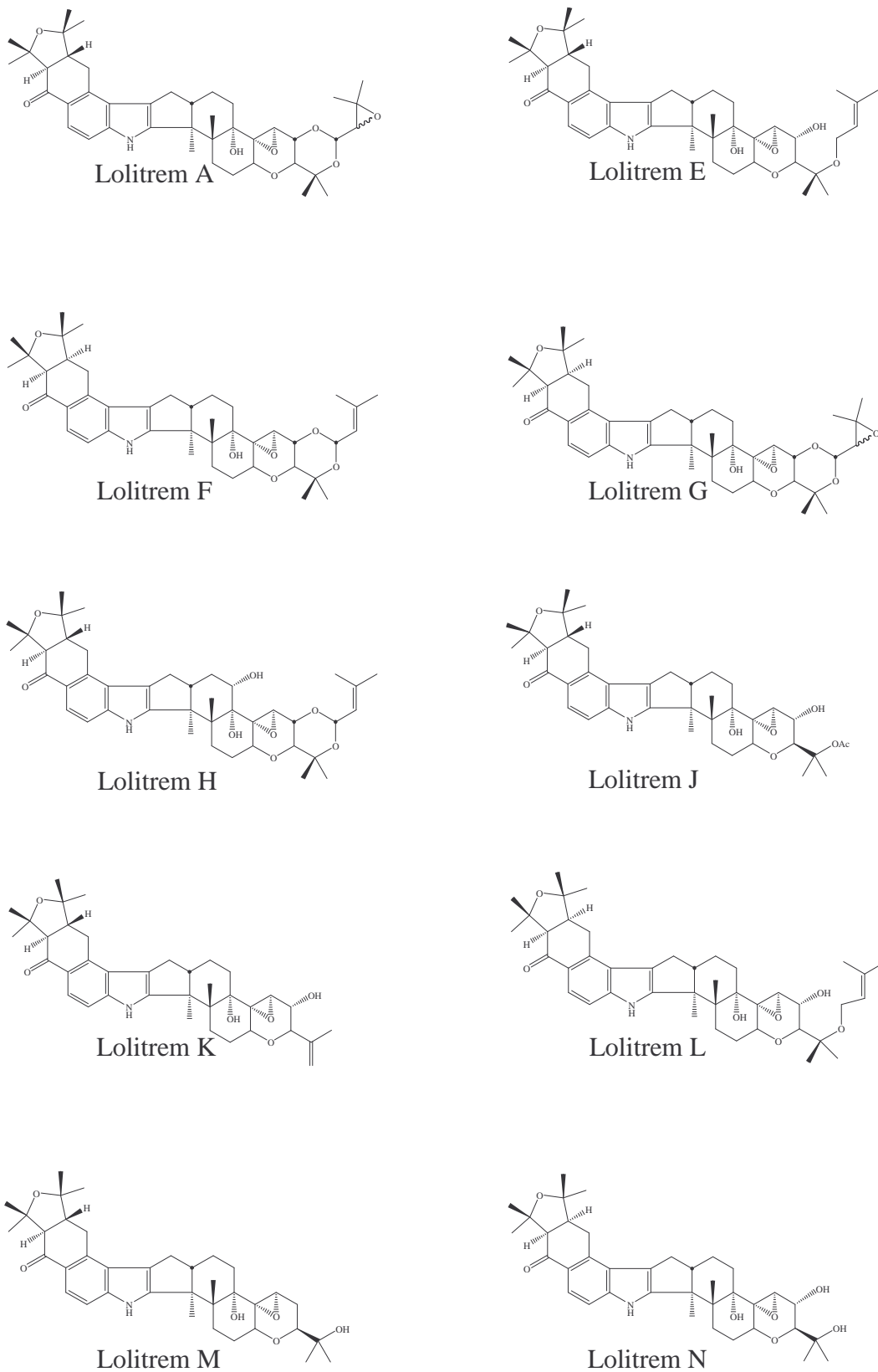


Figure 1.13. Structures of lolitrem A, E, F, G, H, J, K, L, M and N.

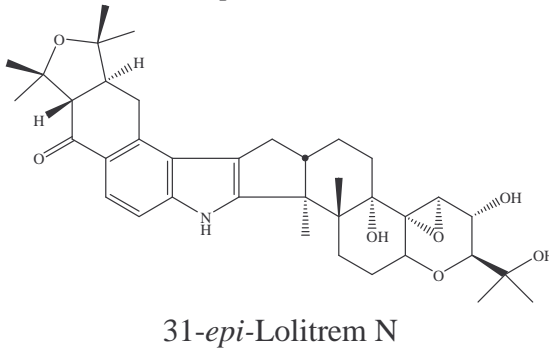
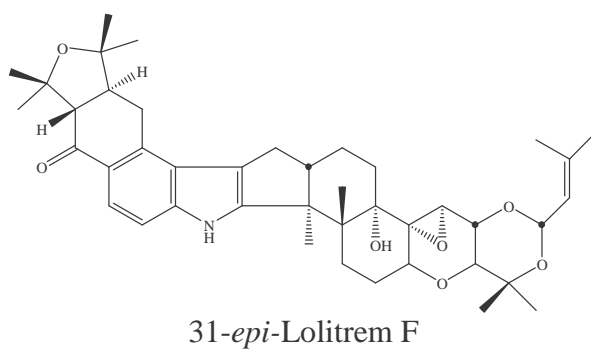
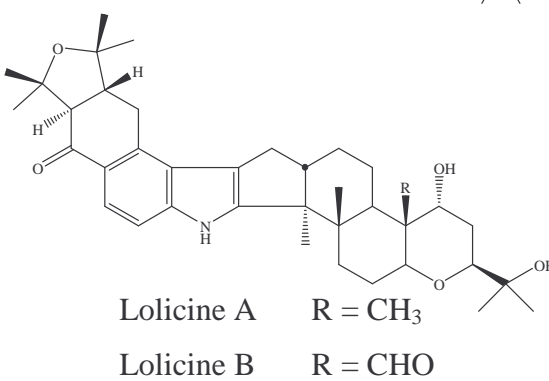
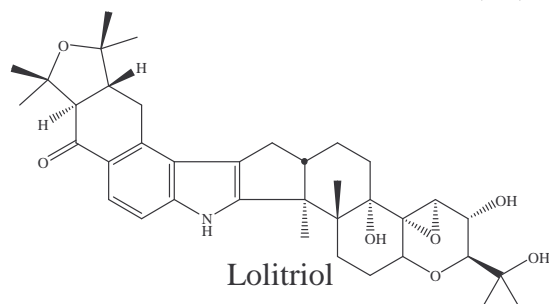
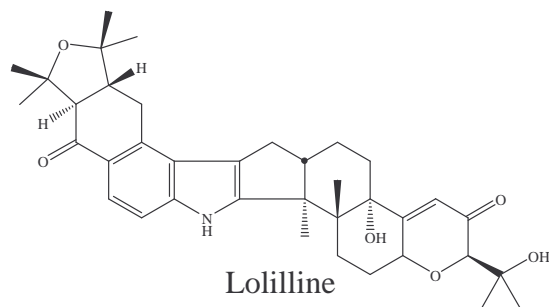


Figure 1.14. Structures of lolilline, lolitriol, lolicines A and B, and 31-*epi*-lolitrems F and N.

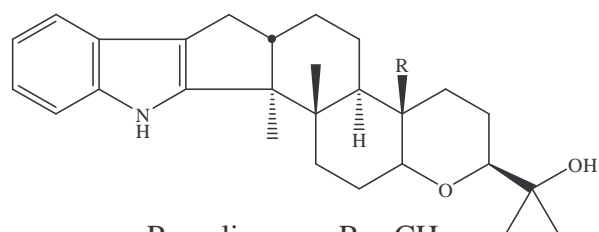
Of the tremorgenic fungal toxins, only certain lolitrems (such as lolitrems A and B) induce a sustained tremor which can last for up to three days in mice dosed intraperitoneally at 4 mg kg⁻¹. In contrast, the other tremorgenic toxins sustain tremors for only a few hours (Munday-Finch, 1997; Munday-Finch et al., 1996b; 1997).

Within the lolitrem class of compounds, the acetal linked isoprene unit (ring I, with the isoprene unit attached to C-43) is important for tremorgenic activity. The A/B rings are also involved in the tremorgenic activity of the lolitrems and appear to be necessary for the slow onset and long duration tremors observed with these compounds (Munday-Finch, 1997).

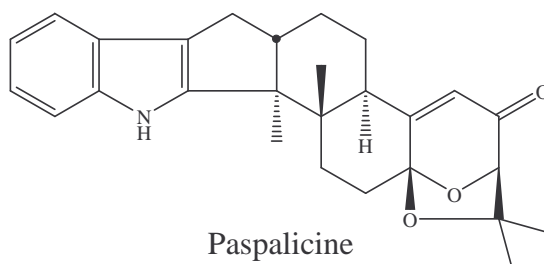
1.4.3 Paspaline

Paspaline and paspalicine (Figure 1.15) are structurally the simplest of the indole-diterpene group (Smith and Cui, 2003). These alkaloids were first reported in 1966 by the Arigoni group (Fehr and Acklin, 1966; Springer and Clardy, 1980) from the ergot fungus *Claviceps paspali*.

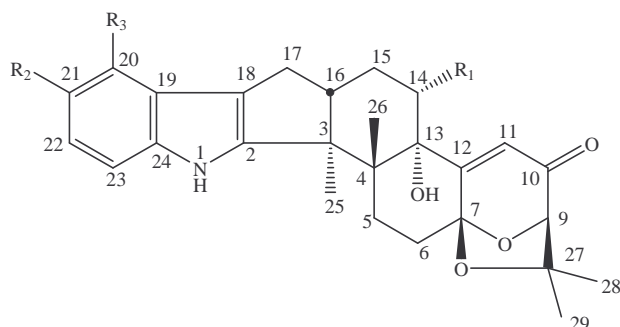
Paspalum staggers (also known as Dallis grass poisoning) is a result of animals ingesting the grass paspalum (*Paspalum dilatatum*) infected with *C. paspali* Stevens and Hall. The fungus invades the pistil of the *P. dilatatum* flower, and the ovary is then destroyed and replaced by a mass of fungal tissue. The fungus is easily spread by insects attracted to the sticky exudate (termed honeydew) produced by the fungus and by cattle walking through the grass (Cole et al., 1977). The symptoms of paspalum staggers include sensitivity to external stimuli and tremors. The tremorgens isolated from *C. paspali* which are responsible for these symptoms include paspalinine and paspalitrems A and B.



Paspaline R = CH₃
 Paspaline B R = CHO



Paspalicine



Paspalinine	R ₁ = H	R ₂ = H	R ₃ = H
14 α -Hydroxypaspalinine	R ₁ = OH	R ₂ = H	R ₃ = H
Paspalitrem A	R ₁ = H	R ₂ = CH ₂ CH=C(CH ₃) ₂	R ₃ = H
Paspalitrem B	R ₁ = H	R ₂ = CH=CHC(CH ₃) ₂ OH	R ₃ = H
Paspalitrem C	R ₁ = H	R ₂ = H	R ₃ = CH ₂ CH=C(CH ₃) ₂

Figure 1.15. Structures of paspaline, paspaline B, paspalicine, 14 α -hydroxypaspalinine, paspalinine and paspalitrem A, B and C.

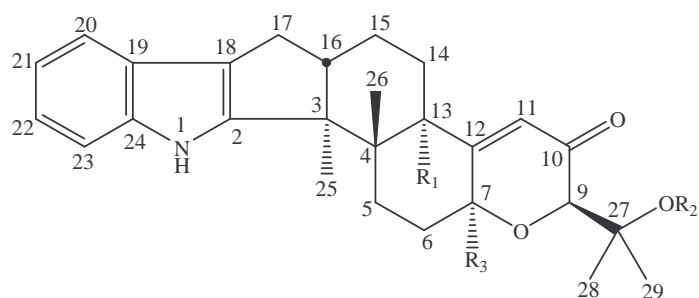
The alkaloids paspalinine (Figure 1.15) (Cole et al., 1977; Gallagher et al., 1980b), paspalicine, paspaline (Springer and Clardy, 1980) and paspalitrem A, B (Figure 1.15) (Cole et al., 1977) and C (Figure 1.15) (Dorner et al., 1984) have all been isolated from *C. paspali*. Paspalinine has also been isolated from

Aspergillus flavus (Cole et al., 1981) and *Eupenicillium shearii* (Belofsky et al., 1995). In addition, paspaline has also been isolated from *Emericella striata* (Nozawa et al., 1988a) and *Albophoma yamanashiensis* (Huang et al., 1995a; b). Paspalitrem A and B have an additional C5 unit located at C-21 of paspalinine. Paspalitrem A and C have also been isolated from the bark of *Cavendishia pubescens* infected with a *Phomopsis* species (Bills et al., 1992). Other paspaline derivatives include paspaline B (Figure 1.15) which was isolated from *Penicillium paxilli* Bainer (Munday-Finch et al., 1996a) and 14 α -hydroxypaspalinine (Figure 1.15) from *Aspergillus nomius* (Staub et al., 1993).

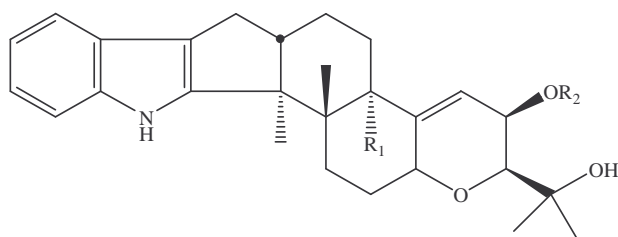
Paspalinine (Cole et al., 1981; Cole et al., 1977) and paspalitrem A and B (Cole et al., 1977) were found to be tremorgenic whereas paspalicine and paspaline (Cole et al., 1977) were non-tremorgenic. The analogues paspaline B, paspalitrem C and 14 α -hydroxypaspalinine have yet to be tested for tremorgenicity.

1.4.4 Paxilline

Paxilline (Figure 1.16) was found to be produced by *P. paxilli* Bainer (which was isolated from insect-damaged pecans) (Cole et al., 1974). A year later the structure of paxilline was elucidated (Springer et al., 1975). Paxilline has also been detected in *N. lolii* (Weedon and Mantle, 1987), *E. striata* (Rai, Tewari and Mujkerji) Malloch & Cain (Kawai and Nozawa, 1988) and *E. shearii* Stork & Scott (Belofsky et al., 1995). Other paxilline derivatives which have been identified include 13-desoxypaxilline and paxilline 27-*O*-acetate from *E. striata* (Kawai and Nozawa, 1988), 7-hydroxy-13-desoxypaxilline from *E. shearii* (Belofsky et al., 1995), PC-M5' and PC-M6 from *P. crustosum* (Hosoe et al., 1990) and paxinorol from *P. paxilli* (Figure 1.16) (Miles et al., 1995b).



Paxilline	$R_1 = \text{OH}$	$R_2 = \text{H}$	$R_3 = \text{H}$
13-Desoxypaxilline	$R_1 = \text{H}$	$R_2 = \text{H}$	$R_3 = \text{H}$
Paxilline 27- <i>O</i> -acetate	$R_1 = \text{OH}$	$R_2 = \text{COCH}_3$	$R_3 = \text{H}$
7-Hydroxy-13-desoxypaxilline	$R_1 = \text{H}$	$R_2 = \text{H}$	$R_3 = \text{OH}$



PC-M5'	$R_1 = \text{OH}$	$R_2 = \text{COCH}_3$
PC-M6	$R_1 = \text{H}$	$R_2 = \text{H}$

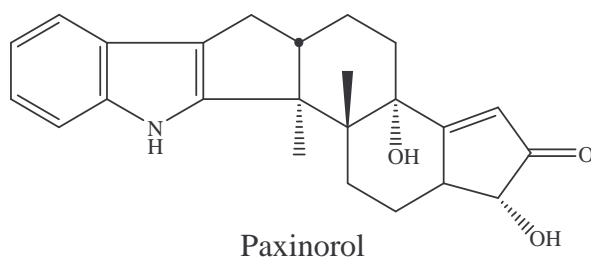


Figure 1.16. Structures of paxilline, 13-desoxypaxilline, paxilline-27-*O*-acetate, 7-hydroxy-13-desoxypaxilline, PC-M5', PC-M6 and paxinorol.

A new congener, 21-isopentenylpaxilline (Figure 1.17), was reported in 1995 (Belofsky et al., 1995). The alkaloid was isolated from *E. shearii* (Belofsky et al., 1995). NMR studies revealed the structure was similar to paxilline and

paspalinine. The tremorgenic activity of this compound has not been evaluated. However, paxilline has been tested and was found to produce short duration tremors at 4 mg kg^{-1} (when injected intraperitoneally into mice) (Miles et al., 1992) whereas 13-desoxypaxilline was non-tremorgenic at a dose rate of 8 mg kg^{-1} (Munday-Finch, 1997).

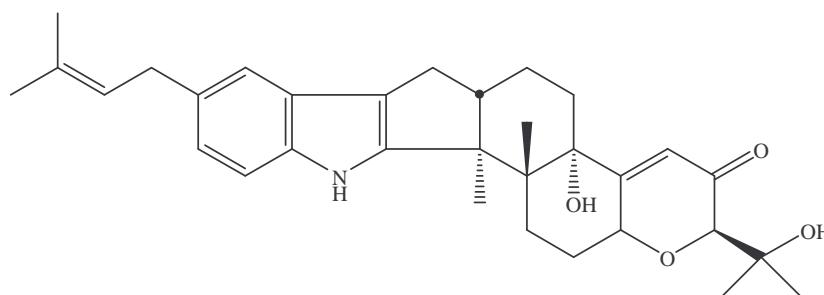
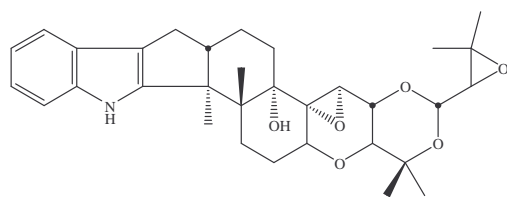


Figure 1.17. Structure of 21-isopentenylpaxilline.

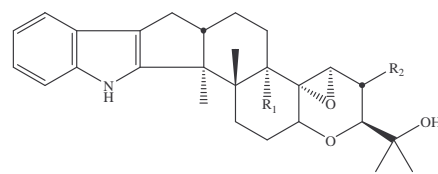
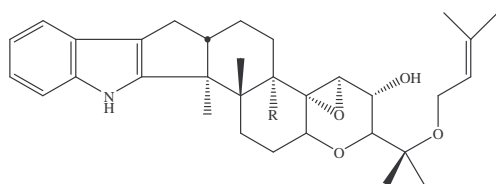
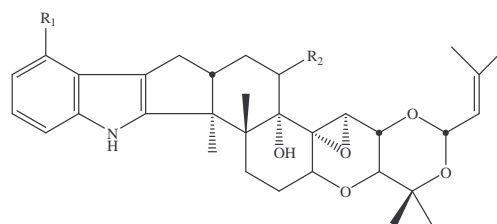
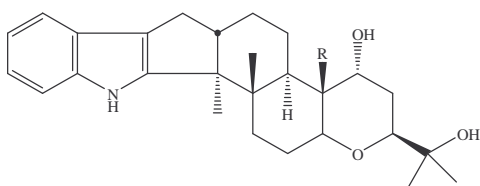
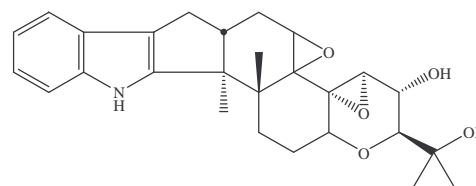
1.4.5 Terpendoles

Huang et al. (1995a) isolated four new metabolites from the culture broth of the fungus *A. yamanashiensis*. These compounds were named terpendoles (A–D) (Figure 1.18) and are acyl–CoA: cholesterol acyltransferase (ACAT) inhibitors.

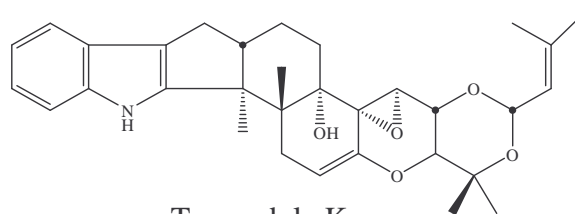
Further investigation led to the discovery of eight additional terpendoles (E–L) (Figures 1.18) (Tomoda et al., 1995). A few years later a further compound, terpendole M (Figure 1.18), was isolated from *N. lolii*-infected perennial ryegrass (Gatenby et al., 1999).



Terpendole A

Terpendole B $R_1 = H$ $R_2 = H$ Terpendole I $R_1 = OH$ $R_2 = OH$ Terpendole D $R = H$ Terpendole J $R = OH$ Terpendole C $R_1 = H$ $R_2 = H$ Terpendole L $R_1 = CH_2CH=C(CH_3)_2$ $R_2 = H$ Terpendole M $R_1 = H$ $R_2 = OH$ Terpendole E $R = CH_3$ Terpendole F $R = CH_2OH$ Terpendole G $R = CHO$ 

Terpendole H



Terpendole K

Figure 1.18. Structures of terpendoles A–M.

Terpendoles D, E, F, G, H and I were found to be non-tremorgenic at a dose of 8 mg kg⁻¹ when injected intraperitoneally into mice (Munday-Finch, 1997). In contrast, terpendole C was found to be strongly tremorgenic at this same dose (Munday-Finch, 1997; Munday-Finch et al., 1997) yielding tremors of short duration.

1.4.6 Sulpinines

The antiinsectan metabolites, the sulpinines, were isolated from the sclerotia of *A. sulphureus* (Laakso et al., 1992). Sclerotia are specialised structures which are able to withstand extreme conditions of temperature, desiccation and nutrient depletion and remain dormant until conditions are favourable for growth. These hardened asexual resting structures are composed of vegetative hyphal cells that can survive for years in soil (Erental et al., 2008). The structures of sulpinines A–C (Figure 1.19) were primarily determined by NMR analysis and by comparison with the structurally-related penitrems. Sulpinine C may be a possible artefact derived from sulpinine A, as paxilline was found to be easily converted to the dioxygenated derivative, 2,18-dioxopaxilline under relatively mild conditions (Munday-Finch, 1997; Mantle et al., 1990).

The three sulpinine metabolites were found to exhibit insecticidal activity against the crop pest *Helicoverpa zea* (Laakso et al., 1992). The sulpinines have not been tested for tremorgenicity.

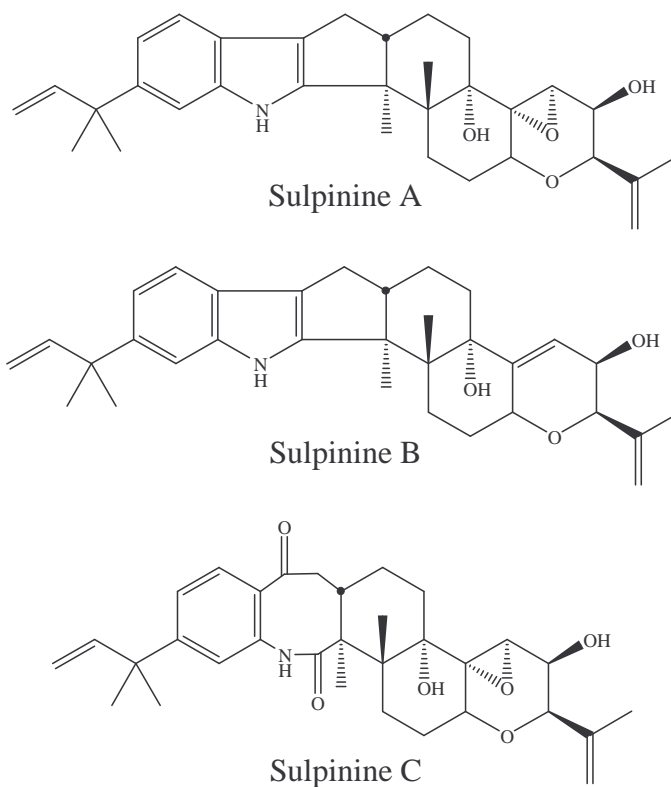
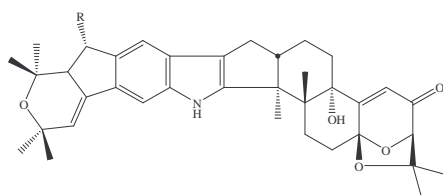


Figure 1.19. Structures of sulpinines A–C.

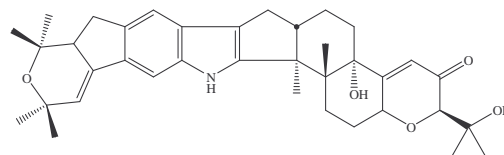
1.4.7 Shearinines

Belofsky et al. (1995) isolated three novel alkaloids, shearinines A, B and C (Figure 1.20), from the ascostromata (hardened structures similar to the sclerotia) of *E. shearii*. Shearinine C may be an artefact derived from shearinine B, as discussed earlier with sulpinine C (Section 1.4.6). The shearinines (which belong to the janthitrem class) were found to exhibit activity against the corn earworm *Helicoverpa zea* and the dried fruit beetle *Carpophilus hemipterus*.

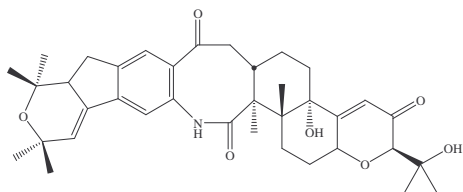


Shearinine A R = H

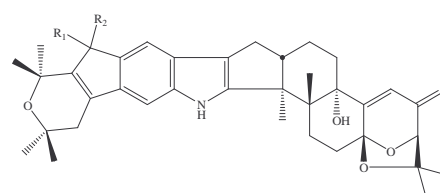
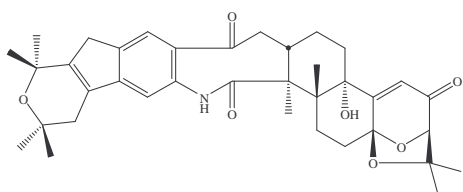
Shearinine D R = OH

Shearinine E R = OCH₃

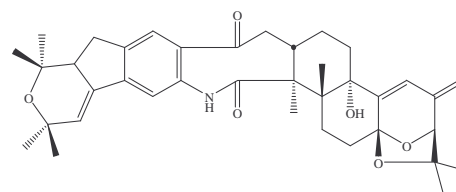
Shearinine B



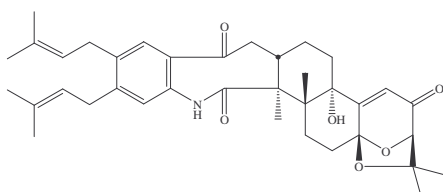
Shearinine C

Shearinine F R₁ = R₂ = HShearinine G R₁ + R₂ = O

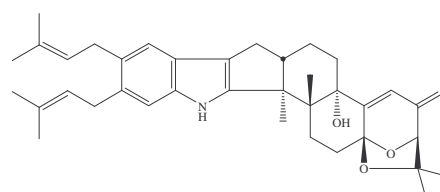
Shearinine H



Shearinine I



Shearinine J



Shearinine K

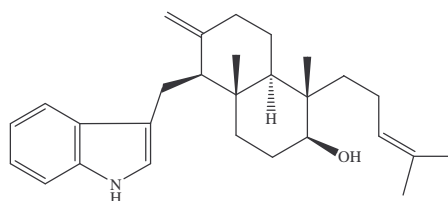
Figure 1.20. Structures of shearinines A–K.

More recently, eight new indole triterpenes, named shearinines D–K (Figure 1.20), have been isolated from a *Penicillium* species (strain HKIO459) obtained from a mangrove plant (Xu et al., 2007). As with shearinine C, shearinines H–J

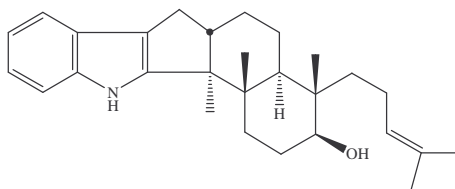
may also be artefacts. These compounds have not been tested for tremorgenic activity.

1.4.8 *Emindoles*

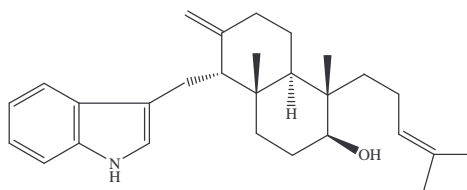
There are a variety of emindole compounds, such as SA, SB, DA and DB (Figure 1.21), which have been isolated. Emindole SA has been isolated from *E. striata* (Kawai and Nozawa, 1988; Nozawa et al., 1988b), SB from *E. striata* and *A. yamanshiensis* (Nozawa et al., 1988a; Tomoda et al., 1995) and DA and DB from *Emericella desertorum* Samson & Mouchacca (Kawai and Nozawa, 1988).



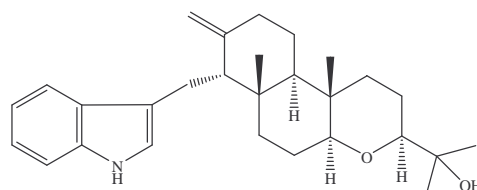
Emindole SA



Emindole SB



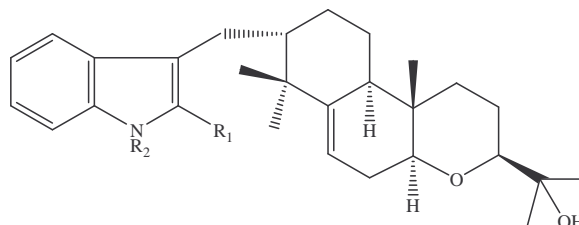
Emindole DA



Emindole DB

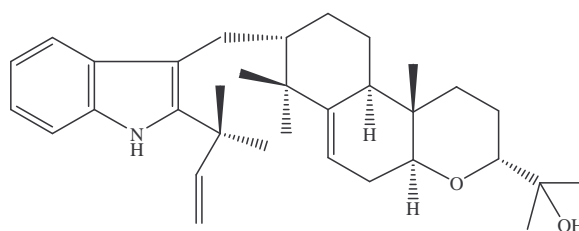
Figure 1.21. Structures of emindoles SA, SB, DA and DB.

More recently three novel emindoles (named PA, PB and PC) (Figure 1.22) were isolated from *Emericella purpurea* (Hosoe et al., 2006). A related compound, emeniveol (Figure 1.22), has also been isolated from *Emericella nivea* (Kimura et al., 1992).

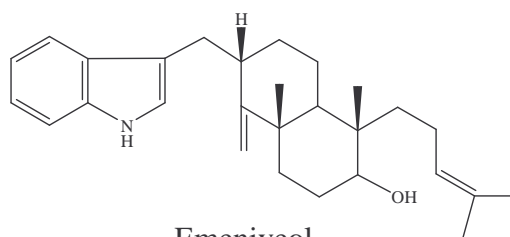


Emindole PA $R_1 = \text{CH}_2\text{C}(\text{CH}_3)_2\text{CHCH}_2$ $R_2 = \text{H}$

Emindole PB $R_1 = \text{H}$ $R_2 = \text{CH}_2\text{C}(\text{CH}_3)_2\text{CHCH}_2$



Emindole PC



Emeniveol

Figure 1.22. Structures of emindoles PA, PB and PC and emeniveol.

1.4.9 Aflatremis

The aflatrem mycotoxins were discovered by Wilson and Wilson (1964). These toxins were produced by a number of *Aspergillus flavus* strains grown on

foodstuffs such as potatoes and rice. The tremorgenic activity of aflatrem (Figure 1.23) was compared to lolitrem B using mice (Gallagher and Hawkes, 1986). Aflatrem induced tremors were shorter in duration but more intense compared to lolitrem B induced tremors.

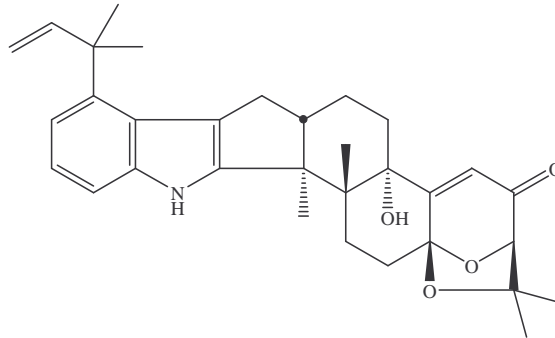


Figure 1.23. Aflatoxin B1.

1.4.10 Janthitrems

Gallagher et al. (1980a) screened twenty one *Penicillium janthinellum* Biourge isolates obtained from ryegrass-staggers-causing pastures to investigate tremorgenic mycotoxins as a cause of ryegrass staggers. Over half of these isolates were found to produce highly fluorescent tremorgenic toxins. Molecular weights were determined by high resolution mass spectrometry for 3 compounds, which were subsequently named janthitrems A (structure unknown), B (Figure 1.24) and C (Figure 1.24) (Gallagher et al., 1980a). Intraperitoneal injection (into the abdominal cavity) of janthitrem B into mice elicited a tremorgenic response as well as incoordination and hypersensitivity to touch and sound. A further compound was later isolated by Lauren and Gallagher (1982) using preparative thin layer chromatography (TLC) which was tentatively named janthitrem D (structure unknown) based on its ultra-violet (UV) and fluorescent properties.

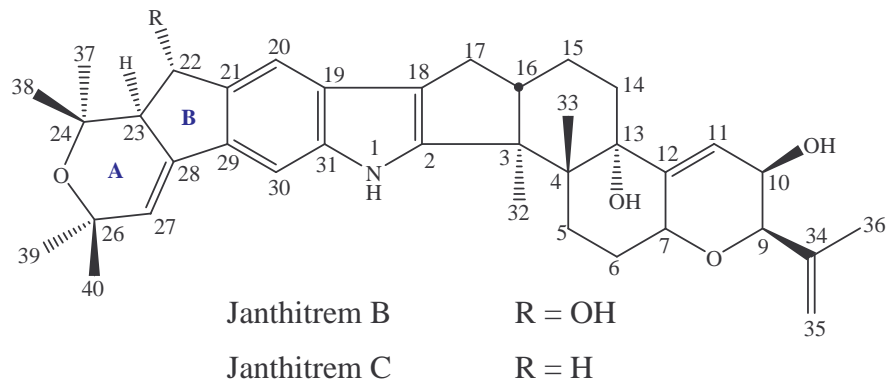


Figure 1.24. Structures of janthitrems B and C.

The structures of three additional similar janthitrem compounds, E, F, and G (Figure 1.25), (discovered from an Australian isolate of *P. janthinellum*) were deduced by de Jesus et al. (1984). Further investigations revealed both New Zealand and Australian isolates of *P. janthinellum* were capable of producing either janthitrems A–D or E–G (Penn et al., 1993). Janthitrems B and C are the two most abundant tremorgenic mycotoxins found in certain isolates of *P. janthinellum* from Australia and New Zealand (Penn et al., 1993).

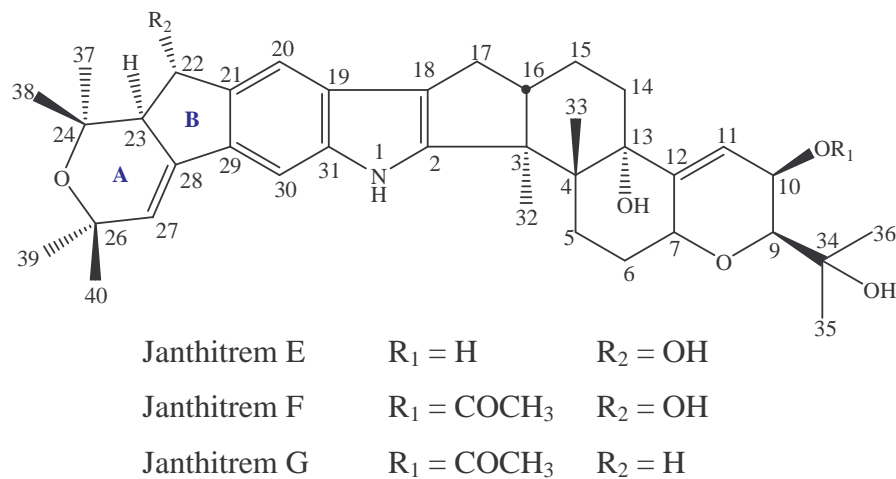


Figure 1.25. Structures of janthitrems E–G.

The structure of janthitrem B was elucidated by Wilkins et al. (1992) using ^1H and ^{13}C NMR, confirming its close structural relationship to janthitrems E–G. The structure of janthitrem C was determined by Penn et al. (1993) by NMR spectroscopy. The NMR assignments were fully corroborated by a full complement of NMR spectral data including NOE measurements. The right-hand side of janthitrems B and C is identical to penitrem D and their spectral data proved to be identical.

Janthitrems B and C have a dehydrated terminal isoprene of the diterpenoid moiety of janthitrems E–G. As with janthitrem E, janthitrem B has a C-22 hydroxyl group whereas janthitrem C, like janthitrem G, lacks this hydroxyl group. Wilkins et al. (1992) also determined the relative configuration of rings A and B of janthitrems B, E and F by NOE (nuclear overhauser effect) difference experiments. Furthermore, the relative stereochemistry at C-22, C-23 of janthitrems E–G was reported for the first time.

The structure of janthitrem A remains unknown due to paucity of material. Likewise, the structure of janthitrem D also remains unknown. More recently, a novel janthitrem named 10-*epi*-11,12-epoxyjanthitrem G (Figure 1.26) was isolated from AR37 endophyte-infected (a novel endophyte as described in Sections 1.7 and 1.8) perennial ryegrass herbage and seed (Tapper and Lane, 2004). The compound was characterised by UV, high resolution mass spectrometry and NMR. Three further structures isolated alongside this compound were assigned 10-deacetyl-10,34-(3-methylbut-2-enyl acetal), 10-deacetyl-34-*O*-(3-methylbut-2-enyl) and 34-*O*-(3-methylbut-2-enyl) derivatives of 10-*epi*-11,12-epoxyjanthitrem G on the basis of LC–MS analysis.

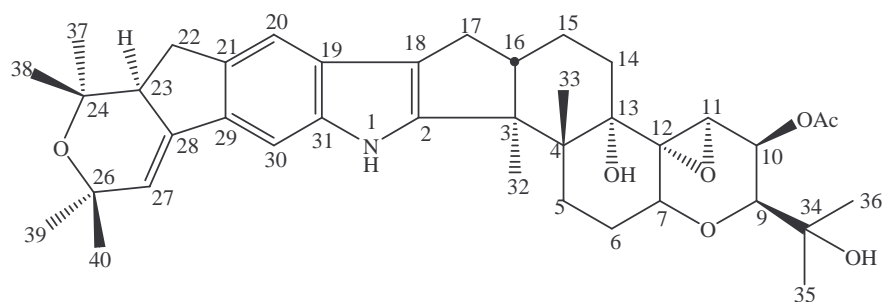


Figure 1.26. 10-*epi*-11,12-epoxyjanthitrem G.

1.5 Biosynthetic Studies

The structures of the metabolites described in the previous section all contain an indole nucleus derived from tryptophan linked to a diterpenoid unit from four mevalonate-derived isoprenes (geranylgeranyl diphosphate) (de Jesus et al., 1983c; Laws and Mantle, 1989; Penn and Mantle, 1994).

Arigoni's group (Acklin et al., 1977) investigated the biosynthesis of paspaline and related metabolites. The group hypothesised the metabolites originated from an indole nucleus and a diterpene unit (Figure 1.27). To confirm this idea, cultures of *C. paspali* were supplemented with ^{13}C labelled acetate. The results showed acetate was readily incorporated into the diterpenoid moiety of paspaline (Figure 1.27). An intermediate in the biosynthesis of paspaline, emindole SB (which is thought to be formed from emeniveol), was isolated by Nozawa et al. (1988a) thus providing further evidence to this proposed pathway (Figure 1.27). Nozawa et al. (1988a; b) then suggested paspaline could be converted to 13-desoxypaxilline (which was isolated from *E. striata*) (Figure 1.27) which was then proposed to be converted to paxilline (Figure 1.27). Paspaline can therefore be regarded as a base structure and a likely key intermediate in the biosynthesis of a number of complex indole-diterpenes.

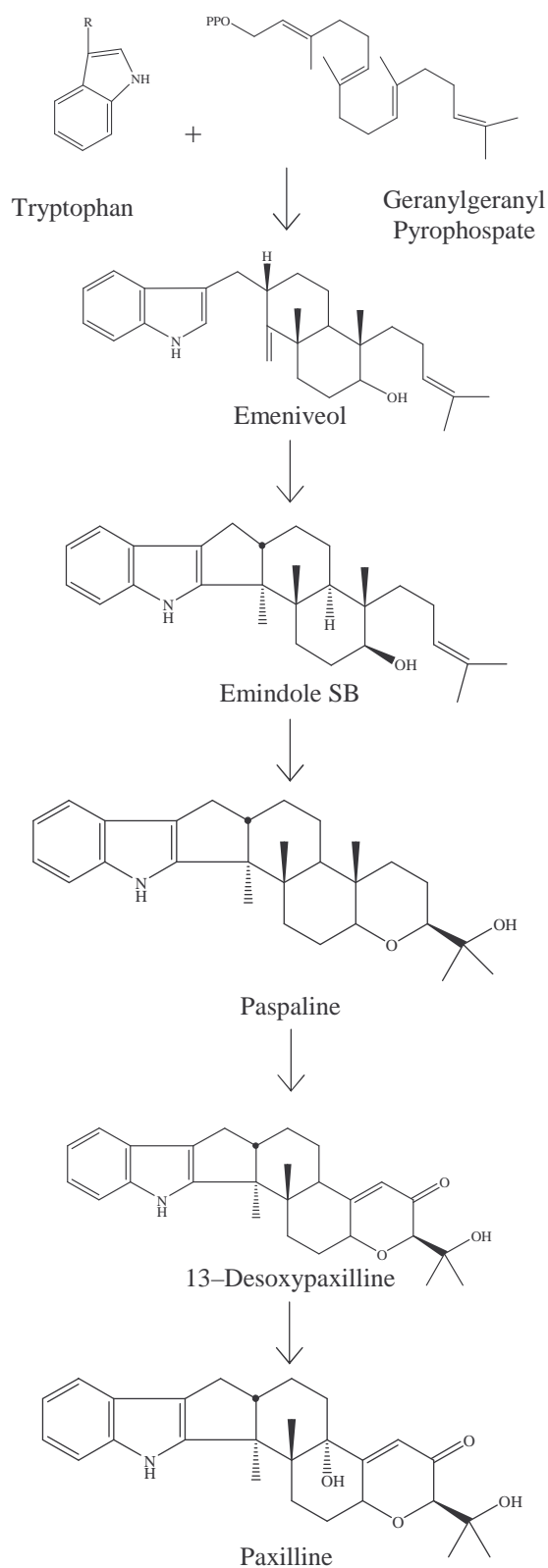


Figure 1.27. Proposed biosynthetic pathway for the early stages of indole-diterpenoid biosynthesis.

Paxilline may also be a key intermediate in biosynthetic pathways. Paxilline and 10 β -hydroxypaxilline are believed to be intermediates in the biosynthesis of the aromatic substituted indole–diterpenoids penitrems and janthitrems (Mantle and Penn, 1989; Penn and Mantle, 1994).

The structure of penitrem A was first proposed by de Jesus et al. (1981) by simultaneous incorporation of spectroscopic studies and biosynthetic reasoning. The biosynthetic study involved feeding labelled tryptophan which showed penitrem A to have a substituted indole nucleus. The biosynthetic pathway of penitrem A proposed by de Jesus et al. (1983c) involved theoretical intermediates with structures similar to paxilline. Consequently, the role of paxilline in the biosynthesis of penitrem was investigated by Mantle and Penn (1989). The study involved feeding ^{14}C labelled paxilline to cultures of *P. janczewskii* which resulted in incorporation of radiolabel into penitrem A thus confirming paxilline was involved in penitrem A biosynthesis.

In a similar vein, janthitrem B was also found to contain radiolabel after feeding cultures of *P. janthinellum* with ^{14}C labelled paxilline indicating paxilline is likely to be involved in the biosynthesis of janthitrem B (Penn and Mantle, 1994).

1.6 Mode of Action of Tremorgenic Mycotoxins

Extensive work was carried out in the 1970s and 1980s to try and determine the mode of action of the tremorgenic mycotoxins. The tremorgenic mycotoxins are lipophilic molecules and consequently have the ability to cross the blood-brain barrier and access the central nervous system (Knaus et al., 1994; Norris et al., 1980). Work was focussed on the possible role of amino acid neurotransmitters

but different studies gave contradicting results and the role of amino acid neurotransmitters was inconclusive.

Recent work has shown indole–diterpenes such as paxilline and lolitrem B to be active on BK channels (Dalziel et al., 2005; Knaus et al., 1994; McMillan et al., 2003; Sanchez and McManus, 1996) using techniques such as patch–clamping.

Ion channels are present in membranes of all cells, from bacteria to humans, and are essential for life. They are responsible for electrical signalling that underlies movement, sensation and thought. The large-conductance calcium-activated potassium channel (BK, *Slo* or maxiK channel) has a specialised role in regulating this electrical signalling and is particularly important in maintaining normal blood pressure and brain activity.

Lolitrem B in particular acts as a very potent BK channel inhibitor but since non-tremorgenic compounds such as paspalicine (Knaus et al., 1994) also induced BK channel inhibition it was initially thought that BK channel activity was unrelated to tremorgenicity. More recently, however, Finch et al. (2006) have used BK channel knock-out mice to investigate this possible link further. Mice lacking BK channels suffered no tremors with doses of lolitrem B and paxilline which would have induced convulsions in wild-type mice. These experiments show that the tremorgenic effects of lolitrem and paxilline are mediated by BK channels. The reason why some compounds show no effect in mice despite having *in vitro* effects on BK channels is not yet clear but may be due to metabolism in the animal rendering them inactive.

1.7 Novel Endophyte Technology

Endophyte–grass combinations produce a number of secondary metabolites which provide both beneficial and detrimental effects. Different endophyte strains produce varying types and concentrations of secondary metabolites which allows for the possibility of selecting an endophyte with a desirable metabolite profile and inserting it into the grass species of your choice. Latch and Christensen (1985) showed that this approach could be successful.

Five endophytic fungi (*N. lolii*, a *Gliocladium*-like species, *Neotyphodium coenophialum*, a *Phialophora*-like species and *Epichloe typhina*) were isolated from different species of New Zealand grasses, cultured and then inoculated into endophyte-free seedlings of tall fescue and ryegrass. This procedure proved successful as four of the five investigated fungi infected the ryegrass. Therefore, this approach can be used to produce cultivars of grasses infected with a chosen endophyte. However, the generation of secondary metabolites is influenced by not only the endophyte, but also the host grass, meaning that a novel endophyte–grass association requires intensive screening to ensure that the association produces (or does not produce) the desired compounds. New classes of beneficial or detrimental products can also be produced, requiring bioactivity testing to be undertaken.

The current commercial novel endophytes include (Ball et al., 2006; Jensen and Popay, 2004; van Zijll de Jong et al., 2008; Wrightson Seeds, 2007):

- MaxP[®]

This tall fescue endophyte provides stronger resistance to pest attack and moisture stress. This endophyte does not produce ergovaline, which is the alkaloid responsible for many of the symptoms associated with tall fescue toxicosis.

- NEA2

Provides insect protection and contains low levels of peramine, ergovaline and very low levels of lolitrem B.

- AR1

Gives excellent animal performance while providing a moderate range of insect protection. Lolitrem B and ergovaline are not produced but the endophyte does produce peramine.

- Endo5

This endophyte does not produce lolitrem B. It provides good resistance to Argentine stem weevil, pasture mealy bug, black beetle and tolerance to root aphid. Endo5 pastures persist better than AR1 in areas where root aphid or black beetle is an issue.

- AR37

AR37 is an endophyte which is able to provide greater insect control compared to the other commercially available endophytes. The endophyte gives protection against Argentine stem weevil, pasture mealy bug, root aphid and black beetle as well as good control of porina. The secondary metabolites responsible for this enhanced protection are not fully understood. AR37 does not produce lolitrem B, but, despite this, sporadic staggers are observed on this pasture type. In general, however, animal performance is good.

1.8 Scope of the Present Study

Endophytic fungi in grasses contain an array of biologically active compounds that profoundly affect the persistence of grasses and the health of the animals that

graze them. Two of the world's most important pastoral grasses (perennial ryegrass and tall fescue) are endophyte-infected. Breeding programmes inserting selected endophytes into selected grasses have led to improvements in persistence and animal health outcomes, and these cultivars have become important to New Zealand's pastoral economy and a major export industry.

A significant new technology recently delivered by AgResearch to New Zealand livestock industries is pasture grass infected with safe endophytic fungi which protect pastures from insect attack, and thus enhances productivity and persistence with minimal animal health issues. Improvements to provide the next generation of these cultivars requires an in-depth understanding of the bioactive compounds produced by the endophyte and their effects on grazing animals and invertebrate pests.

The most recent novel endophyte-infected pasture grass is AR37, a product that has shown great promise. However, despite the absence of lolitrem B, AR37 can still cause ryegrass staggers — though it does occur less frequently and severely.

Several novel janthitrems, including 10-*epi*-11,12-epoxyjanthitrem G, have recently been identified in ryegrass infected with the AR37 endophyte (Tapper and Lane, 2004), leading to renewed interest in the janthitrems. Early work (Section 1.4.10) showed that janthitrems produced by *P. janthinellum* cultures were tremorgenic, but once these compounds were dismissed as the cause of ryegrass staggers, research into janthitrems ceased.

The epoxyjanthitrems isolated from AR37-infected ryegrass are not only a likely candidate for involvement in the staggers observed on this pasture type, but also possibly for the insect resistance observed. This is because good pest protection is found with this product without the production of the known insect anti-feedant

compounds. Further work is therefore required on janthitrems and in particular epoxyjanthitrems. However, the isolation of epoxyjanthitrems from ryegrass is difficult and these compounds have proved to be very unstable, hindering research to date. Therefore, this study will investigate janthitrems from another source, *P. janthinellum* cultures, to determine if suitable related compounds can be isolated.

If suitable compounds can be isolated they can be used in mouse and insect studies to test the hypothesis that epoxyjanthitrems are involved in the animal and insect effects observed with AR37 endophyte-infected ryegrass. The isolated compounds could also be used to study the stability of epoxyjanthitrems so that conditions can be discovered to minimise or prevent degradation during future work on the AR37 compounds.

LC–UV–MS Development

The unexpected discovery of janthitrems produced by a novel endophyte–grass combination proves that these novel products should be screened not only for lolitrems, but also for other classes of indole–diterpenoids. This study will investigate the use of LC–UV–MS for the analysis of a range of indole–diterpenoids including janthitrems, penitrems, lolitrem B, paxilline, paspaline, paspalinine and terpendole C. The development of improved LC–UV–MS methods will allow future endophyte products to be more thoroughly screened for different classes of secondary metabolites.

CHAPTER TWO

Isolation and Structure Elucidation of Janthitrems

2.1 Screening of Cultures

2.1.1 Introduction

Janthitrems produced by *Penicillium janthinellum* cultures are known to be tremorgenic and mycotoxins of this class have been identified in AR37 endophyte-infected perennial ryegrass. A series of *P. janthinellum* strains were therefore grown and extracts of the resulting cultures were analysed for janthitrems and related compounds (Figure 2.1).

P. janthinellum strains were obtained from three sources: (1) freeze-dried preparations made in October 1979 of strains 1–4 (di Menna et al., 1986); (2) isolates obtained by Dr M. E. di Menna from soil of pasture collected from two sites at Ruakura Agricultural Research Centre, Hamilton, New Zealand, in January 2005; and (3) cultures deposited in the PDD culture collection in 1979 by Dr. G. C. M. Latch (originally isolated from soil, sheep dung and ryegrass leaves). In total 31 isolates were grown in culture and extracted as described in Sections 8.1.1 and 8.1.2.

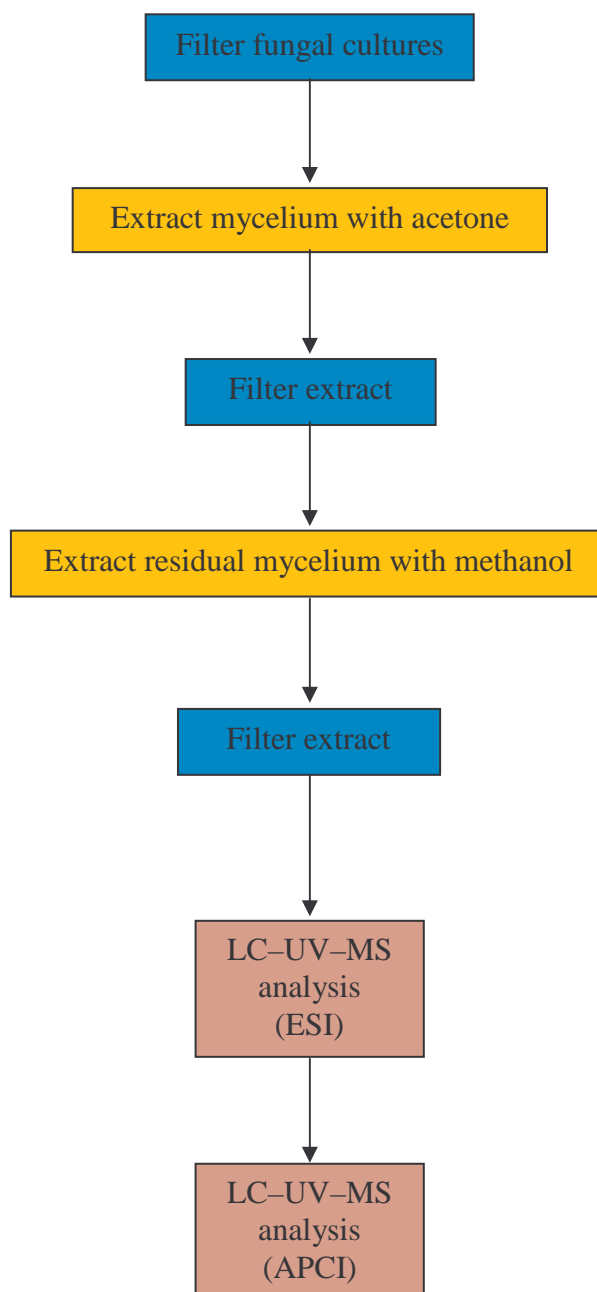


Figure 2.1. Screening of *P. janthinellum* cultures.

2.1.2 LC–UV–MS Analysis of Culture Extracts

Extracts were analysed on an LC–UV–MS system using a Finnigan LTQ Linear Ion Trap mass spectrometer fitted with an ESI interface and coupled to a Surveyor HPLC, autosampler, MS pump and photodiode array (PDA) detector. The fungal culture extracts were also run on a Finnigan LCQ Advantage mass spectrometer fitted with an APCI source. Full experimental details regarding LC–UV–MS analysis can be found in Section 8.1.3.

All cultures were extracted sequentially with acetone and methanol. LC–UV–MS analysis of the extracts indicated that the second extraction of the fungal cultures with methanol was not particularly advantageous since although compounds of interest were extracted, the levels at which they were present were significantly lower than those present in the first acetone extraction (methanol extraction levels were *ca.* 10% of the levels present in acetone extractions). In addition, unwanted compounds that were evident in acetone extracts were still present at similar levels in methanol extracts. On the basis of these observations it was determined that any further extraction of fungal cultures (e.g. preparative cultures) would only be performed with acetone extraction and not further extracted with methanol.

Analysis of the *P. janthinellum* samples by LC–UV–MS (using an ESI source) showed the presence of janthitrems in the majority of the strains. Of particular interest were strains E1 and 5674, which appeared to contain significant amounts of janthitrem B and other janthitrem–related compounds. For this reason, the E1 and 5674 strains were grown on a preparative scale for extraction and isolation of metabolites.

Since later work (Chapter 4, Section 4.2) showed that LC–UV–MS with an APCI source showed significant advantages over that with an ESI source, the 31 fungal isolate extracts were re-analysed using the improved conditions. This identified the possible presence of penitrems in the strain, E2.

The presence of penitrems in a *P. janthinellum* fungal culture has previously been suspected but has not been confirmed (di Menna et al., 1986). The presence of penitrem A in extracts of the E2 culture was initially verified by comparisons of the retention time, mass spectrum, mass spectral fragmentation, and UV spectrum of the E2 metabolite peak and a standard (authentic) specimen of penitrem A (Figure 2.2). In addition, peaks with mass and UV spectral properties consistent with penitrems B–F and roquefortine C were also observed in chromatograms of extracts of strain E2. The mass and UV spectral properties and LC retention times of these peaks were found to be identical to those determined for penitrems B–F and roquefortine C in an extract of a well characterised strain of *P. crustosum* (Rundberget et al., 2004a) grown under identical conditions, and in accordance with chromatographic data reported elsewhere for penitrems (Maes et al., 1982) and roquefortine C (Tor et al., 2006).

The detection of penitrems A–F in extracts of the E2 culture prompted a careful search for the presence of penitrems in extracts of the other investigated cultures. Strain E3 afforded a peak attributable to penitrem A based on comparison with an authentic penitrem A standard, however, in contrast to strain E2, penitrems B–F and roquefortine C were not detected.

P. janthinellum strain identification numbers and compounds detected are listed in Table 2.1.

Table 2.1. Penitrems and janthitrems detected in each strain of *P. janthinellum*.

Fungal Culture	Compounds Present	Fungal Culture	Compounds Present
E1	Janthitrems A, B, C, D	2A7	Janthitrems A, B, C, D
E2	Penitrems A, B, C, D, E, F	2B1	Janthitrems A, B, C, D
E3	Penitrem A	2B2	Janthitrems A, B, C, D
E4	Janthitrems A, B, C, D	2B3	Janthitrems A, B, C, D
1A1	Janthitrems A, B, C, D	2B4	Janthitrems A, B, C, D
1A2	Janthitrems B, C	2B5	Janthitrems A, B, C, D
1A3	Janthitrems A, B, C, D	2B6	Janthitrems A, B, C, D
1A4	Janthitrems A, B, C, D	2B7	Janthitrems A, B, C, D
1A5	Janthitrems A, B, C, D	2B8	Janthitrems A, B, C, D
1A6	Janthitrems A, B, C, D	2B9	Janthitrems A, B, C, D
2A1	None detected	2B10	Janthitrems A, B, C, D
2A2	Janthitrems A, B, C, D	5665	Janthitrems A, B, C, D
2A3	Janthitrems A, B, C, D	5674	Janthitrems A, B, C, D
2A4	Janthitrems A, B, C, D	5685	Janthitrems B, C
2A5	Janthitrems A, B, C, D	5687	Janthitrems A, D
2A6	Janthitrems A, B, C, D		

The results from this investigation confirm that on some occasions penitrems are produced by *P. janthinellum* fungal cultures.

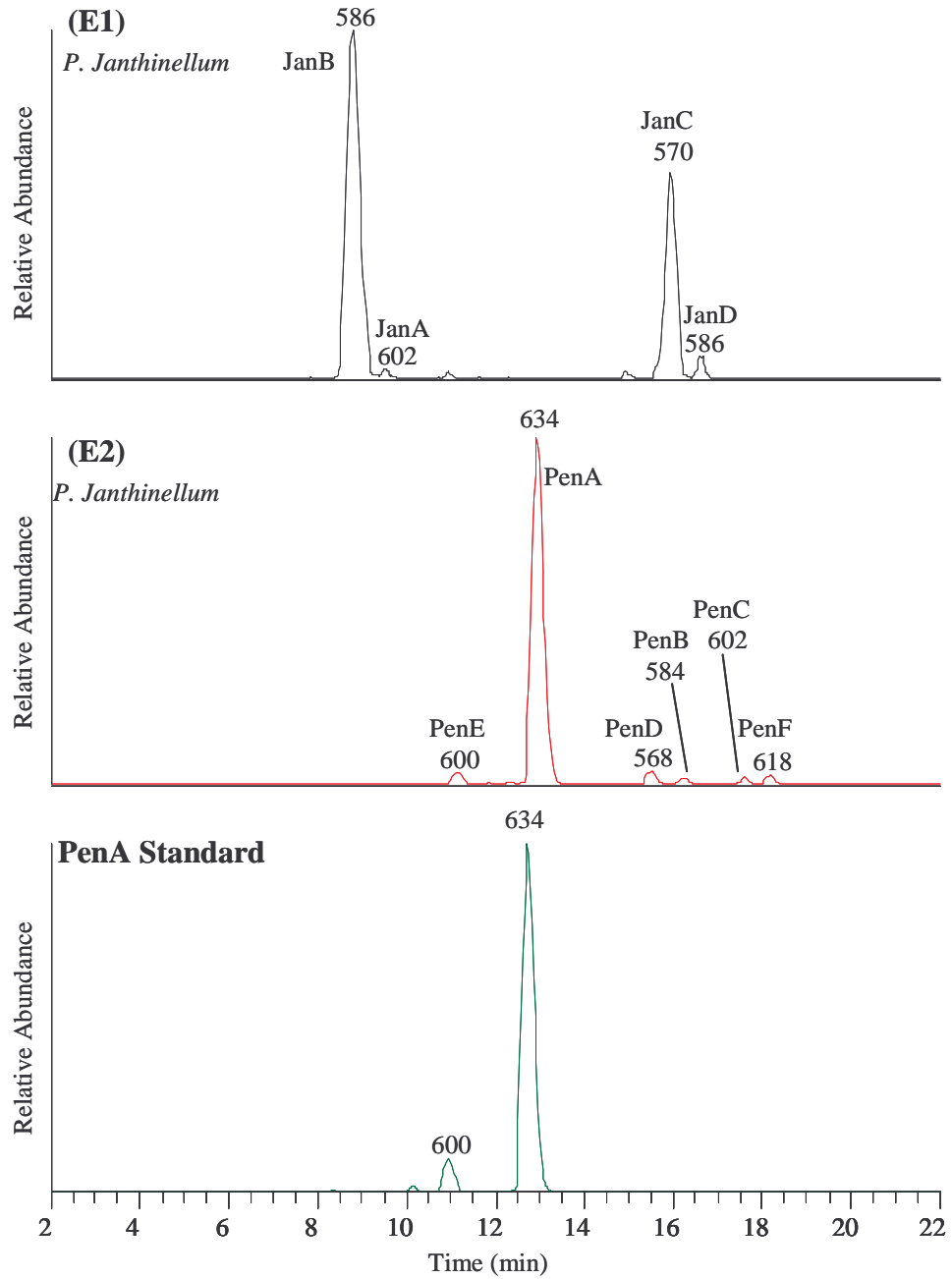


Figure 2.2. LC-MS chromatograms of E1 and E2 and penitrem A standard. Values of m/z for $[M+H]^+$ are given above or below their corresponding peaks.

2.2 Isolation of Janthitrem A and Janthitrem B

A preparative scale culture of *P. janthinellum* strain E1, was grown for isolation of janthitrem A and janthitrem B (Figure 2.3). This strain was selected because LC–UV–MS analysis of the *P. janthinellum* fungal extracts (Section 2.1.2) indicated the presence of janthitrems, with masses corresponding to janthitrems A, B and C.

2.2.1 Extraction and Isolation of Janthitrem A and Janthitrem B

The E1 fungal extract was fractionated by flash column chromatography (details of culturing, extraction, isolation and chromatography procedures are described in Section 8.2).

To determine the ideal solvent system to use as the mobile phase for separation of the janthitrems by flash column chromatography on silica gel, a series of TLC plates were run. Results reported by Wilkins et al. (1992) indicated that toluene and acetone would be suitable solvents, therefore, 80:20, 70:30, 60:40, and 55:45 toluene–acetone mixtures were investigated. These trials showed that the 70:30 toluene–acetone system was likely to be an appropriate mobile phase for flash column chromatography.

Fractions (10 mL) eluted from the silica gel flash column were collected and analysed by TLC (3:2 toluene–acetone) and visualised under short wave (254 nm) and long wave (366 nm) UV light. Upon inspection of the TLC plates, the 10 mL flash column fractions were combined into four bulk fractions on the basis of similar retention times. The first bulked sample comprised fractions 1–4, the second, fractions 5–7, the third, fractions 8–10 and the fourth, fractions 11–14. The remaining fractions were of no interest. The bulked fractions were analysed by HPLC and LC–UV–MS (APCI source) (as described in Sections 8.2.5 and 8.1.3 respectively). This showed that janthitrem B was present in fractions 8–10.

In addition to janthitrems, the flash column fractions also contained fats, oils and other contaminants. Significant clean-up was achieved by de-fatting. After de-fatting, the janthitrem sample was further purified by flash column chromatography (using 17:3 toluene–acetone). The compound of interest, collected based on absorbance at 330 nm, was obtained in a single fraction and evaporated to dryness *in vacuo*. Full details of the de-fatting (of the samples) and chromatography techniques are reported in Sections 8.2.6 and 8.2.7.

The semi-purified material from the second flash column was subjected to a further clean-up via solid phase extraction on a Strata-X column eluted with varying concentrations of methanol. Each fraction was analysed by analytical HPLC which showed that the 80 and 90% (v/v) methanol fractions contained the compounds of interest. These fractions were combined, dried and further purified by semi-preparative HPLC. Semi-preparative HPLC yielded two peaks of interest which were fluorescent, consistent with janthitrem compounds.

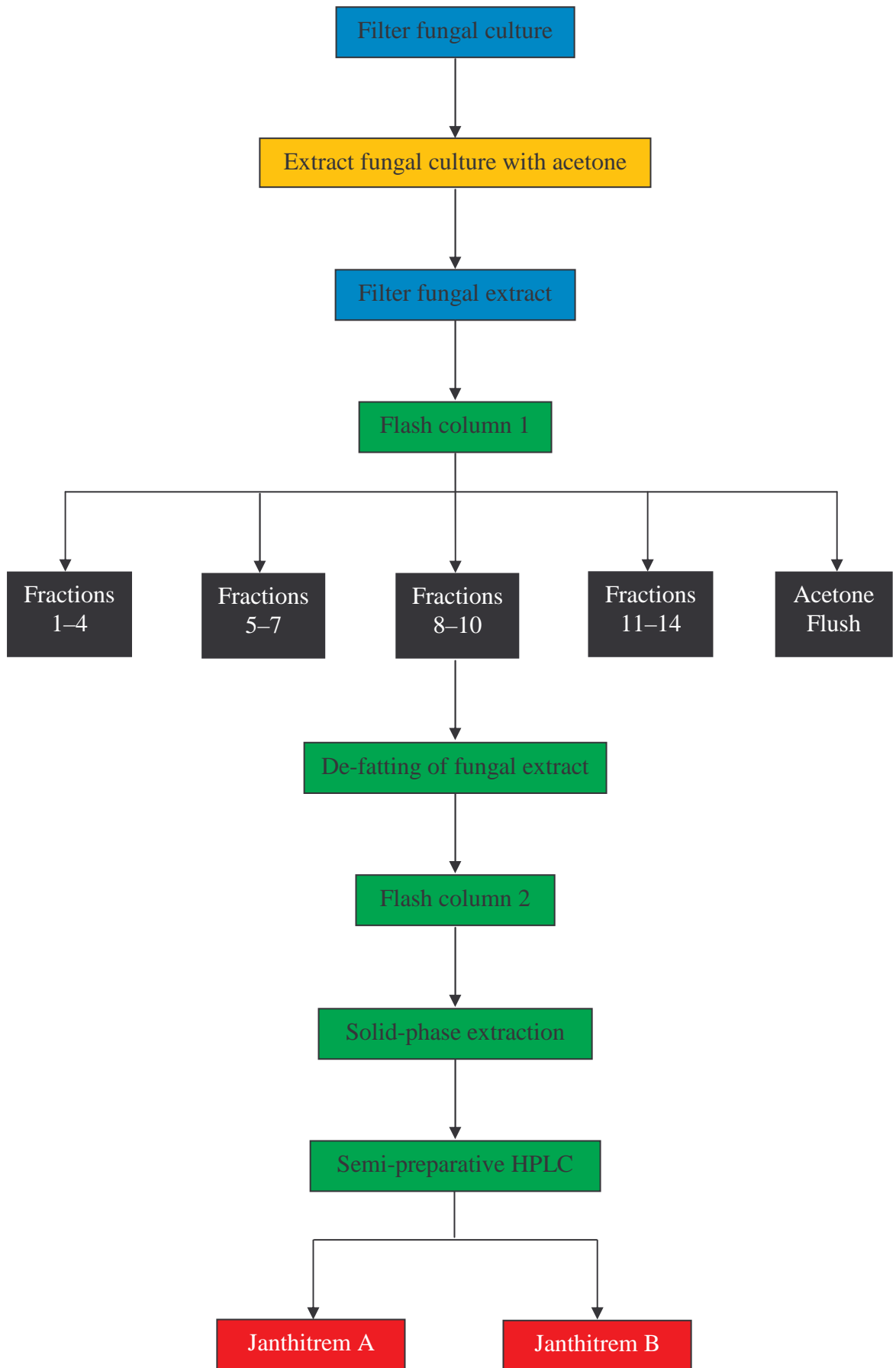


Figure 2.3. The isolation of janthitrem A and janthitrem B.

2.2.2 Analysis of Janthitrem Compounds

LC–UV–MS

Purified janthitrem compounds were analysed by LC–UV–MS using a Finnigan LCQ Advantage mass spectrometer fitted with an APCI source, coupled to a Surveyor HPLC, autosampler, MS pump and PDA detector.

Chromatographic analysis of the janthitrem fractions revealed the presence of two compounds, a major early-eluting peak (9.5 min) and a minor later-eluting peak (11 min). LC–UV–MS analysis of the two isolated compounds indicated that the major peak afforded a $[M+H]^+$ ion at m/z 586 consistent with janthitrem B and the minor peak a $[M+H]^+$ ion at m/z 602 (Figures 2.4 and 2.5).

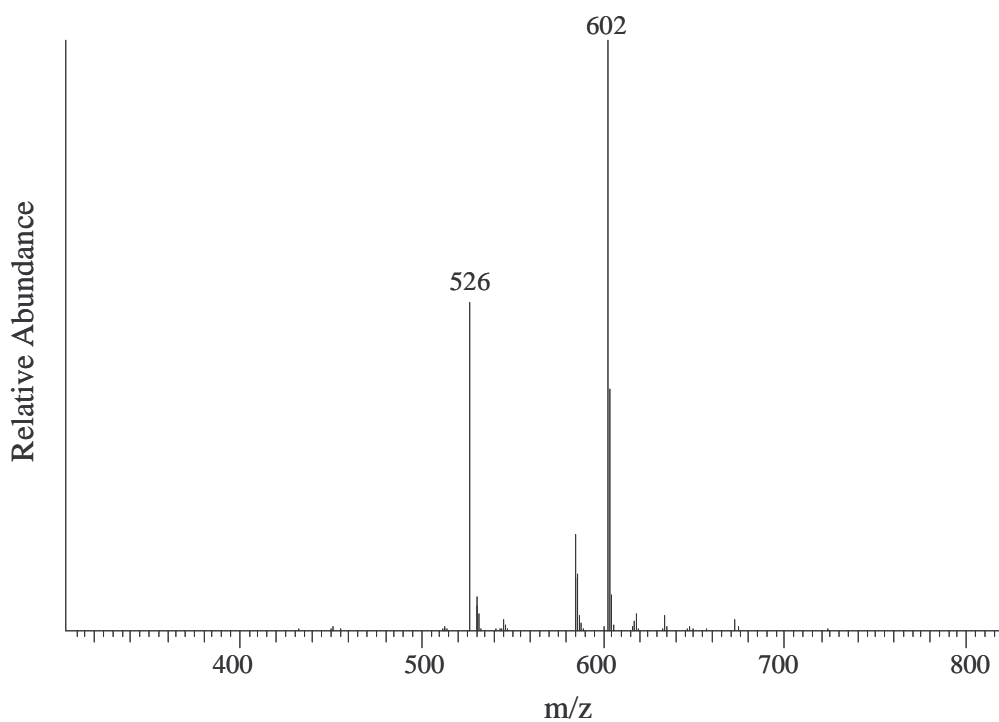


Figure 2.4. Full scan mass spectrum of the minor later-eluting peak. Values of m/z for major ions observed are given.

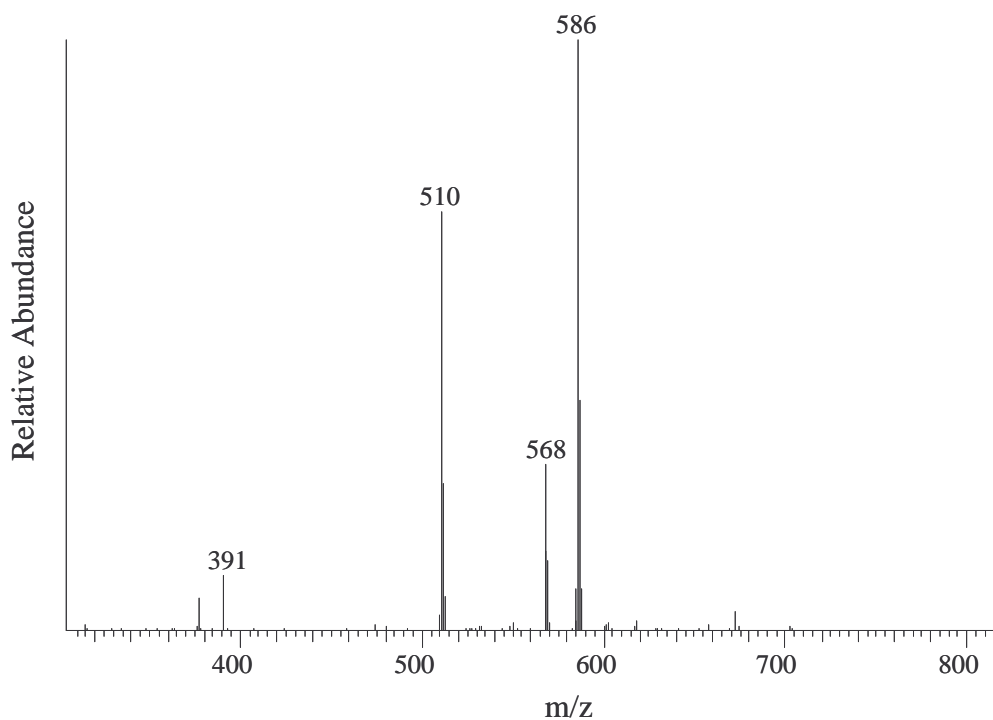


Figure 2.5. Full scan mass spectrum of the major early-eluting peak. Values of m/z for major ions observed are given.

These two isolated compounds also displayed characteristic janthitrem-like UV absorbance spectra with maxima at 260 and 330 nm (Figure 2.6).

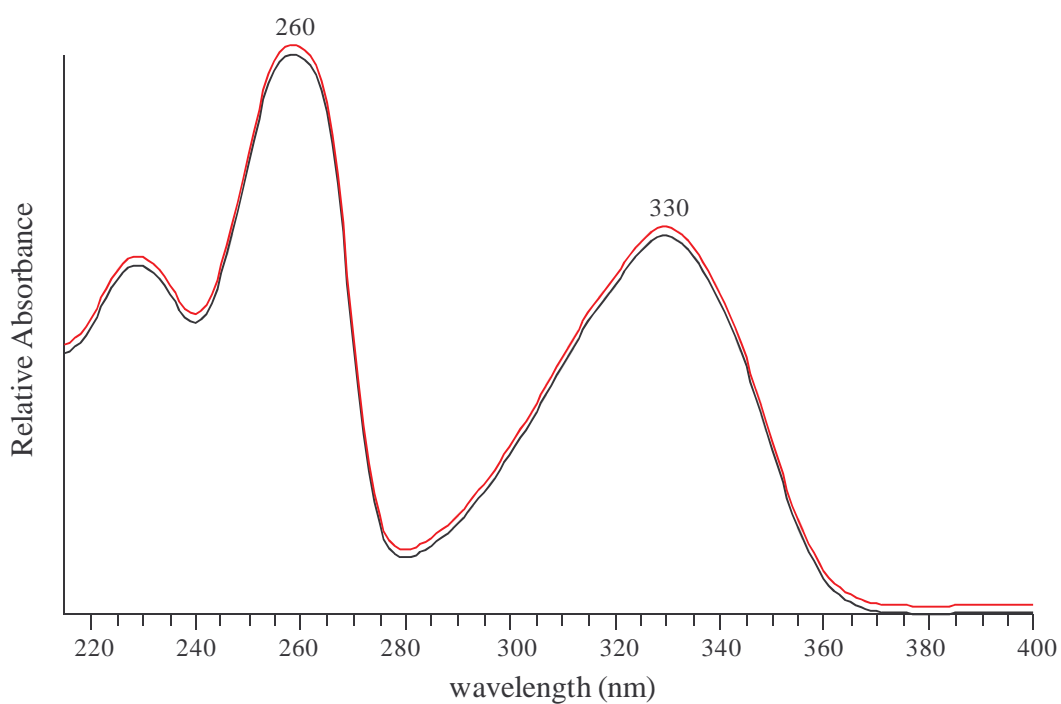


Figure 2.6. Normalised UV absorbance spectra of minor (red) and major (black) peaks.

The atomic compositions of the two isolated compounds were determined by High Resolution Mass Spectrometry (HRMS) (see Section 8.2.10). The molecular formulation of the sample collected from the minor later-eluting peak was established in positive ion mode for its $[M+Na]^+$ ion (found: m/z 624.3276 (error 3.20 ppm); calc. for $C_{37}H_{47}O_6NNa$ m/z 624.3296) while the molecular formulation of the sample collected from the major early-eluting peak was established in negative ion mode for its $[M-H]^-$ ion (found: m/z 584.3381 (error 2.49 ppm); calc. for $C_{37}H_{46}O_5N$ m/z 584.3395), which is consistent with janthitrem B. The results from the HRMS showed the difference between the two compounds related to the presence of an extra oxygen in the minor analogue.

1H and ^{13}C NMR analyses showed the major analogue to be janthitrem B (Chapter 3) after comparison with literature data. The unknown compound was also believed to be a janthitrem analogue due to the similar fragmentation patterns observed between itself and janthitrem B and its janthitrem-like UV and fluorescence.

An examination of the ^{13}C NMR data determined for the unknown compound indicated that the resonances for C-7, C-9, C-10, C-11 and C-12 had shifted markedly relative to the corresponding resonances for janthitrem B, indicating that the extra oxygen may reside in this area of the molecule. Comparison of the carbon resonances of the unknown compound with those of penitrem A (a compound similar in structure to the janthitrems, but with an epoxide in the 11,12 position) revealed almost identical resonances for the carbons of interest (C-7, C-9, C-10, C-11, C-12) (Table 2.2: the numbering system employed is that presented in Chapter 3, Section 3.1). The MS fragmentation (in negative ion mode) was also consistent with the presence of an 11,12-epoxide (Chapter 4, Section 4.5.1) and not with an 11(12)-double bond.

Table 2.2. ^{13}C NMR resonances observed for janthitrem B and the unknown janthitrem analogue and published assignments for penitrem A^a (δ).

	Janthitrem B	Unknown Janthitrem	Penitrem A
C-7	74.3	72.0	72.0
C-9	80.4	74.6	74.7
C-10	64.3	66.2	66.3
C-11	119.5	61.9	61.9
C-12	148.5	66.1	66.1

^a de Jesus et al. (1983a)

Therefore it was believed that the structure of the unknown compound was identical to that of janthitrem B other than for the 11(12)-double bond being replaced by an epoxide. This compound was therefore tentatively named 11,12-epoxyjanthitrem B (Figure 2.7) (refer to poster in Appendix 2). Subsequent ^1H and ^{13}C NMR analysis confirmed the structure of the compound (Chapter 3).

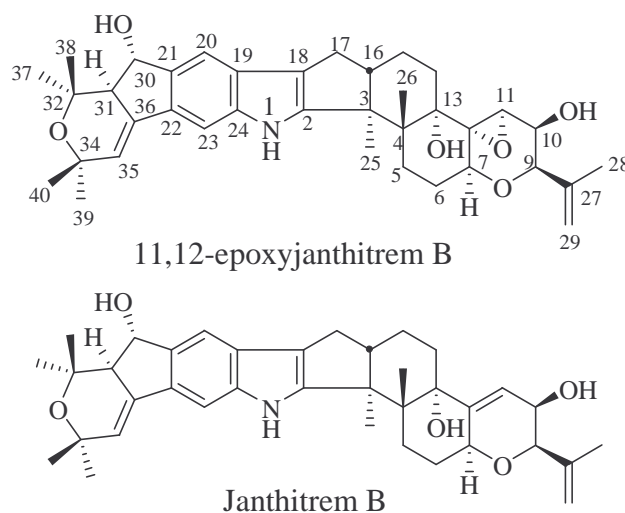


Figure 2.7. Structures of janthitrem B and 11,12-epoxyjanthitrem B.

When evaporated to dryness *in vacuo* the fractions afforded 5.28 mg of janthitrem B and 3.59 mg of 11,12-epoxyjanthitrem B as colourless waxy solids.

Renaming of 11,12-epoxyjanthitrem B

After careful consideration, it was decided that the compound initially referred to as janthitrem B epoxide (11,12-epoxyjanthitrem B) should hereafter be referred to as janthitrem A since 11,12-epoxyjanthitrem B appears to correspond to the partially characterised janthitrem A (identical molecular weights and characteristic UV absorbance spectra) previously detected in extracts of cultures of the same strain of *P. janthinellum* (Gallagher et al., 1980a). At the time however, Gallagher et al. (1980a) were not able to determine the structure of the compound they designated as janthitrem A.

Since no further information concerning the characteristics of their “janthitrem A” have been reported, it is impossible to definitively associate a subsequently obtained structure with their compound. It is proposed that the trivial name janthitrem A be given to the 11,12-epoxyjanthitrem B based on the belief that Gallagher et al.’s (1980a) janthitrem A is likely to have been 11,12-epoxyjanthitrem B.

2.3 Isolation of Janthitrem C and Janthitrem D

As extraction and isolation of janthitrem A and B from the *P. janthinellum* fungal culture, strain E1, was successful, the extraction and isolation of further janthitrem A, in particular janthitrem C, from this fungal culture was attempted (Figure 2.8).

2.3.1 Extraction and Isolation of Janthitrem C and Janthitrem D

A preparative scale culture of *P. janthinellum* strain E1 was grown and extracted as described in Sections 8.2.1 and 8.2.2. Since the de-fatting procedure utilised for the clean-up of the previous E1 extract proved successful, the same procedure

was employed here, but in this case it was utilised prior to the extract being applied to the flash column (refer to Section 8.3.1 for experimental details).

The fungal extract was then fractionated by flash column chromatography using a stepwise solvent gradient. As opposed to the isocratic system employed in the extraction and isolation of janthitrems A and B, a more gradual gradient elution was performed in this instance. Thirty 10 mL fractions were collected together with two 100 mL 100% toluene and 100% acetone fractions, respectively. Full experimental details are reported in Section 8.3.2.

Fractions eluted from the flash column were analysed by TLC (see Section 8.3.3) under short wave (254 nm) and long wave (366 nm) UV light. Analysis of the TLC plates showed that the separation achieved from the flash column was sufficient to allow fractions to be combined into four bulked fractions, each containing different compounds of interest. The first bulked fraction contained fractions 10–13, the second, fractions 14–18, the third, fractions 21–26 and the fourth, fractions 28–30. The remaining fractions were of no interest.

A janthitrem B standard was run on the TLC plate alongside the four bulked fractions which showed that the fourth fraction (28–30) appeared to contain janthitrem B on the basis of identical retention times on the plate. Each of the four bulked fractions were evaporated to dryness *in vacuo*.

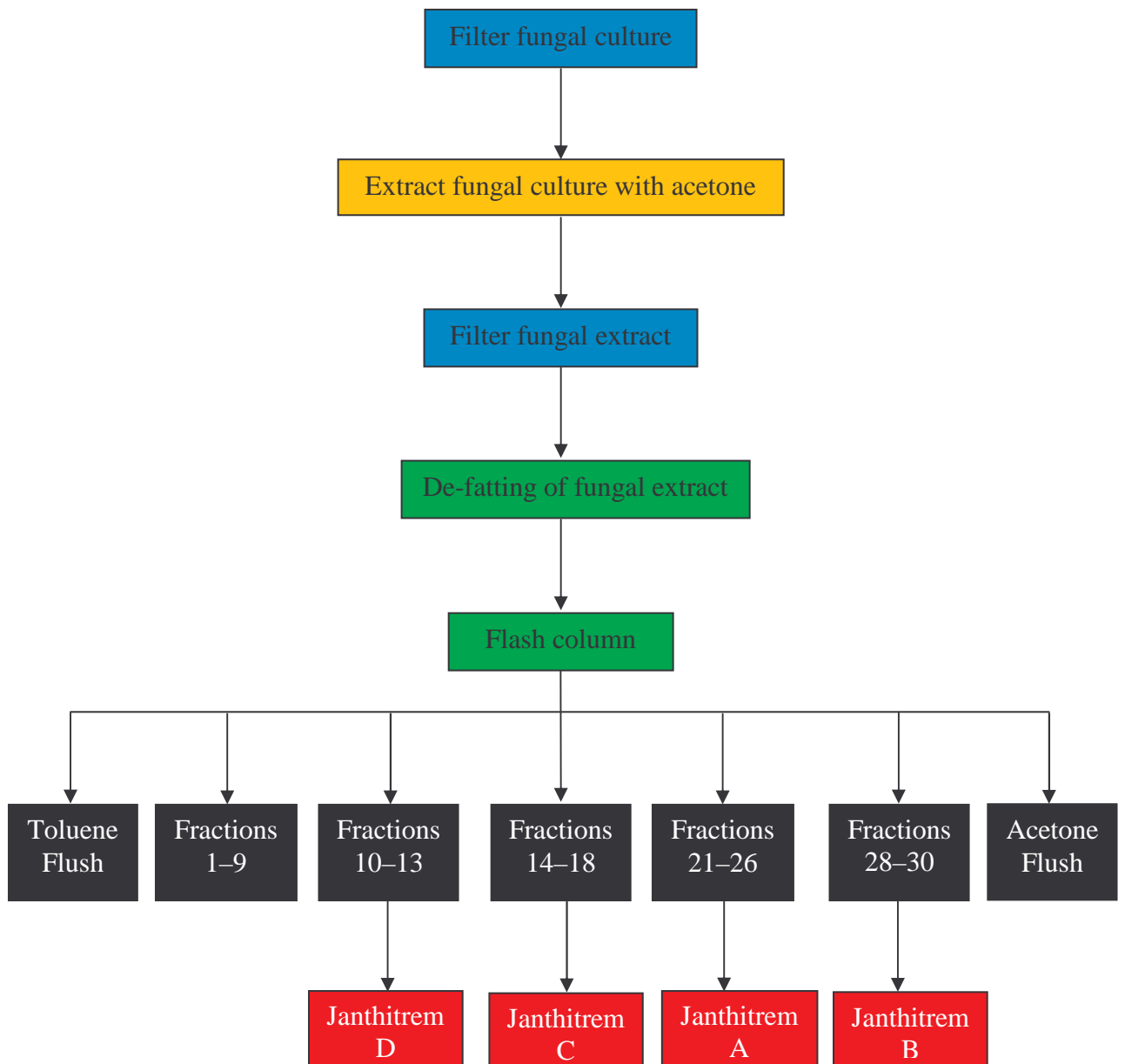


Figure 2.8. Isolation of janthitrem C and janthitrem D.

2.3.2 Analysis of *Janthitrem* Compounds

LC–UV–MS

Prior to analysis of the fractions by ^1H and ^{13}C NMR, the bulked fractions were analysed by both analytical HPLC and LC–UV–MS (as described in Sections 8.2.5 and 8.1.3, respectively).

LC–UV–MS analyses indicated that the third (flash column fractions 21–26) and fourth (flash column fractions 28–30) bulked fractions contained *janthitrem* A and *janthitrem* B based on $[\text{M}+\text{H}]^+$ ions observed at m/z 602 and 586, respectively. The remaining two fractions showed $[\text{M}+\text{H}]^+$ ions at m/z 570 (flash column fractions 14–18) and m/z 586 (flash column fractions 10–13) respectively (Figures 2.9 and 2.10).

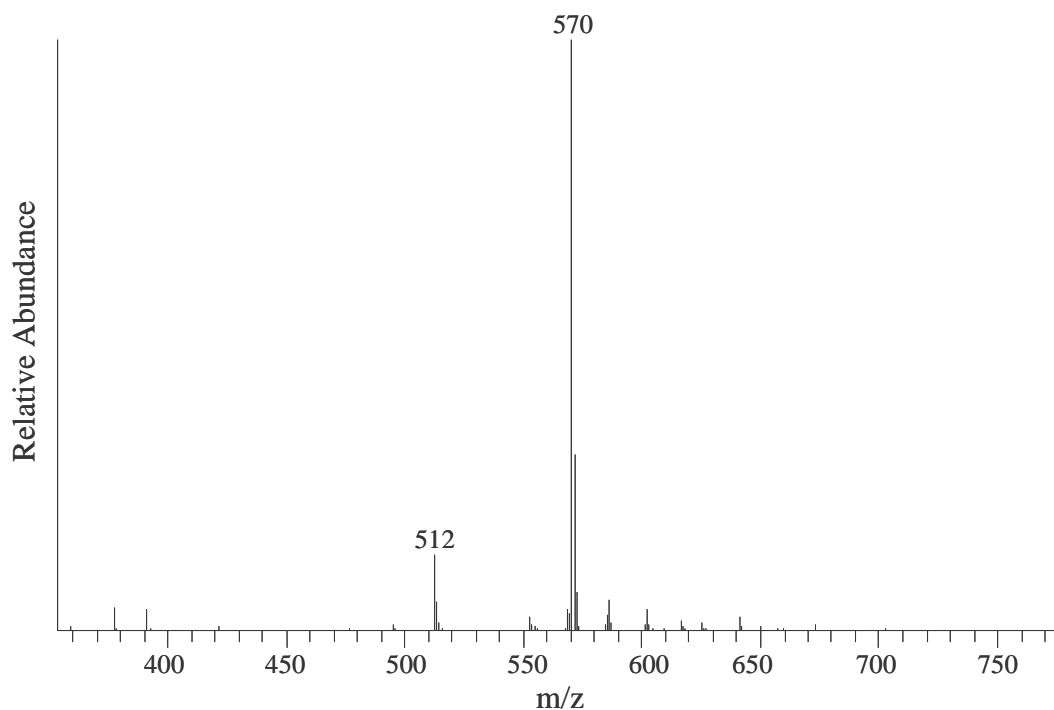


Figure 2.9. Full scan mass spectrum of fractions 14–18. Values of m/z for major ions observed are given.

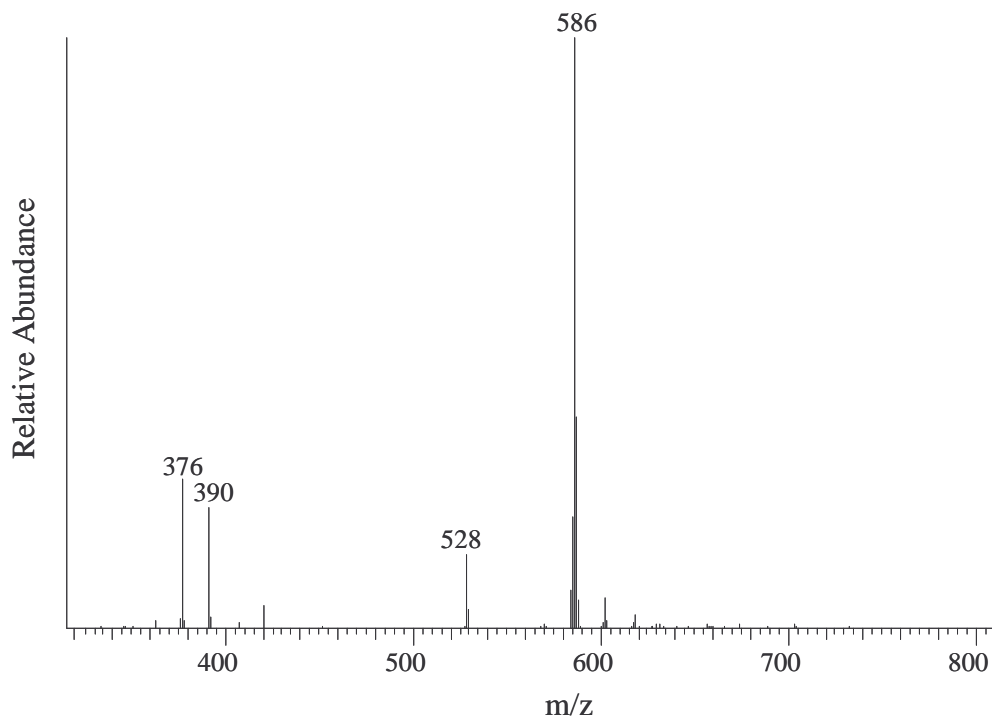


Figure 2.10. Full scan mass spectrum of fractions 10–13. Values of m/z for major ions observed are given.

The compounds which showed $[M+H]^+$ ions at m/z 570 and 586 displayed characteristic janthitrem-like UV absorbance spectra with maxima at 260 and 330 nm (Figure 2.11).

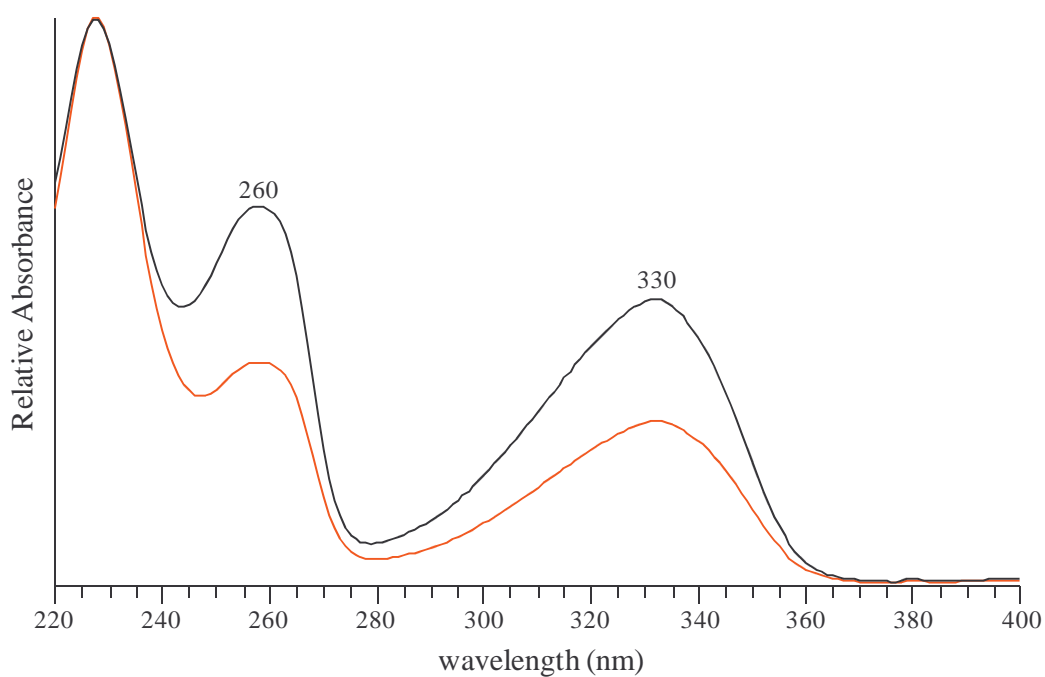


Figure 2.11. Normalised UV absorbance spectra of fractions 14–18 (red) and fractions 10–13 (black).

The masses and atomic compositions of the two compounds were established by HRMS using direct infusion electrospray (refer to Section 8.2.10). Fractions 14–18 was established in positive ion mode for its $[M+H]^+$ ion (found: m/z 569.3500 (error 2.81 ppm); calc. for $C_{37}H_{47}O_4N$ m/z 569.3484) was consistent with the known compound, janthitrem C, while fractions 10–13 in positive ion mode for its $[M+H]^+$ ion (found: m/z 585.3449 (error 4.61 ppm); calc. for $C_{37}H_{47}O_5N$ m/z 585.3422). As was the case with janthitrem A and janthitrem B, HRMS results showed the difference between these two compounds to be the presence of an extra oxygen in the unknown compound.

NMR analysis and comparison with literature data showed fractions 14–18 to contain janthitrem C. The unidentified compound was also believed to belong to the janthitrem family due to fragmentations observed during LC–UV–MS analysis and its janthitrem-like UV and fluorescence. An examination of the ^{13}C NMR data of the unidentified compound indicated that the resonances for C-7, C-9, C-10, C-11 and C-12 had shifted markedly in comparison to those observed for janthitrem C, and that the resonances observed were similar to those for janthitrem A (Table 2.3: the numbering system employed is that presented in Chapter 3, Section 3.1), consistent with an 11,12-epoxide again being present. The MS fragmentation (in negative ion mode) was also consistent with the presence of an 11,12-epoxide (see Chapter 4, Section 4.5.1) and not with an 11(12)-double bond.

Table 2.3. ^{13}C NMR resonances observed for janthitrem A, janthitrem C and the unknown janthitrem analogue (δ).

	Janthitrem C	Unknown Janthitrem	Janthitrem A
C-7	74.3	72.2	72.0
C-9	80.3	74.8	74.6
C-10	64.2	66.4	66.2
C-11	119.5	62.1	61.9
C-12	148.5	66.4	66.1

As a result, a similar structure to that observed for janthitrem A was proposed (Figure 2.12), and hence named 11,12-epoxyjanthitrem C. Subsequent NMR analysis confirmed the structure of the unknown compound (Chapter 3).

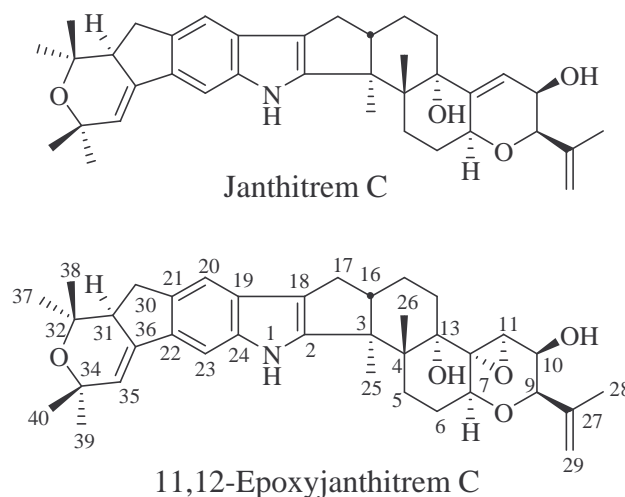


Figure 2.12. Structures of janthitrem C and 11,12-epoxyjanthitrem C.

Initial ^1H NMR analyses of janthitrem C and 11,12-epoxyjanthitrem C showed the samples were not completely pure. However, rather than further purifying the samples, it was decided to continue with the NMR analysis due to the historic instability of these compounds (see Section 2.4). This instability meant that if any further clean-up of the sample was attempted, the sample may decompose to unknown products.

The janthitrem C epoxide was believed to be a new compound as there were no previous reports for the compound in the literature. NMR data for janthitrem C has previously been reported (Penn et al., 1993) but some assignments appear improbable. Therefore, a full NMR analysis of janthitrem C was undertaken in order to unequivocally define its NMR signal assignments (as described in Chapter 3).

The two samples when evaporated to dryness *in vacuo* afforded 2.01 mg of janthitrem C and 2.51 mg of 11,12-epoxyjanthitrem C. These solids were white

with a slight yellow tinge. The yellow tinge may arise from low levels of impurities in the recovered material.

Re-naming of 11,12-epoxyjanthitrem C

As with janthitrem A (11,12-epoxyjanthitrem B), a trivial name for the janthitrem C epoxide (11,12-epoxyjanthitrem C), is proposed. Janthitrem D was originally named in the literature based on its characteristic janthitrem-like UV absorbance spectrum. However, neither a structure, nor a molecular weight was reported for the compound (Lauren and Gallagher, 1982). These authors provided no further information on the characteristics of their “janthitrem D”, so it is impossible to definitively associate a subsequently obtained structure with their compound. For the sake of consistency and completeness in the naming of janthitrem analogues, it is proposed that the janthitrem C epoxide be given the trivial name, janthitrem D.

Acetone Insolubility

After flash column chromatography was performed on the E1 fungal extract, the fraction containing janthitrem A was transferred from a large round-bottom flask to a smaller round-bottom flask using acetone. However, it became apparent that the compounds in the flask were poorly soluble in acetone and were precipitating in solution. The resulting precipitate was collected, and NMR analysis of the precipitate revealed it to be pure janthitrem A. The NMR spectrum of janthitrem A was determined using a saturated acetone solution.

The observed insolubility of janthitrem A in acetone provided a further clean-up method for this compound.

2.4 Janthitrem B Stability Investigations

2.4.1 Introduction

An important consideration when handling new and previously isolated janthitrem is their stability. The successful isolation and experimental manipulation of janthitrem and janthitrem-related compounds requires an understanding of the stability of these compounds. An improved knowledge of experimental conditions which do not promote the degradation of janthitrem is required, particularly so where there is a need to store samples for several years after their initial isolation.

2.4.2 Stability Investigation Conditions

A previously isolated specimen of janthitrem B (Section 2.2) was utilised in a series of experiments directed toward determining 'best practise' storage conditions and solvent handling conditions for janthitrem compounds. Eight test conditions, with variations in solvent, temperature and light, were investigated (Table 2.4) and the rate of degradation (if any) of janthitrem B over time was monitored. Janthitrem B samples were mixed with equal amounts of paxilline, as a reference standard, in each of the trial environments. Paxilline was selected as the reference standard as it is known to be a relatively stable compound and it could be detected and quantified under HPLC conditions appropriate for janthitrem analysis. The area of the UV peak generated by janthitrem B at 248 nm was compared to the area of the UV peak generated by paxilline at 248 nm and the extent to which the ratio of peak area changed over time was determined.

Table 2.4. Conditions used to monitor the stability of janthitrem B.

Test Condition
1) Acetone at room temperature.
2) Methanol at room temperature.
3) DMSO at room temperature.
4) Dry sample at room temperature.
5) Dry sample wrapped in tinfoil at room temperature.
6) Dry sample at 4°C.
7) Dry sample at -20°C.
8) Dry sample at -80°C.

Each of the test samples were analysed after 0, 3, 10, 24, 60, 120, 200 and 300 days. Room temperature was recorded as 20°C.

Test conditions 1–3 (Table 2.4) probed the stability of janthitrem B in three commonly used solvents, namely acetone, methanol and DMSO. Chloroform was not selected as one of the trial solvents since prior experience in our laboratory showed that janthitrem B (and other janthitrems) were progressively degraded in this solvent, or its deuterated analogue during NMR data acquisition, presumably due to the presence of traces of HCl or DCl (Wilkins et al., 1992). The situation with janthitrems appears to be similar to that for penitrems, since penitrem NMR data has been reported only in acetone and not in CDCl₃ (de Jesus et al., 1983a). Full details of the experimental procedure are reported in Section 8.4.

2.4.3 Results of the Stability Investigation

The results of the stability investigation clearly show certain conditions to be more favourable than others for the storage of janthitrem B. Results were considered to be accurate to $\pm 3\%$, with only the 10 day DMSO point showing an apparent greater uncertainty than this.

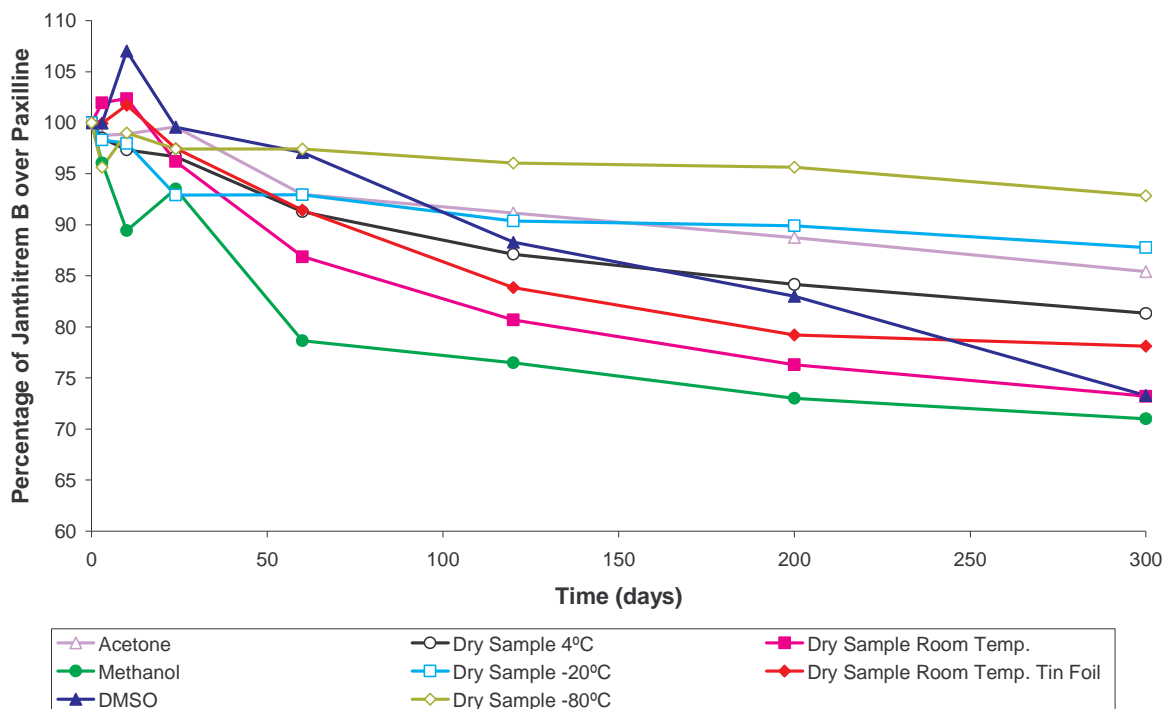


Figure 2.13. Graph displaying stability properties of tested conditions.

Figure 2.13 shows the least favourable test condition to be storage in methanol at room temperature. This resulted in a jantithrem B level of 71% compared to the $t = 0$ level, (i.e. a 29% degradation over the test period of 300 days). The jantithrem B samples stored dry and in DMSO (both at room temperature) showed a similar level of degradation (*ca.* 27% degradation). The jantithrem B sample stored in acetone displayed reasonable stability, showing only a 15% sample loss compared to 29% and 27% loss in methanol and DMSO respectively.

Of all the samples stored at room temperature, the sample stored in acetone displayed the greatest stability, followed by the dry sample wrapped in tin foil. The sample stored in tin foil gave less degradation than the sample stored on the bench (without tinfoil), suggesting jantithrem B may be slightly photosensitive. This sensitivity to light was avoided in the test conditions of 4°C, -20°C and -80°C as samples were stored in a fridge or freezer thus preventing exposure to light.

The results of this investigation indicate that the samples stored dry appear to exhibit greater stability than those stored in solution, with the exception only of

the sample stored in acetone. The remaining samples stored in solution (DMSO and methanol) displayed the greatest extent of degradation. It was also apparent from this stability trial that janthitrem B storage is preferable in colder conditions, where the lower the storage temperature, the greater the stability. Therefore, the dry sample stored at the lowest temperature of -80°C provided the ideal conditions for minimal sample degradation where only 7% degradation was observed over the 300 day stability trial. The next most favourable storage condition for janthitrem B was the sample kept dry at -20°C . The ranking order of the test conditions according to the percentage of janthitrem B degradation is given in Table 2.5.

Table 2.5. Test conditions ranked based on percentage of janthitrem B degraded. Unless otherwise stated, samples were stored at room temperature (20°C).

Test Condition	Percentage of Janthitrem B Degraded (%)
Dry sample, -80°C	7%
Dry sample, -20°C	12%
Acetone	15%
Dry sample at 4°C .	19%
Dry sample wrapped in tinfoil	22%
DMSO	27%
Dry sample	27%
Methanol	29%

2.4.4 Summary of Findings

As a consequence of these findings, all future janthitrem B extractions and handling should be conducted using acetone as the solvent wherever possible. Long term storage of janthitrem B samples should be at -80°C (dry). The capping of samples with nitrogen or argon (which drives out oxygen thus preventing oxidation of samples), as was practiced with NMR samples, will further minimise sample degradation.

CHAPTER THREE

NMR Analysis of Janthitrems A, B, C and D

3.1 Introduction

Detailed analyses of one- and two-dimensional NMR data, including ^1H , ^{13}C , DEPT-135, COSY, TOCSY, g-HSQC, g-HMBC and NOESY NMR spectral data afforded complete ^1H and ^{13}C NMR assignments for janthitrems A, B, C and D. ^1H - ^1H connectivities were established using COSY and TOCSY spectral data and ^1H - ^{13}C connectivities were established using g-HSQC and g-HMBC data. The information provided by the NOESY spectral data allowed the orientation of CH_2 protons (as alpha or beta; axial or equatorial) and of methyl groups of the janthitrems to be defined. Typical NMR acquisition and processing parameters are reported in Section 8.2.11.

Since the use of CDCl_3 results in the progressive decomposition of janthitrems (Wilkins et al., 1992), presumably due to the presence of trace amounts of DCl in the CDCl_3 , all janthitrem samples were made up in acetone- D_6 for NMR analysis.

In this study, the atom numbering used for janthitrems and penitrems (Figure 3.1) has been modified to permit direct comparison of NMR chemical shifts between these compounds and other biosynthetically related indole-diterpenoids, based on the atom numbering proposed for the same reason for lolitrems and paxilline by Miles et al. (1992). It should be noted that the stereochemistry depicted at C-31 of the janthitrems is that proposed recently for a specimen of the structurally related compound shearinine D, isolated from an endophytic *Penicillium* sp. (Xu et al., 2007), although the C-31 stereochemistry of janthitrems remains undefined. All the structures presented in this thesis have been numbered using the revised

numbering system and are depicted as having the shearinine D stereochemistry at C-31.

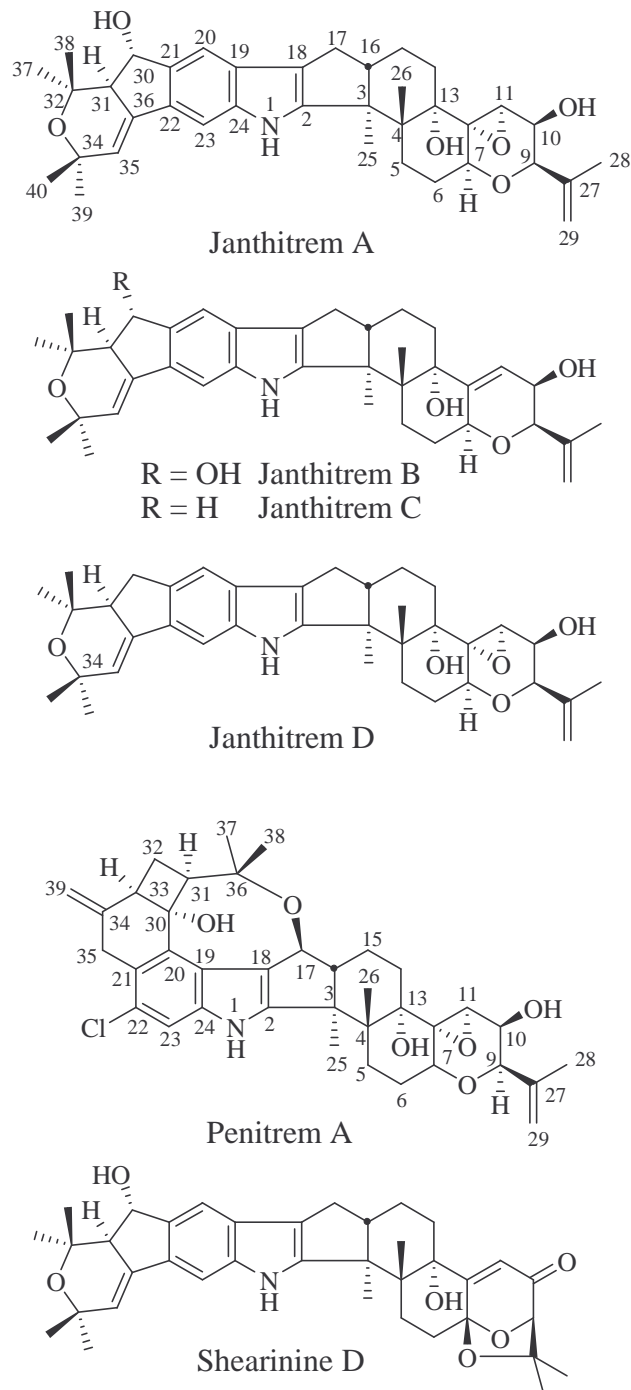


Figure 3.1. Numbered structures for janthitrem A–D, penitrem A and shearinine D.

3.2 Janthitrem B NMR Discussion

One- and two-dimensional NMR data for janthitrem B was acquired and processed as described in Section 8.2.11. Signal assignments for janthitrem B were facilitated by comparison with those previously reported for janthitrem B (Wilkins et al., 1992). A complete assignment of the resonances of janthitrem B is presented in Table 3.1. Methylene proton assignments are reported in the format (H_{α}, H_{β}) based on analyses of coupling constant and/or NOE data. Correlations observed in two-dimensional NMR experiments that substantiated these assignments are reported in Tables 3.2, 3.3, 3.4 and 3.5.

The NMR data reported in this thesis was determined at 400 MHz and are of a higher quality than those previously determined for janthitrem B at 300 MHz (Wilkins et al., 1992). Moreover, due to instrumental limitations, only basic two-dimensional NMR data (COSY and XHCOR spectra) were recorded in the earlier study (Wilkins et al., 1992). During the course of the NMR investigations reported in this chapter it became apparent from analysis of the data reported in Tables 3.1, 3.2, 3.3, 3.4 and 3.5, that some revisions to previously proposed NMR assignments were required, including revised assignments for the H-14 methylene group signals, the H-16 methine signal, and the C-39 and C-40 methyl carbon signals.

3.2.1 1H , ^{13}C , DEPT-135, COSY and TOCSY NMR Spectra of Janthitrem B

^{13}C and DEPT-135 NMR spectra of janthitrem B revealed the presence of 37 carbon resonances (7 methyl, 6 methylene, 10 methine and 14 quaternary). These resonances were for the most part almost identical to those reported by Wilkins et al. (1992) with differences only within the 0.1–0.2 ppm range. Variations of this magnitude can be accounted for by small differences in compound concentration, the level of residual water in the sample and the NMR probe temperature (30°C in

the present study compared to 300 K (26.85°C) in the earlier study (Wilkins et al., 1992)).

The proton resonances for janthitrem B were also very similar to those reported by Wilkins et al. (1992) with the exception of assignments proposed for the H-14 methylene and H-16 methine proton signals.

Table 3.1. ^1H and ^{13}C NMR assignments established for janthitrems A and B and published assignments for penitrem A^a (δ).

	Janthitrem B		Janthitrem A		Penitrem A	
	^{13}C	^1H (α,β)	^{13}C	^1H (α,β)	^{13}C	^1H (α,β)
C-2	155.9		155.4		154.4	
C-3	51.9		51.8		50.1	
C-4	43.5		43.3		43.6	
C-5	28.1	2.61, 1.61	27.2	2.65, 1.60	26.9	2.61, 1.57
C-6	29.2	2.06, 1.82	28.8	2.22, 2.04	28.9	2.22, 2.04
C-7	74.3	4.59	72.0	4.28	72.0	4.29
C-9	80.4	3.79	74.6	4.03	74.7	4.04
C-10	64.3	3.91	66.2	4.04	66.3	4.04
C-11	119.5	5.71	61.9	3.53	61.9	3.57
C-12	148.5		66.1		66.1	
C-13	77.5		78.3		78.2	
C-14	34.7	1.64, 1.81	30.3	1.63, 1.53	30.6	1.68, 1.48
C-15	22.1	2.04, 1.62	21.5	1.97, 1.56	18.6	1.92, 1.78
C-16	50.6	2.73	50.8	2.83	58.8	2.63
C-17	27.9	2.37, 2.66	27.8	2.37, 2.66	72.4	4.93
C-18	116.9		116.6		120.6	
C-19	127.8		127.7		122.0	
C-20	114.1	7.374	103.5	7.366	133.3	
C-21	140.1		140.1		125.8	
C-22	131.7		131.7		124.6	
C-23	103.6	7.366	114.2	7.371	111.9	7.24
C-24	142.2		142.2		139.7	
C-25	16.6	1.34	16.5	1.33	21.4	1.40
C-26	20.1	0.92	18.9	1.20	19.0	1.22
C-27	143.9		143.2		143.3	
C-28	20.0	1.76	19.7	1.70	19.7	1.71
C-29	110.8	5.08 (Z), 4.87 (E)	111.6	5.07 (Z), 4.87 (E)	111.6	5.07, 4.87
C-30	76.4	4.90	76.3	4.89	81.0	
C-31	60.4	2.65	60.3	2.64	52.7	2.49
C-32	74.3		74.3		24.7	2.41, 2.26
C-33					47.0	2.98
C-34	72.6		72.6		149.5	
C-35	120.1	5.97	120.2	5.95	35.1	3.63, 3.26
C-36	137.2		137.1		76.1	
C-37	30.6	1.40	30.6	1.40	20.3	1.75
C-38	23.7	1.09	23.6	1.08	31.1	1.07
C-39	32.5	1.24	32.5	1.24	107.1	5.01, 4.86
C-40	30.4	1.29	30.4	1.28		
10-OH		2.99		3.33		3.40
13-OH		3.30		3.22		3.32
30-OH		4.23		4.21		4.16
NH		9.80		9.89		10.03

^ade Jesus et al. (1983a)

H-14 Signal Assignments

Wilkins et al. (1992) have previously reported that the H-14 methylene protons resonate at 1.58 and 1.70 ppm, however, this was not consistent with the assignments elucidated in this investigation. The g-HSQC NMR spectrum of janthitrem B in this study included correlations between the C-14 carbon signal which occurred at 34.7 ppm and proton signals which resonated at 1.64 and 1.81 ppm, respectively. The C-14 signals resonance position was elucidated by correlations observed in the g-HMBC NMR spectrum, whereby the 13-OH signal showed correlations to three quaternary carbons (C-4, C-12 and C-13) and one methylene carbon (C-14). This readily defined the C-14 carbon resonance as 34.7 ppm.

The H-14 signals were confirmed by correlations observed in the COSY and TOCSY NMR spectra (see Figures 3.2 and 3.3 respectively). The TOCSY NMR spectrum, which emphasised long-range couplings, was determined with a mixing time of 160 msec. Specifically, each of the H-14 signals (1.64 and 1.81 ppm) showed correlations to the H-15 (1.62 and 2.04 ppm) signals in the COSY NMR spectrum and to H-11 (5.71 ppm), 13-OH (3.30 ppm), H-15 (1.62 and 2.04 ppm), H-16 (2.73 ppm) and H-17 (2.37 and 2.66 ppm) in the TOCSY NMR spectrum.

H-16 Signal Assignment

Wilkins et al. (1992) previously reported H-16 to resonate at 2.68 ppm. This was not consistent with the findings of this study since the g-HSQC NMR spectrum of janthitrem B included a correlation between C-16 (50.6 ppm) and its attached methine proton (H-16) at 2.73 ppm. The carbon signal was confirmed by correlations observed in the g-HMBC NMR spectrum, where H-25 showed correlations to three quaternary carbons (C-2, C-3 and C-4) and to one methine carbon (C-16). This readily defined the C-16 resonance as 50.6 ppm. The H-16 proton signal showed correlations to H-15 (1.62 and 2.04 ppm) and H-17 (2.37 and 2.66 ppm) in the COSY NMR spectrum and to H-14 (1.64 and 1.81 ppm), H-

15 (1.62 and 2.04 ppm), H-17 (2.37 and 2.66 ppm) and 13-OH (3.30 ppm) in the TOCSY NMR spectrum, thereby confirming its assignment.

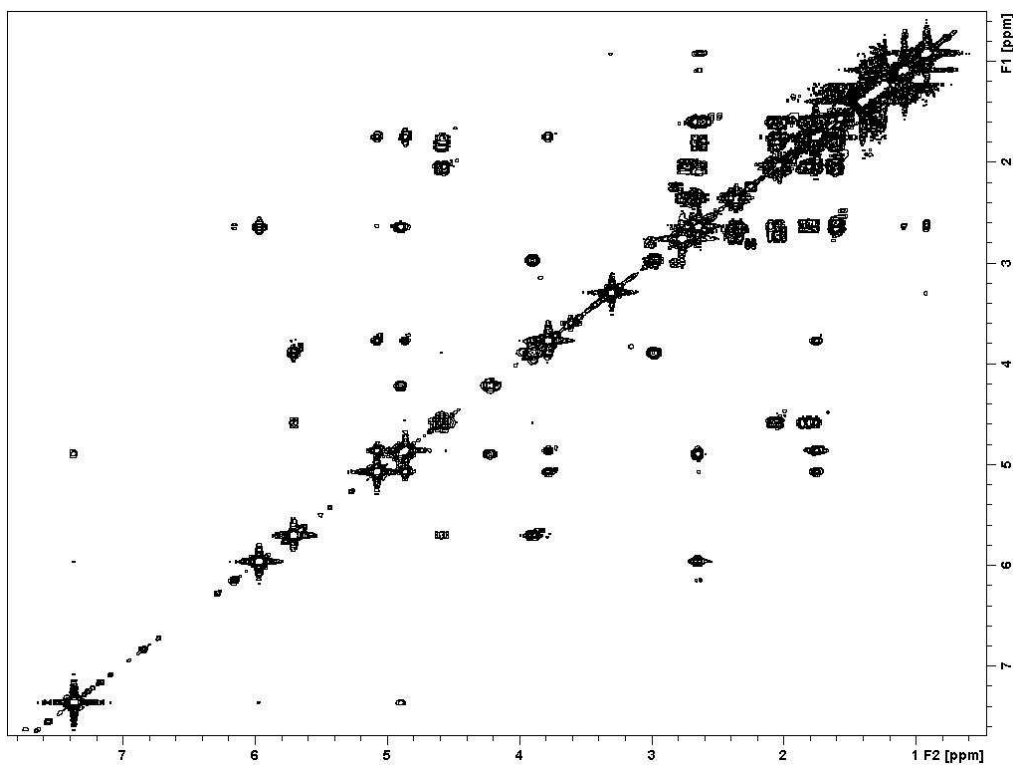


Figure 3.2. The COSY NMR spectrum of janthitrem B.

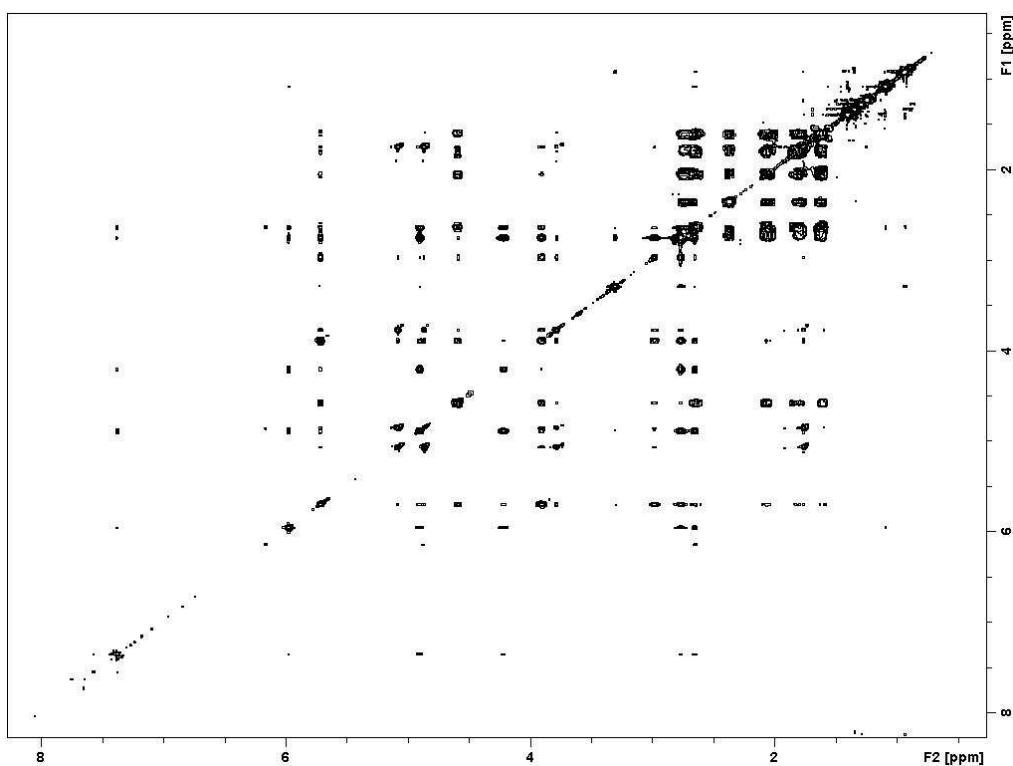


Figure 3.3. The TOCSY NMR spectrum of janthitrem B.

Table 3.2. COSY NMR correlations observed for janthitrem B (δ).

¹ H Signal	Cross peaks observed
0.92 (H-26)	2.61 (H-5 α), 3.30 (13-OH)
1.09 (H-38)	1.40 (H-37), 2.65 (H-31)
1.24 (H-39)	1.29 (H-40)
1.40 (H-37)	1.09 (H-38)
1.61 (H-5 β)	1.82 (H-6 β), 2.06 (H-6 α), 2.61 (H-5 α)
1.62 (H-15 β)	1.81 (H-14 β), 2.04 (H-15 α), 2.73 (H-16)
1.64 (H-14 α)	1.81 (H-14 β), 2.04(H-15 α)
1.76 (H-28)	3.79 (H-9), 4.87 (H-29E), 5.08 (H-29Z)
1.81 (H-14 β)	1.64 (H-14 α), 1.62 (H-15 β), 2.04 (H-15 α)
1.82 (H-6 β)	2.06 (H-6 α), 1.61 (H-5 β), 2.61 (H-5 α), 4.59 (H-7)
2.04 (H-15 α)	1.64 (H-14 α), 1.81 (H-14 β), 1.62 (H-15 β), 2.73 (H-16)
2.06 (H-6 α)	1.82 (H-6 β), 1.61 (H-5 β), 2.61 (H-5 α), 4.59 (H-7)
2.37 (H-17 α)	2.66 (H-17 β), 2.73 (H-16)
2.61 (H-5 α)	0.92 (H-26), 1.82 (H-6 β), 2.06 (H-6 α), 1.61 (H-5 β)
2.65 (H-31)	1.09 (H-38), 4.90 (H-30), 5.97 (H-35)
2.66 (H-17 β)	2.37 (H-17 α), 2.73 (H-16)
2.73 (H-16)	1.62 (H-15 β), 2.04 (H-15 α), 2.37 (H-17 α), 2.66 (H-17 β)
2.99 (10-OH)	3.91 (H-10)
3.30 (13-OH)	0.92 (H-26)
3.79 (H-9)	1.76 (H-28), 3.91 (H-10), 4.87 (H-29E), 5.08 (H-29Z)
3.91 (H-10)	5.71 (H-11), 2.99 (10-OH), 3.79 (H-9)
4.23 (30-OH)	4.90 (H-30)
4.59 (H-7)	1.82 (H-6 β), 2.06 (H-6 α), 5.71 (H-11)
4.87 (H-29E)	1.76 (H-28), 3.79 (H-9), 5.08 (H-29Z)
4.90 (H-30)	2.65 (H-31), 4.23 (30-OH), 7.374 (H-20)
5.08 (H-29Z)	1.76 (H-28), 3.79 (H-9), 4.87 (H-29E)
5.71 (H-11)	3.91 (H-10), 4.59 (H-7)
5.97 (H-35)	2.65 (H-31)
7.38 (H-20)	4.90 (H-30)

Table 3.3. TOCSY NMR correlations observed for janthitrem B (δ).

¹ H Signal	Cross peaks observed
0.92 (H-26)	2.61 (H-5 α), 3.30 (13-OH)
1.09 (H-38)	1.40 (H-37), 2.65 (H-31), 4.23 (30-OH)
1.24 (H-39)	1.29 (H-40), 5.97 (H-35)
1.29 (H-40)	1.24 (H-39)
1.40 (H-37)	1.09 (H-38), 2.65 (H-31), 4.23 (30-OH)
1.61 (H-5 β)	1.82 (H-6 β), 2.06 (H-6 α), 2.61 (H-5 α), 4.59 (H-7)
1.62 (H-15 β)	1.81 (H-14 β), 2.04 (H-15 α), 2.37 (H-17 α), 2.66 (H-17 β), 2.73 (H-16), 3.30 (13-OH)
1.64 (H-14 α)	1.81 (H-14 β), 2.04 (H-15 α), 2.37 (H-17 α), 2.66 (H-17 β), 2.73 (H-16), 3.30 (13-OH), 5.71 (H-11)
1.76 (H-28)	3.79 (H-9), 3.91 (H-10), 2.99 (10-OH), 4.87 (H-29E), 5.08 (H-29Z)
1.81 (H-14 β)	1.64 (H-14 α), 1.62 (H-15 β), 2.04 (H-15 α), 2.37 (H-17 α), 2.66 (H-17 β), 2.73 (H-16), 3.30 (13-OH), 5.71 (H-11)
1.82 (H-6 β)	2.06 (H-6 α), 1.61 (H-5 β), 2.61 (H-5 α), 4.59 (H-7), 5.71 (H-11), 3.30 (13-OH)
2.04 (H-15 α)	1.64 (H-14 α), 1.81 (H-14 β), 1.62 (H-15 β), 2.37 (H-17 α), 2.66 (H-17 β), 2.73 (H-16), 3.30 (13-OH)
2.06 (H-6 α)	1.82 (H-6 β), 1.61 (H-5 β), 2.61 (H-5 α), 4.59 (H-7), 5.71 (H-11), 3.30 (13-OH)
2.37 (H-17 α)	1.34 (H-25), 1.64 (H-14 α), 1.81 (H-14 β), 1.62 (H-15 β), 2.04 (H-15 α), 2.66 (H-17 β), 2.73 (H-16), 7.374 (H-20)
2.61 (H-5 α)	0.92 (H-26), 1.61 (H-5 β), 1.82 (H-6 β), 2.06 (H-6 α), 3.30 (13-OH), 4.59 (H-7)
2.65 (H-31)	1.09 (H-38), 4.23 (30-OH), 4.90 (H-30), 5.97 (H-35)
2.66 (H-17 β)	1.64 (H-14 α), 1.81 (H-14 β), 1.62 (H-15 β), 2.04 (H-15 α), 2.37 (H-17 α), 2.73 (H-16), 7.374 (H-20)
2.73 (H-16)	1.64 (H-14 α), 1.81 (H-14 β), 1.62 (H-15 β), 2.04 (H-15 α), 2.37 (H-17 α), 2.66 (H-17 β), 3.30 (13-OH)
2.99 (10-OH)	1.76 (H-28), 3.30 (13-OH), 3.79 (H-9), 3.91 (H-10), 4.59 (H-7), 4.87 (H-29E), 5.08 (H-29Z), 5.71 (H-11)

Table 3.3 continued

3.30 (13-OH)	0.92 (H-26), 1.64 (H-14 α), 1.81 (H-14 β), 2.99 (10-OH), 3.91 (H-10), 4.59 (H-7), 5.71 (H-11)
3.79 (H-9)	1.76 (H-28), 3.91 (H-10), 4.87 (H-29E), 5.08 (H-29Z), 5.71 (H-11), 4.59 (H-7), 2.99 (10-OH)
3.91 (H-10)	1.76 (H-28), 3.79 (H-9), 4.87 (H-29E), 5.08 (H-29Z), 5.71 (H-11), 4.59 (H-7), 2.99 (10-OH), 3.30 (13-OH)
4.23 (30-OH)	1.09 (H-38), 1.40 (H-37), 2.65 (H-31), 4.90 (H-30), 5.97 (H-35), 7.374 (H-20)
4.59 (H-7)	1.82 (H-6 β), 2.06 (H-6 α), 1.61 (H-5 β), 2.61 (H-5 α), 2.99 (10-OH), 3.79 (H-9), 3.91 (H-10), 5.71 (H-11)
4.87 (H-29E)	1.76 (H-28), 2.99 (10-OH), 3.79 (H-9), 3.91 (H-10), 5.08 (H-29Z)
4.90 (H-30)	2.65 (H-31), 4.23 (30-OH), 5.97 (H-35), 7.374 (H-20)
5.08 (H-29Z)	1.76 (H-28), 2.99 (10-OH), 3.79 (H-9), 3.91 (H-10), 4.87 (H-29E)
5.71 (H-11)	1.76 (H-28), 1.64 (H-14 α), 1.81 (H-14 β), 1.82 (H-6 β), 2.06 (H-6 α), 2.99 (10-OH), 3.30 (13-OH), 3.91 (H-10), 4.59 (H-7)
5.97 (H-35)	1.24 (H-39), 1.29 (H-40), 2.65 (H-31), 4.90 (H-30), 4.23 (30-OH), 7.366 (H-23)
7.366 (H-20) & 7.374 (H-23)	2.65 (H-31), 4.23 (30-OH), 4.90 (H-30), 5.97 (H-35)

3.2.2 *g*-HSQC and *g*-HMBC NMR Spectra of *Janthitrem B*

Analysis of *g*-HSQC and *g*-HMBC NMR spectral data (Figures 3.4 and 3.5 respectively) allowed the unequivocal assignment of C-31, C-32, C-34 and C-35 signals and their attached protons. The *g*-HSQC NMR spectrum showed that the C-37, C-38, C-39 and C-40 methyl carbon signals which resonated at 30.6, 23.7, 32.5 and 30.4 ppm, respectively, exhibited correlations to protons which resonated at 1.40, 1.09, 1.24 and 1.29 ppm, respectively. This data showed that the H-39

and H-40 signals are assigned to C-40 and C-39, respectively, by Wilkins et al. (1992) and should be revised as in Table 3.1.

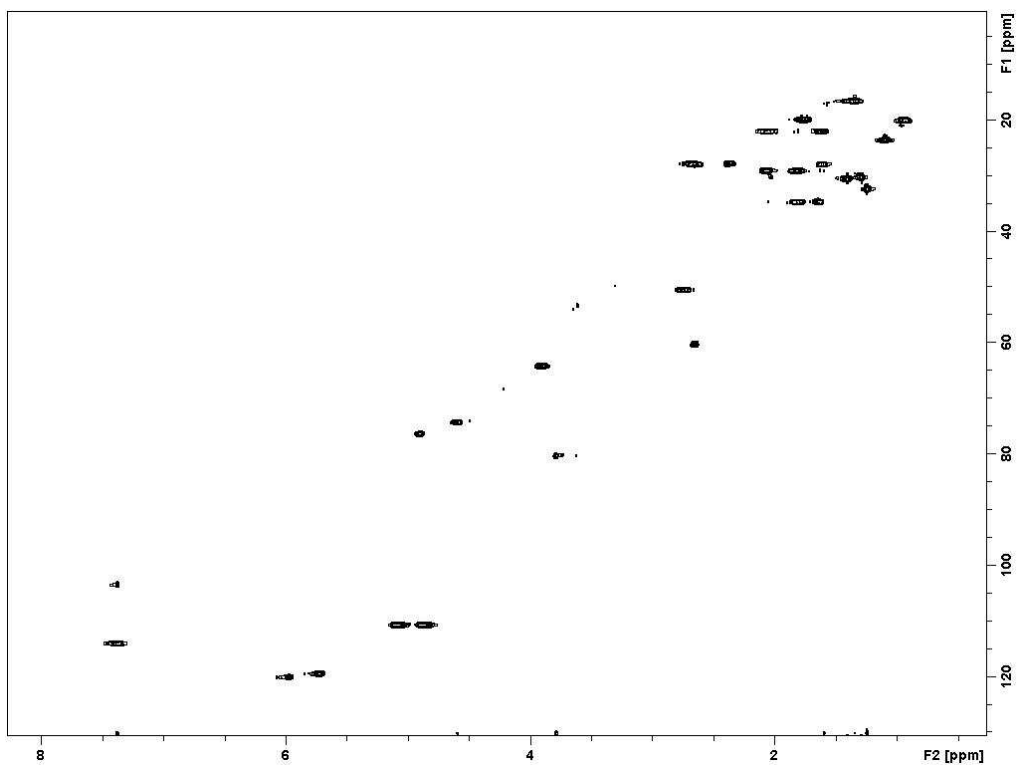


Figure 3.4. The g-HSQC NMR spectrum of janthitrem B.

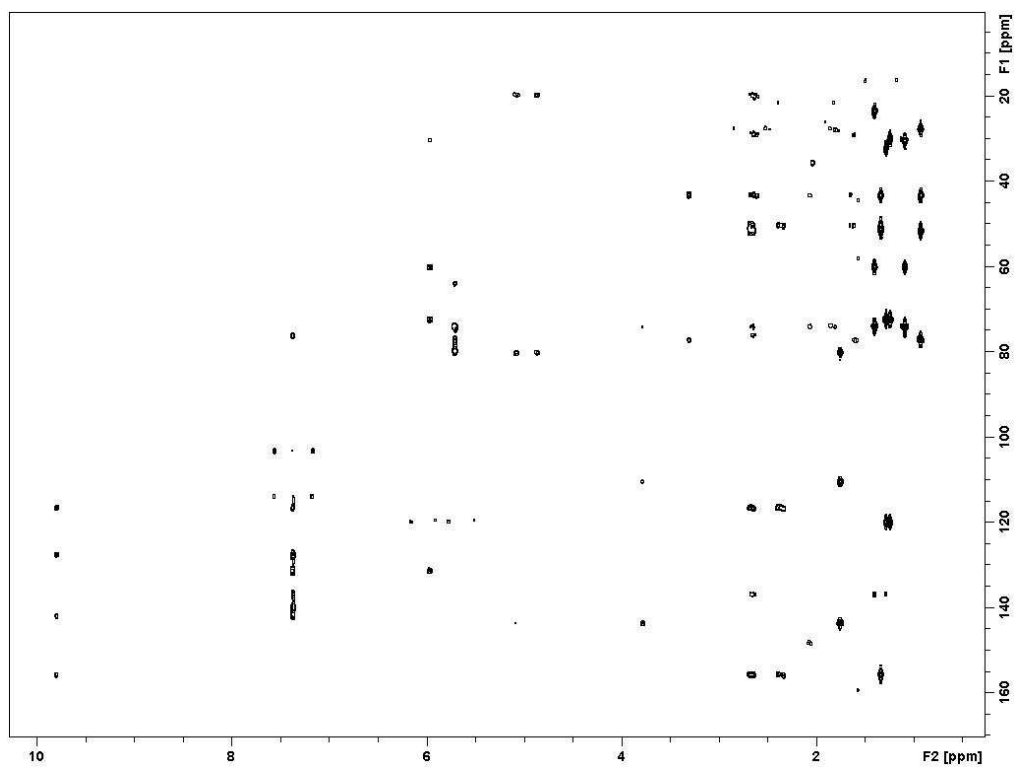


Figure 3.5. The g-HMBC NMR spectrum of janthitrem B.

In the g-HMBC NMR spectrum, H-39 (1.24 ppm) and H-40 (1.29 ppm) both showed correlations to C-34 (72.6 ppm) and C-35 (120.1 ppm), while H-37 (1.40 ppm) and H-38 (1.09 ppm) both showed correlations to C-31 (60.4 ppm) and C-32 (74.3 ppm). The observed g-HMBC correlations are illustrated in Figures 3.6 and 3.7.

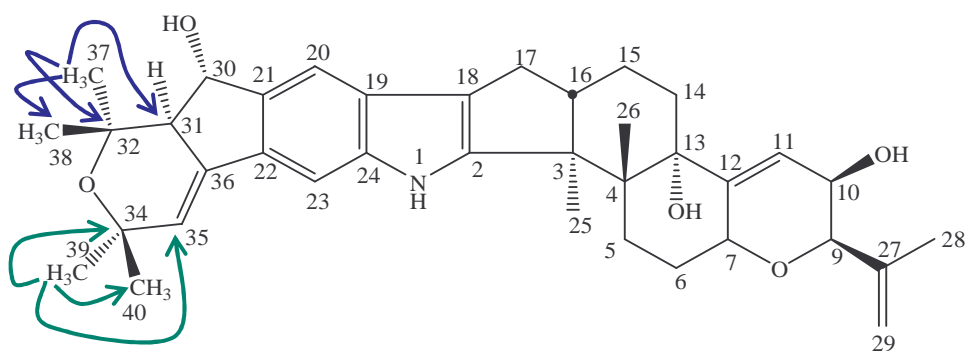


Figure 3.6. Selected g-HMBC correlations observed for H-37 and H-39 of janthitrem B.

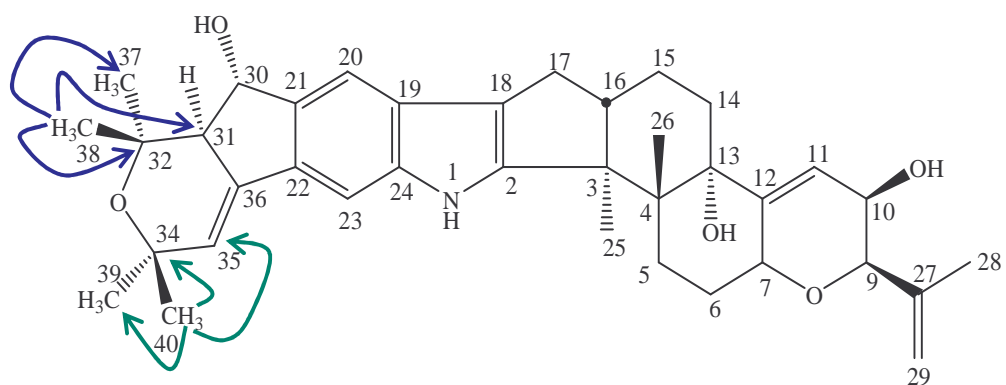


Figure 3.7. Selected g-HMBC correlations observed for H-38 and H-40 of janthitrem B.

Table 3.4. Long-range ^{13}C - ^1H NMR correlations observed in the g-HMBC NMR spectrum of janthitrem B (δ).

^1H Signal	Correlated ^{13}C Signals
0.92 (H-26)	28.1 (C-5), 43.5 (C-4), 51.9 (C-3), 77.5 (C-13)
1.09 (H-38)	30.6 (C-37), 60.4 (C-31), 74.3 (C-32)
1.24 (H-39)	30.4 (C-40), 72.6 (C-34), 120.1 (C-35)
1.29 (H-40)	32.5 (C-39), 72.6 (C-34), 120.1 (C-35)
1.34 (H-25)	43.5 (C-4), 50.6 (C-16), 51.9 (C-3), 155.9 (C-2)
1.40 (H-37)	23.7 (C-38), 60.4 (C-31), 74.3 (C-32)
1.61 (H-5 β)	20.1 (C-26), 29.2 (C-6), 43.5 (C-4), 51.9 (C-3), 74.3 (C-7), 77.5 (C-13)
1.62 (H-15 β)	27.9 (C-17), 34.7 (C-14), 50.6 (C-16), 51.9 (C-3), 77.5 (C-13)
1.64 (H-14 α)	22.1 (C-15), 43.5 (C-4), 50.6 (C-16), 77.5 (C-13), 148.5 (C-12)
1.76 (H-28)	80.4 (C-9), 110.8 (C-29), 143.9 (C-27)
1.81 (H-14 β)	22.1 (C-15), 43.5 (C-14), 50.6 (C-16), 77.5 (C-13), 148.5 (C-12)
1.82 (H-6 β)	28.1 (C-5), 43.5 (C-4), 74.3 (C-7)
2.04 (H-15 α)	27.9 (C-17), 34.7 (C-14), 50.6 (C-16), 51.9 (C-3), 77.5 (C-13)
2.06 (H-6 α)	43.5 (C-4), 28.1 (C-5), 74.3 (C-7), 148.5 (C-12)
2.37 (H-17 α)	22.1 (C-15), 50.6 (C-16), 51.9 (C-3), 116.9 (C-18), 127.8 (C-19), 155.9 (C-2)
2.61 (H-5 α)	20.1 (C-26), 29.2 (C-6), 43.5 (C-4), 51.9 (C-3), 74.3 (C-7), 77.5 (C-13)
2.65 (H-31)	23.7 (C-38), 30.6 (C-37), 74.3 (C-32), 76.4 (C-30), 120.1 (C-35), 131.7 (C-22), 137.2 (C-36), 140.1 (C-21)
2.66 (H-17 β)	22.1 (C-15), 50.6 (C-16), 51.9 (C-3), 116.9 (C-18), 127.8 (C-19), 155.9 (C-2)
2.73 (H-16)	16.6 (C-25), 22.1 (C-15), 27.9 (C-17), 34.7 (C-14), 43.5 (C-4), 51.9 (C-3), 155.9 (C-2)
3.30 (13-OH)	34.7 (C-14), 43.5 (C-4), 148.5 (C-12)
3.79 (H-9)	20.0 (C-28), 64.3 (C-10), 74.3 (C-7), 110.8 (C-29), 143.9 (C-27)
4.59 (H-7)	28.1 (C-5), 29.2 (C-6), 119.5 (C-11), 148.5 (C-12)
4.87 (H-29E)	20.0 (C-28), 80.4 (C-9), 143.9 (C-27)

Table 3.4 continued

5.08 (H-29Z)	20.0 (C-28), 80.4 (C-9), 143.9 (C-27)
5.71 (H-11)	64.3 (C-10), 74.3 (C-7), 77.5 (C-13), 80.4 (C-9), 148.5 (C-12)
5.97 (H-35)	30.4 (C-40), 32.5 (C-39), 60.4 (C-31), 72.6 (C-34), 131.7 (C-22), 137.2 (C-36)
7.374 (H-20) &	76.4 (C-30), 103.6 (C-23), 116.9 (C-18), 114.1 (C-20),
7.366 (H-23)	127.8 (C-19), 131.7 (C-22), 137.2 (C-36), 140.1 (C-21), 142.2 (C-24)
9.80 (NH)	116.9 (C-18), 127.8 (C-19), 142.2 (C-24), 155.9 (C-2)

3.2.3 NOESY NMR Spectrum of *Janthitrem B*

Information concerning the spatial relationships between protons and methyl groups and the orientation of protons was obtained from phase-sensitive two-dimensional NOESY experiments. Molecular modelling (refer to Section 8.2.12 for details on the software used) was used to estimate inter-nuclear distances and to determine whether correlations seen in the NOESY NMR spectrum were feasible (and not COSY-like or symmetrisation artefacts).

The NOESY NMR spectrum (Figure 3.8) served to define the stereochemical dispositions of the H-37, H-38, H-39 and H-40 methyl groups. When NMR assignments were first proposed for *janthitrem B* by Wilkins et al. (1992), the H-37 and H-39 were assigned by convention as being α -oriented (i.e. inclined towards the lower face), while the H-38 and H-40 methyl groups protons were by convention assigned as being β -oriented (i.e. inclined towards the upper face).

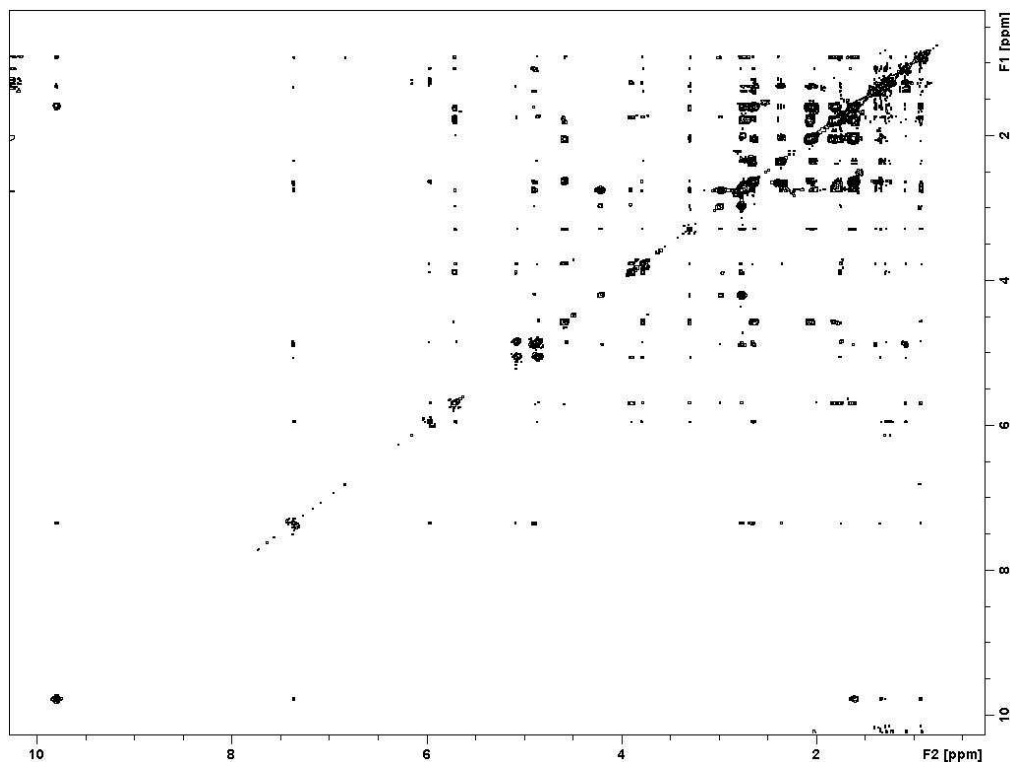


Figure 3.8. The NOESY NMR spectrum of janthitrem B.

The proton signal at 1.40 ppm showed NOESY correlations to signals at 1.09 ppm, 2.65 ppm (H-31) and 4.90 ppm (H-30). The only methyl signal which could be expected to show correlations with these signals is H-37, therefore the signal at 1.40 ppm can be attributed to H-37. Consequently, the signal at 1.09 ppm can be attributed to H-38. This assignment was confirmed by correlations observed in the NOESY NMR spectrum of janthitrem B where the proton signal at 1.09 ppm showed correlations to signals at 4.90 ppm (H-30), 1.40 ppm (H-37) and 1.29 ppm. The only methyl signal which could show correlations to these signals is H-38.

The proton signal at 1.24 ppm showed NOESY correlations to signals at 2.65 ppm (H-31), 5.97 ppm (H-35) and 1.29 ppm. The only methyl signal which could give these correlations is H-39. Since the signal at 1.24 ppm was identified as H-39, the signal at 1.29 ppm can be attributed to H-40. This assignment was confirmed by correlations observed in the NOESY NMR spectrum of janthitrem B where the

proton signal at 1.29 ppm showed correlations to signals at 1.05 ppm (H-38), 1.24 ppm (H-39) and 5.93 ppm (H-35). The only methyl signal which could show correlations to these signals is H-40.

The correlations observed from the NOESY NMR spectrum of janthitrem B also indicated that the H-38 and H-40 methyl group protons must both be oriented towards each other, otherwise a NOESY correlation would not be observed between these two methyl groups, and that the H-37 and H-39 methyl groups must be α -oriented since each of these methyl group protons showed correlations to the α -oriented H-31 proton, while the H-38 and H-40 methyl group protons do not show correlations to H-31. These correlations are illustrated in Figure 3.9.

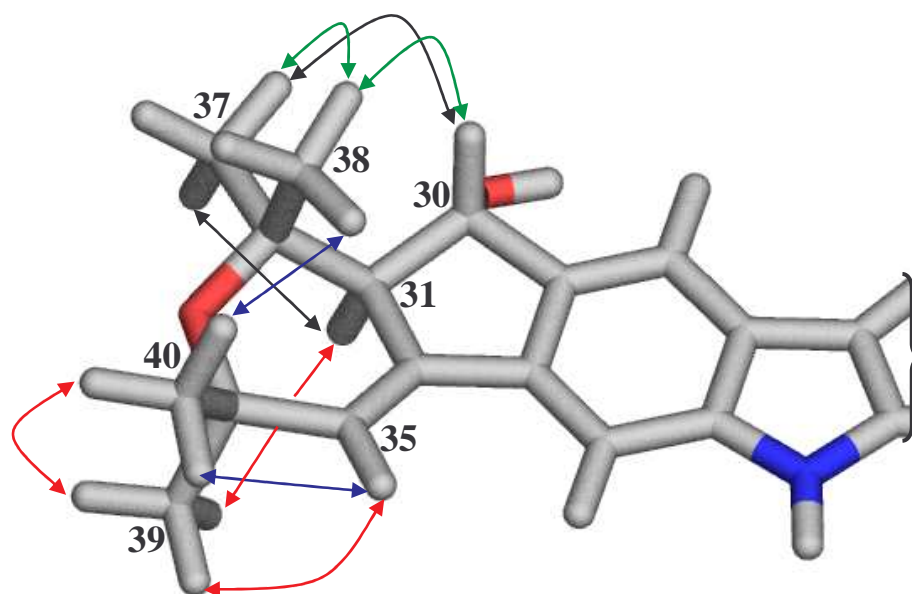


Figure 3.9. NOESY correlations observed for H-37 (black), H-38 (green), H-39 (red) and H-40 (blue) of janthitrem B.

The NOESY NMR spectrum also allowed the α - or β -orientation (i.e. oriented towards the lower or upper face respectively) of methylene protons to be determined. g-HSQC, COSY (Table 3.2) and TOCSY (Table 3.3) NMR data showed that the two H-5 methylene proton signals occurred at 1.61 and 2.61 ppm. The H-5 signal that resonated at 1.61 ppm showed NOESY correlations to signals

which resonated at 0.92 ppm (H-26), 2.06 and 1.82 ppm (H-6), 2.61 ppm (H-5) and 9.80 ppm (NH) (Figure 3.10). The H-5 signal that resonated at 2.61 ppm showed NOESY correlations to signals at 1.34 ppm (H-25), 1.61 ppm (H-5), 2.06 ppm (H-6) and 4.59 ppm (H-7) (Figure 3.10).

The observed correlations are consistent with the H-5 proton that resonated at 1.61 ppm being β -orientated (since it showed a correlation to the β -oriented H-26) and the proton that resonated at 2.61 ppm being α -orientated (since it showed a correlation to the α -oriented H-25). These conclusions were also supported by the appearance in the g-HSQC spectrum of the H-5 β signal (1.61 ppm) of janthitrem B as a doublet like signal, since at two-dimensional resolution H-5 β would be expected to show only a large 2J coupling to H-5 α and smaller (unresolved) 3J equatorial-equatorial and equatorial-axial couplings to H-6 α and H-6 β respectively. The g-HSQC signal arising from H-5 α was partly overlapped and could not be analysed to the same extent.

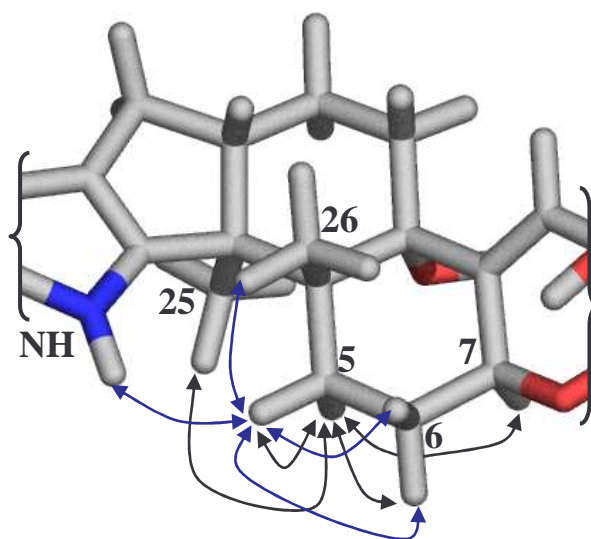


Figure 3.10. NOESY correlations observed for H-5 α (black) and H-5 β (blue) of janthitrem B.

g-HSQC, COSY (Table 3.2) and TOCSY (Table 3.3) NMR data showed that the two H-6 methylene proton signals occurred at 1.82 ppm and 2.06 ppm. The signal

at 1.82 ppm showed NOESY correlations to H-26 (0.92 ppm), H-5 β (1.61 ppm) and H-6 (2.06 ppm). The signal at 2.06 ppm showed NOESY correlations to H-5 α (2.61 ppm), H-5 β (1.61 ppm), H-6 (1.82 ppm) and H-7 (4.59 ppm). These observations showed the H-6 signal at 2.06 ppm to be α -oriented since it showed a correlation to the α -oriented H-7 and the H-6 signal at 1.82 ppm to be β -oriented since it showed a correlation to the β -oriented H-26. The aforementioned correlations are depicted in Figure 3.11.

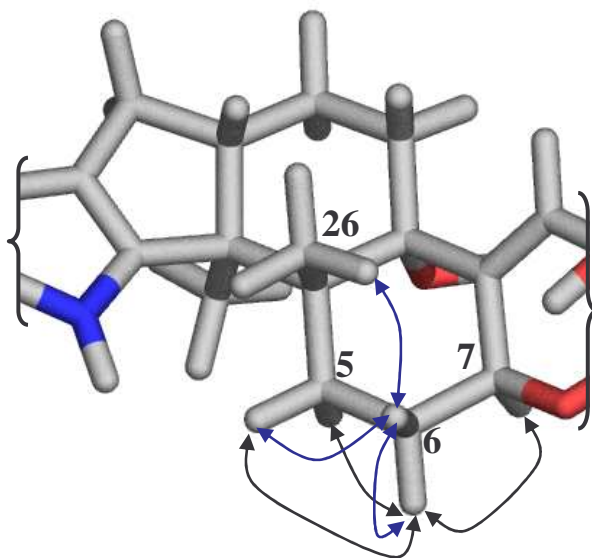


Figure 3.11. NOESY correlations observed for H-6 α (black) and H-6 β (blue) of janthitrem B.

The H-14 signal at 1.64 ppm showed NOESY correlations to 1.81 ppm (H-14), 2.04 ppm (H-15), 3.30 ppm (13-OH) and 5.71 ppm (H-11), whilst the H-14 signal at 1.81 ppm showed correlations with signals at 0.92 ppm (H-26), 1.62 ppm (H-15), 1.64 ppm (H-14), 2.73 ppm (H-16) and 5.71 ppm (H-11) (as shown in Figure 3.12). The H-15 signal at 2.04 ppm showed NOESY correlations to 1.34 ppm (H-25), 1.62 ppm (H-15), 1.64 ppm (H-14), 2.37 ppm (H-17) and 3.30 ppm (13-OH) while the H-15 signal at 1.62 ppm showed correlation to signals at 1.81 ppm (H-14), 2.04 ppm (H-15), 2.37, 2.66 ppm (H-17) and 2.73 ppm (H-16) (as shown in Figure 3.13).

Since only the H-14 signal at 1.81 ppm showed correlations to H-16 and H-26, both of which are β -oriented, this H-14 signal must also be β -oriented, whilst the H-14 signal at 1.64 ppm must be α -oriented as it showed correlations to the α -oriented H-11 and 13-OH.

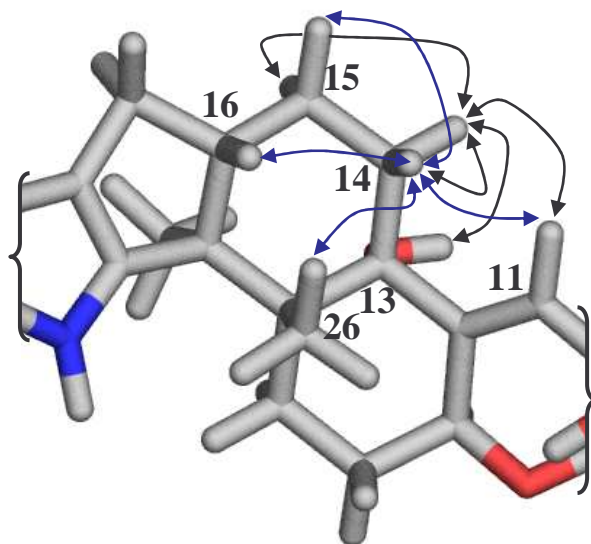


Figure 3.12. NOESY correlations observed for H-14 α (black) and H-14 β (blue) of janthitrem B.

The H-15 signal at 2.04 ppm was determined to be α -oriented since it showed a correlation to the α -oriented H-25 while the H-15 signal at 1.62 ppm was determined to be β -oriented since it showed a correlation to the β -oriented H-16.

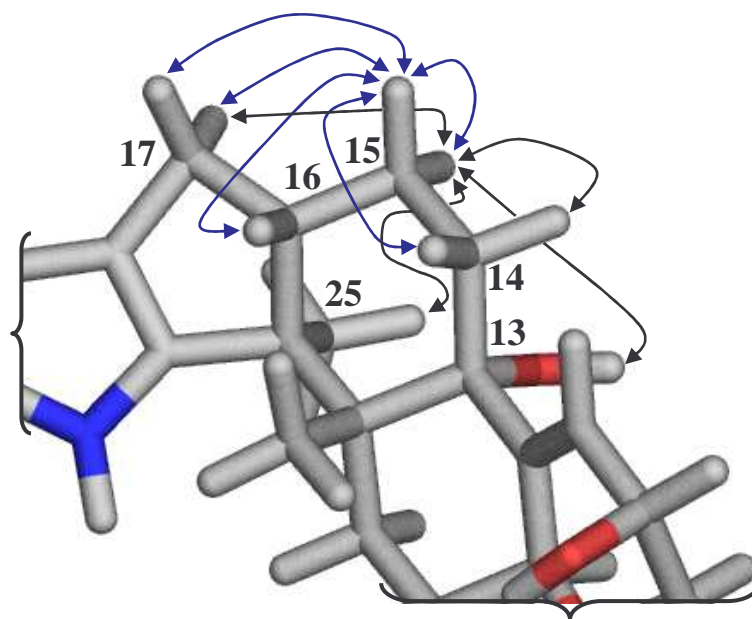


Figure 3.13. NOESY correlations observed for H-15 α (black) and H-15 β (blue) of janthitrem B.

The H-17 signal that resonated at 2.37 ppm showed NOESY correlations to signals at 1.34 ppm (H-25), 2.04 ppm (H-15 α) and 2.66 ppm (H-17) (Figure 3.14), enabling it to be assigned as α -oriented since it showed a correlation to the α -oriented H-25. The H-17 signal that resonated at 2.66 ppm showed NOESY correlations to signals at 1.62 ppm (H-15 β), 2.37 ppm (H-17), 2.73 ppm (H-16) and 7.374 ppm (H-20) (Figure 3.14) allowing it to be assigned as β -oriented since it showed a correlation to the β -oriented H-16.

The pair of H-17 resonances could be readily identified in the one-dimensional NMR spectrum, and their coupling constants determined. Thus H-17 α (2.37 ppm, dd, $J = 12.7, 10.6$ Hz) showed coupling constants consistent with a pseudo trans diaxial relationship between H-17 α and H-16 ($J = 10.6$ Hz), whereas H-17 β (2.66 ppm, dd, $J = 12.7, 6.1$ Hz) showed coupling constants consistent with a pseudo equatorial-axial relationship between H-17 β and H-16. Each of H-17 α and H-17 β showed a mutual 2J coupling of 12.7 Hz. The NOESY correlations observed for H-17 α and H-17 β are consistent with the pseudo axial and pseudo equatorial orientations established for these protons via coupling constants.

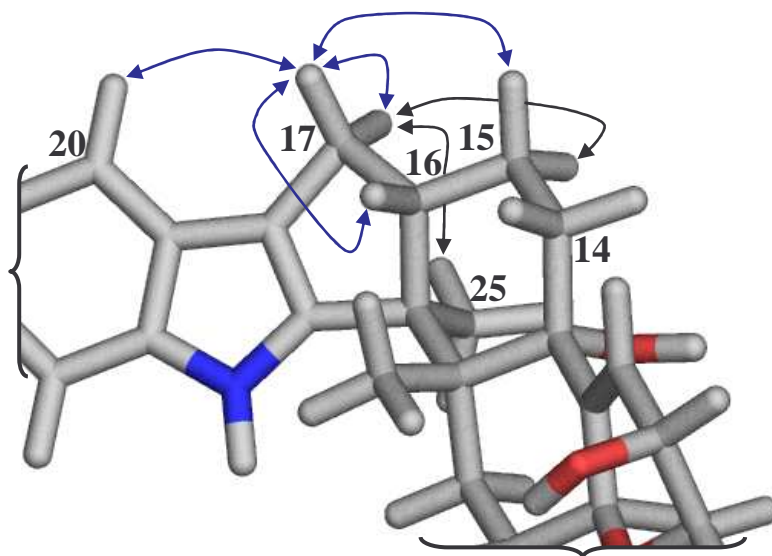


Figure 3.14. NOESY correlations observed for H-17 α (black) and H-17 β (blue) of janthitrem B.

The assignments reported in Table 3.5 for H-5, H-6 and H-17 are in agreement with those proposed by Wilkins et al. (1992) for H-5 α , H-5 β , H-6 α , H-6 β , H-15 α , H-15 β , H-17 α and H-17 β .

Protons attached to the C-29 methylene group can be designated as having *E*, or *Z* orientations based on the Cahn–Ingold–Prelog (CIP) priority rules. In the case of double bonds, the stereochemical descriptor *Z* (from the German *zusammen*, meaning together) is assigned when the two groups of highest priority are on the same side of the reference plane and the stereochemical descriptor *E* (from the German *entgegen*, meaning opposite) is assigned when the two highest priority groups are on opposite sides of the reference plane (Blackwood et al., 1968).

The H-29 signal at 4.87 ppm showed NOESY correlations to H-28 (1.76 ppm) and the H-29 signal at 5.08 ppm. The other H-29 (5.08 ppm) signal showed NOESY correlations to H-9 (3.79 ppm), H-10 (3.91 ppm) and H-29 (4.87 ppm). These correlations are illustrated in Figure 3.15. Based on the CIP priority rules, the H-29 proton (5.08 ppm) showing correlations to H-9 and H-10 is of higher priority and so is assigned as *Z*, while the H-29 proton (4.87 ppm) showing correlations to H-28 is of lower priority and so is assigned as *E*.

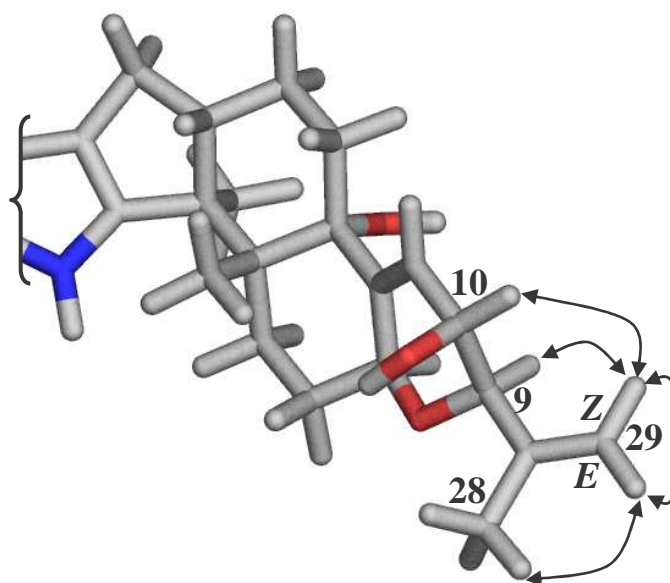


Figure 3.15. NOESY correlations observed for H-29*E* and H-29*Z* of janthitrem B.

NOESY NMR data also served to differentiate the pair of aromatic signals (H-20 and H-23) which occurred at almost identical chemical shifts (7.366 and 7.374 ppm). The signal at 7.366 ppm showed correlations to the H-35 (5.97 ppm) and NH (9.80 ppm) signals, showing it must be H-23, while the signal at 7.374 ppm showed correlations to H-17 β (2.66 ppm), 30-OH (4.23 ppm) and H-30 (4.90 ppm) (Figure 3.16), thereby demonstrating it to be the H-20 resonance.

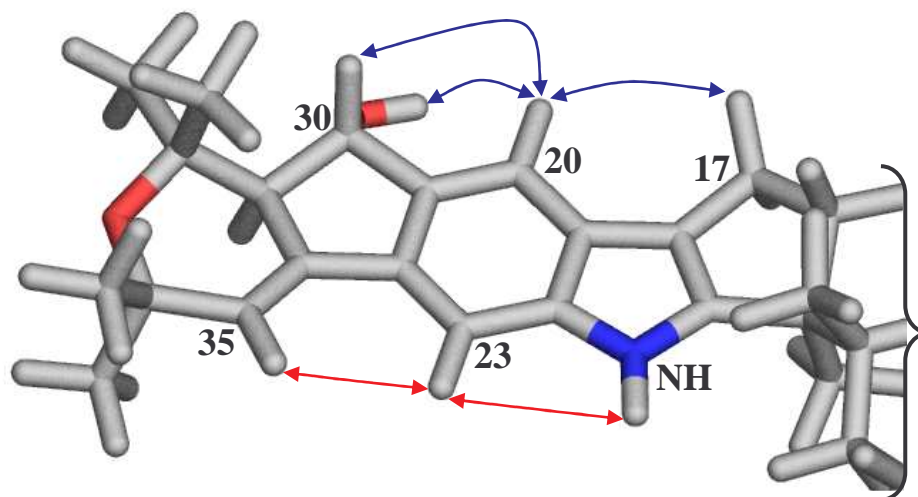


Figure 3.16. NOESY correlations observed for H-20 (blue) and H-23 (red) of janthitrem B.

Table 3.5. NOESY NMR correlations observed for janthitrem B (δ).

^1H Signal	Cross peaks observed
0.92 (H-26)	1.81 (H-14 β), 1.61 (H-5 β), 1.82 (H-6 β), 2.73 (H-16), 4.59 (H-11), 9.80 (NH)
1.09 (H-38)	1.29 (H-40), 1.40 (H-37), 4.90 (H-30)
1.24 (H-39)	1.29 (H-40), 2.65 (H-31), 5.97 (H-35)
1.29 (H-40)	1.09 (H-38), 1.24 (H-39), 5.97 (H-35)
1.34 (H-25)	2.04 (H-15 α), 2.37 (H-17 α), 2.61 (H-5 α), 3.30 (13-OH)
1.40 (H-37)	1.09 (H-38), 2.65 (H-31), 4.90 (H-30)
1.62 (H-15 β)	1.81 (H-14 β), 2.04 (H-15 α), 2.37 (H-17 α), 2.66 (H-17 β), 2.73 (H-16)
1.61 (H-5 β)	0.92 (H-26), 1.82 (H-6 β), 2.06 (H-6 α), 2.61 (H-5 α), 9.80 (NH)
1.64 (H-14 α)	1.81 (H-14 β), 2.04 (H-15 α), 3.30 (13-OH), 5.71 (H-11)

Table 3.5 continued

1.76 (H-28)	3.79 (H-9), 3.91 (H-10), 4.87 (H-29E)
1.81 (H-14 β)	0.92 (H-26), 1.62 (H-15 β), 1.64 (H-14 α), 2.73 (H-16), 5.71 (H-11)
1.82 (H-6 β)	0.92 (H-26), 2.06 (H-6 α), 1.61 (H-5 β)
2.04 (H-15 α)	1.34 (H-25), 1.62 (H-15 β), 1.64 (H-14 α), 2.37 (H-17 α), 3.30 (13-OH)
2.06 (H-6 α)	1.61 (H-5 β), 2.61 (H-5 α), 1.82 (H-6 β), 4.59 (H-7)
2.37 (H-17 α)	1.34 (H-25), 2.04 (H-15 α), 2.66 (H-17 β)
2.61 (H-5 α)	1.34 (H-25), 1.61 (H-5 β), 2.06 (H-6 α), 4.59 (H-7)
2.65 (H-31)	1.24 (H-39), 1.40 (H-37), 4.90 (H-30)
2.66 (H-17 β)	1.62 (H-15 β), 2.37 (H-17 α), 2.73 (H-16), 7.374 (H-20)
2.73 (H-16)	0.92 (H-26), 1.81 (H-14 β), 1.62 (H-15 β), 2.04 (H-15 α), 2.66 (H-17 β)
3.30 (13-OH)	1.34 (H-25), 1.64 (H-14 α), 2.04 (H-15 α), 4.59 (H-7)
2.99 (10-OH)	3.91(H-10)
3.79 (H-9)	1.76 (H-28), 3.91 (H-10), 4.59 (H-7), 5.08 (H-29Z)
3.91 (H-10)	1.76 (H-28), 2.99 (10-OH), 3.79 (H-9), 5.71 (H-11), 5.08 (H-29Z)
4.23 (30-OH)	4.90 (H-30), 7.366 (H-23)
4.59 (H-7)	1.82 (H-6 β), 2.06 (H-6 α), 2.61 (H-5 α), 3.30 (13-OH), 3.79 (H-9)
4.87 (H-29E)	1.76 (H-28), 5.08 (H-29Z)
4.90 (H-30)	1.09 (H-38), 1.40 (H-37), 2.65 (H-31), 4.23 (30-OH), 7.374 (H-20)
5.08 (H-29Z)	3.79 (H-9), 3.91 (H-10), 4.87 (H-29E)
5.71 (H-11)	0.92 (H-26), 1.81 (H-14 β), 3.91 (H-10)
5.97 (H-35)	1.24 (H-39), 1.29 (H-40), 7.366 (H-23)
7.366 (H-23)	5.97 (H-35), 9.80 (NH)
7.374 (H-20)	2.66 (H-17 β), 4.23 (30-OH), 4.90 (H-30)
9.80 (NH)	0.92 (H-26), 1.61 (H-5 β), 7.366 (H-23)

3.2.4 Summary; *Janthitrem B* NMR Assignments

Generally the ^1H and ^{13}C NMR signal assignments determined in the present investigation for *janthitrem B* agreed with those reported by Wilkins et al. (1992) with the exception of revised assignments for H-14 and H-16 and C-39 and C-40.

3.3 *Janthitrem A* NMR Discussion

A complete assignment of the resonances of *janthitrem A* is presented in Table 3.1. Methylene proton assignments are reported in the format ($\text{H}_\alpha, \text{H}_\beta$) based on analyses of coupling constant and/or NOESY data. Correlations observed in two-dimensional NMR experiments that substantiated these assignments are reported in Tables 3.6, 3.7, 3.8 and 3.9.

The NMR data was determined at 400 MHz. When *janthitrem A* was first detected by Gallagher et al. (1980a), only a molecular weight was determined (by high resolution mass spectrometry). While this data showed *janthitrem A* possessed an additional oxygen atom compared to *janthitrem B*, it did not define either the nature of the oxygen atom (e.g. presence of an additional epoxy or hydroxyl group) or the location of the additional oxygen atom. The structure of this compound was unequivocally defined for the first time during the present investigation. A comparison of selected NMR chemical shift data that demonstrates the presence of an 11,12-epoxy functionality in *janthitrem A* is reported in Chapter 2, Section 2.2.2. A complete assignment of the ^1H and ^{13}C NMR signals of *janthitrem A* is reported in this Chapter (see below).

Signal assignments for *janthitrem A* were facilitated by comparison with acquired *janthitrem B* data and those previously reported for *penitrem A* (de Jesus et al., 1983a). This is because while *janthitrem A* and *janthitrem B* are the same at the left-hand end of the molecule, *janthitrem A* contains an 11,12-epoxy group

analogous to that found in penitrem A. Since the right-hand end of janthitrem A and penitrem A are the same, and the left-hand end of janthitrem A and janthitrem B are the same, together they were the perfect model compound.

3.3.1 ^1H , ^{13}C , DEPT-135, COSY and TOCSY NMR Spectra of Janthitrem A

^{13}C and DEPT-135 NMR spectra of janthitrem A revealed the presence of 37 carbon resonances (7 methyl, 6 methylene, 10 methine and 14 quaternary). The carbon and proton resonances for janthitrem A were consistent with those observed for janthitrem B for the left-hand half of the molecule. The difference in carbon and proton resonances between janthitrem A and B can be ascribed to the replacement of the double bond at C-11 and C-12 with an epoxide. This resulted in significant shifts in the proton resonances for H-7, H-9, H-10 and H-11 (see Table 3.1).

H-7 Signal Assignment

Since the C-7 signal can be inferred from data presented in Table 2.2 (see Chapter 2, Section 2.2.2), the resonance of H-7 can be identified from the g-HSQC NMR spectrum of janthitrem A, where a correlation between C-7 (72.0 ppm) and its attached methane proton (H-7) at 4.28 ppm was observed. The COSY NMR spectrum showed H-7 correlated with H-6 (2.22 and 2.04 ppm) and H-11 (3.53 ppm) while the TOCSY NMR spectrum showed correlations with H-6 (2.22 and 2.04 ppm), H-5 (2.65 and 1.60 ppm), 10-OH (3.33 ppm), H-11 (3.53 ppm), H-9 (4.03 ppm) and H-10 (4.04 ppm).

The significant difference observed between the H-7 resonances of janthitrem A and janthitrem B can be explained by the presence of the epoxide in janthitrem A. As H-7 in janthitrem A is situated close to the epoxide, the proton resonance has, as expected, shifted from 4.59 ppm (janthitrem B) to 4.28 ppm. The H-7

resonance for janthitrem A was in close agreement with the 4.29 ppm value reported for penitrem A (de Jesus et al., 1983a).

H-9 and H-10 Signal Assignments

As was the case for C-7, the C-9 and C-10 signal assignments can be inferred from data presented in Table 2.2 (see Chapter 2, Section 2.2.2). The resonances of H-9 and H-10 can be identified from correlations observed in the g-HSQC NMR spectrum. Thus, H-9 and H-10 were observed to resonate at 4.03 and 4.04 ppm respectively. In penitrem A, the reported chemical shift for both H-9 and H-10 was 4.04 ppm (de Jesus et al., 1983a), in agreement with the assignments determined here for H-9 and H-10 of janthitrem A.

The overlapping H-9 and H-10 signals (4.03 and 4.04 ppm) showed correlations to H-11 (3.53 ppm), 10-OH (3.33 ppm), H-28 (1.70 ppm) and H-29 (4.87 and 5.07 ppm) in the COSY NMR spectrum and H-28 (1.70 ppm), 10-OH (3.33 ppm), H-11 (3.53 ppm), H-7 (4.28 ppm) and H-29 (4.87 and 5.07 ppm) in the TOCSY NMR spectrum.

H-11 Signal Assignment

In a like manner (see preceding paragraph), g-HSQC data showed that C-11 (61.9 ppm, see Table 2.2) correlated to the proton resonating at 3.53 ppm. H-11 (3.53 ppm) showed correlations to 10-OH (3.33 ppm), H-10 (4.04 ppm) and H-7 (4.28 ppm) in the COSY NMR spectrum and H-6 (2.22 and 2.04 ppm), H-5 (2.65 and 1.60 ppm), 10-OH (3.33 ppm), H-9 (4.03 ppm), H-10 (4.04 ppm) and H-7 (4.28 ppm) in the TOCSY NMR spectrum. In penitrem A (de Jesus et al., 1983a), H-11 resonated at 3.57 ppm, in close agreement to the chemical shift of H-11 observed for janthitrem A.

H-26 Signal Assignment

Two of the seven methyl groups, H-26 and H-28, showed significant changes in their proton resonances compared to the values observed in janthitrem B (Table 3.1). This is because these methyl groups are close to the epoxide at C-11 and C-12. The g-HSQC NMR spectrum for janthitrem A showed a correlation between C-26 (18.9 ppm) and its attached proton (H-26) at 1.20 ppm. In the TOCSY NMR spectrum H-26 (1.20 ppm) showed long range correlations to H-5 (2.65 ppm) and 13-OH (3.22 ppm). The corresponding H-26 resonance of janthitrem B occurred at 0.92 ppm (Table 3.1).

The H-26 resonance of penitrem A was reported at 1.22 ppm (de Jesus et al., 1983a), in close agreement with the value observed for janthitrem A.

H-28 Signal Assignment

As mentioned above, H-28, showed a significant change in its proton resonance compared to the value observed for janthitrem B, due to its proximity to the 11,12-epoxy group (as opposed to an 11(12)-double bond in janthitrem B). g-HSQC and g-HMBC data showed H-28 to resonate at 1.70 ppm compared to 1.76 ppm for janthitrem B (Table 3.1). The H-28 signal (1.70 ppm) of janthitrem A showed correlations to H-9 (4.03 ppm) and H-29 (4.87 and 5.07 ppm) in the COSY NMR spectrum and to H-9 (4.03 ppm), H-10 (4.04 ppm) and H-29 (4.87 and 5.07 ppm) in the TOCSY NMR spectrum. de Jesus et al. (1983a) reported the H-28 signal of penitrem A to resonate at 1.71 ppm, almost identical to the resonance observed for janthitrem A.

The remaining five methyl groups for janthitrem A, H-25, H-37, H-38, H-39 and H-40 (1.33, 1.40, 1.08, 1.24 and 1.29 ppm respectively) showed proton resonances that were either identical or in close agreement with those observed for janthitrem B.

NH and OH Signal Assignments

The janthitrem A NH signal occurred at 9.89 ppm, as opposed to 9.80 ppm for janthitrem B (Table 3.1). The 10-OH and 13-OH chemical shifts of janthitrem A also varied from those observed for janthitrem B. These OH groups are in close proximity to the point of structural difference between the respective molecules (namely an 11,12-epoxy group vs. a 11(12)-double bond).

g-HMBC, COSY and TOCSY data showed that the 10- and 13-OH signals of janthitrem A occurred at 3.33 and 3.22 ppm respectively. The signal at 3.33 ppm (10-OH) showed correlations to signals at 3.53 (H-11), 4.03 (H-9) and 4.04 ppm (H-10) in the COSY spectrum and to signals at 3.53 (H-11), 4.03 (H-9), 4.04 (H-10) and 4.28 ppm (H-7) in the TOCSY spectrum. The signal at 3.22 ppm (13-OH) showed correlations to H-26 (1.20 ppm) in the COSY spectrum and to H-26 (1.20 ppm) and H-14 (1.63 ppm) in the TOCSY spectrum.

The janthitrem A resonances for 10-OH (3.33 ppm) and 13-OH (3.22 ppm) can be compared to the janthitrem B values of 2.99 and 3.30 ppm (see Table 3.1). de Jesus et al. (1983a) reported 10-OH and 13-OH in penitrem A as 3.40 and 3.32 ppm, respectively. The resonances of OH protons are known to be sensitive to conditions such as temperature, concentration and the level of residual water in an NMR sample, therefore this difference in chemical shift is not significant.

Table 3.6. COSY NMR correlations observed for janthitrem A (δ).

¹ H Signal	Cross peaks observed
1.08 (H-38)	1.40 (H-37)
1.40 (H-37)	1.08 (H-38)
1.53 (H-14 β)	1.63 (H-14 α), 1.97 (H-15 α), 1.56 (H-15 β)
1.56 (H-15 β)	1.63 (H-14 α), 1.53 (H-14 β), 1.97 (H-15 α)
1.60 (H-5 β)	2.22 (H-6 α), 2.04 (H-6 β), 2.65 (H-5 α)
1.63 (H-14 α)	1.53 (H-14 β), 1.97 (H-15 α), 1.56 (H-15 β)
1.70 (H-28)	4.03 (H-9), 5.07 (H-29Z), 4.87 (H-29E)
1.97 (H-15 α)	1.56 (H-15 β), 1.63 (H-14 α), 1.53 (H-14 β), 2.83 (H-16)
2.04 (H-6 β)	2.22 (H-6 α), 2.65 (H-5 α), 1.60 (H-5 β), 4.28 (H-7)
2.22 (H-6 α)	2.04 (H-6 β), 2.65 (H-5 α), 1.60 (H-5 β), 4.28 (H-7)
2.37 (H-17 α)	2.66 (H-17 β), 2.83 (H-16)
2.64 (H-31)	4.89 (H-30), 5.95 (H-35)
2.65 (H-5 α)	1.20 (H-26), 1.60 (H-5 β), 2.22 (H-6 α), 2.04 (H-6 β)
2.66 (H-17 β)	2.37 (H-17 α), 2.83 (H-16)
2.83 (H-16)	1.97 (H-15 α), 2.37 (H-17 α), 2.66 (H-17 β)
3.22 (13-OH)	1.20 (H-26)
3.33 (10-OH)	3.53 (H-11), 4.03 (H-9), 4.04 (H-10)
3.53 (H-11)	3.33 (10-OH), 4.04 (H-10), 4.28 (H-7)
4.03 (H-9) & 4.04(H-10)	1.70 (H-28), 3.33 (10-OH), 3.53 (H-11), 5.07 (H-29Z), 4.87 (H-29E)
4.21 (30-OH)	2.64 (H-31), 4.89 (H-30)
4.28 (H-7)	2.22 (H-6 α), 2.04 (H-6 β), 3.53 (H-11)
4.87 (H-29E)	1.70 (H-28), 4.03 (H-9), 5.07 (H-29Z)
4.89 (H-30)	2.64 (H-31), 4.21 (30-OH), 7.366 (H-20)
5.07 (H-29Z)	1.70 (H-28), 4.03 (H-9), 4.87 (H-29E)
5.95 (H-35)	2.64 (H-31)
7.366 (H-20) & 7.371 (H-23)	4.89 (H-30), 9.89 (NH)
9.89 (NH)	7.371 (H-23)

Table 3.7. TOCSY NMR correlations observed for janthitrem A (δ).

¹ H Signal	Cross peaks observed
1.08 (H-38)	1.40 (H-37), 2.64 (H-31), 4.21 (30-OH)
1.20 (H-26)	2.65 (H-5 α), 3.22 (13-OH)
1.24 (H-39)	1.28 (H-40), 5.95 (H-35)
1.28 (H-40)	1.24 (H-39), 5.95 (H-35)
1.40 (H-37)	1.08 (H-38), 2.64 (H-31), 4.21 (30-OH)
1.53 (H-14 β)	1.63 (H-14 α), 1.97 (H-15 α), 2.37 (H-17 α), 2.66 (H-17 β), 2.83 (H-16)
1.56 (H-15 β)	1.97 (H-15 α), 1.63 (H-14 α), 2.37 (H-17 α), 2.66 (H-17 β), 2.83 (H-16)
1.60 (H-5 β)	2.22 (H-6 α), 2.04 (H-6 β), 2.65 (H-5 α), 4.28 (H-7)
1.63 (H-14 α)	1.53 (H-14 β), 1.97 (H-15 α), 1.56 (H-15 β), 2.37 (H-17 α), 2.66 (H-17 β), 2.83 (H-16), 3.22 (13-OH), 3.53 (H-11)
1.70 (H-28)	4.03 (H-9), 4.04 (H-10), 5.07 (H-29Z), 4.87 (H-29E)
1.97 (H-15 α)	1.56 (H-15 β), 1.63 (H-14 α), 1.53 (H-14 β), 2.37 (H-17 α), 2.66 (H-17 β), 2.83 (H-16)
2.04 (H-6 β)	2.22 (H-6 α), 2.65 (H-5 α), 1.60 (H-5 β), 3.53 (H-11), 4.28 (H-7)
2.22 (H-6 α)	2.04 (H-6 β), 2.65 (H-5 α), 1.60 (H-5 β), 3.53 (H-11), 4.28 (H-7)
2.37 (H-17 α)	1.63 (H-14 α), 1.53 (H-14 β), 1.97 (H-15 α), 1.56 (H-15 β), 2.66 (H-17 β), 2.83 (H-16)
2.64 (H-31)	1.08 (H-38), 4.21 (30-OH), 4.89 (H-30), 5.95 (H-35)
2.65 (H-5 α)	1.20 (H-26), 1.60 (H-5 β), 2.22 (H-6 α), 2.04 (H-6 β), 4.28 (H-7)
2.66 (H-17 β)	1.63 (H-14 α), 1.53 (H-14 β), 1.97 (H-15 α), 1.56 (H-15 β), 2.37 (H-17 α), 2.83 (H-16), 7.366 (H-20)
2.83 (H-16)	1.97 (H-15 α), 1.56 (H-15 β), 2.37 (H-17 α), 2.66 (H-17 β), 1.63 (H-14 α), 1.53 (H-14 β)
3.22 (13-OH)	1.20 (H-26), 1.63 (H-14 α)
3.33 (10-OH)	3.53 (H-11), 4.03 (H-9), 4.04 (H-10), 4.28 (H-7)
3.53 (H-11)	2.22 (H-6 α), 2.04 (H-6 β), 2.65 (H-5 α), 1.60 (H-5 β), 3.33 (10-OH), 4.03 (H-9), 4.04 (H-10), 4.28 (H-7)

Table 3.7 continued

4.03 (H-9) & 4.04 (H-10)	1.70 (H-28), 3.33 (10-OH), 3.53 (H-11), 4.28 (H-7), 5.07 (H-29Z), 4.87 (H-29E)
4.21 (30-OH)	1.08 (H-38), 1.40 (H-37), 2.64 (H-31), 4.89 (H-30), 5.95 (H-35), 7.366 (H-20), 7.371 (H-23)
4.28 (H-7)	2.22 (H-6 α), 2.04 (H-6 β), 2.65 (H-5 α), 1.60 (H-5 β), 3.33 (10-OH), 3.53 (H-11), 4.03 (H-9), 4.04 (H-10)
4.87 (H-29E)	1.70 (H-28), 3.33 (10-OH), 3.53 (H-11), 4.03 (H-9), 4.04 (H-10), 5.07 (H-29Z)
4.89 (H-30)	2.64 (H-31), 4.21 (30-OH), 5.95 (H-35), 7.366 (H-20)
5.07 (H-29Z)	1.70 (H-28), 3.33 (10-OH), 3.53 (H-11), 4.03 (H-9), 4.04 (H-10), 4.87 (H-29E)
5.95 (H-35)	1.24 (H-39), 1.28 (H-40), 2.64 (H-31), 4.21 (30-OH), 4.89 (H-30), 7.371 (H-23)
7.366 (H-20) & 7.371 (H-23)	2.64 (H-31), 4.21 (30-OH), 4.89 (H-30), 5.95 (H-35), 9.89 (NH)
9.89 (NH)	7.371 (H-23)

3.3.2 *g*-HSQC and *g*-HMBC NMR Spectra of *Janthitrem A*

As was the case with *janthitrem B*, analysis of *g*-HMBC and *g*-HSQC NMR spectral data allowed the unequivocal assignment of the C-31, C-32, C-34 and C-35 signals and their attached protons. The *g*-HSQC NMR spectrum showed that the C-37, C-38, C-39 and C-40 methyl carbon signals which resonated at 30.6, 23.6, 32.5 and 30.4 ppm, respectively, exhibited correlations to protons which resonated at 1.40, 1.08, 1.24 and 1.28 ppm, respectively. These values were in close agreement with those observed for *janthitrem B* and confirmed that the C-39 and C-40 signal assignments proposed by Wilkins et al. (1992) should be reversed.

In the *g*-HMBC NMR spectrum, H-39 (1.24 ppm) and H-40 (1.28 ppm) showed correlations to C-34 (72.6 ppm) and C-35 (120.2 ppm) while H-37 (1.40 ppm) and

H-38 (1.08 ppm) showed correlations to C-31 (60.3 ppm) and C-32 (74.3 ppm). These values were almost identical to those observed for janthitrem B.

As noted above for janthitrem B, by convention lower numbers are assigned to the lower face, α -oriented, methyl groups (H-37 and H-39), and higher numbers to the upper face, β -oriented, methyl groups (H-38 and H-40).

Table 3.8. Long-range ^{13}C - ^1H NMR correlations observed in the g-HMBC NMR spectrum of janthitrem A (δ).

^1H Signal	Correlated ^{13}C Signals
1.08 (H-38)	30.6 (C-37), 60.3 (C-31), 74.3 (C-32)
1.20 (H-26)	27.2 (C-5), 43.3 (C-4), 51.8 (C-3), 78.3 (C-13)
1.24 (H-39)	30.4 (C-40), 72.6 (C-34), 120.2 (C-35)
1.28 (H-40)	32.5 (C-39), 72.6 (C-34), 120.2 (C-35)
1.33 (H-25)	43.3 (C-4), 51.8 (C-3), 155.4 (C-2)
1.40 (H-37)	23.6 (C-38), 60.3 (C-31), 74.3 (C-32)
1.70 (H-28)	74.6 (C-9), 111.6 (C-29), 143.2 (C-27)
7.366 (H-20) &	76.3 (C-30), 116.6 (C-18), 127.7 (C-19), 131.7 (C-22),
7.371 (H-23)	137.1 (C-36), 140.1 (C-21), 142.2 (C-24)

3.3.3 NOESY NMR Spectrum of Janthitrem A

NOESY data served to define the stereochemical dispositions of the H-37, H-38, H-39 and H-40 methyl groups, as was also the case for janthitrem B (Section 3.2.3). As previously mentioned, NMR assignments originally proposed for janthitrem B by Wilkins et al. (1992) were based on a numbering convention in which H-37 and H-39 were assigned as α -oriented (i.e. inclined towards the lower face), while the H-38 and H-40 methyl group protons were assigned as β -oriented (i.e. inclined towards the upper face).

The methyl group signal at 1.40 ppm displayed NOESY correlations with signals at 1.08 ppm, 2.64 ppm (H-31) and 4.89 ppm (H-30). On the basis of these observations, the signal at 1.40 ppm can be attributed to H-37. The signal at 1.08 ppm showed NOESY correlations to signals at 4.89 ppm (H-30), 1.40 ppm (H-37) and 1.28 ppm. This signal can only be attributed to H-38 based on the NOESY correlations observed. The proton signal at 1.24 ppm showed NOESY correlations to signals at 2.64 ppm (H-31), 5.95 ppm (H-35) and 1.28 ppm while the signal at 1.28 ppm showed correlations to signals at 1.08 ppm (H-38), 1.24 ppm and 5.95 ppm (H-35). On the basis of these observations the signals at 1.24 and 1.28 ppm can be attributed to H-39 and H-40, respectively.

The foregoing NOESY correlations showed that H-38 and H-40 must both be oriented towards each other and that H-37 and H-39 must be α -oriented since they showed correlations to the α -oriented H-31 proton, while H-38 and H-40 do not. These assignments are in accord with those established for the equivalent signals of janthitrem B (Section 3.2.3).

NOESY data, in combination with g-HSQC and COSY data, served to define the α - or β -orientation of the H-5, H-6, H-14, H-15 and H-17 methylene protons. g-HSQC, COSY (Table 3.6) and TOCSY (Table 3.7) data showed that these protons occurred at 2.65 and 1.60 ppm (H-5), 2.22 and 2.04 ppm (H-6), 1.63 and 1.53 ppm (H-14), 1.97 and 1.56 ppm (H-15) and 2.37 and 2.66 ppm (H-17), respectively.

The H-5 signal at 2.65 ppm showed NOESY correlations to H-25 (1.33 ppm), H-5 (1.60 ppm) and H-6 (2.22 ppm) (Figure 3.17). The H-5 signal at 1.60 ppm correlated with H-26 (1.20 ppm), H-6 (2.22, 2.04 ppm), H-5 (2.65 ppm) and NH (9.89 ppm) in the NOESY spectrum (Figure 3.17). Since the H-5 signal at 2.65 ppm showed a correlation to the α -oriented H-25, this H-5 signal must also be α -

oriented. Similarly, since the H-5 signal at 1.60 ppm showed a correlation to the β -oriented H-26, this H-5 signal must also be β -oriented.

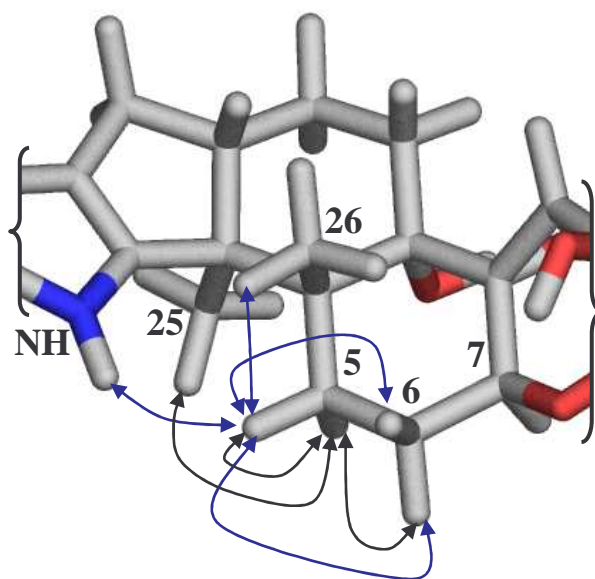


Figure 3.17. NOESY correlations observed for H-5 α (black) and H-5 β (blue) of janthitrem A.

The H-6 signal which resonated at 2.22 ppm showed NOESY correlations to signals at 2.65 ppm (H-5 α), 1.60 ppm (H-5 β), 2.04 ppm (H-6) and 4.28 ppm (H-7). The H-6 signal which resonated at 2.04 ppm showed NOESY correlations to signals at 1.20 ppm (H-26), 1.60 ppm (H-5 β) and 2.22 ppm (H-6). These observations are consistent with the H-6 signal which resonated at 2.22 ppm being α -oriented (since it showed a correlation to the α -oriented H-7) and the signal which resonated at 2.04 ppm being β -oriented (since it showed a correlation to the β -oriented H-26). The observed H-6 correlations are illustrated in Figure 3.18.

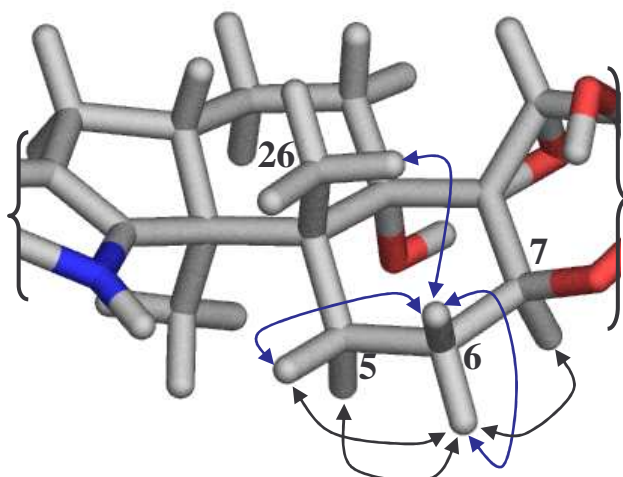


Figure 3.18. NOESY correlations observed for H-6 α (black) and H-6 β (blue) of janthitrem A.

The H-14 signal at 1.63 ppm showed NOESY correlations to H-14 (1.53 ppm), H-15 (1.97 ppm), 13-OH (3.22 ppm) and H-11 (3.53 ppm). The signal at 1.53 ppm showed NOESY correlations to H-26 (1.20 ppm), H-14 (1.63 ppm), H-16 (2.83 ppm) and H-11 (3.53 ppm). These observations showed the H-14 signal at 1.63 ppm to be α -oriented since it showed correlations to the α -oriented H-11 and 13-OH and the H-14 signal at 1.53 ppm to be β -oriented since it showed correlations to the β -oriented H-16 and H-26. These correlations are depicted in Figure 3.19.

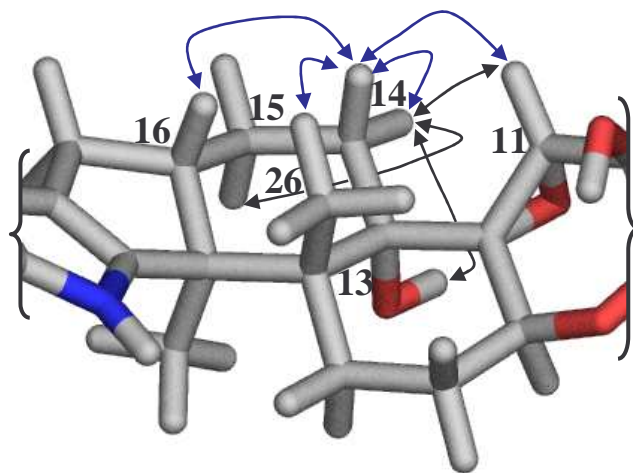


Figure 3.19. NOESY correlations observed for H-14 α (black) and H-14 β (blue) of janthitrem A.

H-15 (1.97 ppm) showed NOESY correlations to signals at 1.33 ppm (H-25), 1.56 ppm (H-15), 1.63 ppm (H-14 α) and 2.37 ppm (H-17). H-15 (1.56 ppm) showed NOESY correlations to signals at 1.97 ppm (H-15), 2.37 and 2.66 ppm (H-17) and 2.83 ppm (H-16). Since the H-15 signal which resonated at 1.97 ppm showed a correlation to the α -oriented H-25, this signal in turn must also be α -oriented. The H-15 signal which resonated at 1.56 ppm showed a correlation to the β -oriented H-16, thus this signal must also be β -oriented. NOESY correlations for H-15 are depicted in Figure 3.20.

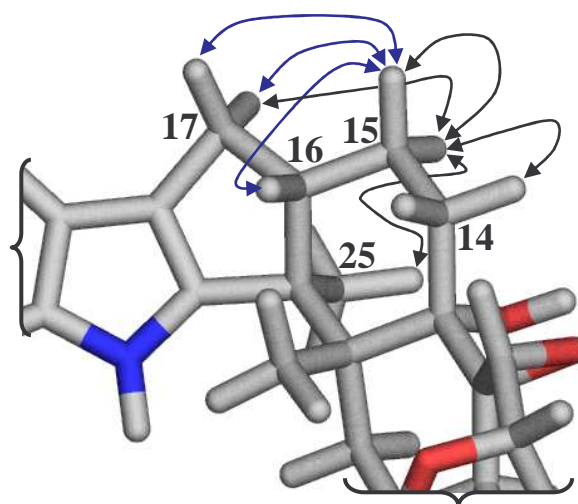


Figure 3.20. NOESY correlations observed for H-15 α (black) and H-15 β (blue) of janthitrem A.

The H-17 methylene proton which resonated at 2.37 ppm showed NOESY correlations to H-25 (1.33 ppm), H-15 α (1.97 ppm) and H-17 (2.66 ppm) (Figure 3.21). These correlations are consistent with the α -orientation of the H-17 proton which resonated at 2.37 ppm. In contrast the H-17 signal which resonated at 2.66 ppm showed correlations in the NOESY spectrum to H-15 β (1.56 ppm), H-17 (2.37 ppm), H-16 (2.83 ppm) and H-20 (7.366 ppm) (Figure 3.21). These correlations are consistent with the β -orientation of the H-17 proton which resonated at 2.37 ppm.

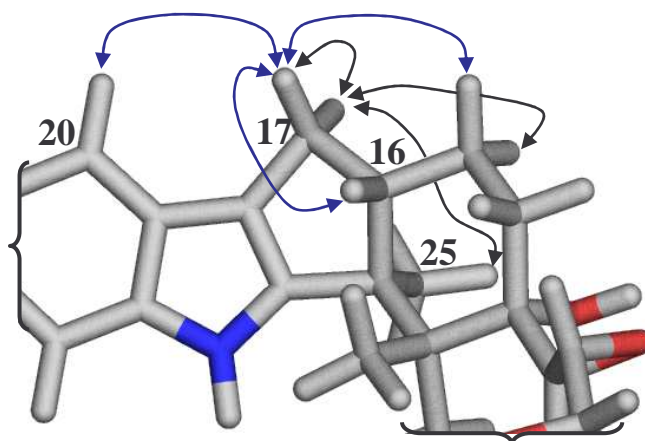


Figure 3.21. NOESY correlations observed for H-17 α (black) and H-17 β (blue) of janthitrem A.

As with janthitrem B, the protons attached to the C-29 methylene group were designated as having *E* or *Z* orientations based on the CIP priority rules (as discussed in Section 3.2.3).

COSY and TOCSY experiments confirmed the proton resonances of H-29 as 4.87 and 5.07 ppm. The H-29 signal at 4.87 ppm showed NOESY correlations to signals attributable to H-28 (1.70 ppm) and H-29 (5.07 ppm). The H-29 signal at 5.07 ppm showed NOESY correlations to signals attributable to H-9 (4.03 ppm) and H-29 (4.87 ppm). Based on the CIP priority rules, the proton showing correlations to H-9 is of higher priority and so is assigned as *Z*, while the proton showing correlations to H-28 is of lower priority and so is assigned as *E*. Therefore the H-29 signal resonating at 4.87 ppm was assigned *E* and the signal resonating at 5.07 ppm was assigned *Z*. The observed NOESY correlations for H-29 are illustrated in Figure 3.22.

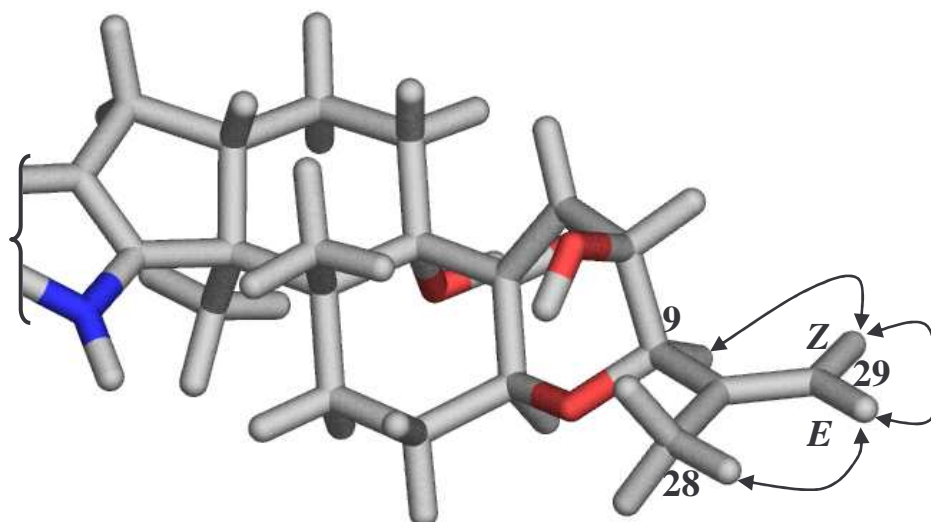


Figure 3.22. NOESY correlations observed for H-29*E* and H-29*Z* of janthitrem A.

NOESY data also enabled distinction between the aromatic protons, H-20 and H-23 to be made. These two signals resonated at almost identical chemical shifts, 7.366 and 7.371 ppm. The proton resonance at 7.366 ppm showed correlations to signals attributable to H-17 β (2.66 ppm) and H-30 (4.89 ppm), whereas the signal at 7.371 ppm correlated to signals attributable to H-35 (5.95 ppm) and NH (9.89 ppm). On the basis of these observations, the signal at 7.366 ppm can be attributed to H-20 while the signal at 7.371 ppm can be attributed to H-23.

Table 3.9. NOESY NMR correlations observed for janthitrem A (δ).

¹ H Signal	Cross peaks observed
1.08 (H-38)	1.28 (H-40), 1.40 (H-37), 4.89 (H-30)
1.20 (H-26)	1.53 (H-14 β), 1.60 (H-5 β), 2.04 (H-6 β), 2.83 (H-16), 3.53 (H-11), 9.89 (NH)
1.24 (H-39)	1.28 (H-40), 2.64 (H-31), 5.95 (H-35)
1.28 (H-40)	1.08 (H-38), 1.24 (H-39), 5.95 (H-35)
1.33 (H-25)	1.97 (H-15 α), 2.37 (H-17 α), 2.65 (H-5 α), 1.60 (H-5 β)
1.40 (H-37)	1.08 (H-38), 2.64 (H-31), 4.89 (H-30)
1.53 (H-14 β)	1.20 (H-26), 1.63 (H-14 α), 2.83 (H-16), 3.53 (H-11)
1.56 (H-15 β)	1.97 (H-15 α), 2.37 (H-17 α), 2.66 (H-17 β), 2.83 (H-16)
1.60 (H-5 β)	1.20 (H-26), 2.22 (H-6 α), 2.04 (H-6 β), 2.65 (H-5 α), 9.89 (NH)
1.63 (H-14 α)	1.53 (H-14 β), 1.97 (H-15 α), 3.22 (13-OH), 3.53 (H-11)
1.70 (H-28)	4.03 (H-9), 4.04 (H-10), 4.87 (H-29E)
1.97 (H-15 α)	1.33 (H-25), 1.56 (H-15 β), 1.63 (H-14 α), 2.37 (H-17 α)
2.04 (H-6 β)	1.20 (H-26), 2.22 (H-6 α), 1.60 (H-5 β)
2.22 (H-6 α)	2.65 (H-5 α), 1.60 (H-5 β), 2.04 (H-6 β), 4.28 (H-7)
2.37 (H-17 α)	1.33 (H-25), 1.97 (H-15 α), 2.66 (H-17 β)
2.64 (H-31)	1.24 (H-39), 1.40 (H-37), 4.89 (H-30)
2.65 (H-5 α)	1.33 (H-25), 1.60 (H-5 β), 2.22 (H-6 α), 4.28 (H-7)
2.66 (H-17 β)	1.56 (H-15 β), 2.37 (H-17 α), 2.83 (H-16), 7.366 (H-20)
2.83 (H-16)	1.20 (H-26), 1.53 (H-14 β), 1.97 (H-15 α), 1.56 (H-15 β), 2.66 (H-17 β)
3.22 (13-OH)	1.33 (H-25), 1.63 (H-14 α), 4.28 (H-7)
3.33 (10-OH)	4.03 (H-9), 4.04 (H-10)
3.53 (H-11)	1.20 (H-26), 1.53 (H-14 β), 4.04 (H-10)
4.03 (H-9) & 4.04 (H-10)	1.70 (H-28), 3.33 (10-OH), 3.53 (H-11), 4.28 (H-7), 5.07 (H-29Z)
4.21 (30-OH)	4.89 (H-30), 7.371 (H-23)
4.28 (H-7)	2.22 (H-6 α), 2.65 (H-5 α), 3.22 (13-OH), 4.03 (H-9)
4.87 (H-29E)	1.70 (H-28), 5.07 (H-29Z)
4.89 (H-30)	1.08 (H-38), 1.40 (H-37), 2.64 (H-31), 4.21 (30-OH), 7.366 (H-20)

Table 3.9 continued

5.07 (H-29Z)	4.03 (H-9), 4.87 (H-29E)
5.95 (H-35)	1.24 (H-39), 1.28 (H-40), 7.371 (H-23)
7.366 (H-20)	2.66 (H-17 β), 4.89 (H-30)
7.371 (H-23)	5.95 (H-35), 9.89 (NH)
9.89 (NH)	1.20 (H-26), 1.60 (H-5 β), 7.371 (H-23)

3.3.4 Summary; *Janthitrem A* NMR Assignments

Generally the ^1H and ^{13}C NMR signal assignments determined in the present investigation for *janthitrem A* agreed with those observed for *janthitrem B* (Table 3.1) for the left-hand half of the molecule and those reported for *penitrem A* by de Jesus et al. (1983a) for the right-hand half of the molecule. The analysis of the *janthitrem A* data supported the view that the C-39 and C-40 signal assignments proposed by Wilkins et al. (1992) for *janthitrem B* should be revised to those reported in Table 3.1.

3.4 *Janthitrem C* NMR Discussion

Detailed analyses of one- and two-dimensional NMR data, including ^1H , COSY, TOCSY, g-HSQC and g-HMBC NMR spectral data afforded complete ^1H and partial ^{13}C NMR assignments for *janthitrem C*. Due to a paucity of material for *janthitrem C*, ^{13}C , DEPT-135 and NOESY NMR spectral data were unable to be obtained. ^{13}C signals were therefore assigned on the basis of the lower resolution g-HMBC and g-HSQC NMR spectral data.

One- and two-dimensional NMR data for *janthitrem C* was acquired and processed as described in Section 8.3.4. Signal assignments for *janthitrem C* were facilitated by comparison with those previously reported for *janthitrem B* (Section 3.2) and *janthitrem C* (Penn et al., 1993). The NMR data reported in this thesis

was determined at 400 MHz whereas the janthitrem C data reported by Penn et al. (1993) was determined at 500 MHz (^1H) or 125.8 MHz (^{13}C).

A complete assignment of the resonances is presented in Table 3.10. Methylene proton assignments are not reported in the format ($\text{H}_\alpha, \text{H}_\beta$) as NOESY spectral data was not acquired. It was apparent, from analysis of the data reported in Tables 3.10, 3.11, 3.12 and 3.13 that some revisions to previously proposed NMR assignments of Penn et al. (1993) were required.

3.4.1 ^1H , ^{13}C , DEPT-135, COSY and TOCSY NMR Spectra of Janthitrem C

Since ^{13}C and DEPT-135 NMR spectra for janthitrem C were unable to be obtained due to paucity of material (since a large portion of the original material decomposed rapidly), carbon resonances were assigned on the basis of lower resolution two-dimensional g-HSQC and g-HMBC spectral data and comparison with assignments for janthitrems B and D (Sections 3.2 and 3.5 respectively). Analysis of NMR spectral data revealed the presence of 37 carbon resonances (7 methyl, 7 methylene, 9 methine and 14 quaternary), which is consistent with the structure of janthitrem C. These resonances were, for the most part, almost identical to those reported for janthitrems B and D with differences only within the 0.1–0.2 ppm range. Variations of this magnitude can be accounted for by small differences in compound concentration, the level of residual water in the sample and NMR probe temperature (30°C in the present study). The carbon resonances for janthitrem C reported by Penn et al. (1993) were for the most part similar to those observed for janthitrem C, however significant differences were observed for C-25, C-39 and C-40.

The proton resonances for janthitrem C were similar to those reported by Penn et al. (1993) with the exception of assignments proposed for the H-5, H-14, H-15, H-16, H-25, H-26, H-35 and H-38 signals.

Table 3.10. ^1H and ^{13}C NMR assignments established for janthitrem C and published assignments for janthitrem C^a (δ).

	Janthitrem C		Janthitrem C ^a	
	^{13}C	^1H	^{13}C	^1H
C-2	155.3		155.6	
C-3	51.9		51.7	
C-4	43.5		43.4	
C-5	27.9	2.63, 1.62	27.8	1.61, 2.94
C-6	29.1	2.08, 1.82	28.0	1.81, 2.05
C-7	74.3	4.62	74.3	4.59
C-9	80.3	3.79	80.3	3.79
C-10	64.2	3.89	64.2	3.92
C-11	119.5	5.75	119.4	5.71
C-12	*		148.5	
C-13	78.4		77.5	
C-14	34.7	1.72, 2.01	34.7	1.56, 1.64
C-15	22.0	1.67, 2.04	22.0	1.59, 2.02
C-16	50.6	2.85	50.5	2.79
C-17	27.7	2.37, 2.65	27.8	2.35, 2.63
C-18	*		116.4	
C-19	127.9		127.7	
C-20	114.2	7.16	114.1	7.20
C-21	141.1		140.9	
C-22	133.6		133.3	
C-23	103.9	7.37	104.1	7.40
C-24	141.5		141.2	
C-25	16.5	1.37	14.3	0.86
C-26	20.0	1.02	20.1	0.92
C-27	143.4		143.8	
C-28	19.8	1.76	20.0	1.75
C-29	110.7	5.07, 4.86	110.7	5.09, 4.88
C-30	33.5	3.08, 2.64	33.5	3.09, 2.66
C-31	49.7	2.84	49.8	2.86
C-32	74.8		74.7	
C-34	73.0		72.9	
C-35	119.5	5.91	119.5	5.97
C-36	*		136.8	
C-37	30.3	1.26	22.5	1.07
C-38	22.4	1.04	30.4	1.28
C-39	32.3	1.24	32.4	1.25
C-40	30.4	1.28	16.6	1.31
10-OH		*		3.35
13-OH		*		
NH		9.76		9.85

* Signal not identified

^a Penn et al. (1993)

C-25 and H-25 Signal Assignments

Penn et al. (1993) reported the C-25 signal of janthitrem C to occur at 14.3 ppm and the H-25 signal to occur at 0.86 ppm. This was not, however, consistent with the assignments established in this study. The g-HMBC NMR spectrum of janthitrem C showed correlations between the proton signal at 1.37 ppm and ^{13}C signals attributable to C-4 (43.5 ppm), C-16 (50.6 ppm), C-3 (51.9 ppm) and C-2 (155.3 ppm). The only methyl signal which could give these correlations is H-25. This revised assignment was confirmed by correlations observed in the TOCSY NMR spectrum whereby H-25 (1.37 ppm) showed a correlation to H-16 (2.85 ppm). The H-25 signal of janthitrem B was observed to resonate at 1.34 ppm (Table 3.1), in close vicinity to the value observed for janthitrem C (1.37 ppm).

The g-HSQC NMR spectrum showed a correlation between H-25 (1.37 ppm) and a ^{13}C signal at 16.5 ppm which can be attributable to C-25. This chemical shift is consistent with that observed for janthitrem A (16.5 ppm), janthitrem B (16.6 ppm) and janthitrem D (16.6 ppm).

C-37 and H-37 Signal Assignments

Penn et al. (1993) reported the C-37 and H-37 signals to resonate at 22.5 and 1.07 ppm, respectively. This was however in contrast to the resonances of 30.3 and 1.26 ppm respectively determined in this study. The g-HMBC NMR spectrum of janthitrem C showed the proton signal at 1.26 ppm correlated to a methyl carbon (either C-37 or C-38), a methine carbon (C-31) and a quaternary carbon (C-32). The methyl signals which could be responsible for these correlations were H-38 or H-37. The signal at 1.26 ppm was attributed to H-37 after analysis of the NOESY NMR data generated for janthitrem D (Section 3.5.3). This methyl group signal (1.26 ppm) showed 4J correlations in the COSY and TOCSY NMR spectra to H-38 (1.04 ppm).

The g-HSQC NMR spectrum of janthitrem C showed a correlation between H-37 (1.26 ppm) and a ^{13}C signal at 30.3 ppm, which can be attributable to C-37. This chemical shift is consistent with that observed for janthitrem A (30.6 ppm), janthitrem B (30.6 ppm) and janthitrem D (30.5 ppm).

C-38 and H-38 Signal Assignments

The C-38 and H-38 signals for janthitrem C were reported by Penn et al. (1993) to resonate at 30.4 and 1.28 ppm respectively. These resonances correspond closely to those established in this study for C-37 and H-37 respectively (see above). The g-HMBC NMR spectrum of janthitrem C showed correlations between the proton signal at 1.04 ppm and ^{13}C signals attributable to C-37 (30.3 ppm), C-31 (49.7 ppm) and C-32 (74.8 ppm). The only methyl signal which could give these correlations is H-38. This assignment was consistent with the mutual 4J correlations observed between H-38 (1.04 ppm) and H-37 (1.26 ppm) in the COSY and TOCSY NMR spectra of janthitrem C.

The g-HSQC NMR spectrum showed a correlation between H-38 and a ^{13}C signal at 22.4 ppm, which can be attributed to C-38. This signal was confirmed by a correlation observed in the g-HMBC NMR spectrum where H-37 (1.26 ppm) showed a correlation to a methyl carbon (C-38) which resonated at 22.4 ppm. This chemical shift was consistent with that observed for janthitrem D (22.6 ppm) (see Table 3.14).

C-40 Signal Assignment

In the g-HMBC NMR spectrum of janthitrem C, H-39 (1.24 ppm) showed correlations to a quaternary carbon (C-34), a methine carbon (C-35) and a methyl carbon. The only methyl carbon which could correlate to H-39 is C-40, hence the signal at 30.4 ppm can be attributed to C-40, however Penn et al. (1993) reported the C-40 signal of janthitrem C to occur at 16.6 ppm. Similar shifts were also

observed for the C-40 of janthitrem A (30.4 ppm), janthitrem B (30.4 ppm) and janthitrem D (30.7 ppm).

H-5 Signal Assignment

Penn et al. (1993) reported the pair of H-5 methylene protons to resonate at 1.61 and 2.94 ppm in contrast to the resonances of 1.62 and 2.63 ppm elucidated in this investigation. The C-5 carbon signal (27.9 ppm) was identified by correlations in the g-HMBC NMR spectrum whereby H-26 (1.02 ppm) showed correlations to three quaternary carbons (C-3, C-4 and C-13 at 51.9, 43.5 and 78.4 ppm, respectively) and to a methylene carbon (C-5 at 27.9 ppm). g-HSQC data showed that the C-5 signal (27.9 ppm) exhibited correlations to methylene protons which occurred at 2.63 and 1.62 ppm.

These assignments were confirmed by correlations observed in the COSY and TOCSY NMR spectra. Each of the H-5 methylene proton signals showed correlations to the pair of H-6 methylene protons (2.08 and 1.82 ppm) in the COSY NMR spectrum and to the pair of H-6 protons (2.08 and 1.82 ppm) and H-7 (4.62 ppm) proton in the TOCSY NMR spectrum. H-5 (2.63 ppm) also showed a correlation to H-26 (1.02 ppm) in the TOCSY NMR spectrum. The H-5 signal assignments determined for janthitrem B (2.61 and 1.61 ppm: see Table 3.1 and Section 3.2) are in accordance with the assignments reported here for janthitrem C.

H-14 Signal Assignments

The H-14 methylene protons were reported by Penn et al. (1993) to resonate at 1.56 and 1.64 ppm. However, this was not consistent with the assignments elucidated in this study. The g-HSQC NMR spectrum of janthitrem C showed a correlation between two connected proton signals at 1.72 and 2.01 ppm and a ^{13}C signal at 34.7 ppm. Each of these proton signals showed correlations to H-15 (1.67 and 2.04 ppm) in the COSY NMR spectrum and H-15 (1.67 and 2.04 ppm),

H-16 (2.85 ppm) and H-17 (2.37 and 2.65 ppm) in the TOCSY NMR spectrum, readily defining the signals as the H-14 methylene proton signals.

H-15 Signal Assignments

g-HSQC, COSY and TOCSY spectral data showed that the H-15 methylene signals resonated at 1.67 and 2.04 ppm as opposed to 1.59 and 2.02 ppm as reported by Penn et al. (1993). Each of the H-15 protons showed COSY correlations to H-14 (1.72 and 2.01 ppm) and H-16 (2.85 ppm) and TOCSY correlations to H-14 (1.72 and 2.01 ppm), H-16 (2.85 ppm) and H-17 (2.37 and 2.65 ppm).

H-16 Signal Assignment

Penn et al. (1993) reported the H-16 signal of janthitrem C to occur at 2.79 ppm, whereas it was found to resonate at 2.85 ppm in the present investigation. In the *g*-HMBC NMR spectrum H-25 showed correlations to three quaternary carbons (C-2, C-3 and C-4 at 155.3, 51.9 and 43.5 ppm, respectively) and to one methine carbon (C-16 at 50.6 ppm). This readily defined the C-16 resonance as 50.6 ppm. The *g*-HSQC NMR spectrum of janthitrem C included a correlation between the C-16 (50.6 ppm) signal and its attached methane proton (H-16) at 2.85 ppm.

The proton signal at 2.85 ppm was observed to correlate with the H-15 (1.67 and 2.04 ppm) and H-17 (2.37 and 2.65 ppm) signals in the COSY NMR spectrum and the H-14 (1.72 and 2.10 ppm), H-15 (1.67 and 2.04 ppm) and H-17 (2.37 and 2.65 ppm) signals in the TOCSY NMR spectrum.

H-26 Signal Assignment

The H-26 signal of janthitrem C was reported by Penn et al. (1993) at 0.90 ppm, in contrast to 1.02 ppm as determined in this investigation. The *g*-HMBC NMR spectrum of janthitrem C showed correlations between the proton signal at 1.02 ppm and ¹³C signals attributable to C-5 (27.9 ppm), C-4 (43.5 ppm), C-3 (51.9

ppm) and C-13 (78.4 ppm). The only methyl signal which could give these correlations is H-26. In the COSY NMR spectrum H-26 (1.02 ppm) showed a 4J correlation to H-5 (2.63 ppm). The TOCSY spectrum included correlations between H-26 (1.02 ppm) and H-5 (2.63 ppm) and H-25 (1.37 ppm).

H-35 Signal Assignment

H-35 was reported to resonate at 5.97 ppm by Penn et al. (1993) whereas it was observed to occur at 5.91 ppm in this study. In the g-HMBC NMR spectrum of janthitrem C, both H-39 and H-40 showed correlations to a methyl carbon (C-40 for H-39 and C-39 for H-40), a quaternary carbon (C-34) and a methine carbon (C-35). This methine carbon resonated at 119.5 ppm, identical to the value reported for C-35 by Penn et al. (1993). The g-HSQC NMR spectrum for janthitrem C included a correlation between C-35 (119.5 ppm) and its attached proton at 5.91 ppm. The COSY NMR spectrum included a correlation between the proton signal at 5.91 ppm and H-31 (2.84 ppm) while the TOCSY NMR spectrum included correlations between H-35 (5.91 ppm) and H-23 (7.37 ppm), H-30 (2.64 and 3.08 ppm) and H-31 (2.84 ppm).

Table 3.11. COSY NMR correlations observed for janthitrem C (δ).

¹ H Signal	Cross peaks observed
1.02 (H-26)	2.63 (H-5)
1.04 (H-38)	1.26 (H-37)
1.26 (H-37)	1.04 (H-38)
1.62 (H-5)	1.82, 2.08 (H-6), 2.63 (H-5)
1.67 (H-15)	2.01 (H-14), 2.04 (H-15), 2.85 (H-16)
1.72 (H-14)	2.01 (H-14), 2.04 (H-15)
1.76 (H-28)	3.79 (H-9), 5.07, 4.86 (H-29)
1.82 (H-6)	2.08 (H-6), 2.63, 1.62 (H-5), 4.62 (H-7)
2.01 (H-14)	1.72 (H-14), 1.67 (H-15)
2.04 (H-15)	1.67 (H-15), 1.72 (H-14), 2.85 (H-16)
2.08 (H-6)	1.82 (H-6), 2.63, 1.62 (H-5), 4.62 (H-7)
2.37 (H-17)	2.65 (H-17), 2.85 (H-16)
2.63 (H-5)	2.08, 1.82 (H-6), 1.62 (H-5)
2.64 (H-30)	2.84 (H-31), 3.08 (H-30)
2.65 (H-17)	2.37 (H-17), 2.85 (H-16)
2.84 (H-31)	3.08, 2.64 (H-30), 5.91 (H-35)
2.85 (H-16)	2.04, 1.67 (H-15), 2.37, 2.65 (H-17)
3.08 (H-30)	2.64 (H-30), 2.84 (H-31)
3.79 (H-9)	1.76 (H-28), 3.89 (H-10), 5.07, 4.86 (H-29)
3.89 (H-10)	3.79 (H-9), 5.75 (H-11)
4.62 (H-7)	2.08, 1.82 (H-6), 5.75 (H-11)
4.86 (H-29)	1.76 (H-28), 3.79 (H-9), 5.07 (H-29)
5.07 (H-29)	1.76 (H-28), 3.79 (H-9), 4.86 (H-29)
5.75 (H-11)	3.89 (H-10), 4.62 (H-7)
5.91 (H-35)	2.84 (H-31)

Table 3.12. TOCSY NMR correlations observed for janthitrem C (δ).

¹ H Signal	Cross peaks observed
1.02 (H-26)	1.37 (H-25), 2.63 (H-5), 3.33 (13-OH)
1.04 (H-38)	1.26 (H-37)
1.24 (H-39)	1.28 (H-40)
1.26 (H-37)	1.04 (H-38)
1.28 (H-40)	1.24 (H-39)
1.37 (H-25)	2.85 (H-16)
1.62 (H-5)	2.08, 1.82 (H-6), 2.63 (H-5), 4.62 (H-7)
1.67 (H-15)	2.04 (H-15), 2.01, 1.72 (H-14), 2.37, 2.65 (H-17), 2.85 (H-16)
1.72 (H-14)	2.01 (H-14), 2.04, 1.67 (H-15), 2.37, 2.65 (H-17), 2.85 (H-16)
1.76 (H-28)	3.79 (H-9), 3.89 (H-10), 5.07, 4.86 (H-29)
1.82 (H-6)	2.63, 1.62 (H-5), 2.08 (H-6), 4.62 (H-7), 5.75 (H-11)
2.01 (H-14)	1.72 (H-14), 1.67 (H-15), 2.37, 2.65 (H-17), 2.85 (H-16)
2.04 (H-15)	1.72 (H-14), 1.67 (H-15), 2.37, 2.65 (H-17), 2.85 (H-16)
2.08 (H-6)	1.82 (H-6), 2.63, 1.62 (H-5), 4.62 (H-7), 5.75 (H-11)
2.37 (H-17)	2.01, 1.72 (H-14), 2.04, 1.67 (H-15), 2.65 (H-17), 2.85 (H-16)
2.65 (H-17)	1.67, 2.04 (H-15), 1.72, 2.01 (H-14), 2.37 (H-17), 2.85 (H-16)
2.63 (H-5)	1.02 (H-26), 2.08, 1.82 (H-6), 1.62 (H-5), 4.62 (H-7)
2.64 (H-30)	2.84 (H-31), 3.08 (H-30), 5.91 (H-35), 7.16 (H-20)
2.84 (H-31)	2.64, 3.08 (H-30), 5.91 (H-35), 7.16 (H-20)
2.85 (H-16)	2.01, 1.72 (H-14), 2.04, 1.67 (H-15), 2.37, 2.65 (H-17)
3.08 (H-30)	2.64 (H-30), 2.84 (H-31), 5.91 (H-35), 7.16 (H-20)
3.79 (H-9)	1.76 (H-28), 5.07, 4.86 (H-29), 4.62 (H-7), 3.89 (H-10)
3.89 (H-10)	1.76 (H-28), 3.79 (H-9), 4.62 (H-7), 5.07, 4.86 (H-29), 5.75 (H-11)
4.62 (H-7)	2.04, 1.82 (H-6), 2.63, 1.62 (H-5), 3.79 (H-9), 3.89 (H-10), 5.75 (H-11)
4.86 (H-29)	1.76 (H-28), 3.79 (H-9), 3.89 (H-10), 5.07 (H-29)
5.07 (H-29)	1.76 (H-28), 3.79 (H-9), 3.89 (H-10), 4.86 (H-29)
5.75 (H-11)	2.08, 1.82 (H-6), 5.07, 4.86 (H-29), 3.79 (H-9), 3.89 (H-10), 4.62 (H-7)
5.91 (H-35)	2.64, 3.08 (H-30), 2.84 (H-31), 7.37 (H-23)
7.16 (H-20)	2.64, 3.08 (H-30), 2.84 (H-31), 7.37 (H-23)
7.37 (H-23)	3.08, 2.64 (H-30), 7.16 (H-23)

3.4.2 *g*-HSQC and *g*-HMBC NMR Spectra of *Janthitrem C*

Analysis of *g*-HMBC and *g*-HSQC NMR spectral data allowed the unequivocal assignment of C-31, C-32, C-34 and C-35 and their attached protons. The *g*-HSQC NMR spectrum showed that the C-37, C-38, C-39 and C-40 methyl carbon signals which resonated at 30.3, 22.4, 32.3 and 30.4 ppm respectively exhibited correlations to protons which resonated at 1.26, 1.04, 1.24 and 1.28 ppm respectively. In the *g*-HMBC NMR spectrum, each of H-39 (1.24 ppm) and H-40 (1.28 ppm) showed correlations to C-34 (73.0 ppm) and C-35 (119.5 ppm), while each of H-37 (1.26 ppm) and H-38 (1.04 ppm) showed correlations to C-31 (49.7 ppm) and C-32 (74.8 ppm).

Table 3.13. Long-range ^{13}C - ^1H NMR correlations observed in the *g*-HMBC NMR spectrum of *janthitrem C* (δ).

^1H Signal	Correlated ^{13}C Signals
1.04 (H-38)	30.3 (C-37), 49.7 (C-31), 74.8 (C-32)
1.02 (H-26)	27.9 (C-5), 43.5 (C-4), 51.9 (C-3), 78.4 (C-13)
1.24 (H-39)	30.4 (C-40), 73.0 (C-34), 119.5 (C-35)
1.28 (H-40)	32.3 (C-39), 73.0 (C-34), 119.5 (C-35)
1.26 (H-37)	22.4 (C-38), 49.7 (C-31), 74.8 (C-32)
1.37 (H-25)	43.5 (C-4), 50.6 (C-16), 51.9 (C-3), 155.3 (C-2)
1.76 (H-28)	80.3 (C-9), 110.7 (C-29), 143.4 (C-27)
7.16 (H-20)	127.9 (C-19), 141.1 (C-21)
7.37 (H-23)	133.6 (C-22), 141.5 (C-24)

3.4.3 *Summary; Janthitrem C* NMR Assignments

The ^{13}C NMR data of *janthitrem C* was generally in accordance with that reported previously (Penn et al., 1993), with the exception of C-25, C-37, C-38 and C-40 only. However, greater differences were observed for the ^1H assignments, with the H-5, H-14, H-15, H-16, H-25, H-26, H-35, H-37 and H-38 signals all exhibiting significant changes to those proposed by Penn et al. (1993). These

changes were confirmed by observations in the COSY, TOCSY, g-HSQC and g-HMBC NMR spectra of janthitrem C. Due to a paucity of material, no carbon data for C-12, C-18 and C-36 was able to be attained, nor were the 10-OH and 13-OH resonances identified.

3.5 Janthitrem D NMR Discussion

Detailed analyses of one- and two-dimensional NMR data, including ^1H , ^{13}C , DEPT-135, COSY, TOCSY, g-HSQC, g-HMBC and NOESY NMR spectral data afforded complete ^1H and ^{13}C NMR assignments for janthitrem D. ^1H - ^1H connectivities and ^1H - ^{13}C connectivities were established using COSY and TOCSY experiments and g-HSQC and g-HMBC experiments respectively. The information provided by the NOESY experiment allowed the orientation of the CH_2 protons (as alpha or beta; axial or equatorial) and of the methyl groups of janthitrem D to be defined.

One- and two-dimensional janthitrem D NMR data was acquired and processed as described in Section 8.3.4. Signal assignments for janthitrem D were facilitated by comparison with those previously reported for janthitrem A (Section 3.3), janthitrem C (Section 3.4) and penitrem A (de Jesus et al., 1983a).

A complete assignment of the resonances of janthitrem D is presented in Table 3.14. Methylene proton assignments are reported in the format ($\text{H}_\alpha, \text{H}_\beta$) based on analyses of coupling constant and/or NOE data. Correlations observed in two-dimensional NMR experiments that substantiated these assignments are reported in Tables 3.15, 3.16, 3.17 and 3.18.

The NMR data reported in Table 3.14 was determined at 400 MHz, as was the case with janthitrem A, B and C. Analysis of the data reported in Tables 3.14,

3.15, 3.16, 3.17 and 3.18 for janthitrem D confirmed the revisions of assignments proposed for janthitrem C.

3.5.1 ^1H , ^{13}C , DEPT-135, COSY and TOCSY NMR Spectra of Janthitrem D

^{13}C and DEPT-135 NMR spectra of janthitrem D revealed the presence of 37 carbon resonances (7 methyl, 7 methylene, 9 methine and 14 quaternary). Janthitrem C and D differ only at the right-hand end of the molecule, at C-11 and C-12, where an epoxide resides in janthitrem D as opposed to the double bond present in janthitrem C. Janthitrem A and D both possess this epoxide, but differ at the left-hand end of the molecule, by an OH group present at C-30 in janthitrem A compared to a hydrogen in janthitrem D. Therefore, both janthitrem A and C can act as suitable models for comparison of NMR data produced by janthitrem D; janthitrem A for the signals produced by the right-hand side of the molecule and janthitrem C for signals produced by the left-hand side of the molecule.

The carbon and proton resonances for janthitrem D were consistent with those observed for janthitrem C for the left-hand half of the molecule. As mentioned previously, the difference in carbon and proton resonances between janthitrem C and D can be ascribed to the replacement of the double bond at C-11 and C-12 with an epoxide. This resulted in significant shifts in the proton resonances of H-7, H-9, H-10, H-11, H-26 and H-28 in particular.

Table 3.14. ^1H and ^{13}C NMR assignments established for janthitrem D (δ).

	^{13}C	^1H (α,β)		^{13}C	^1H (α,β)
C-2	155.3		C-23	104.2	7.38
C-3	51.9		C-24	141.5	
C-4	43.5		C-25	16.6	1.32
C-5	27.3	2.65, 1.62	C-26	19.0	1.18
C-6	29.0	2.22, 2.04	C-27	143.4	
C-7	72.2	4.27	C-28	19.8	1.70
C-9	74.8	4.025	C-29	111.7	5.07 (<i>Z</i>), 4.87 (<i>E</i>)
C-10	66.4	4.032	C-30	33.7	3.08, 2.64
C-11	62.1	3.52	C-31	50.0	2.85
C-12	66.4		C-32	74.8	
C-13	78.4		C-34	73.0	
C-14	30.4	1.64, 1.47	C-35	119.7	5.93
C-15	21.7	1.97, 1.56	C-36	137.0	
C-16	51.0	2.79	C-37	30.5	1.27
C-17	27.9	2.34, 2.63	C-38	22.6	1.05
C-18	116.9		C-39	32.5	1.24
C-19	127.9		C-40	30.7	1.29
C-20	114.4	7.16	10-OH		3.33
C-21	141.1		13-OH		3.22
C-22	133.6		NH		9.89

H-7 Signal Assignment

Since the C-7 signal can be inferred from data presented in Table 2.3 (see Chapter 2, Section 2.3.2), the resonance of H-7 can be identified from the g-HSQC NMR spectrum of janthitrem D where a correlation between C-7 (72.2 ppm) and its attached methane proton (H-7) at 4.27 ppm was observed. This assignment was confirmed by correlations observed in both the COSY and TOCSY NMR spectra where H-7 showed correlations to signals attributable to H-6 (2.22 and 2.04 ppm) and H-11 (3.52 ppm) in the COSY NMR spectrum and to H-5 (2.65 and 1.62 ppm), H-6 (2.22 and 2.04 ppm) and H-11 (3.52 ppm) in the TOCSY NMR spectrum. Almost identical resonances were observed for H-7 in janthitrem A, (4.28 ppm, see Table 3.1), and penitrem A (4.29 ppm) (de Jesus et al., 1983a).

H-9 and H-10 Signal Assignments

As with C-7, the C-9 and C-10 signals can be inferred from data presented in Table 2.3 (see Chapter 2, Section 2.3.2). Accordingly the resonance of H-9 and H-10 can be identified from correlations observed in the g-HSQC NMR spectrum where H-9 was observed to resonate at the lower chemical shift value of 4.025 ppm and H-10 was observed to resonate at 4.032 ppm. In the COSY and TOCSY NMR spectra, the overlapping H-9 and H-10 signals showed correlations to H-11 (3.52 ppm), H-28 (1.70 ppm) and H-29 (5.07 and 4.87 ppm), confirming their assignments.

The proton resonances elucidated for H-9 and H-10 were in close agreement with those reported for janthitrem A and penitrem A. In janthitrem A, H-9 and H-10 were observed to resonate at 4.03 and 4.04 ppm, respectively (Table 3.1), while in penitrem A both H-9 and H-10 were reported to occur at 4.04 ppm (de Jesus et al., 1983a).

H-11 Signal Assignment

The g-HSQC experiment showed that C-11, which resonated at 62.1 ppm (see Table 2.3, Chapter 2, Section 2.3.2), exhibited a correlation to H-11 (3.52 ppm). This value was almost identical to that observed for this proton in janthitrem A (3.53 ppm, see Table 3.1), and slightly lower than the reported value for penitrem A (3.57 ppm) (de Jesus et al., 1983a). In the COSY and TOCSY NMR spectra, H-11 (3.52 ppm) showed correlations to signals at 4.27 ppm (H-7), 4.025 ppm (H-9) and 4.032 ppm (H-10) as expected.

H-26 Signal Assignment

Two of the seven methyl groups, namely H-26 and H-28, showed significant changes in their proton resonances compared to the values observed for janthitrem C (Table 3.10). This pair of methyl groups are in close proximity to the 11,12-epoxy group. The g-HMBC NMR spectrum for janthitrem D showed correlations

between a proton signal at 1.18 ppm and ^{13}C signals attributable to C-5 (27.3 ppm), C-4 (43.5 ppm), C-3 (51.9 ppm) and C-13 (78.4 ppm). The only methyl signal which could give rise to these correlations is H-26, thereby establishing that the signal at 1.18 ppm is attributable to H-26. This assignment was confirmed by long range correlations observed in the COSY and TOCSY NMR spectra between H-26 (1.18 ppm) and H-5 (2.65 ppm).

The H-26 chemical shift determined for janthitrem D (1.18 ppm) can be compared to that found for the corresponding methyl group of penitrem A (1.22 ppm) (de Jesus et al., 1983a) and janthitrem A (1.20 ppm).

H-28 Signal Assignment

As noted above, H-28 showed a significant change in its resonance compared to that observed for janthitrem C (Table 3.10). The g-HMBC NMR spectrum of janthitrem D showed a correlation between the proton signal at 1.70 ppm and ^{13}C signals attributable to C-9 (74.8 ppm), C-29 (111.7 ppm) and C-27 (143.4 ppm). The only methyl signal which could give rise to these correlations is H-28, hence the signal at 1.70 ppm can be attributed to H-28. This assignment was confirmed by correlations observed in the COSY and TOCSY NMR spectra. H-28 (1.70 ppm) showed correlations to H-9 (4.025 ppm) and H-29 (5.07 and 4.87 ppm) in the COSY NMR spectrum and to H-9 (4.025 ppm), H-10 (4.032 ppm) and H-29 (5.07 and 4.87 ppm) in the TOCSY NMR spectrum.

The H-28 (1.70 ppm) resonance determined for janthitrem D was identical to that determined for janthitrem A (Table 3.1) and differed by only 0.01 ppm from that reported by de Jesus et al. (1983a) for penitrem A (1.71 ppm).

Table 3.15. COSY NMR correlations observed for janthitrem D (δ).

¹ H Signal	Cross peaks observed
1.05 (H-38)	1.27 (H-37)
1.18 (H-26)	2.65 (H-5 α)
1.27 (H-37)	1.05 (H-38)
1.47 (H-14 β)	1.64 (H-14 α), 1.97 (H-15 α), 1.56 (H-15 β)
1.56 (H-15 β)	1.64 (H-14 α), 1.47 (H-14 β), 1.97 (H-15 α), 2.79 (H-16)
1.62 (H-5 β)	2.22 (H-6 α), 2.04 (H-6 β), 2.65 (H-5 α)
1.64 (H-14 α)	1.47 (H-14 β), 1.97 (H-15 α), 1.56 (H-15 β)
1.70 (H-28)	4.025 (H-9), 5.07 (H-29 Z), 4.87 (H-29E)
1.97 (H-15 α)	1.56 (H-15 β), 1.64 (H-14 α), 1.47 (H-14 β), 2.79 (H-16)
2.04 (H-6 β)	2.22 (H-6 α), 2.65 (H-5 α), 1.62 (H-5 β), 4.27 (H-7)
2.22 (H-6 α)	2.04 (H-6 β), 2.65 (H-5 α), 1.62 (H-5 β), 4.27 (H-7)
2.34 (H-17 α)	2.63 (H-17 β), 2.79 (H-16)
2.63 (H-17 β)	2.34 (H-17 α), 2.79 (H-16)
2.65 (H-5 α)	2.22 (H-6 α), 2.04 (H-6 β), 1.62 (H-5 α)
2.64 (H-30 β)	2.85 (H-31), 3.08 (H-30 α)
2.79 (H-16)	1.97 (H-15 α), 1.56 (H-15 β), 2.34 (H-17 α), 2.63 (H-17 β)
2.85 (H-31)	3.08 (H-30 α), 2.64 (H-30 β), 5.93 (H-35)
3.08 (H-30 α)	2.64 (H-30 β), 2.85 (H-31)
3.52 (H-11)	4.025 (H-9), 4.032 (H-10), 4.27 (H-7)
4.025 (H-9)	1.70 (H-28), 5.07 (H-29Z), 4.87 (H-29E)
4.032 (H-10)	3.52 (H-11)
4.27 (H-7)	2.22 (H-6 α), 2.04 (H-6 β), 3.52 (H-11)
4.87 (H-29E)	1.70 (H-28), 4.025 (H-9), 5.07 (H-29Z)
5.07 (H-29Z)	1.70 (H-28), 4.025 (H-9), 4.87 (H-29E)
5.93 (H-35)	1.24 (H-39), 1.29 (H-40), 2.85 (H-31)

Table 3.16. TOCSY NMR correlations observed for janthitrem D (δ).

¹ H Signal	Cross peaks observed
1.05 (H-38)	1.27 (H-37)
1.18 (H-26)	2.65 (H-5 α)
1.24 (H-39)	1.29 (H-40), 5.93 (H-35)
1.27 (H-37)	1.05 (H-38)
1.29 (H-40)	1.24 (H-39), 5.93 (H-35)
1.32 (H-25)	2.79 (H-16)
1.47 (H-14 β)	1.64 (H-14 α), 1.97 (H-15 α), 1.56 (H-15 β), 2.34 (H-17 α), 2.63 (H-17 β), 2.79 (H-16)
1.56 (H-15 β)	1.64 (H-14 α), 1.47 (H-14 β), 1.97 (H-15 α), 2.34 (H-17 α), 2.63 (H-17 β), 2.79 (H-16)
1.62 (H-5 β)	2.22 (H-6 α), 2.04 (H-6 β), 2.65 (H-5 α), 4.27 (H-7)
1.64 (H-14 α)	1.47 (H-14 β), 1.97 (H-15 α), 1.56 (H-15 β), 2.34 (H-17 α), 2.63 (H-17 β), 2.79 (H-16)
1.70 (H-28)	4.025 (H-9), 4.032 (H-10), 5.07 (H-29Z), 4.87 (H-29E)
1.97 (H-15 α)	1.56 (H-15 β), 1.64 (H-14 α), 1.47 (H-14 β), 2.34 (H-17 α), 2.63 (H-17 β), 2.79 (H-16)
2.04 (H-6 β)	2.22 (H-6 α), 2.65 (H-5 α), 1.62 (H-5 β), 4.27 (H-7)
2.22 (H-6 α)	2.04 (H-6 β), 2.65 (H-5 α), 1.62 (H-5 β), 4.27 (H-7)
2.34 (H-17 α)	1.64 (H-14 α), 1.47 (H-14 β), 1.97 (H-15 α), 1.56 (H-15 β), 2.63 (H-17 β), 2.79 (H-16)
2.63 (H-17 β)	1.64 (H-14 α), 1.47 (H-14 β), 1.97 (H-15 α), 1.56 (H-15 β), 2.34 (H-17 α), 2.79 (H-16)
2.65 (H-5 α)	1.62 (H-5 β), 2.22 (H-6 α), 2.04 (H-6 β), 4.27 (H-7)
2.64 (H-30 β)	2.85 (H-31), 3.08 (H-30 α)
2.79 (H-16)	1.64 (H-14 α), 1.47 (H-14 β), 1.97 (H-15 α), 1.56 (H-15 β), 2.34 (H-17 α), 2.63 (H-17 β)
2.85 (H-31)	3.08 (H-30 α), 2.64 (H-30 β), 5.93 (H-35)
3.08 (H-30 α)	2.64 (H-30 β), 2.85 (H-31)
3.52 (H-11)	4.025 (H-9), 4.032 (H-10), 4.27 (H-7)
4.025 (H-9)& 4.032 (H-10)	1.70 (H-28), 5.07 (H-29Z), 4.87 (H-29E), 3.52 (H-11)
4.27 (H-7)	2.22 (H-6 α), 2.04 (H-6 β), 2.65 (H-5 α), 1.62 (H-5 β), 3.52 (H-11)
4.87 (H-29E)	1.70 (H-28), 4.025 (H-9), 4.032 (H-10), 5.07 (H-29Z)
5.07 (H-29Z)	1.70 (H-28), 4.025 (H-9), 4.032 (H-10), 4.87 (H-29E)
5.93 (H-35)	1.24 (H-39), 1.29 (H-40), 2.85 (H-31)

3.5.2 *g*-HSQC and *g*-HMBC NMR Spectra of *Janthitrem D*

As with *janthitrem*s A, B and C, analysis of *g*-HMBC and *g*-HSQC NMR spectral data allowed the unequivocal assignment of the C-31, C-32, C-34 and C-35 signals and their attached protons. The *g*-HSQC NMR spectrum for *janthitrem D* showed that the C-37, C-38, C-39 and C-40 methyl carbon signals which resonated at 30.5, 22.6, 32.5 and 30.7 ppm, respectively, exhibited correlations to protons which resonated at 1.27, 1.05, 1.24 and 1.29 ppm, respectively. These assignments were in close agreement with those observed for *janthitrem C* (Table 3.10), as was expected.

In the *g*-HMBC NMR spectrum, each of H-39 (1.24 ppm) and H-40 (1.29 ppm) showed correlations to C-34 (73.0 ppm) and C-35 (119.7 ppm), while each of H-37 (1.27 ppm) and H-38 (1.05 ppm) showed correlations to C-31 (50.0 ppm) and C-32 (74.8 ppm). These assignments were in close agreement with those established for *janthitrem C* (Table 3.10).

Table 3.17. Long-range ^{13}C - ^1H NMR correlations observed in the *g*-HMBC NMR spectrum of *janthitrem D* (δ).

^1H Signal	Correlated ^{13}C Signals
1.05 (H-38)	30.5 (C-37), 50.0 (C-31), 74.8 (C-32)
1.18 (H-26)	27.3 (C-5), 43.5 (C-4), 51.9 (C-3), 78.4 (C-13)
1.24 (H-39)	30.7 (C-40), 73.0 (C-34), 119.7 (C-35)
1.29 (H-40)	32.5 (C-39), 73.0 (C-34), 119.7 (C-35)
1.27 (H-37)	22.6 (C-38), 50.0 (C-31), 74.8 (C-32)
1.32 (H-25)	43.5 (C-4), 51.0 (C-16), 51.9 (C-3), 155.3 (C-2)
1.70 (H-28)	74.8 (C-9), 111.7 (C-29), 143.4 (C-27)
5.93 (H-35)	50.0 (C-31), 73.0 (C-34), 133.6 (C-22), 137.0 (H-36)
7.16 (H-20)	33.7 (C-30), 116.9 (C-18), 127.9 (C-19), 133.6 (C-22), 141.1 (C-21), 141.5 (C-24)
7.38 (H-23)	127.9 (C-19), 133.6 (C-22), 137.0 (C-36), 141.1 (C-21), 141.5 (C-24)

3.5.3 NOESY NMR Spectrum of Janthitrem D

NOESY data served to define the stereochemical dispositions of the H-37, H-38, H-39 and H-40 methyl groups of janthitrem D. As previously mentioned in this chapter (Section 3.2.3), Wilkins et al. (1992) proposed NMR signal assignments for the methyl group protons of janthitrem B based on the convention that H-37 and H-39 were α -oriented (i.e. inclined towards the lower face), while H-38 and H-40 were β -oriented (i.e. inclined towards the upper face). This convention was also employed here for janthitrem D.

The methyl group proton signal at 1.27 ppm displayed NOESY correlations with signals at 1.05 ppm, 2.85 ppm (H-31) and 2.64 and 3.08 ppm (H-30). Since H-31 is α -oriented this proton signal can be attributed to H-37. The signal at 1.05 ppm showed NOESY correlations to 2.64 ppm (H-30), 1.27 ppm (H-37) and 1.29 ppm and hence must be attributable to H-38. The signal at 1.24 ppm showed NOESY correlations to signals at 2.85 ppm (H-31), 5.93 ppm (H-35) and 1.29 ppm, showing it to be attributable to H-39. The signal at 1.29 ppm correlated to signals at 1.05 ppm (H-38) and 5.93 ppm (H-35) and hence must be attributable to H-40. The foregoing correlations are depicted in Figure 3.23 and are in accordance with signal assignments established for janthitrem A and janthitrem B (Table 3.1).

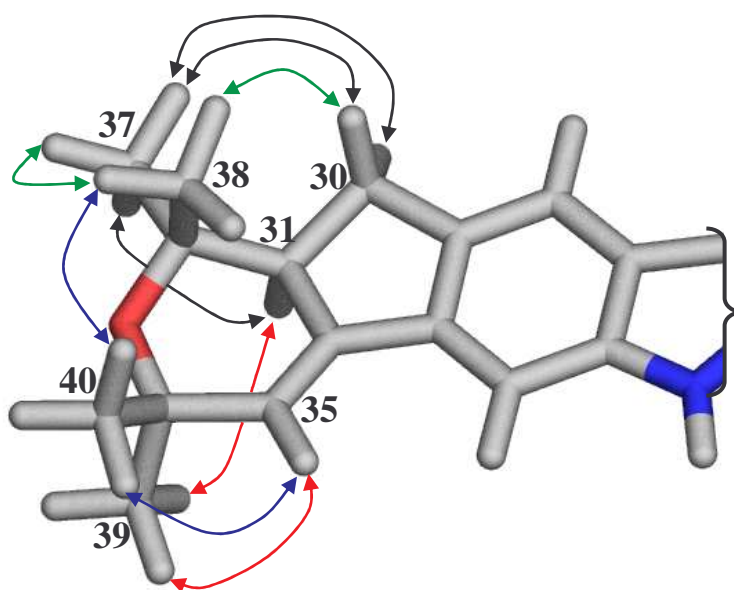


Figure 3.23. NOESY correlations observed for H-37 (black), H-38 (green), H-39 (red) and H-40 (blue) of janthitrem D.

The NOESY experiment also served to differentiate the stereochemical dispositions of the methylene proton signals for each of H-5, H-6, H-14, H-15, H-17 and H-30 as either α -oriented or β -oriented (i.e. oriented towards the lower or upper face respectively). g-HSQC, COSY (Table 3.15) and TOCSY (Table 3.16) data confirmed the assignments of H-5 as 2.65 and 1.62 ppm, H-6 as 2.22 and 2.04 ppm, H-14 as 1.64 and 1.47 ppm, H-15 as 1.97 and 1.56 ppm, H-17 as 2.34 and 2.63 ppm and H-30 as 2.64 and 3.08 ppm.

The H-5 signal at 2.65 ppm showed NOESY correlations to H-25 (1.32 ppm), H-5 (1.62 ppm), H-6 (2.04 and 2.22 ppm) and H-7 (4.27 ppm). The H-5 signal at 1.62 ppm correlated with H-26 (1.18 ppm), H-25 (1.32 ppm), H-6 (2.04 and 2.22 ppm) and H-5 (2.65 ppm) in the NOESY NMR spectrum. These observations showed the H-5 signal at 2.65 ppm to be α -oriented since it showed a correlation to the α -oriented H-25. The H-5 signal at 1.62 ppm was determined to be β -oriented since it showed a correlation to the β -oriented H-26. H-5 NOESY correlations are depicted in Figure 3.24.

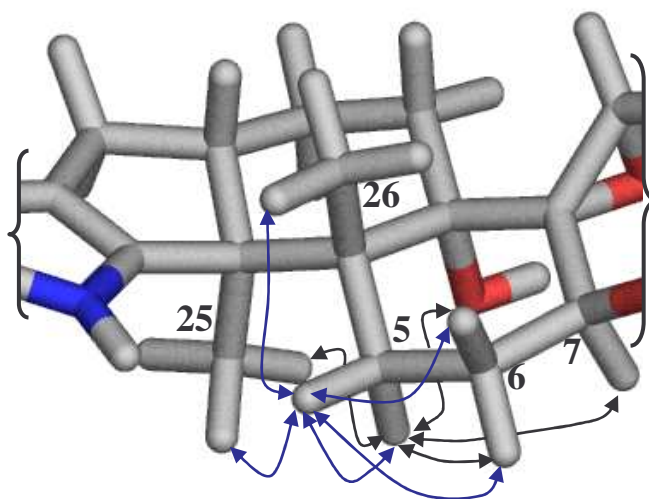


Figure 3.24. NOESY correlations observed for H-5 α (black) and H-5 β (blue) of janthitrem D.

The H-6 signal that resonated at 2.22 ppm showed NOESY correlations to signals at 2.65 (H-5 α), 1.60 ppm (H-5 β), 2.04 ppm (H-6) and 4.27 ppm (H-7). The H-6

signal that resonated at 2.04 ppm showed NOESY correlations to signals at 1.18 ppm (H-26), 2.22 ppm (H-6), 2.65 ppm (H-5 α) and 1.62 ppm (H-5 β). Since the H-6 signal at 2.22 ppm showed a correlation to the α -oriented H-7, it in turn must also be α -oriented. In a like manner, since the H-6 signal at 2.04 ppm showed a NOESY correlation to the β -oriented H-26, it must also be β -oriented. NOESY correlations observed for H-6 are depicted in Figure 3.25.

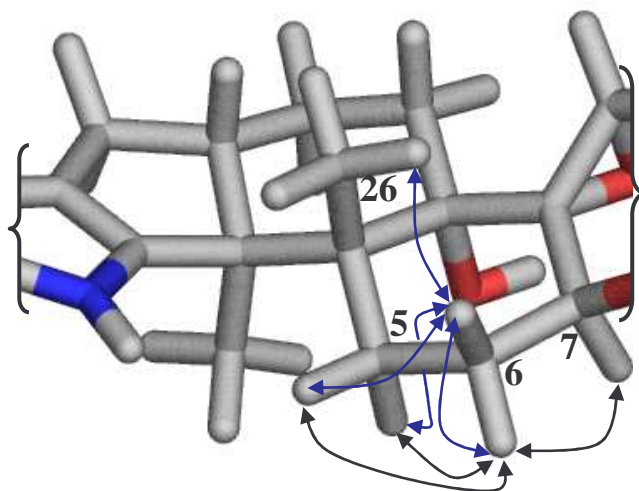


Figure 3.25. NOESY correlations observed for H-6 α (black) and H-6 β (blue) of janthitrem D.

The H-14 signal at 1.64 ppm showed NOESY correlations to H-14 (1.47 ppm) and H-15 (1.97 ppm) (Figure 3.26). The signal at 1.47 ppm showed NOESY correlations to H-26 (1.18 ppm), H-14 (1.64 ppm), H-16 (2.79 ppm) and H-11 (3.52 ppm) (Figure 3.26). Since only the H-14 signal at 1.47 ppm showed correlations to H-16 and H-26, both of which are β -oriented, this H-14 signal must also be β -oriented, whilst the H-14 signal at 1.64 ppm must be α -oriented as it showed correlations to the α -oriented H-11 and 13-OH.

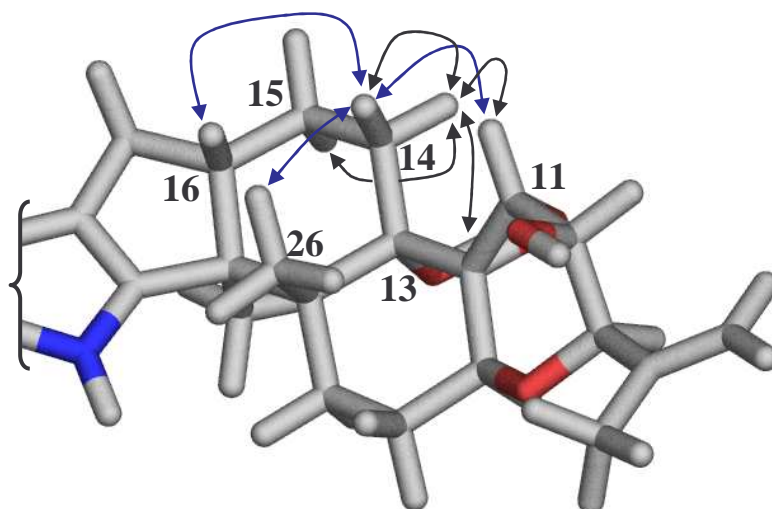


Figure 3.26. NOESY correlations observed for H-14 α (black) and H-14 β (blue) of janthitrem D.

H-15 (1.97 ppm) showed NOESY correlations to signals at 1.32 ppm (H-25), 1.56 ppm (H-15), 1.64 ppm (H-14 α) and 2.34 ppm (H-17). H-15 (1.56 ppm) showed NOESY correlations to signals at 1.64 ppm (H-14 α), 1.47 ppm (H-14 β), 1.97 ppm (H-15), 2.63 ppm (H-17) and 2.79 ppm (H-16). These correlations are consistent with the H-15 signal that resonated at 1.97 ppm being α -oriented (since it showed a correlation to the α -oriented H-25) and the H-15 signal that resonated at 1.56 ppm being β -oriented (since it correlated with the β -oriented H-16). These correlations are illustrated in Figure 3.27.

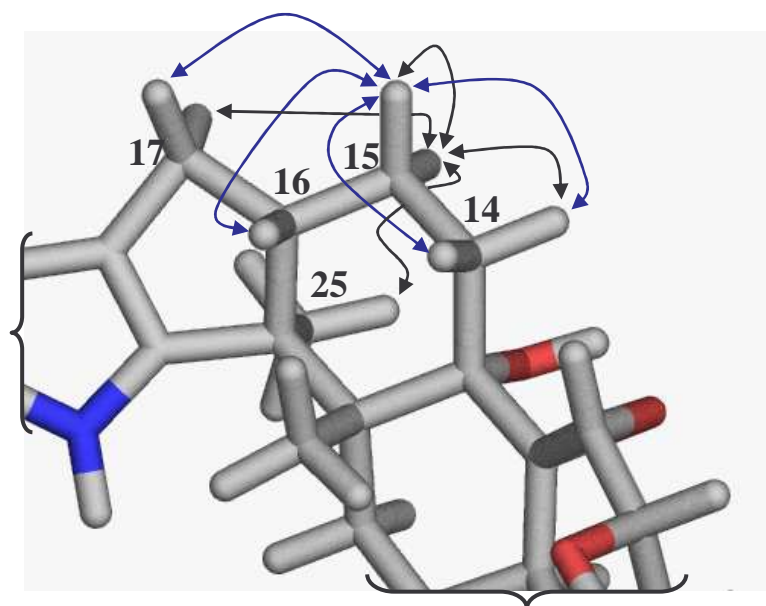


Figure 3.27. NOESY correlations observed for H-15 α (black) and H-15 β (blue) of janthitrem D.

The H-17 methylene proton resonance at 2.34 ppm showed correlations in the NOESY NMR spectrum to H-25 (1.32 ppm), H-15 α (1.97 ppm) and H-17 (2.63 ppm). The H-17 signal resonating at 2.63 ppm showed correlations in the NOESY spectrum to H-15 β (1.56 ppm), H-17 (2.34 ppm) and H-16 (2.79 ppm). Since the H-17 signal at 2.34 ppm showed a NOESY correlation to the α -oriented H-25, it was consequently assigned as being α -oriented. Since the H-17 signal at 2.63 ppm showed a correlation to the β -oriented H-16, it was also determined to be β -oriented. NOESY correlations observed for H-17 are depicted in Figure 3.28.

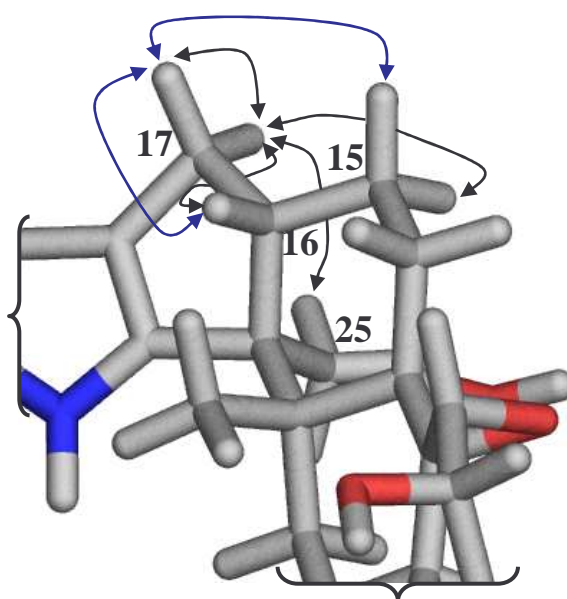


Figure 3.28. NOESY correlations observed for H-17 α (black) and H-17 β (blue) of janthitrem D.

The H-30 methylene signal at 2.64 ppm showed NOESY correlations to signals at 1.05 ppm (H-38), 1.27 ppm (H-37) and 3.08 ppm (H-30), whilst the signal at 3.08 ppm showed correlations to signals at 1.27 ppm (H-37), 2.64 ppm (H-30) and 2.85 ppm (H-31). The foregoing correlations are consistent with the H-30 signal that resonated at 2.64 ppm being β -oriented since it showed a correlation to the β -oriented H-38, while the H-30 signal at 3.08 ppm must be α -oriented since it showed a correlation to the α -oriented H-31. The NOESY correlations shown by H-30 are depicted in Figure 3.29.

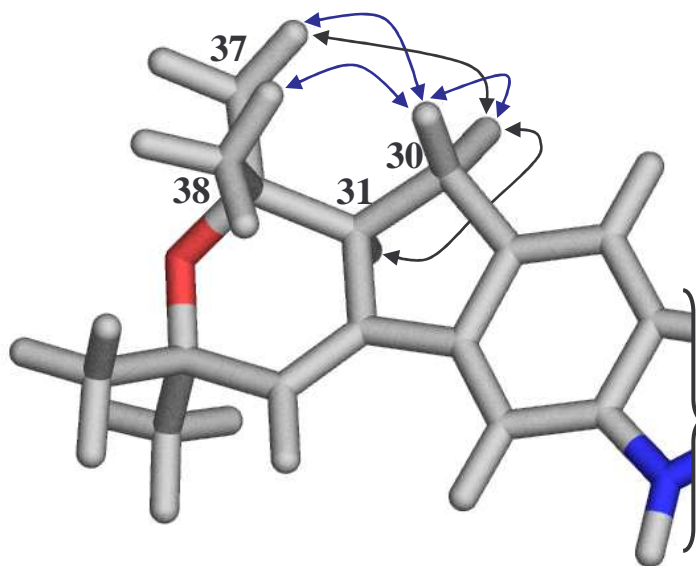


Figure 3.29. NOESY correlations observed for H-30 α (black) and H-30 β (blue) of janthitrem D.

As with janthitrems A and B, the protons attached to the C-29 methylene group were designated as having *E* or *Z* orientations based on the CIP priority rules (Section 3.2.3). *g*-HSQC, COSY and TOCSY data showed that the pair of H-29 methylene protons resonated at 4.87 and 5.07 ppm. The H-29 signal at 4.87 ppm showed NOESY correlations to signals attributable to H-28 (1.70 ppm) and H-29 (5.07 ppm) (Figure 3.30). The H-29 signal at 5.07 ppm showed NOESY correlations to signals attributable to H-9 (4.025 ppm) and H-29 (4.87 ppm) (Figure 3.30).

Based on the CIP priority rules, the proton showing correlations to H-9 is of higher priority and so is assigned as *Z*, while the proton showing correlations to H-28 is of lower priority and so is assigned as *E* (Blackwood et al., 1968). Therefore the H-29 signal resonating at 4.87 ppm was assigned *E* and the signal resonating at 5.07 ppm was assigned *Z*. This was the same conclusion reached for janthitrem A and janthitrem B (Sections 3.2.3 and 3.3.3).

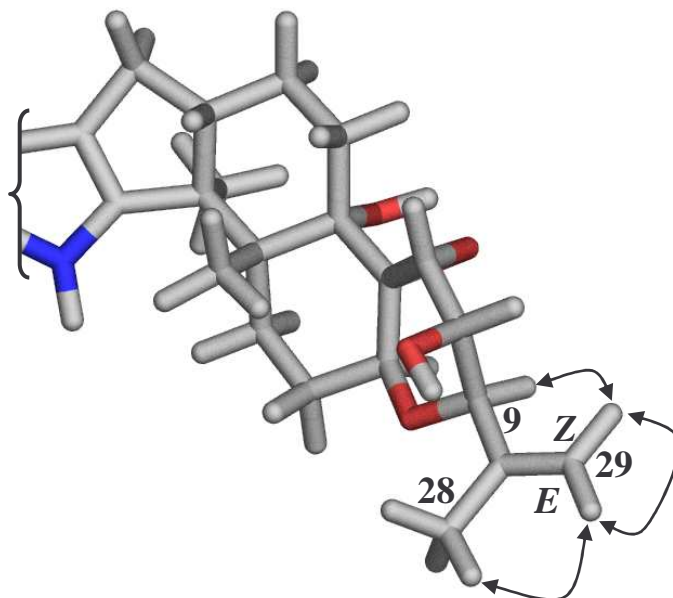


Figure 3.30. NOESY correlations observed for H-29E and H-29Z of janthitrem D.

Table 3.18. NOESY NMR correlations observed for janthitrem D.

¹ H Signal	Cross peaks observed
1.05 (H-38)	1.27 (H-37), 1.29 (H-40), 2.64 (H-30β)
1.18 (H-26)	1.47 (H-14β), 1.62 (H-5β), 2.04 (H-6β), 2.79 (H-16), 3.52 (H-11)
1.24 (H-39)	1.29 (H-40), 2.85 (H-31), 5.93 (H-35)
1.27 (H-37)	1.05 (H-38), 2.64 (H-30β), 3.08 (H-30α), 2.85 (H-31)
1.29 (H-40)	1.24 (H-39), 1.05 (H-38), 5.93 (H-35)
1.32 (H-25)	2.34 (H-17α), 2.65 (H-5α), 1.62 (H-5β), 1.97 (H-15α), 3.22 (13-OH)
1.47 (H-14β)	1.18 (H-26), 1.64 (H-14α), 2.79 (H-16), 3.52 (H-11)
1.56 (H-15β)	1.64 (H-14α), 1.47 (H-14β), 1.97 (H-15α), 2.63 (H-17β), 2.79 (H-16)
1.62 (H-5β)	1.18 (H-26), 1.32 (H-25), 2.22 (H-6α), 2.04 (H-6β), 2.65 (H-5α)
1.64 (H-14α)	1.47 (H-14β), 1.97 (H-15α), 3.22 (13-OH), 3.52 (H-11)
1.70 (H-28)	4.025 (H-9), 4.032 (H-10), 4.87 (H-29E)
1.97 (H-15α)	1.32 (H-25), 1.56 (H-15β), 1.64 (H-14α), 2.34 (H-17α)
2.04 (H-6β)	1.18 (H-26), 2.22 (H-6α), 2.65 (H-5α), 1.62 (H-5β)

Table 3.18 continued

2.22 (H-6 α)	2.04 (H-6 β), 2.65 (H-5 α), 1.62 (H-5 β), 4.27 (H-7)
2.34 (H-17 α)	2.63 (H-17 β), 1.32 (H-25), 1.97 (H-15 α)
2.63 (H-17 β)	1.56 (H-15 β), 2.34 (H-17 α), 2.79 (H-16)
2.64 (H-30 β)	1.05 (H-38), 1.27 (H-37), 3.08 (H-30 α)
2.65 (H-5 α)	1.32 (H-25), 2.22 (H-6 α), 2.04 (H-6 β), 1.62 (H-5 β), 4.27 (H-7)
2.79 (H-16)	1.18 (H-26), 1.47 (H-14 β), 1.97 (H-15 α), 1.56 (H-15 β), 2.63 (H-17 β)
2.85 (H-31)	1.27 (H-37), 3.08 (H-30 α)
3.08 (H-30 α)	1.27 (H-37), 2.64 (H-30 β), 2.85 (H-31)
3.22 (13-OH)	1.32 (H-25), 1.64 (H-14 α)
3.52 (H-11)	1.18 (H-26), 1.47 (H-14 β), 1.64 (H-14 α), 4.032 (H-10)
4.025 (H-9)	1.70 (H-28), 5.07 (H-29Z)
4.032 (H-10)	1.70 (H-28), 3.52 (H-11), 5.07 (H-29Z)
4.27 (H-7)	2.22 (H-6 α), 2.65 (H-5 α), 4.025 (H-9)
4.87 (H-29E)	1.70 (H-28), 5.07 (H-29Z)
5.07 (H-29Z)	4.025 (H-9), 4.87 (H-29E)
5.93 (H-35)	1.24 (H-39), 1.29 (H-40)

3.5.4 Summary; *Janthitrem D* NMR Assignments

Generally, the ^1H and ^{13}C assignments of *janthitrem D* determined in the present investigation agreed with those observed for *janthitrem C* (Table 3.10) for the left-hand half of the molecule and for *janthitrem A* (Table 3.1) for the right-hand half of the molecule. NOESY NMR spectral data allowed the orientation of CH_2 groups and methyl groups to be determined. No NMR data for *janthitrem D* has previously been reported.

CHAPTER FOUR

LC–UV–MS Analysis of Indole–Diterpenoids

4.1 Introduction

LC–UV–MS is a highly effective tool for identification and analysis of a range of compounds. When methods and techniques are developed that allow in-depth analysis of a class of compounds (in this case indole–diterpenoids), a new understanding of the behaviour of the compounds and their properties can be gained.

This chapter reports an investigation of the positive and negative ion LC–UV–MS spectra of indole–diterpenoids, determined under a variety of conditions including different ionisation methods (APCI and ESI) and in the presence of different buffers (acetic acid and formic acid). Hitherto, no account of the negative ion spectra of indole–diterpenoids has appeared in the literature. As no significant differences were observed in the spectra of samples acquired using either acetic acid or formic acid as the buffer, all data was obtained using acetic acid as the buffer.

The development of enhanced and sensitive LC–UV–MS methods allowed the rapid analysis of crude cultures and of any isolated samples. This in turn greatly facilitated the identification and quantification of culture metabolites.

During the course of the investigations reported in this thesis, there was a requirement to determine the identity of compounds present in extracts of a culture derived from a mouldy walnut sample (Chapter 6). Detailed LC–UV–MS

analyses of the mouldy walnut extracts using the positive and negative ion LC–UV–MS procedures developed for janthitrem metabolites showed that penitrems A–F were present in the mouldy walnut extracts.

4.2 Comparison of an APCI and ESI Source in an LC–UV–MS System

An LC–UV–MS method for the analysis of janthitrems, penitrems and other indole–diterpenoids was required. Since all previous LC–UV–MS data which had been reported by AgResearch for samples submitted for indole–diterpenoid analyses had been obtained using an LC–UV–MS system fitted with an ESI source, this configuration was initially employed to analyse the penitrem containing samples on The University of Waikato’s LC–UV–MS system. When standard positive ion LC–UV–MS procedures were applied to the mouldy walnut extracts, UV and mass spectral peaks attributable to penitrem A were observed, although the mass spectral ion current peak appeared to be suppressed (Figure 4.1). Typically the signal to noise ratio of the UV response at 233 nm was *ca.* 3 times that of the full scan ESI ion current.

Rundberget and Wilkins (2002b) have reported that penitrem A and related analogues show greater responses when an LC–UV–MS system fitted with an APCI source was used as opposed to an ESI source. Consequently, a comparative study of APCI versus ESI responses was performed.

While the work reported in this thesis was in progress, an opportunity arose for penitrem containing samples to be run on a higher sensitivity LTQ LC–UV–MS system at the National Veterinary Institute in Oslo, Norway as opposed to the LCQ Advantage system available at The University of Waikato (refer to Section 8.5.1 for full details). Penitrems A–F were analysed using APCI and ESI sources on the LTQ system.

The chromatograms determined using the LTQ system at the National Veterinary Institute, Oslo, Norway showed that the APCI source was superior (typically by a factor of *ca.* 5–20) to the ESI source for the analysis of penitrems. Experiments carried out at The University of Waikato, New Zealand to verify these findings provided unequivocal evidence that APCI was a better source than ESI for the analysis of penitrems.

The APCI and ESI experiments were run consecutively so that the samples were exposed to the same conditions and instrument settings for the purpose of direct comparison. The indole–diterpenoids that were utilised in these comparative investigations were samples of janthitrems A–D and standards of penitrem A, lolitrem B, paxilline, paspaline, paspalinine and terpendole C. The APCI and ESI $[M+H]^+$ ion peak responses for the indole–diterpenoids were determined and compared to their respective UV absorption maxima at 260 nm for the janthitrems, 235 nm for paxilline and paspaline, 230 nm for paspalinine and terpendole C, 233 nm for penitrem A and 268 nm for lolitrem B. Results, expressed as the % ratio of the $[M+H]^+$ ion mass spectral peak area divided by the UV peak area at the selected wavelength, are presented in Table 4.1.

Table 4.1. % UV versus APCI or ESI [M+H]⁺ peak area responses.

Indole–Diterpenoid Standard	APCI % Ratio (Mass/UV)	ESI % Ratio (Mass/UV)	Improvement Factor
Paspaline	540.4	705.1	0.8
Paspalinine	433.2	25.9	16.7
Paxilline	1673.3	72.0	23.2
Penitrem A	29.0	3.0	9.7
Janthitrem A	24.6	5.4	4.6
Janthitrem B	34.0	5.8	5.9
Janthitrem C	19.0	4.0	4.8
Janthitrem D	11.8	9.1	1.3
Lolitrem B	409.1	12.7	32.2
Terpendole C	194.1	77.4	2.5

An improved [M+H]⁺/UV ratio was observed for all compounds run using the APCI source with the exception of paspaline. An improvement factor greater than one indicates a greater APCI response (relative to the ESI response). The sensitivity gain was more marked for some analogues than others (see Table 4.1). In accordance with the findings of Rundberget and Wilkins (2002b), penitrem A was found to give a greater response in APCI mode than in ESI mode (Figures 4.1 and 4.2). Consequently, all subsequent LC–UV–MS data acquisitions were performed using an APCI source.

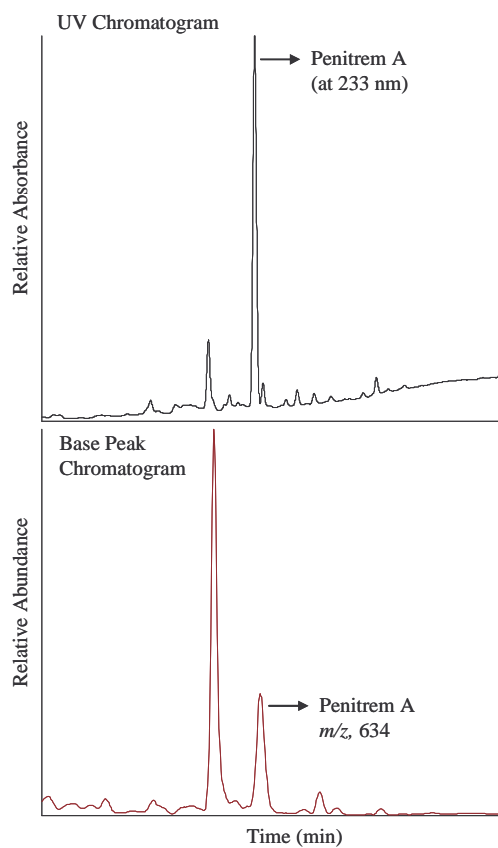


Figure 4.1. LC–UV–MS spectrum of penitrem A (ESI) at 233 nm (upper profile) and m/z 634, $[M+H]^+$ (lower profile).

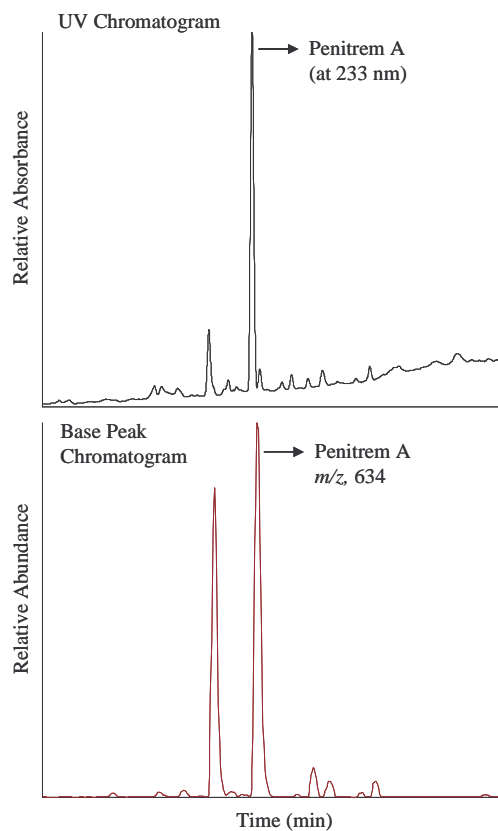


Figure 4.2. LC–UV–MS spectrum of penitrem A (APCI) at 233 nm (upper profile) and m/z 634, $[M+H]^+$ (lower profile).

4.3 APCI Vapourisation Temperature

Since the majority of samples investigated during the course of this research tended to be indole–diterpenoid compounds, a janthitrem B standard was run on The University of Waikato LC–UV–MS system using a range of APCI vaporisation temperatures in order to determine the optimal vapourisation temperature for indole–diterpenoid compounds (refer to Section 8.5.2 for full experimental details). Five vapourisation temperatures were evaluated; namely 250, 300, 350, 400 and 450°C.

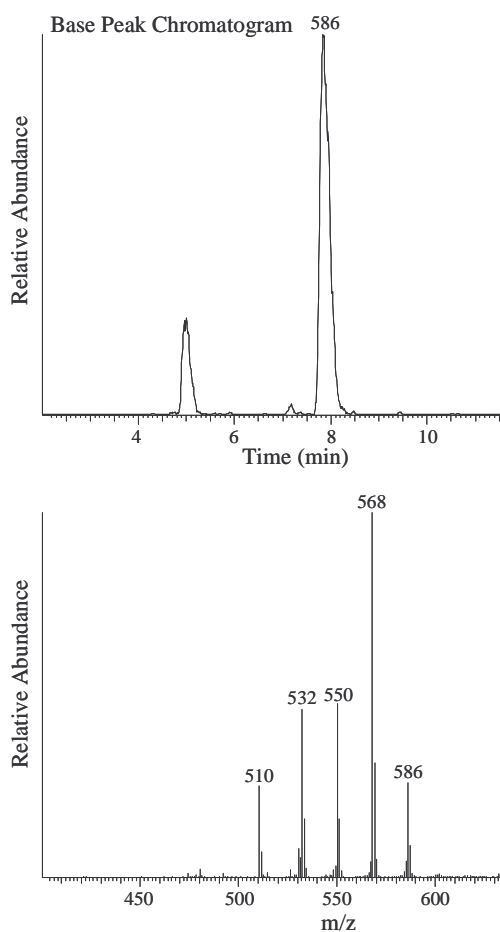


Fig 4.3. 250°C APCI mass spectrum. Values of m/z for major ions observed for the 586 peak are given.

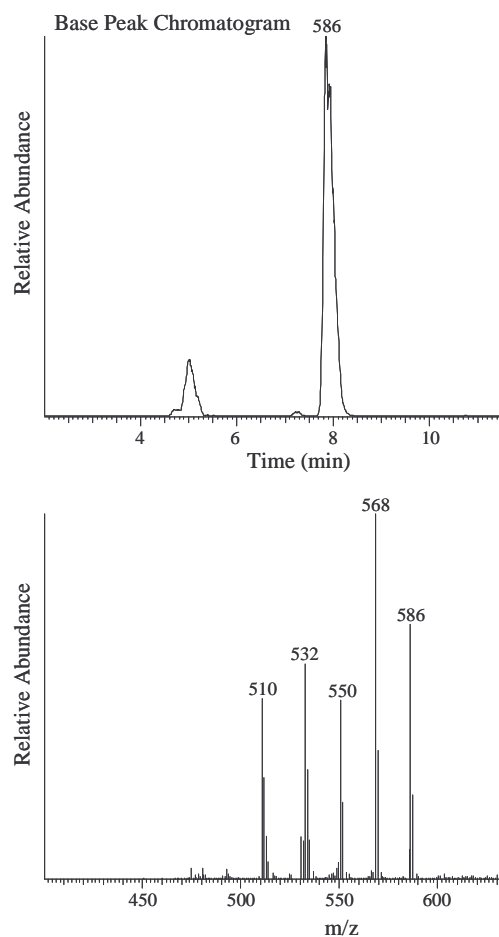


Figure 4.4. 300°C APCI mass spectrum. Values of m/z for major ions observed for the 586 peak are given.

The two initial injections of janthitrem B were performed with vapourisation temperatures of 250°C and 300°C respectively. The resulting spectra (see Figures

4.3 and 4.4 respectively) showed that neither of these temperatures were ideal. At both 250°C and 300°C, the base peak ion occurred at, m/z 568 $[M+H-water]^+$, rather than at m/z 586 $[M+H]^+$. The desired $[M+H]^+$ ion was only observed as a small contributor to the total ion current. The m/z 568 (water loss) ion can arise as a consequence of either or both thermally induced, or acetic acid catalysed dehydration processes during the passage of analyte molecules through the heated zone of the APCI inlet.

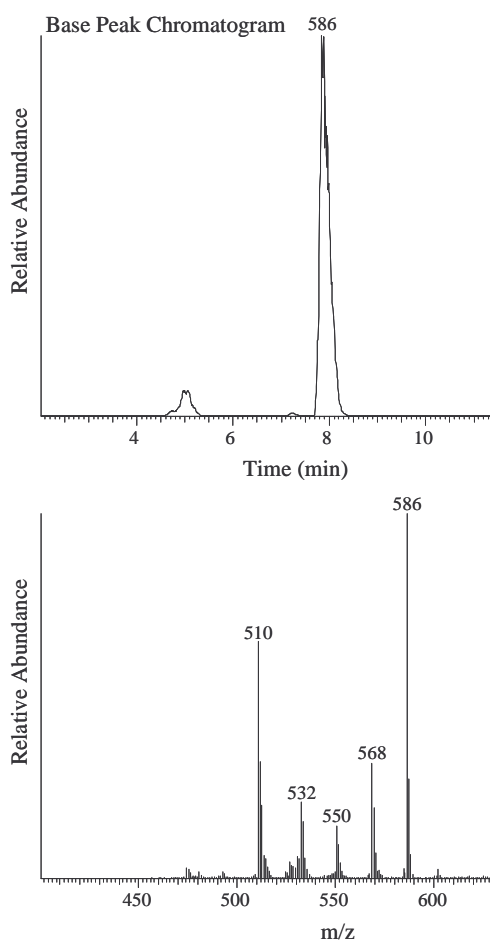


Figure 4.5. 350°C APCI spectrum. Values of m/z for major ions observed for the 586 peak are given.

At 350°C, the expected m/z 586 $[M+H]^+$ ion was the dominant ion observed. However, a significant water loss ion, at m/z 568, was still observable (*ca.* 50% of the $[M+H]^+$ ion). A substantial m/z 510 ion, attributable to the loss of acetone (58

amu) and water (18 *amu*) (total 76 *amu*) from the $[M+H]^+$ ion was also observed (Figure 4.5).

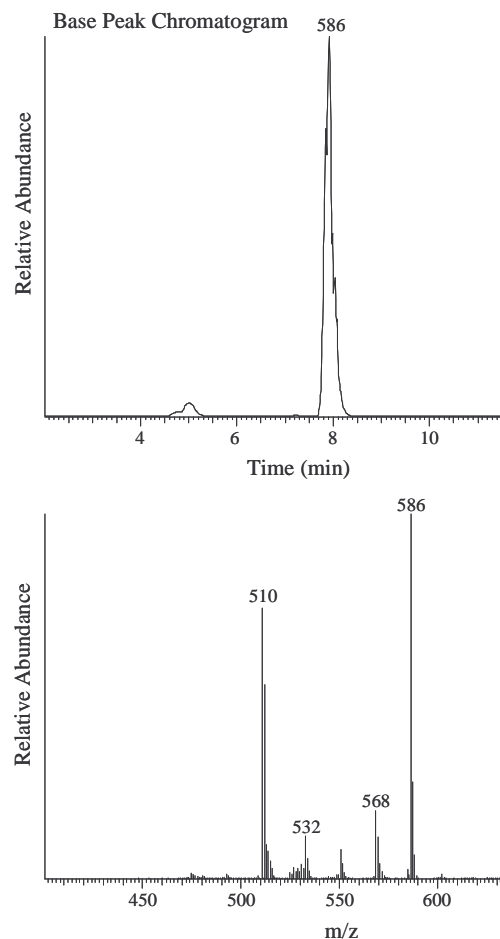


Figure 4.6. 400°C APCI spectrum. Values of m/z for major ions observed for the 586 peak are given.

A vapourisation temperature of 400°C gave a similar result to that obtained at 350°C, with the m/z 586 $[M+H]^+$ ion the dominant fragment ion, together with a strong m/z 510 ion (Figure 4.6). However, the m/z 568, $[M+H-\text{water}]^+$ ion was largely suppressed. A possible explanation for this is that at 400°C, it is less likely that residual acetic acid will be present in vapour exiting from the APCI heated region prior to material being introduced to the MS source through the mass spectrometer's heated capillary interface (which was maintained at 250°C during each of the evaluation experiments).

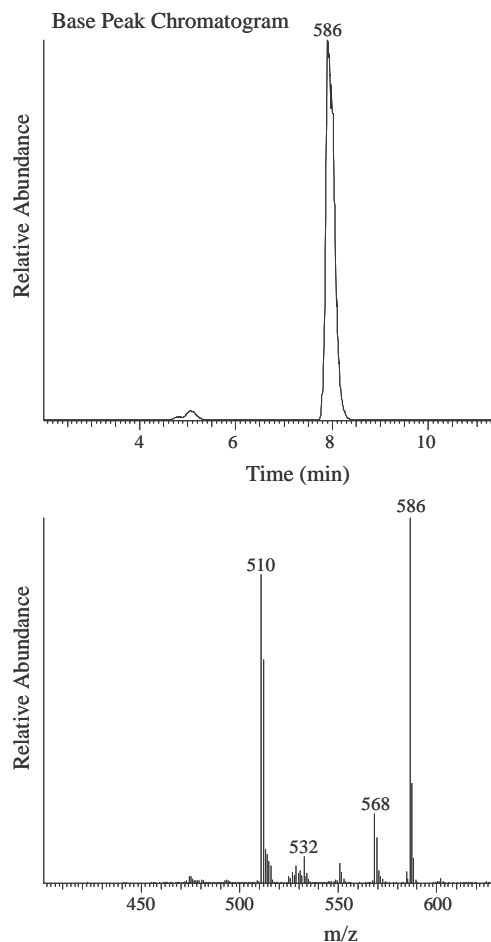


Figure 4.7. 450°C APCI spectrum. Values of m/z for major ions observed for the 586 peak are given.

At 450°C, as at 400°C, the m/z 586 $[M+H]^+$ ion was the dominant peak with the m/z 510 ion the only other significant fragment (Figure 4.7). At 450°C the m/z 568 ($[M+H-\text{water}]^+$) ion was almost completely suppressed.

Summary of Findings

APCI heater temperatures of 250°C and 300°C afforded an appreciable level of the m/z 568 (water loss) ion, whereas the preference is for the $[M+H]^+$ ion to be the dominant peak. Temperatures in the range of 350–450°C afforded the desired m/z 586 $[M+H]^+$ ion as the major fragment, together with lesser levels of m/z 568 $[M+H-\text{water}]^+$ and 510 $[M+H-\text{acetone}-\text{water}]^+$ ions.

A 350°C vapourisation temperature was considered ideal for janthitrem B analysis on the basis that it afforded a more favourable ratio between the desired m/z 586 $[M+H]^+$ ion and m/z 568 (water loss) or 510 (acetone plus water loss) ions. It was also believed that a lower APCI heater temperature of 350°C (rather than 400°C or 450°C) would be less likely to affect any samples being analysed in an adverse way by (for example) facilitating thermal dehydration and/or molecular rearrangement processes.

4.4 LC–UV–MS APCI and ESI Positive Ion Modes

The LC–UV–MS characteristics of some indole–diterpenoid compounds and their MS^n fragmentation pathways were investigated in positive ion mode using an LC–UV–MS system fitted with either an ESI source or an APCI source. The indole–diterpenoid compounds analysed were janthitrems A–D, penitrems A–F, lolitrem B, paxilline, terpendole C and paspalinine. Full experimental details are described in Section 8.5.3.

Significant differences were observed in the MS^2 and MS^3 fragmentation pathways determined for janthitrems A–D, penitrems A–F, lolitrem B, paxilline, terpendole C and paspalinine. Some of the differences were found to be dependent on their structural features and the type of source employed.

4.4.1 Fragmentation of Janthitrems

Each of janthitrems A, B, C and D fragmented under positive ion full scan conditions to afford an $[M-58]^+$ ion corresponding to the loss of acetone and an $[M-76]^+$ ion, which is believed to be due to the sequential loss of acetone and water. These ions were also observed in the MS^2 spectra of the janthitrems. The loss of 58 *amu* can be attributed to the loss of an acetone molecule from the

bridging $-\text{C}(\text{CH}_3)_2-\text{O}-$ ether linkage (Naude et al., 2002), via a retro Diels–Alder (RDA) rearrangement (Figure 4.8).

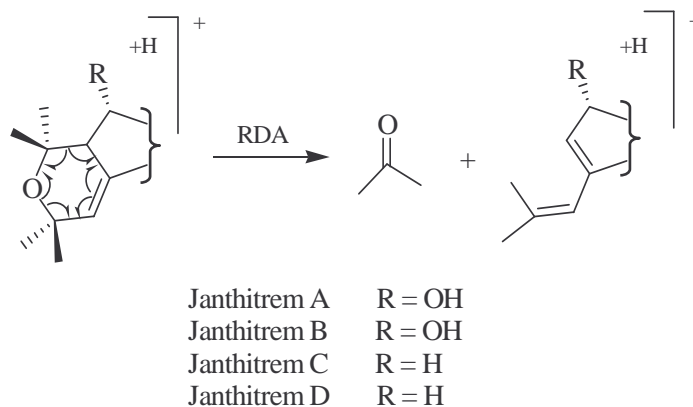


Figure 4.8. Loss of acetone in janthitrem A–D.

Janthitrem A

Identical MS^2 fragmentation was observed for janthitrem A under positive ion conditions, regardless of the source employed, be it ESI or APCI. Under MS^2 conditions the m/z 602 $[\text{M}+\text{H}]^+$ ion of janthitrem A fragmented to generate m/z 544 $[\text{M}-58]^+$ and m/z 526 $[\text{M}-76]^+$ ions, as observed in the full scan spectrum. As noted above, these ions are believed to arise from the loss of acetone (58 *amu* loss) and acetone plus water (76 *amu* loss). A plausible structure for the acetone loss fragment observed in the MS and MS^2 mass spectra of all of the janthitrem A is given in Figure 4.8.

The loss of water could be due to the loss of any of the three OH groups present in janthitrem A (at C-10, C-13 or C-30). One such water loss is shown in Figure 4.9. Fragmentation of the m/z 544 (acetone loss) ion under MS^3 conditions afforded an m/z 526 ion (–18 *amu*), thereby supporting the proposal that the latter ion arises via the sequential loss of acetone and water rather than by the direct loss of a 76 *amu* fragment.

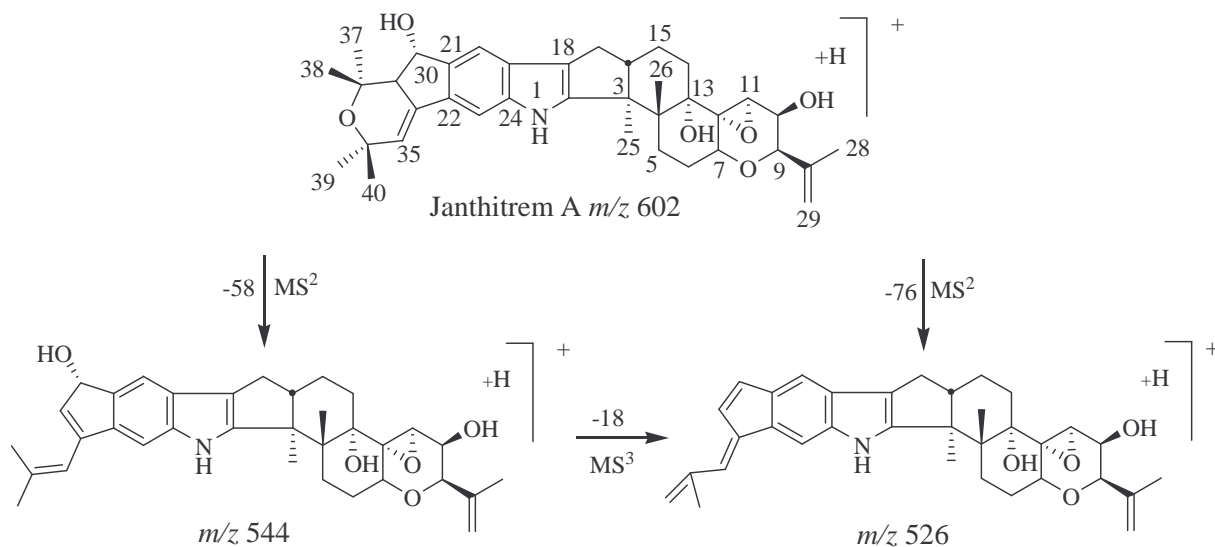


Figure 4.9. Fragmentation of janthitrem A in positive ion MS^2 and MS^3 spectra.

Janthitrem B

Fragmentation of the m/z 586 janthitrem B $[M+H]^+$ ion under ESI conditions afforded an m/z 528 ion (58 *amu* loss). This loss can be attributed to the loss of acetone via a retro Diels–Alder rearrangement (Figure 4.8). Further fragmentation of the m/z 528 ion under MS^3 conditions afforded an m/z 510 ion (water loss peak). The loss of a water molecule may occur via the loss of any of the three OH groups (C-10, C-13 or C-30) present in janthitrem B. One such loss is shown in Figure 4.10.

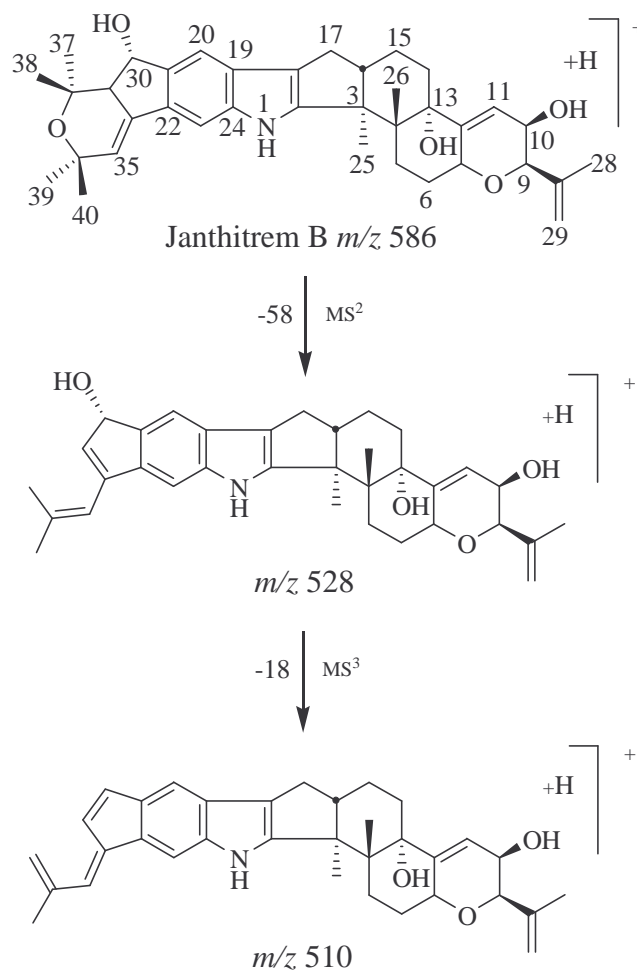


Figure 4.10. Fragmentation of janthitrem B in positive ion MS^2 and MS^3 spectra (ESI).

The fragmentation behaviour of janthitrem B under APCI conditions differed from that observed under ESI conditions. In APCI, fragmentation of the m/z 586 $[M+H]^+$ ion under MS^2 conditions predominantly afforded m/z 568 and m/z 510 ions, corresponding to the loss of water, and water plus acetone respectively (as opposed to the loss of acetone observed under ESI conditions). Further fragmentation of the m/z 510 ion under MS^3 conditions afforded an m/z 440 (loss of 70 *amu* from the m/z 510 ion) fragment (Figure 4.11). The loss of 70 *amu* can be ascribed to the loss of a C_4H_6O residue as a C_3H_5-CHO molecule from the right-hand terminal ring via a retro Diels–Alder mechanism, as illustrated in Figure 4.12. The m/z 440 ion would have an enol group which would be expected to equilibrate to the corresponding aldehyde form.

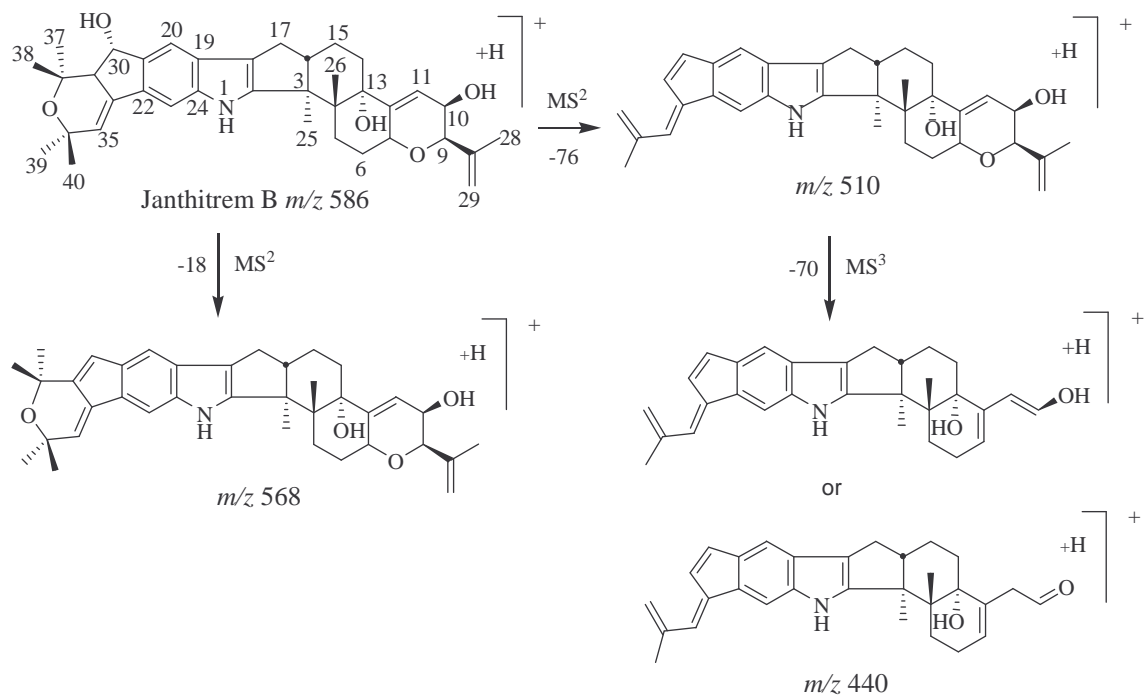


Figure 4.11. Fragmentation of janthitrem B in positive ion MS² and MS³ spectra (APCI).

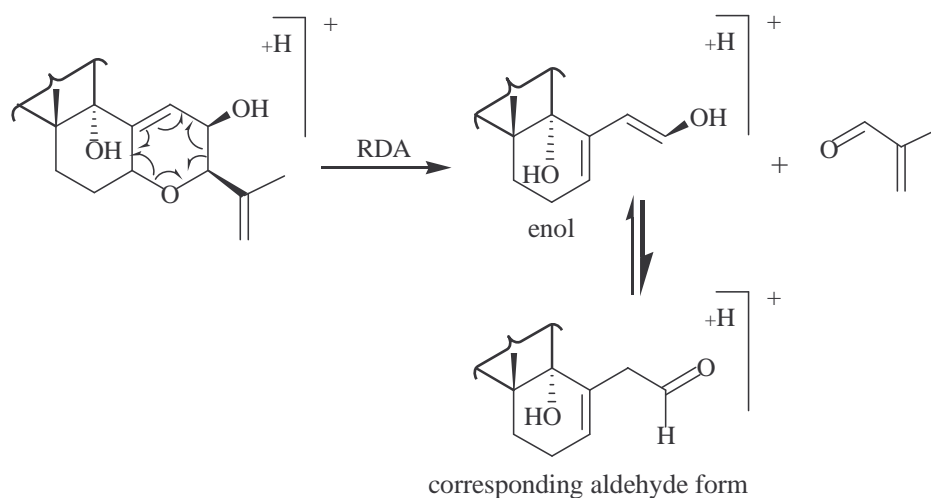


Figure 4.12. Retro Diels–Alder rearrangement of janthitrem B involving formation of an enol group which equilibrates to the corresponding aldehyde form.

Janthitrem C

Fragmentation of the m/z 570 $[M+H]^+$ ion of janthitrem C under ESI MS² conditions afforded an m/z 554 ion (-16 amu). The loss of 16 amu could arise from either the loss of an oxygen atom or the loss of a methane group. Both of

these losses are rarely encountered in mass spectrometry. On balance, it is considered to be more likely that the 16 *amu* loss arises from the loss of a methane molecule rather than an oxygen atom.

HRMS data could differentiate between an oxygen versus methane loss, however, the LCQ system used in this investigation did not have high resolution capabilities. Possibly, under ESI conditions, the loss of 16 *amu* may be explained by the loss of a methane molecule through the loss of the C-25 methyl group or via loss of an oxygen atom from either the C-13 or C-10 hydroxyl group or by ring contraction of a 6-membered oxido ring to afford a cyclopentene ring (Figure 4.13).

Fragmentation of the *m/z* 554 ion under MS³ conditions afforded an *m/z* 496 ion (58 *amu* loss). This loss was observed for janthitrems A and B, albeit in the MS² spectrum, and is believed to arise through the loss of acetone via a retro Diels–Alder rearrangement at the left-hand end of the molecule (Figure 4.8).

Under APCI conditions, the losses of 58 *amu* and 16 *amu* were both observed during MS² analysis. Under MS³ conditions, further fragmentation of the *m/z* 512 (acetone loss) ion afforded an *m/z* 442 ion arising from the loss of 70 *amu*, as observed for janthitrem B (Figure 4.14). As in janthitrem B, the 70 *amu* loss can be attributed to the loss of a C₃H₅–CHO molecule via a retro Diels–Alder pathway (Figure 4.12).

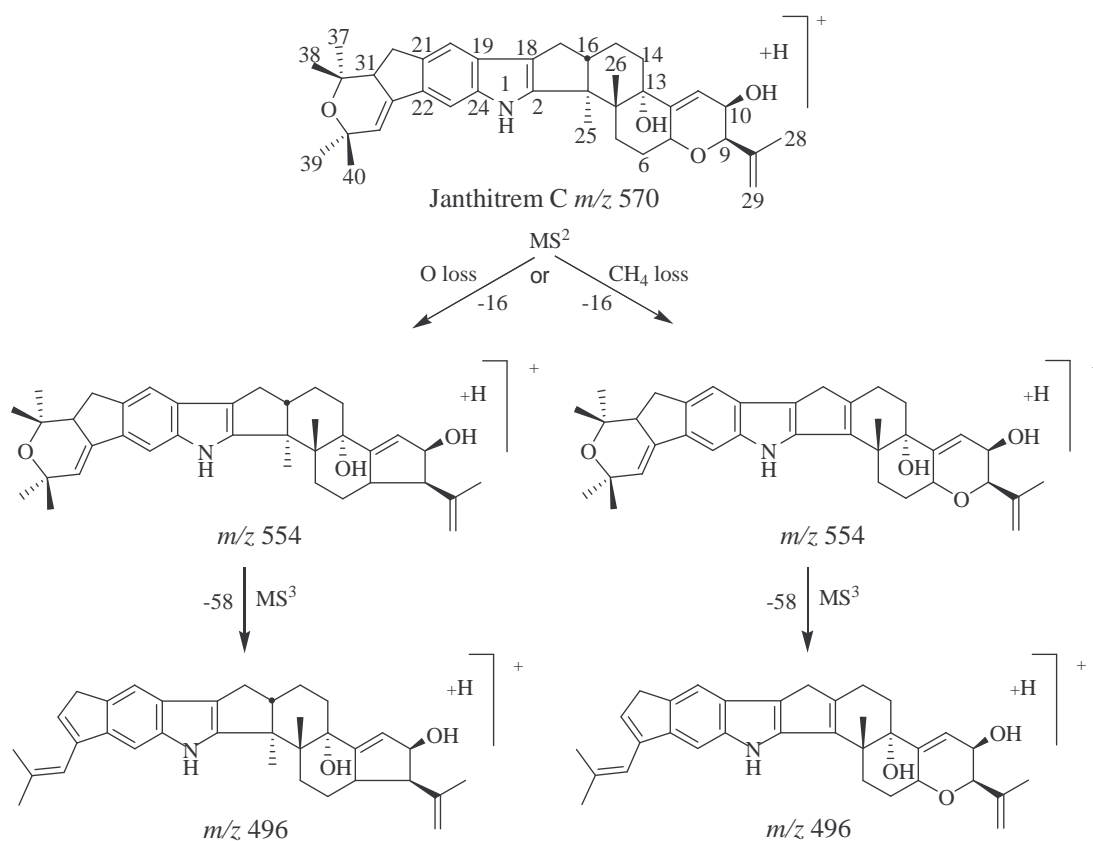


Figure 4.13. Fragmentation of janthitrem C in positive ion MS² and MS³ spectra (ESI).

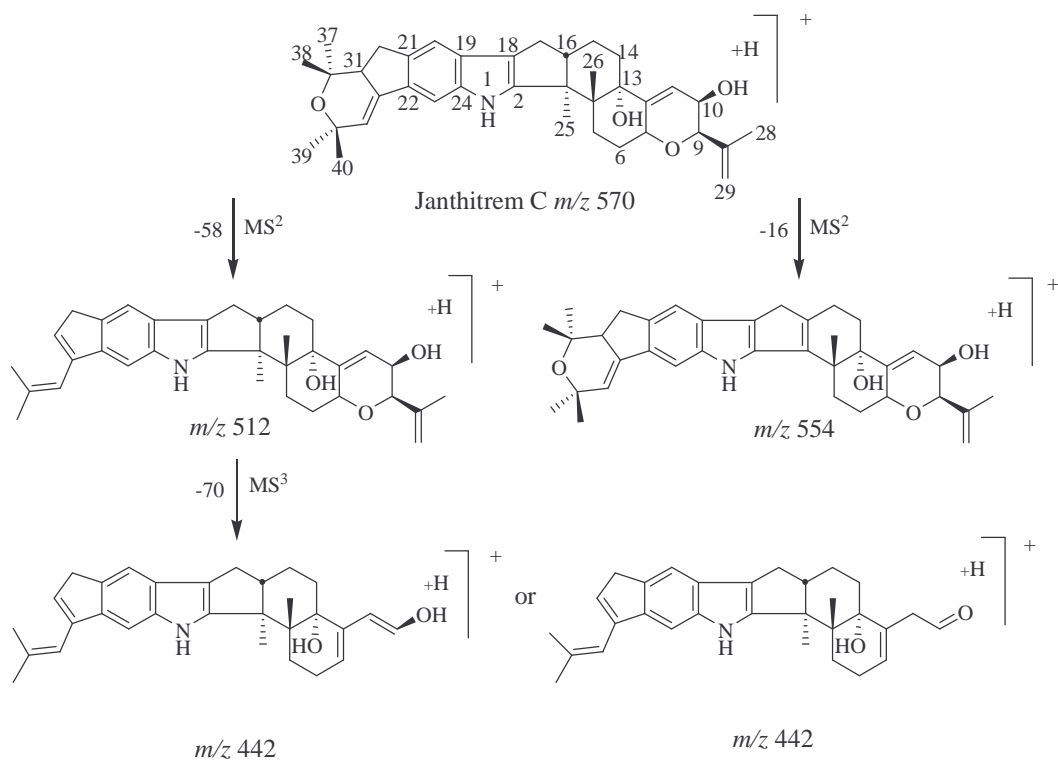


Figure 4.14. Fragmentation of janthitrem C in positive ion MS² and MS³ spectra (APCI).

Janthitrem D

A similar series of fragment ions were observed in positive ion ESI and APCI MS spectra of janthitrem D. Fragmentation of the m/z 586 $[M+H]^+$ ion afforded m/z 528 (58 *amu* loss) and m/z 570 (16 *amu* loss) ions. Analogous losses of acetone (58 *amu*) were observed for janthitrem A, B and C and of methane (or oxygen) (16 *amu*) for janthitrem C. These losses are accounted for in Figure 4.15.

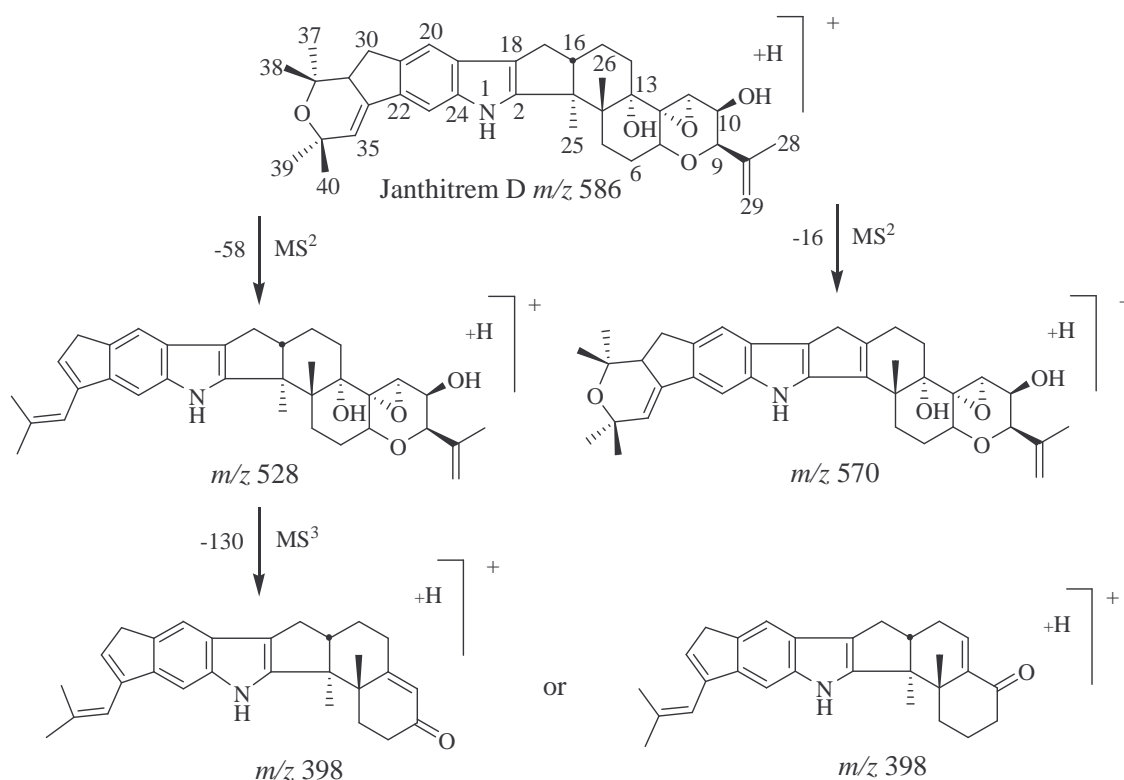


Figure 4.15. Fragmentation of janthitrem D in positive ion MS^2 and MS^3 spectra.

Under MS^3 conditions, fragmentation of the m/z 528 ion (acetone loss ion) afforded an m/z 398 ion (loss of 130 *amu*). The loss of 130 *amu* can only be ascribed to the loss of $C_{10}H_{10}$, C_9H_6O , $C_8H_2O_2$ or $C_6H_{10}O_3$. Since the chlorine atom is retained in the 130 *amu* loss ions observed for penitrem A and E (see Section 4.4.2), and if these losses are analogous, the loss of a $C_{10}H_{10}$ fragment from the left-hand portion of the janthitrem D structure is not plausible, nor is the loss of a $C_8H_2O_2$ formulation due to the inadequate number of hydrogen atoms present.

Similarly, it is difficult to envisage how a C₉H₆O fragment could be lost from the tri-oxygenated right-hand portion of the janthitrem D structure. On the other hand, the loss of a C₆H₁₀O₃ fragment as HC(=O)–CHOH–CHOH–C₃H₅ from the right-hand terminal ring of janthitrem D can be readily envisaged. This would, with appropriate hydrogen transfers, afford an *m/z* 398 ion for which a possible structure is shown in Figure 4.15. Alternatively, concerted loss of the 13-OH group as a water molecule followed by loss of C₆H₈O₃ (overall C₆H₁₀O₃ loss) can be envisaged as affording a conjugated enone structure that retains the C-7 oxygen atom as a keto group. A plausible ion structure for this option is shown in Figure 4.15. It is of note that janthitrem analogues that possess a C-11 and C-12 double bond show a retro Diels–Alder type 70 *amu* loss under MS³ conditions, whereas those possessing an 11,12-epoxide show a 130 *amu* loss.

Summary of Findings

Generally, janthitrem analogues showed 18 (water), 58 (acetone) or 76 (58 + 18) *amu* losses in full scan and MS² spectra under both APCI and ESI conditions. Under APCI conditions, janthitrem A and B were observed to lose 18 *amu*, whereas janthitrem C and D were observed to lose 16 *amu*, corresponding to the loss of either a methane molecule or an oxygen atom. The most significant difference in fragmentation patterns observed for janthitrem A and B under APCI and ESI conditions was the observation of an increased number of water losses under APCI conditions. These losses may primarily arise from thermal dehydration of the vapourising analyte (Rundberget and Wilkins, 2002b).

4.4.2 Fragmentation of Penitrem A

The MS² and MS³ fragmentation patterns observed for penitrem A, B, C, D, E and F during positive ion APCI LC–UV–MS analyses served to divide the penitrem A analogues into three sub-groups, based on structural variations in their right-hand ring structures in the vicinity of C-7 to C-11. Thus, the MSⁿ fragmentation of

penitrem A corresponded closely with that of penitrem E, with the ion masses differing only due to the presence of a chlorine atom in penitrem A rather than a proton in penitrem E. Similarly, after allowing for the presence or absence of a chlorine atom, the MSⁿ features of penitrem C corresponded closely with that of penitrem D, as did those of penitrems B and F. Furthermore, the behaviour of the three sub-groups of penitrems under both APCI and ESI conditions were essentially identical up to the MS³ stage. Because ESI ion currents and peak intensities were less than those generated under APCI conditions, MS⁴ data was not generated for the six penitrems under ESI conditions.

Ions observed in the full scan, MS², MS³ and MS⁴ spectra of the penitrems A–F (Figure 4.16) are listed in Table 4.2. Dominant ions (*ca.* 50% of base peak) are shown in bold type whilst the smaller, less significant ions (*ca.* < 50% of base peak) are presented in plain text. Plausible structures have been proposed for dominant ions wherever possible, and for selected lower intensity ions.

Table 4.2. Ions observed in MS spectra of penitrems A–F under positive ion conditions.

Penitrem	Full Scan [MH] ⁺ (m/z)	MS ² Ions (m/z)	MS ³ Ions (m/z)	MS ⁴ Ions (m/z)
Penitrem A	634	558, 616 , 598, 540	540, 332 , 368, 522, 412	332, 410 , 440, 522, 504, 456
Penitrem E	600	524, 582 , 564	506, 298 , 334, 488	298, 376 , 488, 406
Penitrem B	584	566, 514 , 497, 548	496 , 414, 478	396, 478 , 366
Penitrem F	618	600, 548 , 531, 582	530 , 448, 280	512, 430, 400 , 418, 382, 494
Penitrem C	602	584, 532 , 566, 514, 496	462, 514 , 532, 496	444, 496 , 426, 478
Penitrem D	568	550, 498 , 532, 480	428, 480 , 410	410 , 462

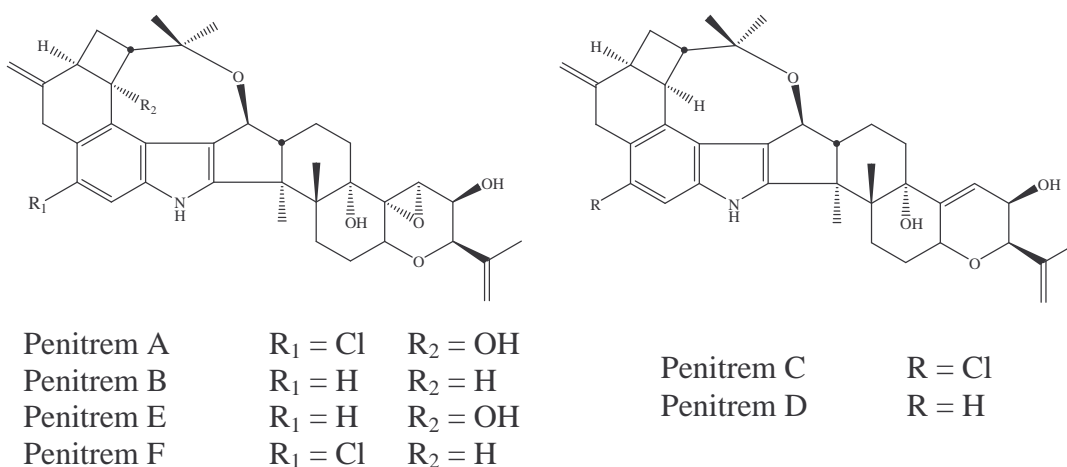


Figure 4.16. Structures of penitrems A–F.

Penitrem A and Penitrem E

In full scan APCI and ESI mode, penitrems A and E each showed [M+H]⁺ as well as [M+H–18]⁺ and [M+H–58–18]⁺ ions, corresponding to the loss of water and water plus acetone molecules. These ions were also observed in the MS² spectra

of penitrems A and E. The loss of 58 *amu* can be attributed to the loss of acetone from the C-17 to C-31 ether bridge. Possibly, this loss is enhanced by the presence of a gamma-hydroxyl group at C-30 since the equivalent 58 *amu* loss is not seen in the MSⁿ spectra of penitrems B, C, D and F, all of which are devoid of a 30-OH group. Ion structures presented in Figure 4.17 have been formulated as arising from the loss of the 30-OH group, rather than the 13- or 10-OH groups.

Further fragmentation of the *m/z* 558 (76 *amu* loss) ion of penitrem A under MS³ conditions afforded fragment ions at *m/z* 540 and 332, arising from the loss of 18 *amu* (water) and 226 *amu* respectively. Plausible structures for these ions are proposed in Figure 4.17. The loss of 226 *amu* may be ascribed to the loss of a C₁₂H₁₈O₄ molecule. Since the chlorine atom is retained in the chlorinated *m/z* 332 variant of the *m/z* 298 ion, it appears that these ions arise by loss of the two right-hand rings, via a pathway involving cleavage, rearrangement and/or ring contraction in the vicinity of C-13 (Figure 4.17). As observed for the MS² spectra, the loss of water (18 *amu*) in the MS³ spectra can be explained by the loss of any of the remaining OH groups.

Fragmentation of the *m/z* 540 and 506 ions (from penitrems A and E, respectively) generated under MS³ conditions afforded MS⁴ data. Ions corresponding to the loss of 130 *amu* and 208 *amu* were observed in the MS⁴ spectra. An analogous 130 *amu* loss was observed in the MS² and MS³ spectra of janthitrem D (Section 4.4.1). This loss can be attributed to the concerted loss of a C₆H₁₀O₃ fragment as HC(=O)-CHOH-CHOH-C₃H₅ or alternatively to the sequential loss of water and a C₆H₈O₂ species. The 208 *amu* loss, which appears to arise by loss of C₁₂H₁₆O₃ in the vicinity of C-13, may involve similar fragmentation to that observed during the loss of 226 *amu*, other than for the prior loss of water (18 *amu*).

Additional, comparatively low intensity fragment ions arising from the loss of 100 *amu* or 18 *amu* (water) were also observed in the MS⁴ spectra of penitrems A and

E. The loss of 100 *amu* can only be ascribed to the loss of $C_6H_{12}O$, $C_5H_8O_2$, or $C_4H_4O_3$. Given the disposition of carbon and oxygen atoms in penitrems A and E, only the loss of $C_5H_8O_2$ from the O-8-C-9-C-10 portion of the molecule as $HOH_2C-C(=O)C_3H_5$ appears plausible (see Figure 4.17).

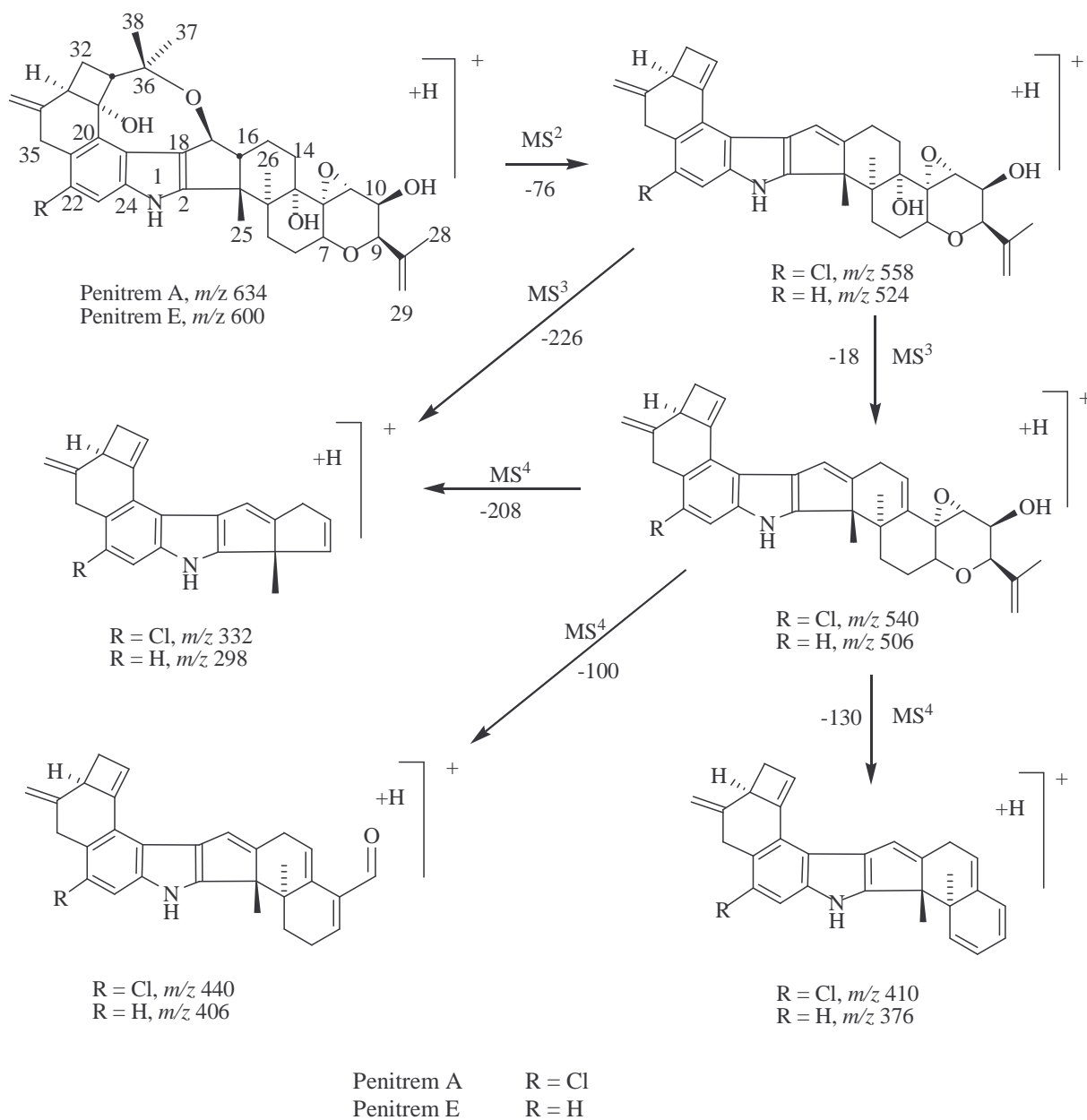


Figure 4.17. Fragmentation of penitrems A and E in positive ion MS^2 , MS^3 and MS^4 spectra.

Penitrems B and Penitrem F

Penitrems B and F exhibited losses of 70 *amu* and 18 *amu* (water) under MS² conditions. The loss of 70 *amu* is not believed to be analogous to that observed for janthitrem C since their right-hand rings differ (11,12-epoxide in penitrems B and F as opposed to an 11(12)-double bond in janthitrem C), making retro Diels–Alder loss of 70 *amu* non-usable. The 70 *amu* loss observed in the MS² spectra of penitrems B and F is instead believed to arise via cleavage and rearrangement of the top left-hand end of the molecules (Figure 4.18) and can be ascribed to the loss of a C₅H₁₀ residue.

Further fragmentation of the 70-*amu*-loss-ions under MS³ conditions afforded losses of 100 *amu* and 18 *amu* (water). The loss of 18 *amu* can be attributed to the loss of any of the OH groups as a water molecule. A loss of 100 *amu* was also observed for penitrems A and E (see above) and is most likely due to the loss of C₅H₈O₂ from the O-8–C-9–C-10 portion of the molecule as HOH₂C–C(=O)C₃H₅ (Figure 4.18).

MS⁴ fragmentation of the MS³ water loss peaks afforded ions corresponding to the loss of 18 *amu*, 100 *amu* and 130 *amu*. Losses of 18 *amu* and 100 *amu* were also observed under MS² and MS³ conditions (see Figure 4.18). The 130 *amu* loss is analogous to that observed for janthitrem D. Since the right-hand ends of the janthitrem D and penitrems B and F are identical, a similar fragmentation is proposed as shown in Figure 4.18 (see Section 4.4.1). Each of these compounds possess an 11,12-epoxy group which is believed to promote the loss of a 130 *amu* residue.

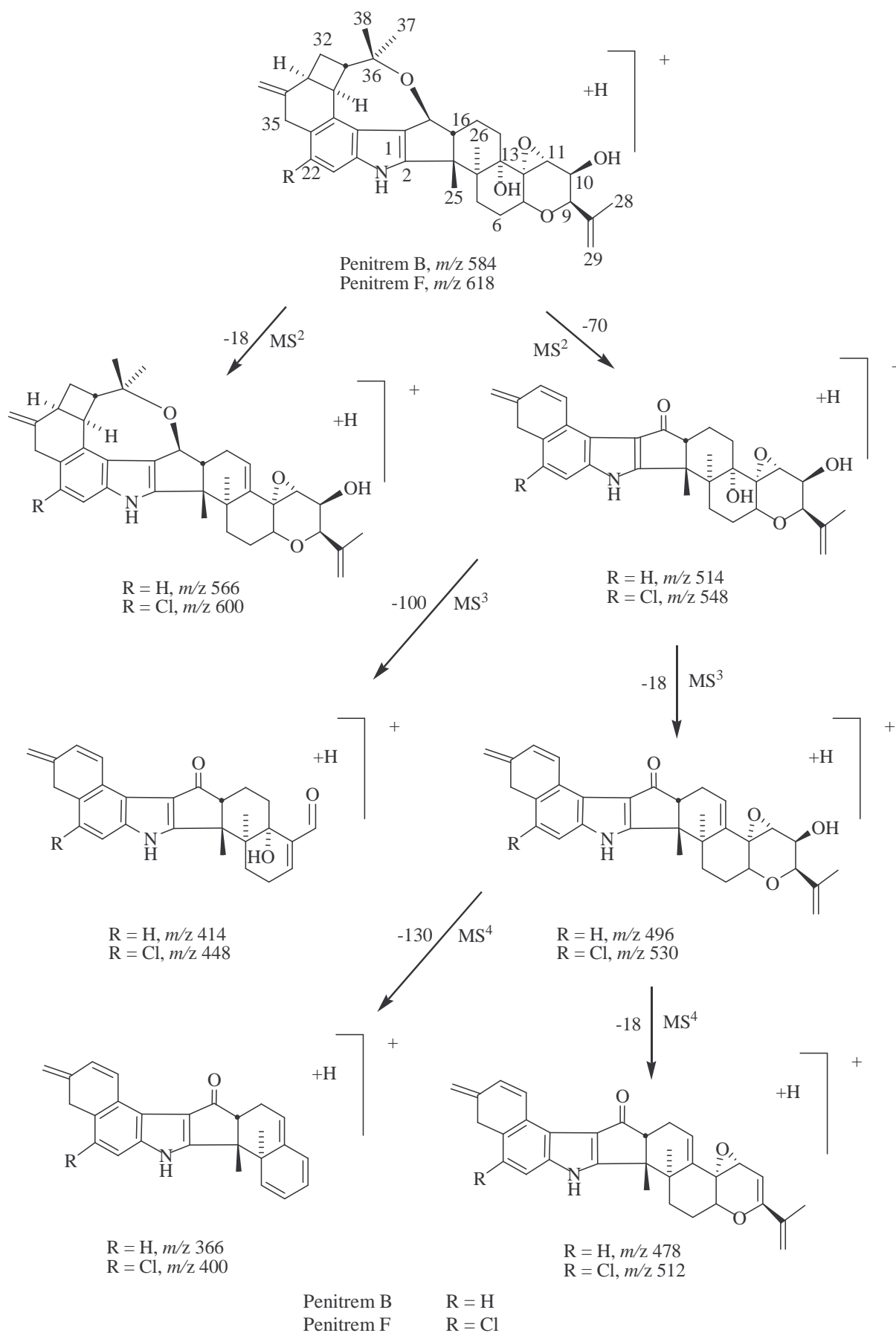


Figure 4.18. Fragmentation of penitrems B and F in positive ion MS², MS³ and MS⁴ spectra.

Penitrem C and Penitrem D

Penitrems C and D exhibited losses of 70 *amu* and 18 *amu* (water) under MS² conditions. The 18 *amu* loss can be attributed to the loss of any of the hydroxyl groups as a water molecule (as observed for janthitrems A and B and penitrems A, B, E and F). The loss of 70 *amu* was analogous to that observed in the MS² spectra of penitrems B and F (loss of a C₅H₁₀ residue). Since the left-hand portions of these molecules' structures are identical, identical fragmentation is proposed (see Figure 4.19).

Fragmentation of the 70 *amu* loss ions under MS³ conditions afforded ions arising from a further loss of 70 *amu* and/or 18 *amu* (water). The second loss of 70 *amu* is believed to correspond to the 70 *amu* loss observed for janthitrems B and C under positive ion APCI conditions (Section 4.4.1). This loss can be ascribed to the loss of a C₄H₆O residue as C₃H₅-CHO from the right-hand terminal ring via a retro Diels-Alder like mechanism (Figure 4.19).

MS⁴ fragmentation of the MS³ water loss peaks also affords losses of 18 *amu* (water) and 70 *amu* fragments. Plausible structures for these losses are proposed in Figure 4.19. The loss of a water molecule (18 *amu*) is believed to arise through loss of the remaining OH group at C-10, whilst the loss of 70 *amu* arises via a retro Diels-Alder mechanism outlined in the MS³ stage (see above) through the loss of a C₄H₆O fragment.

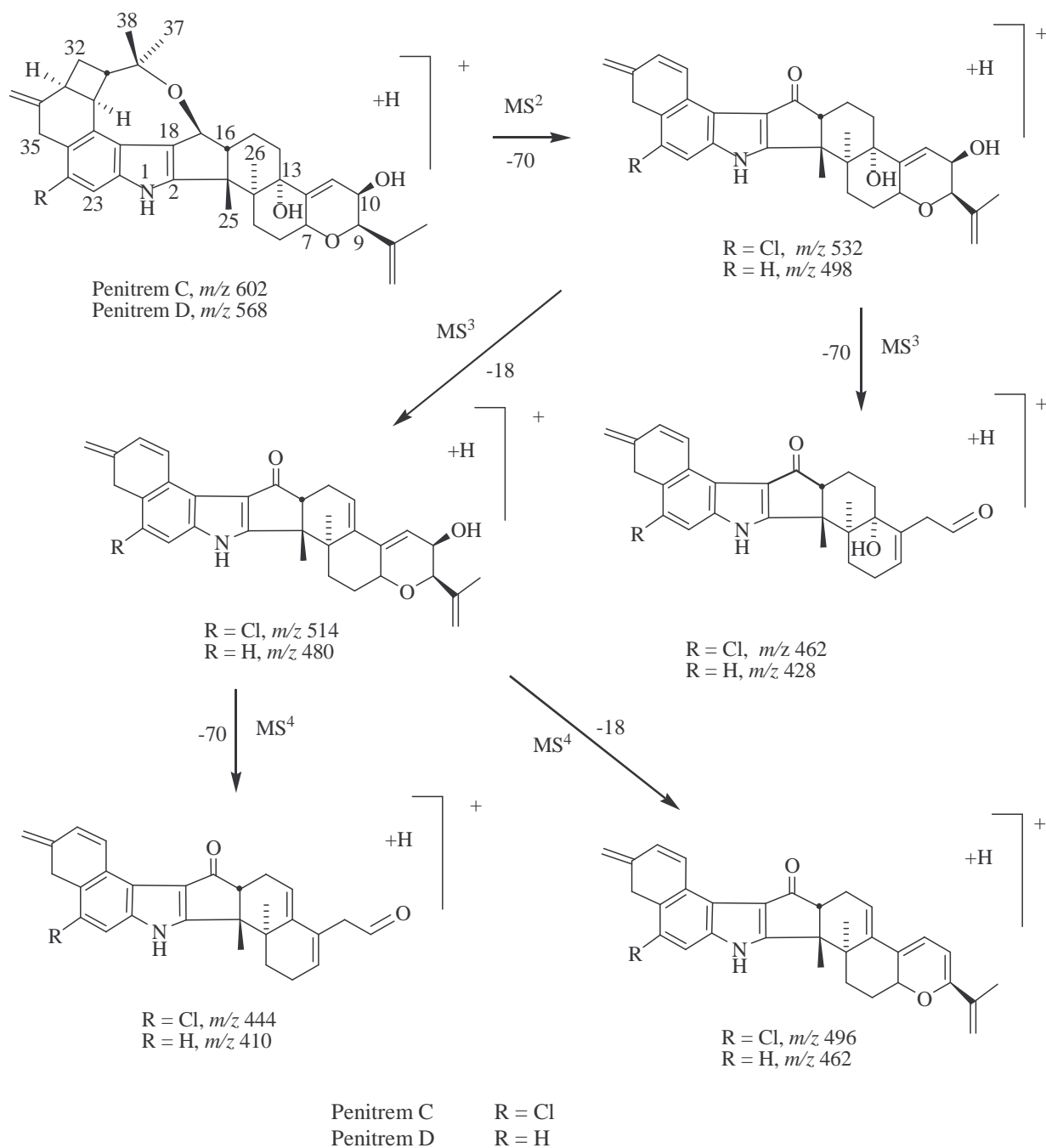


Figure 4.19. Fragmentation of penitrems C and D in positive ion MS^2 , MS^3 and MS^4 spectra.

4.4.3 Fragmentation of Lolitrem B

Fragmentation of the m/z 686 $[M+H]^+$ ion under MS^2 conditions using an ESI source afforded an m/z 670 ion (-16 *amu*). Further fragmentation of the m/z 670 ion under MS^3 conditions afforded an m/z 612 ion (-58 *amu*). The loss of 16 *amu*

is most likely due to the loss of a methane molecule through the loss of the methyl group at C-25 as shown in Figure 4.20. The loss of 16 *amu* may also be due to the loss of an oxygen atom. The loss of 58 *amu* is indicative of the loss of an acetone molecule from the left-hand portion of the molecule (Figure 4.20).

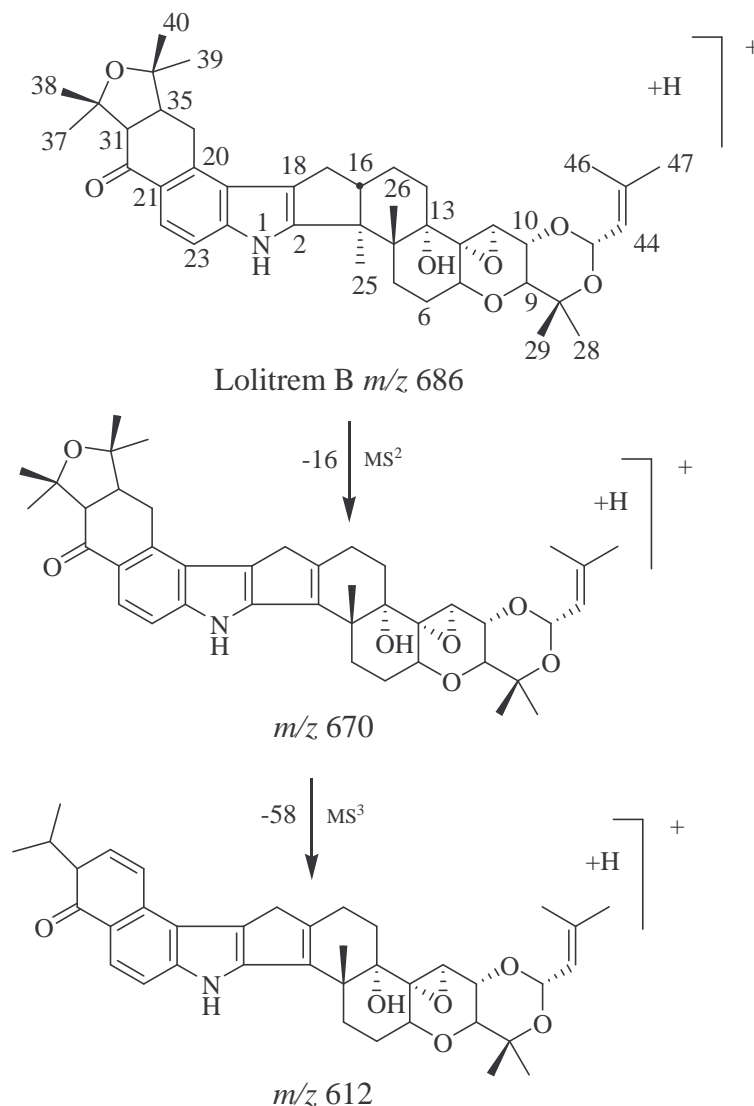


Figure 4.20. Fragmentation of lolitrem B in positive ion MS^2 and MS^3 spectra (ESI).

The behaviour of lolitrem B under APCI conditions was similar in some respects to that observed under ESI conditions, with both 16 *amu* and 18 *amu* losses being observed under MS^2 conditions to afford m/z 670 and m/z 668 ions respectively. The loss of 18 *amu* is most likely attributable to the loss of water via the

elimination of the 13-OH group (Figure 4.21). The loss of 16 *amu* may arise from the loss of a methane molecule or through the loss of any of the available oxygen atoms.

Further fragmentation of the m/z 668 (water loss) ion under MS^3 conditions afforded m/z 566 and 524 ions, corresponding to the loss of 102 *amu* and 144 *amu* respectively. Plausible structures for resulting ions are given in Figure 4.21. Since these losses were only observed in the MS^3 spectra of lolitrem B (and not other indole-diterpenoids) it can be reasoned that the losses are associated with the C-43 to C-47 acetal portion of lolitrem B.

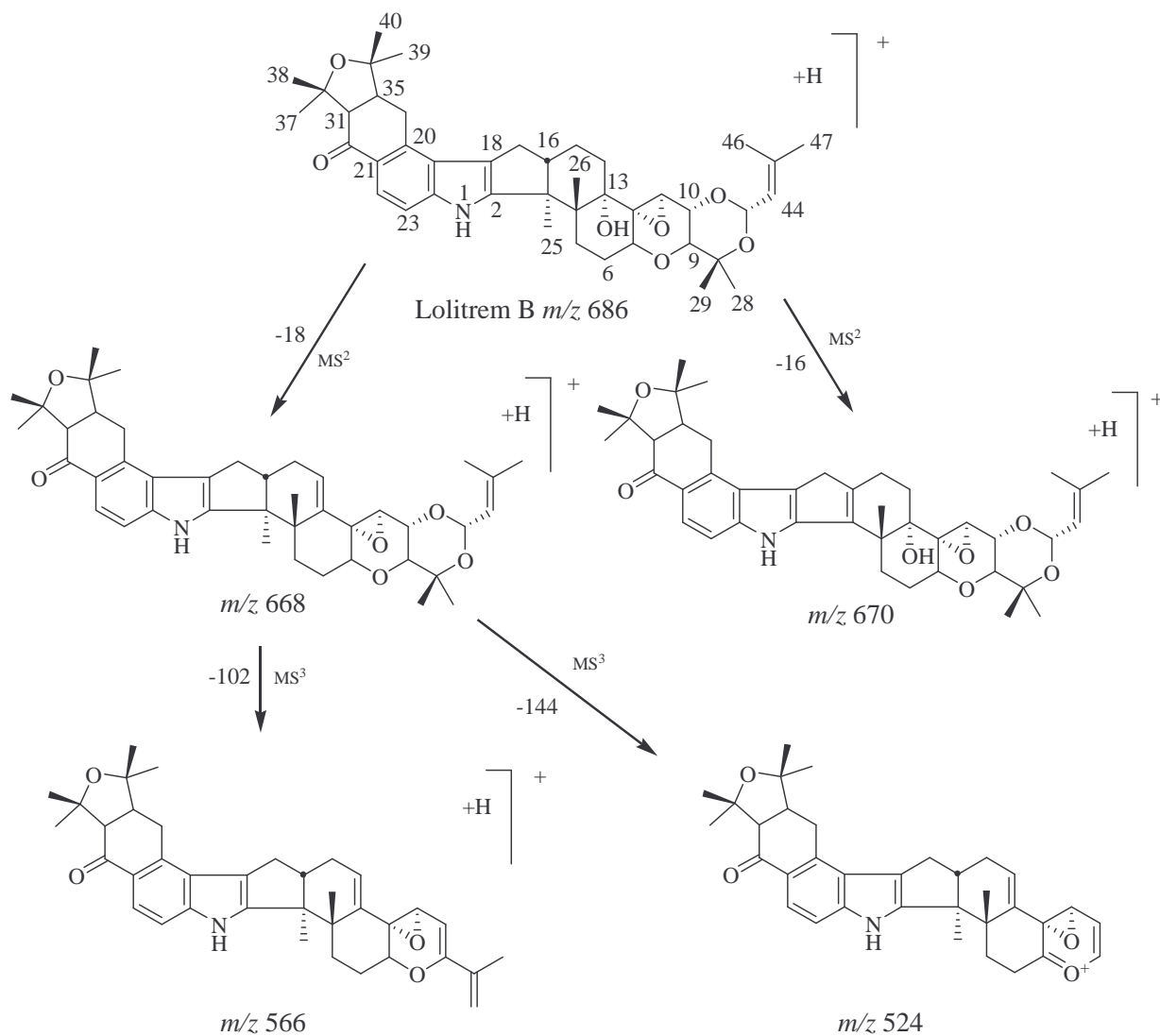


Figure 4.21. Fragmentation of lolitrem B in positive ion MS^2 and MS^3 spectra (APCI).

4.4.4 Fragmentation of Paxilline

Essentially identical fragmentation under APCI and ESI conditions was observed for paxilline, with losses of 16 *amu* (*m/z* 420) and 18 *amu* (*m/z* 418) being observed under MS² conditions using an APCI source and only 16 *amu* (*m/z* 420) being observed using an ESI source (Figure 4.22). The loss of 18 *amu* can be attributed to the loss of either the 13-OH or 27-OH groups as a water molecule. Loss of the 13-OH group is shown in Figure 4.23. As noted previously, the loss of 16 *amu* could arise from either the loss of a methane molecule or the loss of an oxygen atom. The former (loss of a methane molecule) appears to be the more likely than the latter (loss of an oxygen atom). Fragmentation of the *m/z* 418 ion under APCI conditions resulted in the loss of a second water molecule to afford an *m/z* 400 ion, or the loss of 58 *amu* to afford an *m/z* 360 ion. This loss can be attributed to the loss of an acetone molecule from the C-9 hydroxyisopropyl group.

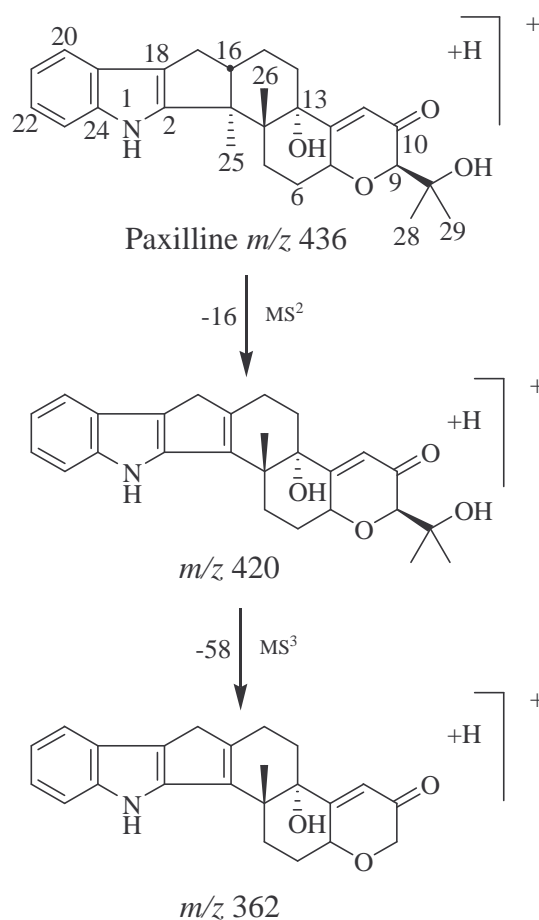


Figure 4.22. Fragmentation of paxilline in positive ion MS² and MS³ spectra (ESI).

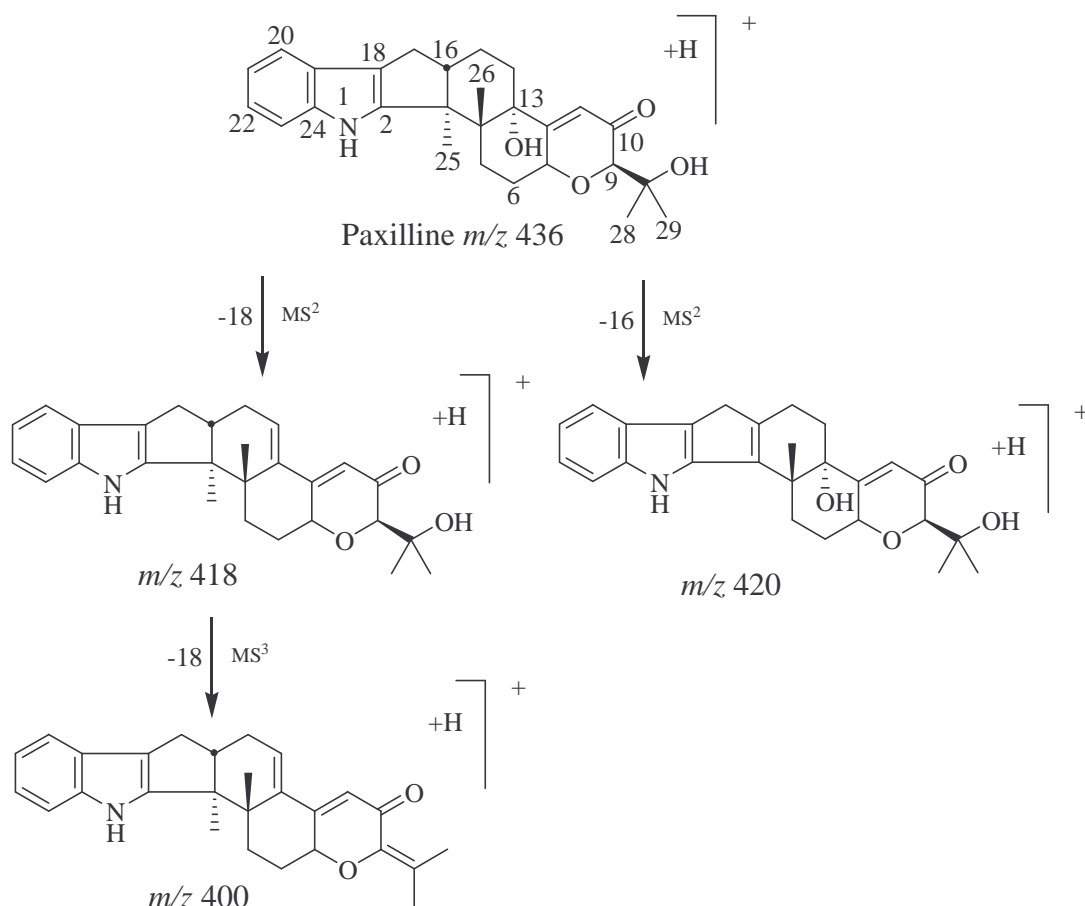


Figure 4.23. Fragmentation of paxilline in positive ion MS^2 and MS^3 spectra (APCI).

4.4.5 Fragmentation of Terpendole C

The fragmentation patterns exhibited by terpendole C under positive ion conditions using either an ESI source or an APCI source (Figures 4.24 and 4.25 respectively) were virtually identical, the difference being the generation of an extra peak under APCI MS^2 conditions. In both cases, fragmentation of the m/z 520 $[M+H]^+$ ion under MS^2 conditions gave an m/z 504 ion (-16 *amu*). This loss may be attributable to the loss of a methane molecule through the elimination of the C-25 methyl group. Loss of 18 *amu* was also observed under APCI MS^2 conditions. This loss can be attributed to the loss of water via the loss of the 13-OH group (Figure 4.25).

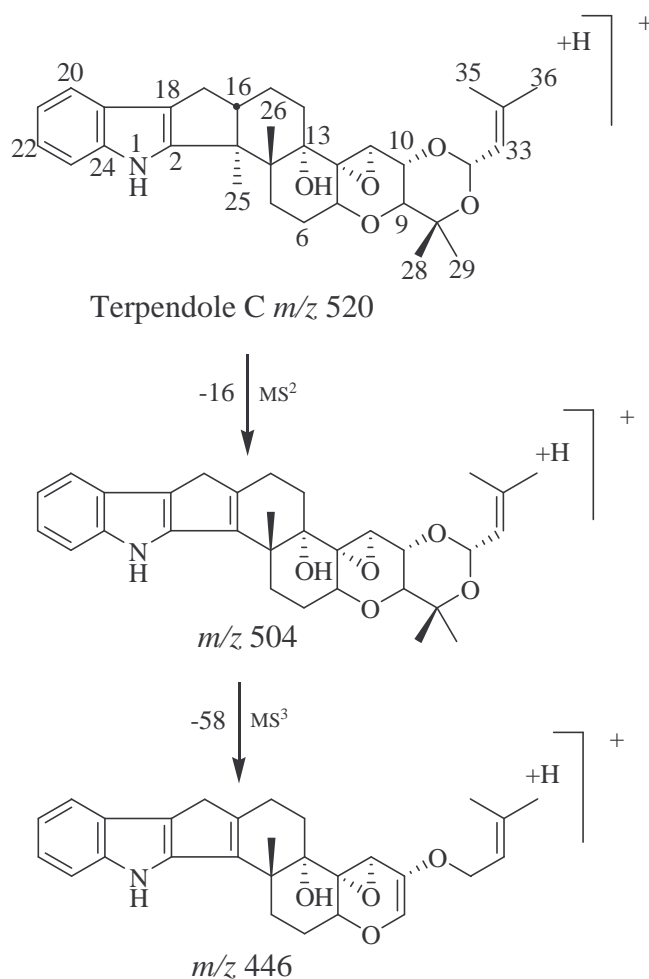


Figure 4.24. Fragmentation of terpendole C in positive ion MS^2 and MS^3 spectra (ESI).

Fragmentation of the m/z 504 ion (-16 *amu*) under MS^3 conditions (ESI source) afforded an m/z 446 ion (-58 *amu*). Loss of 58 *amu* was also observed under MS^3 conditions (APCI source), albeit following fragmentation of the water loss ion as opposed to fragmentation of the oxygen loss ion. The loss of 58 *amu* can be attributed to the loss of acetone, as commonly observed for the janthitrems A, B, C and D, lolitrem B (ESI source only) and paxilline, with the proviso that different structural sub-units are responsible for the acetone losses in the respective groups of indole–diterpenoids.

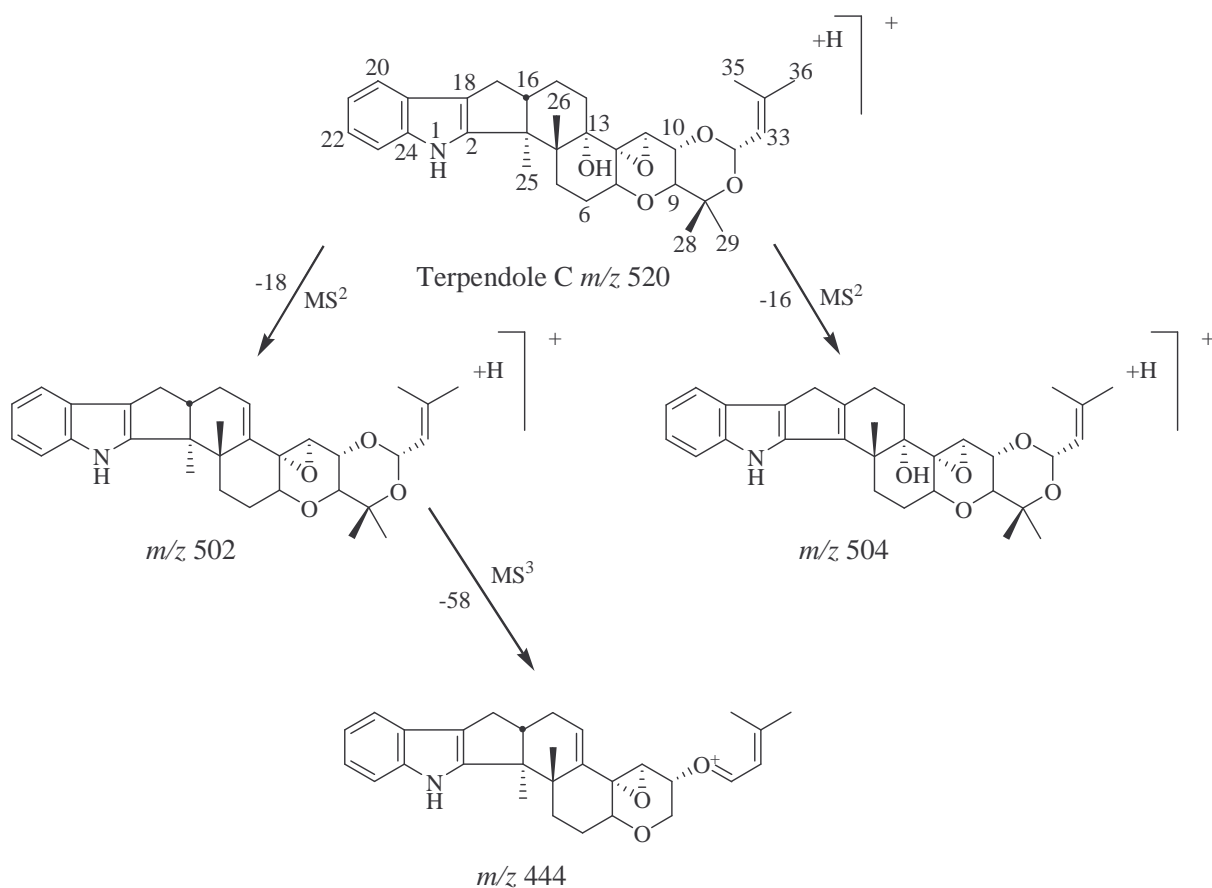


Figure 4.25. Fragmentation of terpendole C in positive ion MS^2 and MS^3 spectra (APCI).

4.4.6 Fragmentation of Paspalinine

The $[M+H]^+$ ion of paspalinine, which occurred at m/z 434, showed a loss of 16 *amu* under ESI MS^2 conditions and a loss of 18 *amu* under APCI MS^2 conditions to afford m/z 418 and 416 ions respectively. The loss of 16 *amu*, though uncommon in mass spectrometry, most likely arises from the loss of a methane molecule or an oxygen atom. The ion structure presented in Figure 4.26 arbitrarily shows the 16 *amu* loss as arising from the loss of a methane molecule through elimination of the C-25 methyl group, rather than via the loss of any of the oxygen atoms. These options however cannot be unequivocally excluded. High resolution data could differentiate between an oxygen or methane loss.

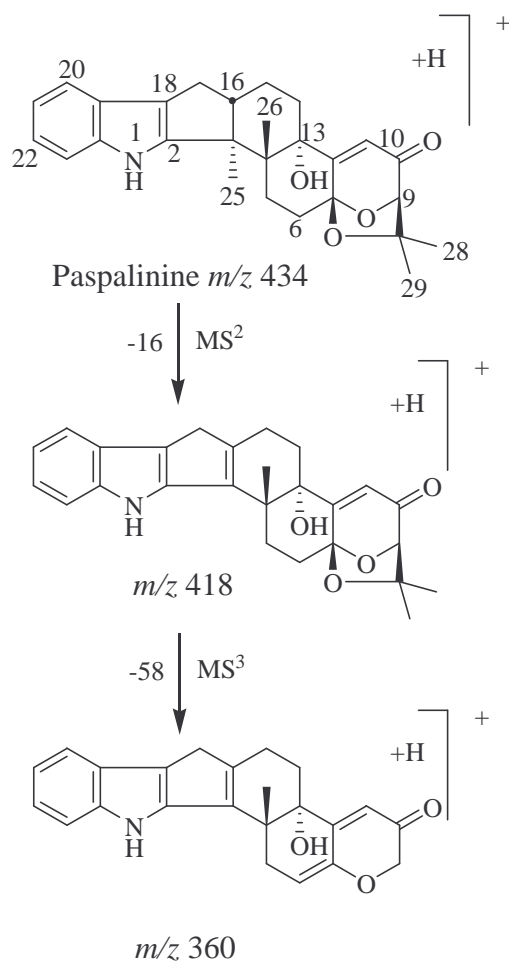


Figure 4.26. Fragmentation of paspalinine in positive ion MS² and MS³ spectra (ESI).

Under ESI MS³ conditions the m/z 418 ion fragmented to afford an m/z 360 ion (58 *amu* loss) presumably via acetone loss from the bridging 7,27-oxido linkage. Fragmentation of the m/z 416 (water loss) ion generated under APCI MS² conditions also resulted in the loss of 58 *amu* (Figure 4.27).

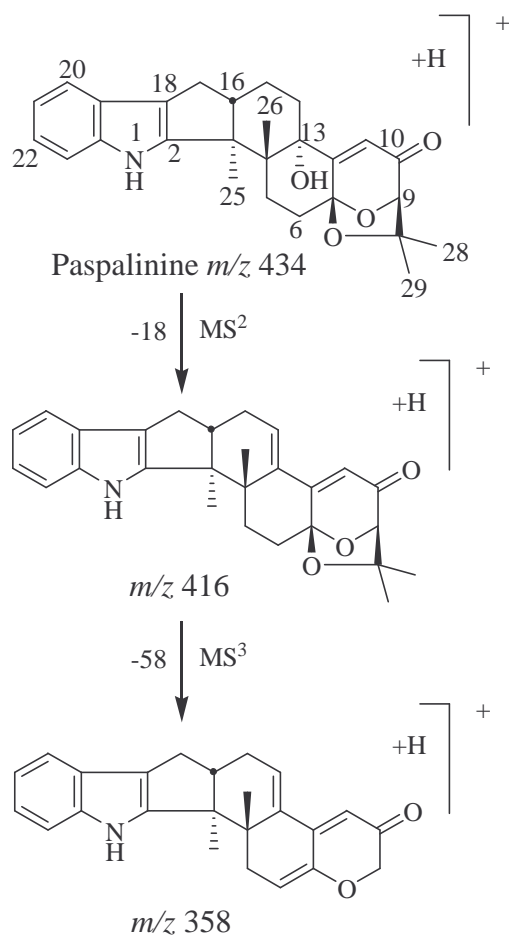


Figure 4.27. Fragmentation of paspalinine in positive ion MS^2 and MS^3 spectra (APCI).

4.5 LC–UV–MS APCI Negative Ion Mode

Full scan, MS^2 and MS^3 spectra of a range of indole–diterpenoids were also acquired in negative ion mode using an APCI source. These analyses were directed towards the identification of structurally significant fragments that appear in the mass spectra of several groups of indole–diterpenoids. Analysis was carried out as described in Section 8.5.4. No previous account of the behaviour of indole–diterpenoid compounds in negative ion APCI MS and MS^n modes has appeared in the literature.

The expectation with compounds run in the negative ion mode was that $[M-H]^-$ ions would be observed in full scan spectra and that fragmentation of this ion would afford MS^n spectra. However, unlike in the positive ion APCI and ESI mode analyses, one of the more dominant ions observed was an adduct ion arising from addition of an acetate ion when 0.1% (v/v) CH_3COOH was present in the eluent or formate ion when 0.1% (v/v) $HCOOH$ was present in the eluent.

An $[M+OAc]^-$ (+59 *amu*) adduct ion was observed as the second most dominant peak (*ca.* 50% the intensity of the major $[M-H]^-$ ion) in the full scan APCI mass spectra of janthitrems A, B (Figure 4.28), C and D, penitrems A, B, C, D, E and F, lolitrem B and paxilline acquired with acetic acid as the eluent modifier. In the case of terpendole C (Figure 4.29) and paspalinine, the acetate adduct ion, $[M+OAc]^-$ was the most dominant peak in full scan mass spectra acquired with acetic acid as the eluent modifier. By contrast, an $[M+H]^+$ ion was the dominant peak in all full scan positive ion LC–UV–MS analyses.

Attempts were made to fragment the adduct ions observed in the negative ion mass spectra, however, efforts to obtain MS^2 data were futile. The collision energy (CE) was increased progressively from 5% fragmentation up to 60%, but with no success. The failure of these experiments was presumably due to the loss of an $[X]^-$ ion from the $[M+X]^-$ adduct ion leaving an uncharged M species.

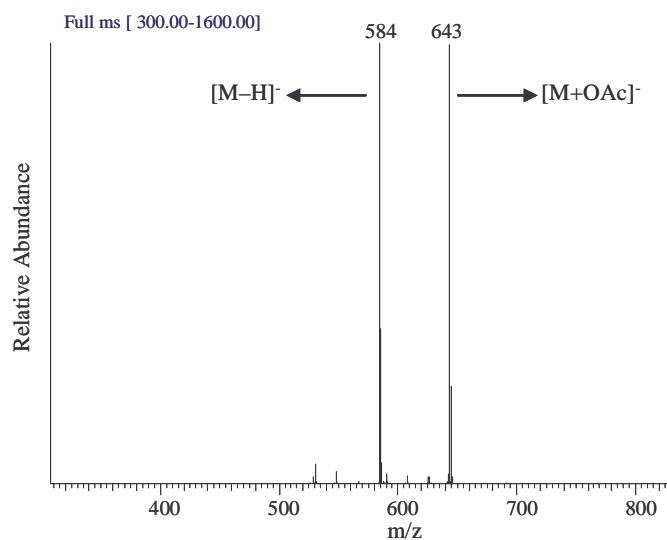


Figure 4.28. Full scan negative ion spectrum of janthitrem B.

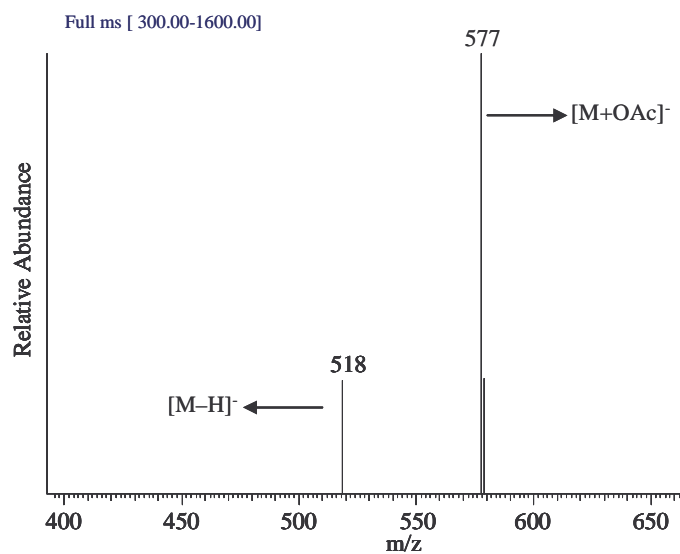


Figure 4.29. Full scan negative ion spectrum of terpendole C.

In situations such as these, prior experience in the Chemistry Department (The University of Waikato) is that acquisition of full scan MS data with source-induced dissociation (SID) can suppress the tendency to form adduct ions and increase the $[M-H]^-$ ion current.

Utilisation of this approach resulted in essentially the complete suppression of acetate (or formate) adduct ions (Figures 4.30 and 4.31). Full scan negative ion indole–diterpenoid mass spectra were therefore routinely acquired with 25–30 V SID. Thereafter, MS² and MS³ spectral data were recorded using a CE of 60%. SID was only applied during the initial full scan stage, and not in subsequent MS² or MS³ data acquisition stages.

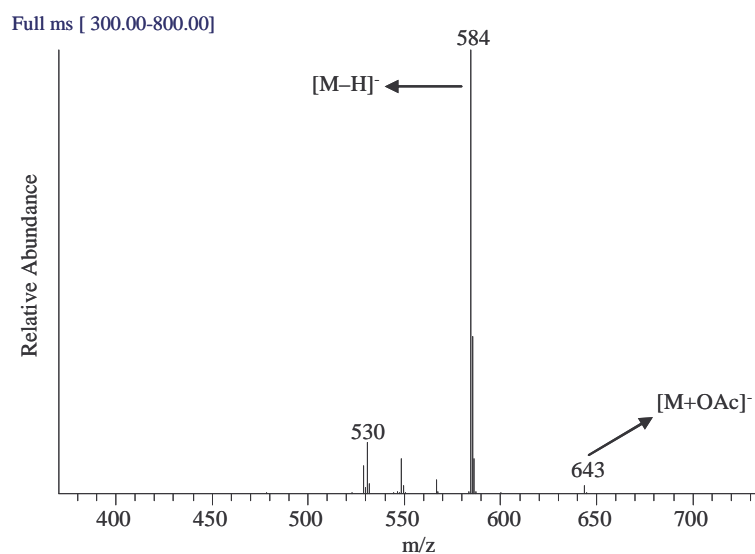


Figure 4.30. Full scan negative ion spectrum of janthitrem B with SID.

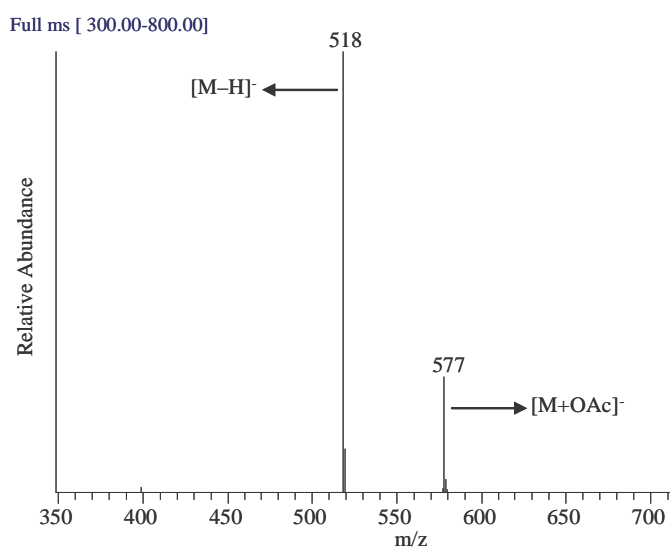


Figure 4.31. Full scan negative ion spectrum of terpendole C with SID.

4.5.1 Fragmentation of Janthitrem

The four janthitrem compounds examined, janthitrem A, B, C and D, all fragmented under the influence of 20 V SID and 35% collision energy to afford $[M-58]^-$ ions. This loss (as mentioned previously in Section 4.4.1) is believed to arise by the loss of an acetone molecule from the bridging $C(CH_3)_2-O$ -ether linkage (Naude et al., 2002), via a retro Diels–Alder rearrangement (Figure 4.32).

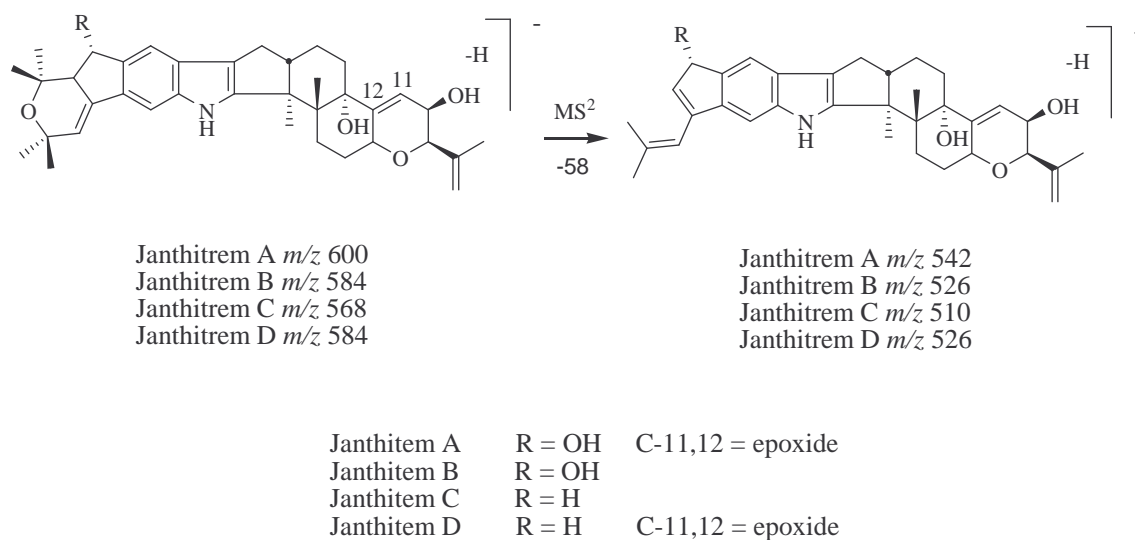


Figure 4.32. Ions generated through loss of acetone from janthitrem A–D.

Janthitrem A

Janthitrem A lost acetone (58 *amu*) and water (18 *amu*) under MS^2 conditions and acetone (58 *amu*) from the $[M-H-18]^-$ ion under MS^3 conditions (Figures 4.33, 4.34 and 4.35). The loss of water could be explained by the loss of any of the three OH groups at C-10, C-13 and C-30. Loss of the 30-OH group is shown in Figure 4.36.

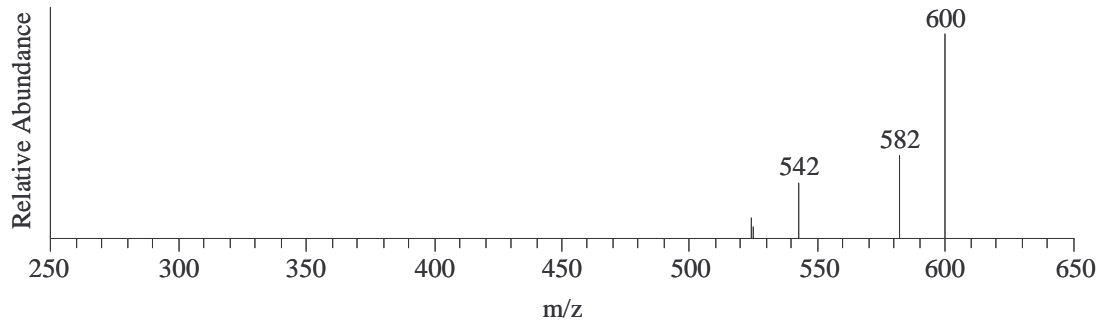


Figure 4.33. Janthitrem A full scan negative ion mass spectrum.

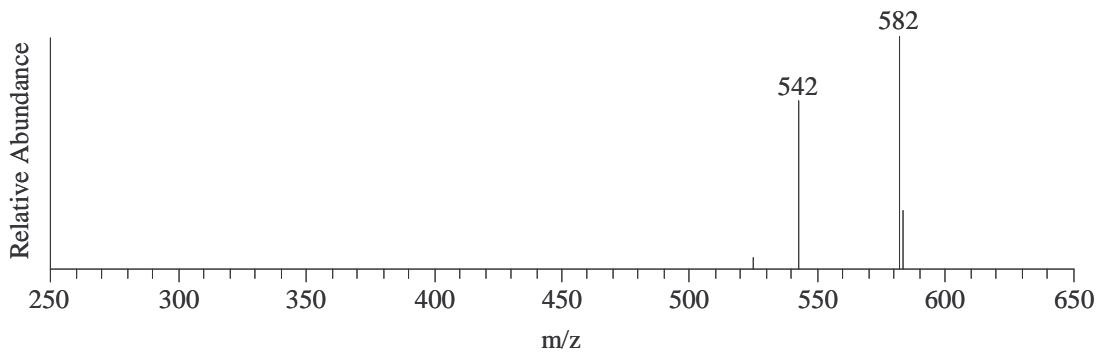


Figure 4.34. Janthitrem A negative ion MS^2 spectrum (m/z 600).

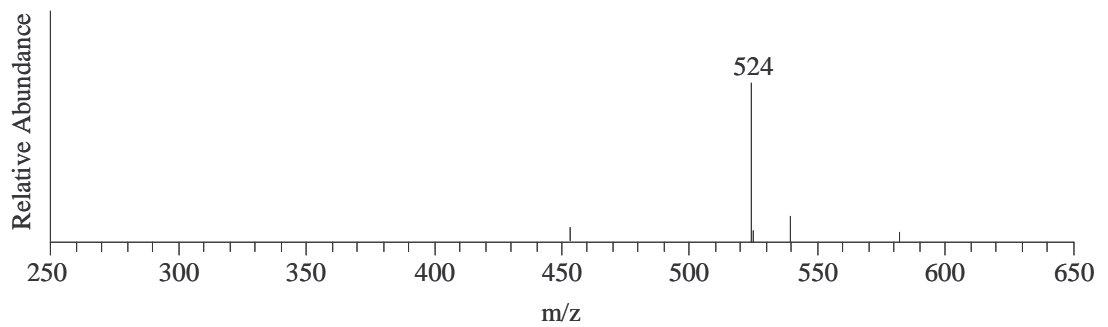


Figure 4.35. Janthitrem A negative ion MS^3 spectrum (m/z 600 \rightarrow m/z 582).

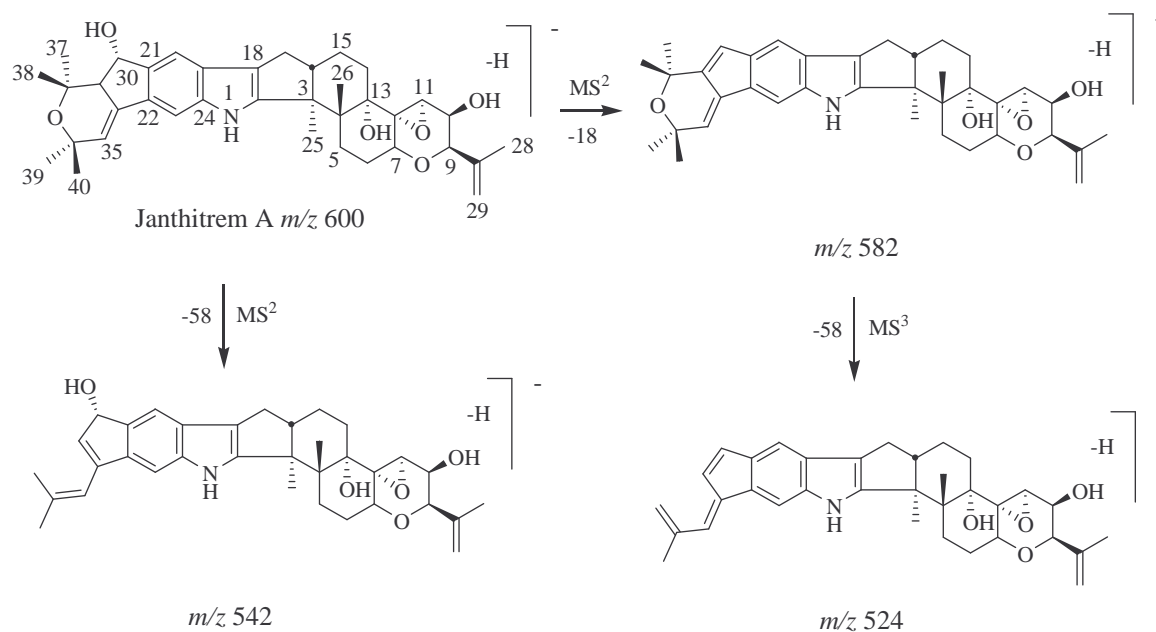


Figure 4.36. Fragmentation of janthitrem A in negative ion MS^2 and MS^3 spectra.

Janthitrem B

Janthitrem B was observed to lose 58 *amu* (acetone loss) under MS^2 conditions and subsequently 18 *amu* or 70 *amu* under MS^3 conditions (Figures 4.37, 4.38 and 4.39).

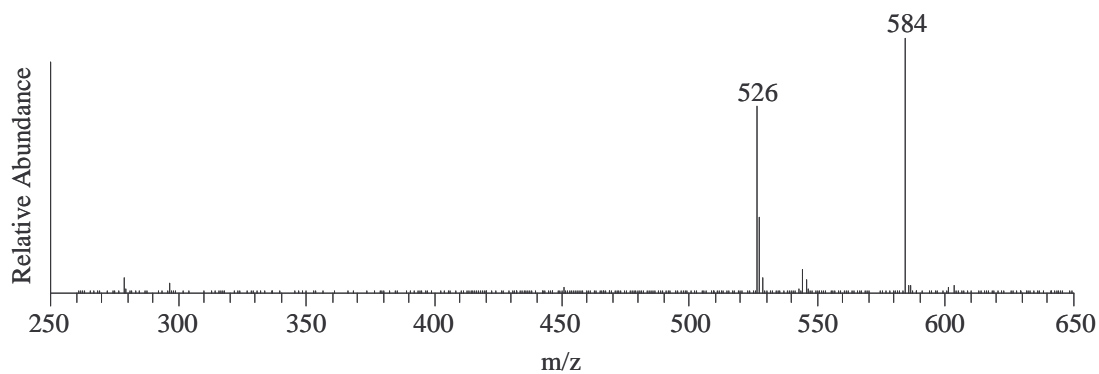


Figure 4.37. Janthitrem B full scan negative ion mass spectrum.

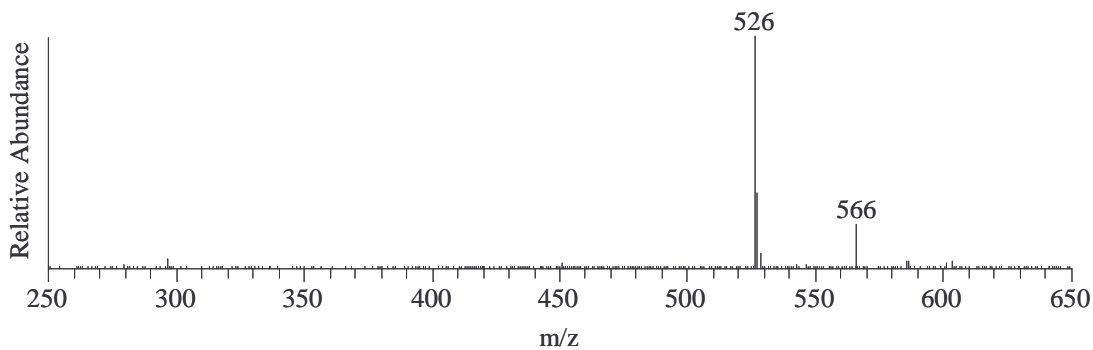


Figure 4.38. Janthitrem B negative ion MS² spectrum (m/z 584).

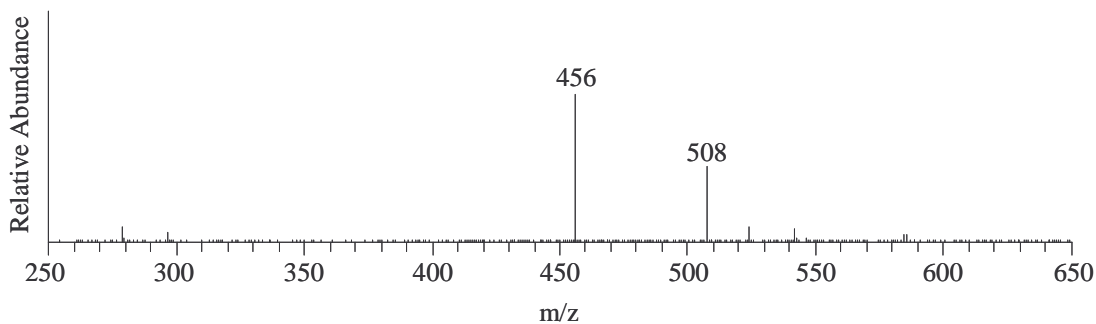


Figure 4.39. Janthitrem B negative ion MS³ spectrum (m/z 584 \rightarrow m/z 526).

The loss of 18 *amu* can be attributed to the loss of water via elimination of any of the C-10, C-13 or C-30 hydroxyl groups, as also observed for janthitrem A. Since the loss of water in the MS² step is only observed in janthitrem A and B, and not janthitrem C and D, it is likely that this water loss may arise from the loss of the 30-OH group which only janthitrem A and B possess. Possible ion structures arising from the loss of the 30-OH group and the 58 *amu* and 70 *amu* losses are given in Figure 4.40.

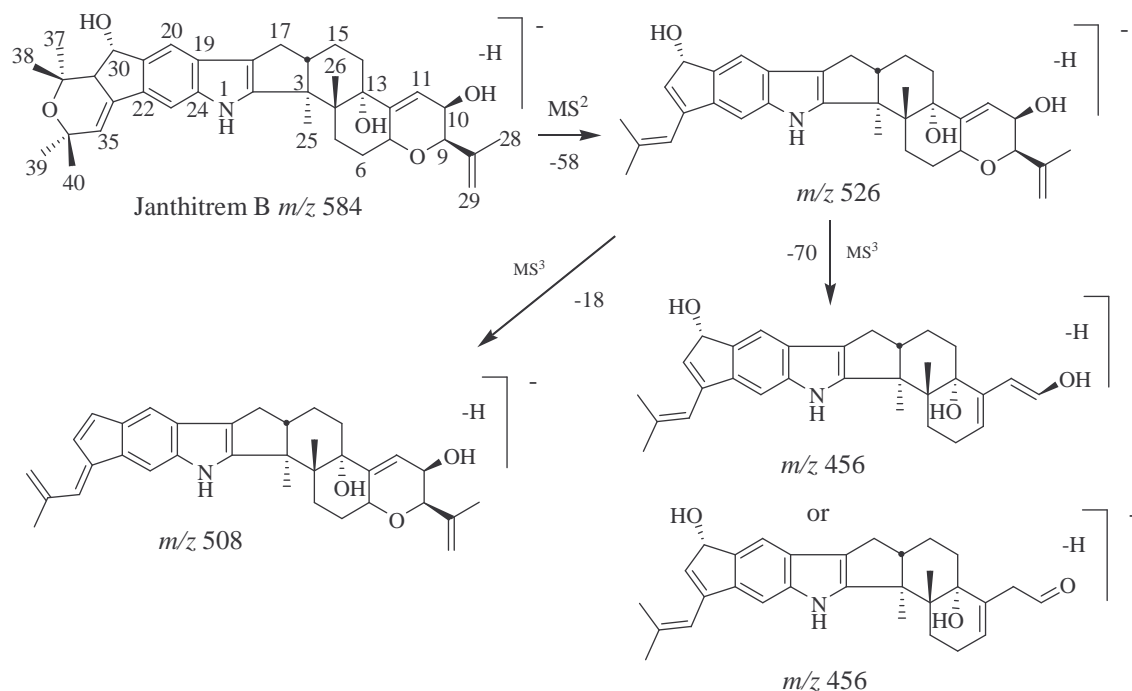


Figure 4.40. Fragmentation of janthitrem B in negative ion MS^2 and MS^3 spectra.

The loss of 70 *amu* can be ascribed to the loss of a $\text{C}_4\text{H}_6\text{O}$ residue as a $\text{C}_3\text{H}_5\text{-CHO}$ molecule from the right-hand terminal ring via a retro Diels–Alder mechanism. The initially generated *m/z* 456 product ion would have an enol group which would be expected to equilibrate to the corresponding aldehyde form (Figure 4.41). Similar losses of 70 *amu* were observed in the positive ion spectra MS^3 stage of janthitrems B and C (APCI only) and penitrems C and D (ESI and APCI).

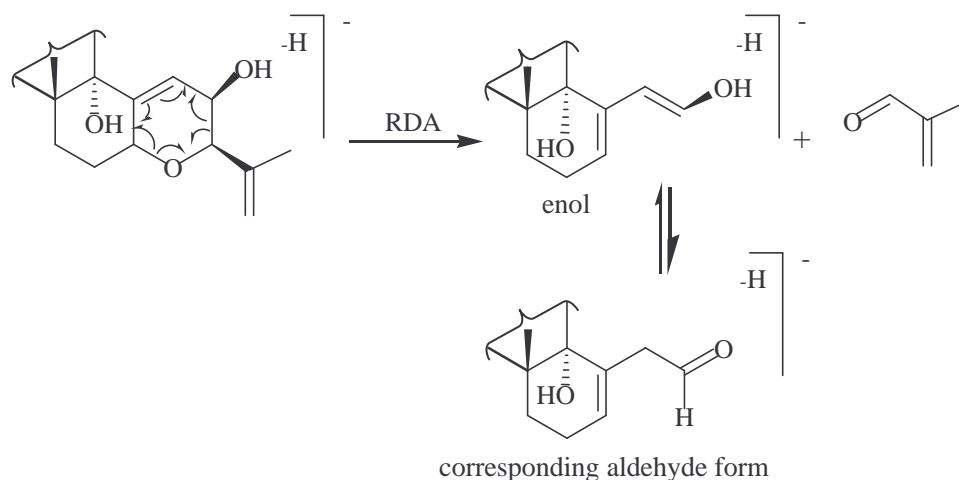


Figure 4.41. Retro Diels–Alder rearrangement of janthitrem B involving formation of an enol group which equilibrates to the corresponding aldehyde form.

Janthitrem C

Janthitrem C showed a 58 *amu* (acetone) loss under MS² conditions, followed by the loss of 70 *amu* (as also seen for janthitrem B: see above) under MS³ conditions (Figure 4.42). As noted above, this loss can be envisaged as occurring via a retro Diels–Alder like pathway (Figure 4.41).

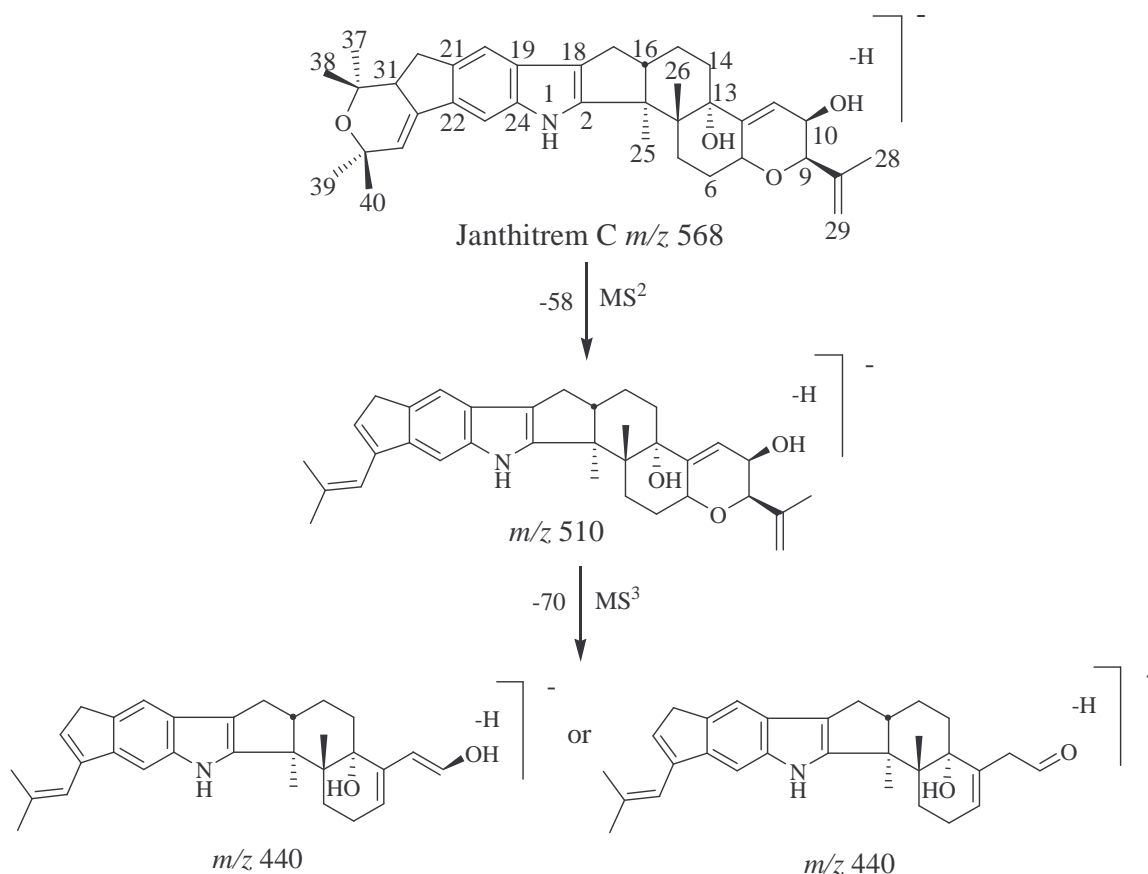


Figure 4.42. Fragmentation of janthitrem C in negative ion MS² and MS³ spectra.

Janthitrem D

The loss of acetone (58 *amu*) from janthitrem D under MS² conditions was followed by a further loss of 130 *amu* under MS³ conditions. Two possible plausible structures for the resulting m/z 396 ion are presented in Figure 4.43. The loss of 130 *amu* is believed to arise from the loss of a C₆H₁₀O₃ molecule as HC(=O)–CHOH–CHOH–C₃H₅ from the right-hand terminal ring of janthitrem D (Figure 4.43). An analogous loss of 130 *amu* is observed under positive ion

conditions for janthitrem D and for penitremes A, B, E and F (Sections 4.4.1 and 4.4.2).

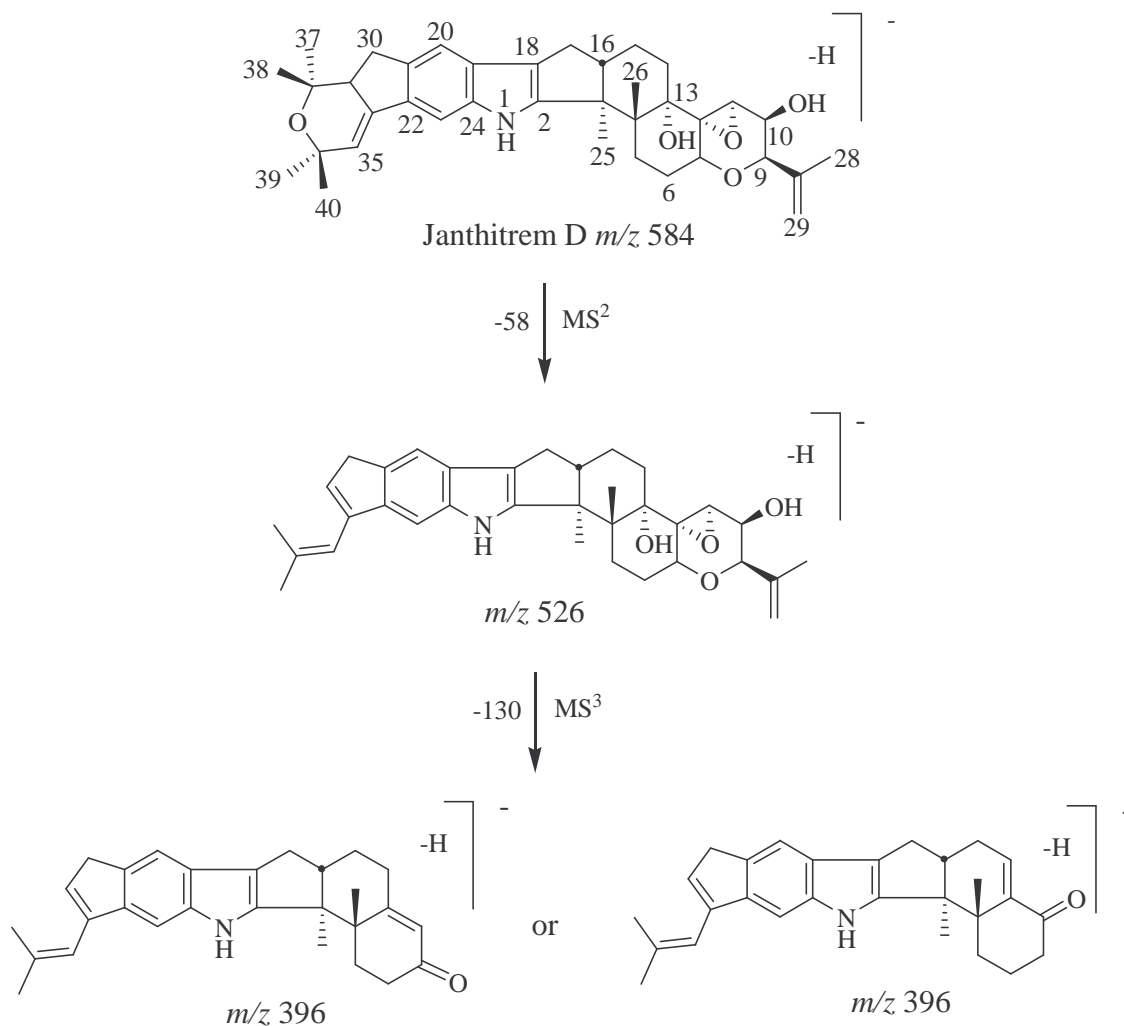


Figure 4.43. Fragmentation of janthitrem D in negative ion MS^2 and MS^3 spectra.

4.5.2 Fragmentation of Penitremes

Three distinctive negative ion fragmentation patterns were recognised amongst the six penitremes (penitremes A–F) that were examined in this investigation. The MS^n characteristics of penitremes A and E, penitremes B and F and penitremes C and D were similar. These pairs of compounds afforded MS^n spectra which differed only to the extent that the presence of a chlorine atom in penitremes A, C and F afforded fragment ions which differed by 34 *amu* from those observed for

penitrems E, D and B, respectively. The full scan, MS² and MS³ spectra of penitrems A, C and F determined under APCI negative ion conditions are depicted in Figures 4.44–4.46, 4.48–4.50 and 4.52–4.54 respectively.

The ions observed for penitrems A–F are detailed in Table 4.3. Ions presented in bold in Table 4.3 are dominant ions, *ca.* 50% of base peak, whilst the smaller, less significant ions, *ca.* < 50% of base peak, are presented in plain text. Ion structures have been proposed for dominant ions where possible, and for selected, lower intensity ions.

Table 4.3. Ions observed in full scan, MS² and MS³ spectra of penitrems A–F under negative ion conditions.

Penitrem	Full Scan Ions (<i>m/z</i>)	MS² Ions (<i>m/z</i>)	MS³ Ions (<i>m/z</i>)
Penitrem A	632	546	416, 296, 362, 401
Penitrem E	598	512	382, 262
Penitrem B	582	452, 524, 330, 366	366
Penitrem F	616	558, 486, 400, 530, 364	400, 428
Penitrem C	600	514, 530, 444, 542	444, 400
Penitrem D	566	480, 496, 508, 410	410

Penitrem A and Penitrem E

Penitrems A and E were both observed to lose 86 *amu* under negative ion MS² conditions. This loss may arise from cleavage across the C-30–C-31, C-32–C-33 bonds and C-17–O bonds to give the conjugated enol ion structure shown in Figure 4.47. An alternative ion structure would be that in which the 30(33)-en-30-ol was present as the 30-keto variant.

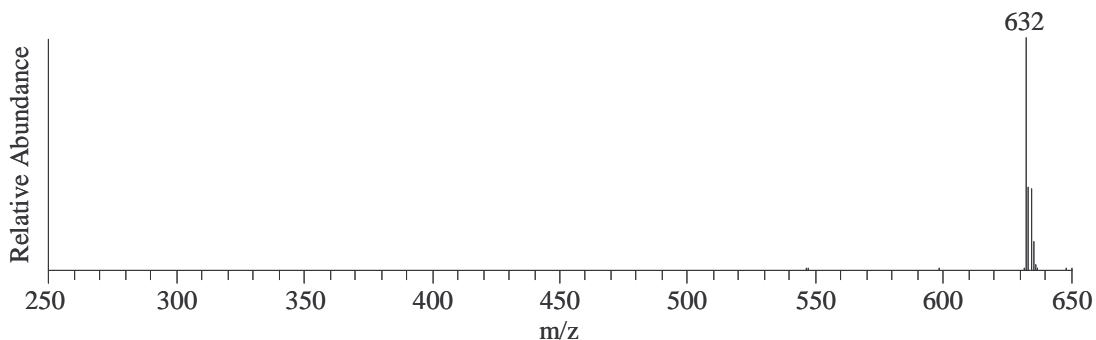


Figure 4.44. Penitrem A full scan negative ion mass spectrum.

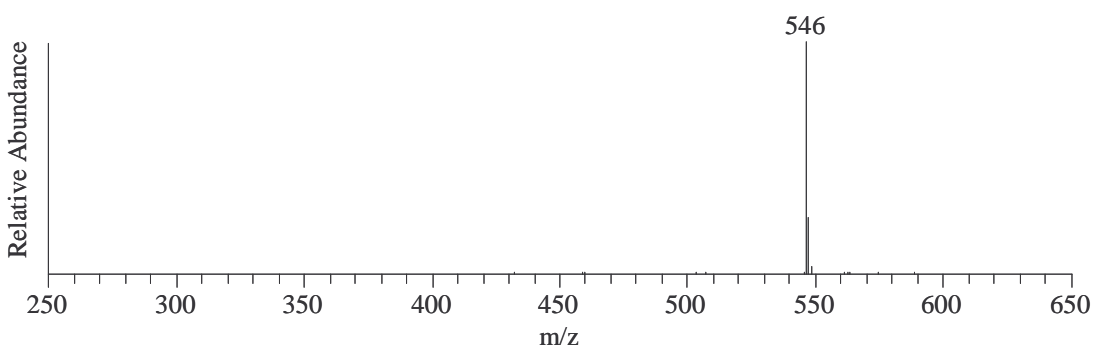


Figure 4.45. Penitrem A negative ion MS^2 spectrum (m/z 632).

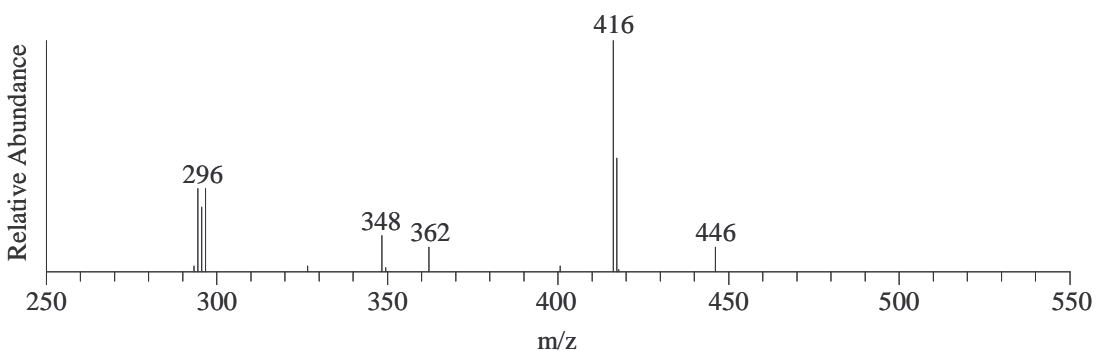


Figure 4.46. Penitrem A negative ion MS^3 spectrum (m/z 632 \rightarrow m/z 546).

The loss of 86 *amu* can be ascribed to the loss of either a C_6H_{14} or (more probably) a $C_5H_{10}O$ residue, possibly by fragmentation and rearrangement of the left-hand end of penitrems A and E. Further fragmentation of the $[M-H-86]^-$ ion under MS^3 conditions afforded fragments arising from 130 and 250 *amu* losses (Figure 4.47). Both these fragments are believed to originate from cleavages of right-hand portions of the molecule. The 130 *amu* loss is believed to arise from

the loss of a $C_6H_{10}O_3$ molecule and is comparable to that observed for janthitrem D (see Section 4.5.1).

The 250 *amu* loss can be explained by cleavage across the C-3–C-4 and C-13–C-14 bonds with the loss a $C_{14}H_{18}O_4$ residue to afford *m/z* 296 or 262 ions (penitrems A and E, respectively).

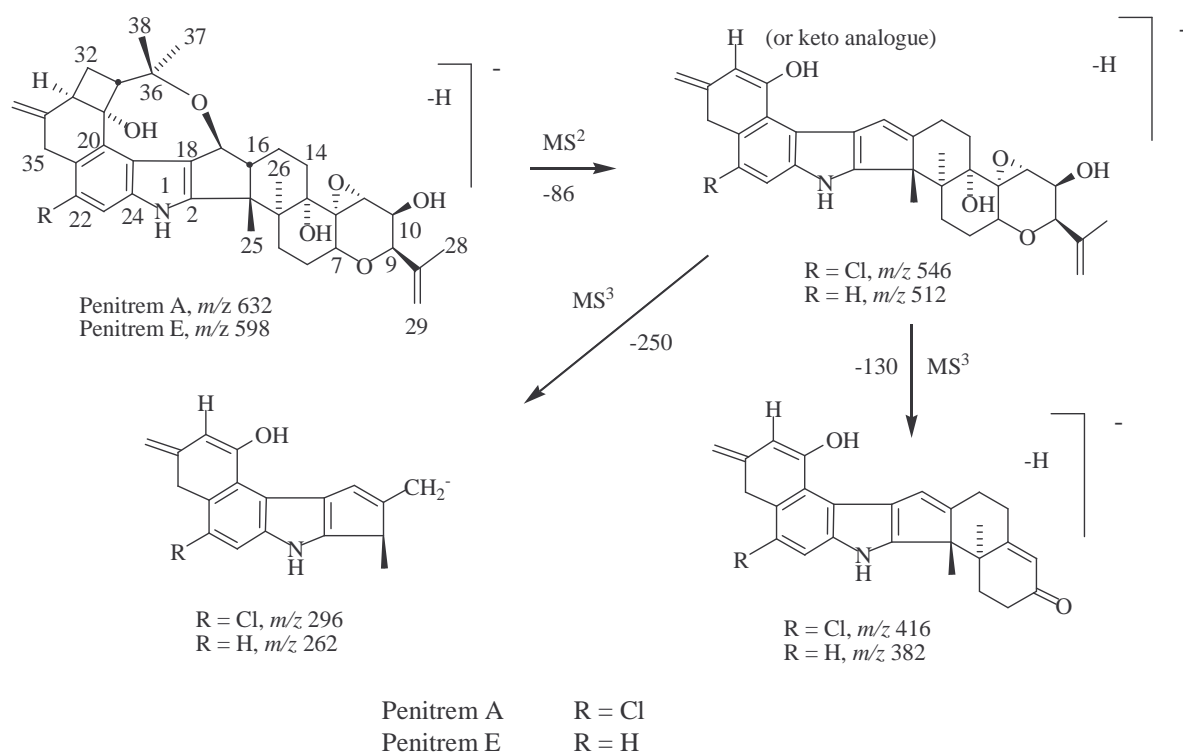


Figure 4.47. Fragmentation of penitrems A and E in negative ion MS^2 and MS^3 spectra.

Penitrem C and Penitrem D

Penitrems C and D showed approximately equal losses of 70 and 86 *amu* under MS^2 conditions. The 86 *amu* loss is consistent with that observed for penitrems A and E and, as in penitrems A and E, is considered to arise via cleavage of the C-30–C-31, C-32–C-33 and C-17–O bonds (see Figure 4.51). As discussed above, it is thought the 86 *amu* loss is due to the loss of a $C_5H_{10}O$ molecule. It can be proposed that the 70 *amu* loss arises by loss of a C_3H_5-CHO molecule from the lower right-hand portion of the penitrems C and D structures via a retro Diels–

Alder mechanism. An analogous loss is observed for janthitrems B and C under MS^3 conditions, and since the right-hand ends of the janthitrems B and C and penitrems C and D molecules are identical, identical fragmentation is proposed as shown in Figure 4.51.

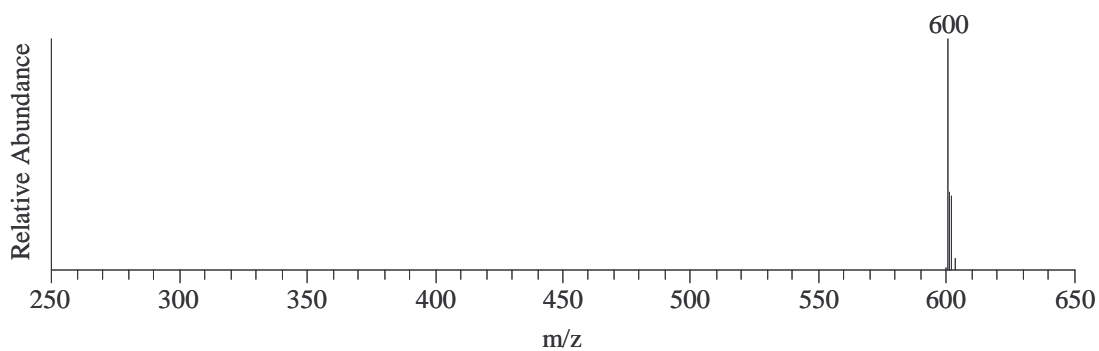


Figure 4.48. Penitrem C full scan negative ion mass spectrum.

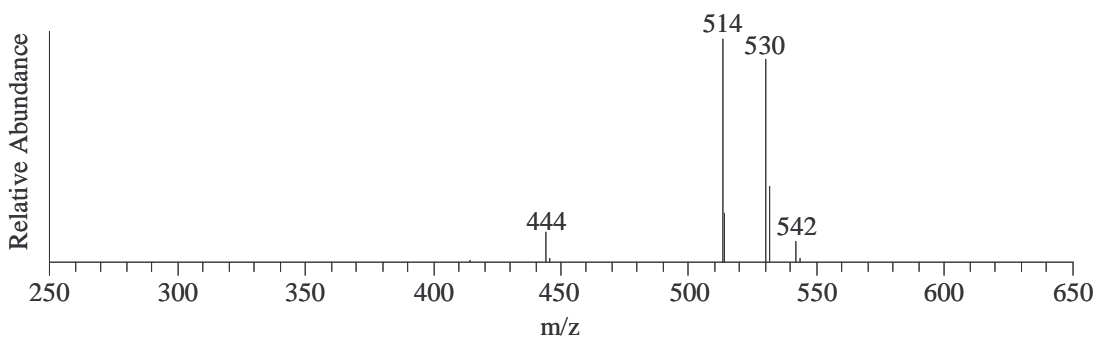


Figure 4.49. Penitrem C negative ion MS^2 spectrum (m/z 600).

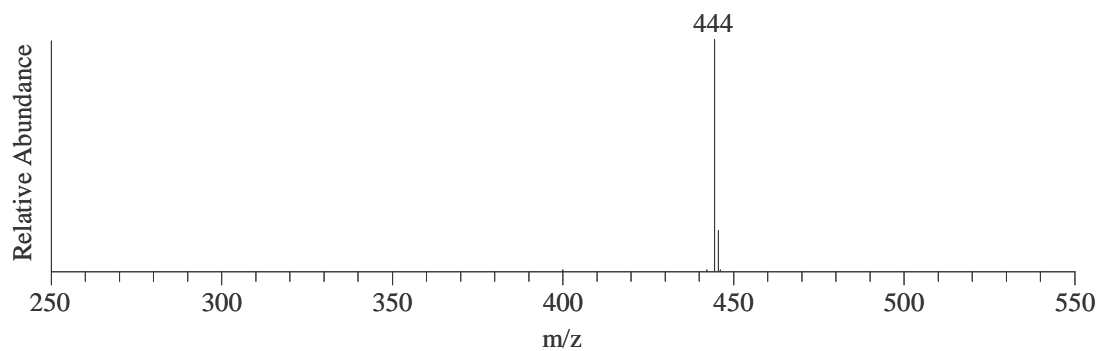


Figure 4.50. Penitrem C negative ion MS^3 spectrum (m/z 600 \rightarrow m/z 514).

The presence in penitrems C and D of an 11(12)-double bond is required for the retro Diels–Alder loss of the C_3H_5-CHO molecule. Compounds possessing an 11,12-epoxy group (and a 10-OH group) as is the case for penitrems A, B, E and F and janthitrems A and D do not show the loss of 70 *amu* in their negative ion MS^2 or MS^3 spectra.

A weak loss of 156 *amu*, attributable to the loss of both 86 and 70 *amu* fragments, is also seen in the MS^2 spectra of penitrems C and D. Under MS^3 conditions, the $[M-H-86]^-$ ions of penitrems C and D each predominantly afforded $[M-H-86-70]^-$ ions.

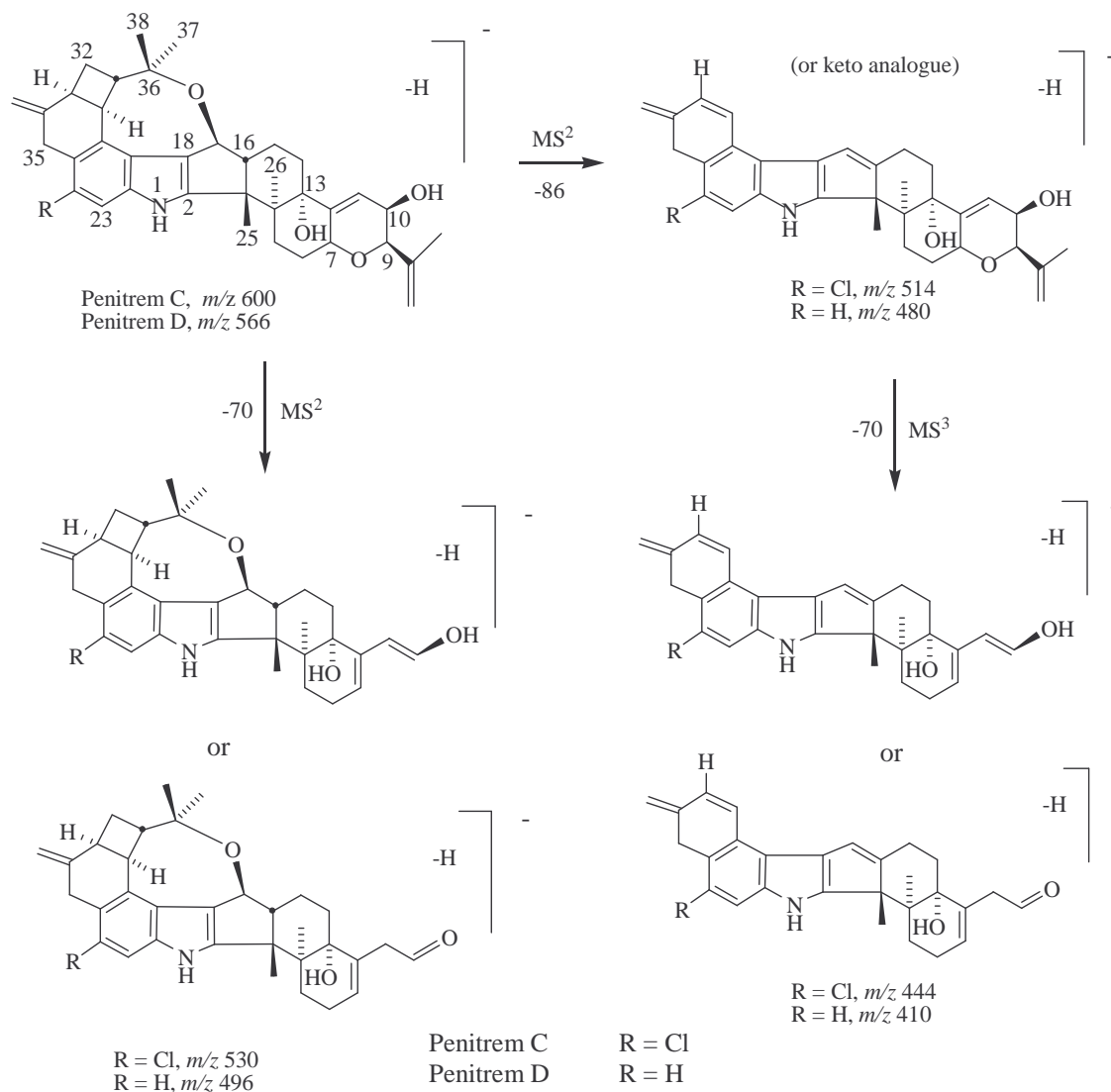


Figure 4.51. Fragmentation of penitrems C and D in negative ion MS^2 and MS^3 spectra.

Penitrem B and Penitrem F

Unlike penitrems A, E, C and D, a loss of 86 *amu* was not observed as one of the dominant fragments in the MS² or MS³ spectra of penitrems B and F. Rather, under MS² conditions, a loss of 130 *amu* was observed.

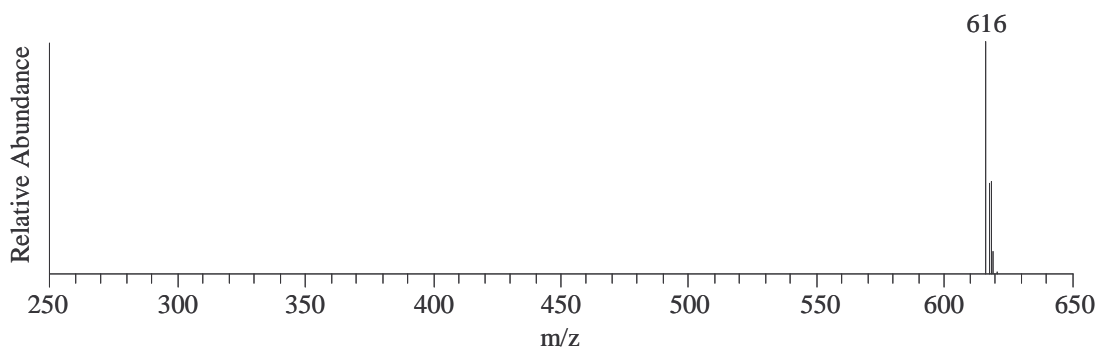


Figure 4.52. Penitrem F full scan negative ion mass spectrum.

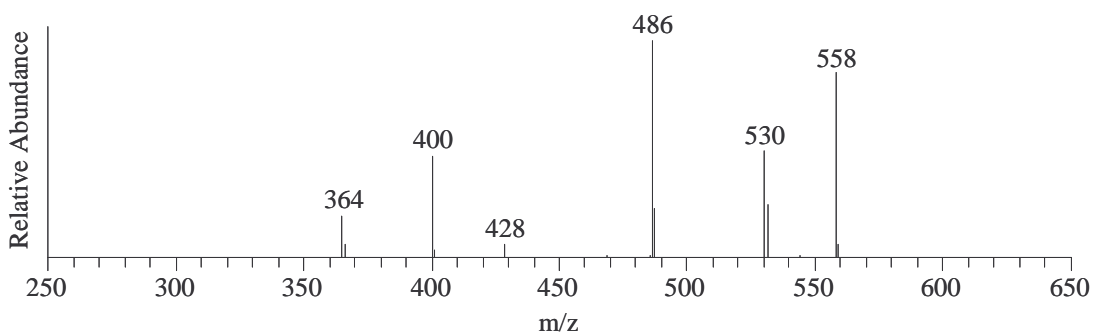


Figure 4.53. Penitrem F negative ion MS² spectrum (*m/z* 616).

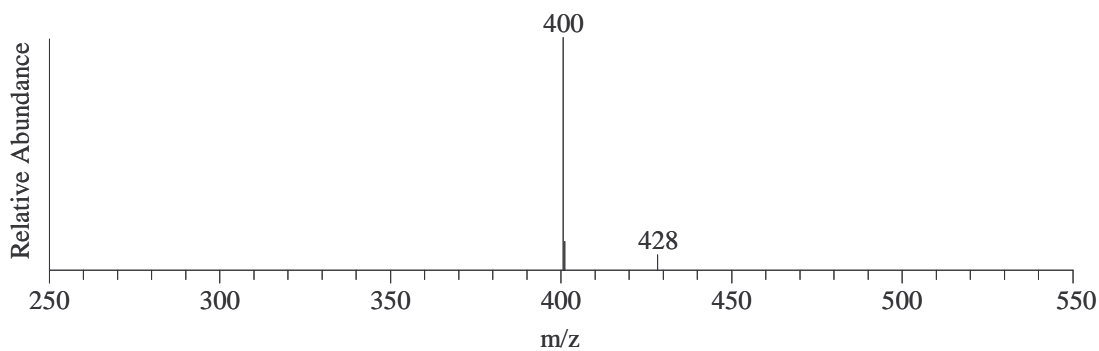


Figure 4.54. Penitrem F negative ion MS³ spectrum (*m/z* 616 → *m/z* 486).

The loss of 130 *amu* is consistent with that observed for janthitrem D and penitrems A and E and is believed to arise via fragmentation of the common right-hand portions of janthitrem D and penitrems B and F ($C_6H_{10}O_3$) (see Figure 4.55). A 58 *amu* (acetone) loss was also observed under MS^2 conditions. Plausible structure ions, accounting for the losses of 130 *amu* and 58 *amu*, are shown in Figure 4.55.

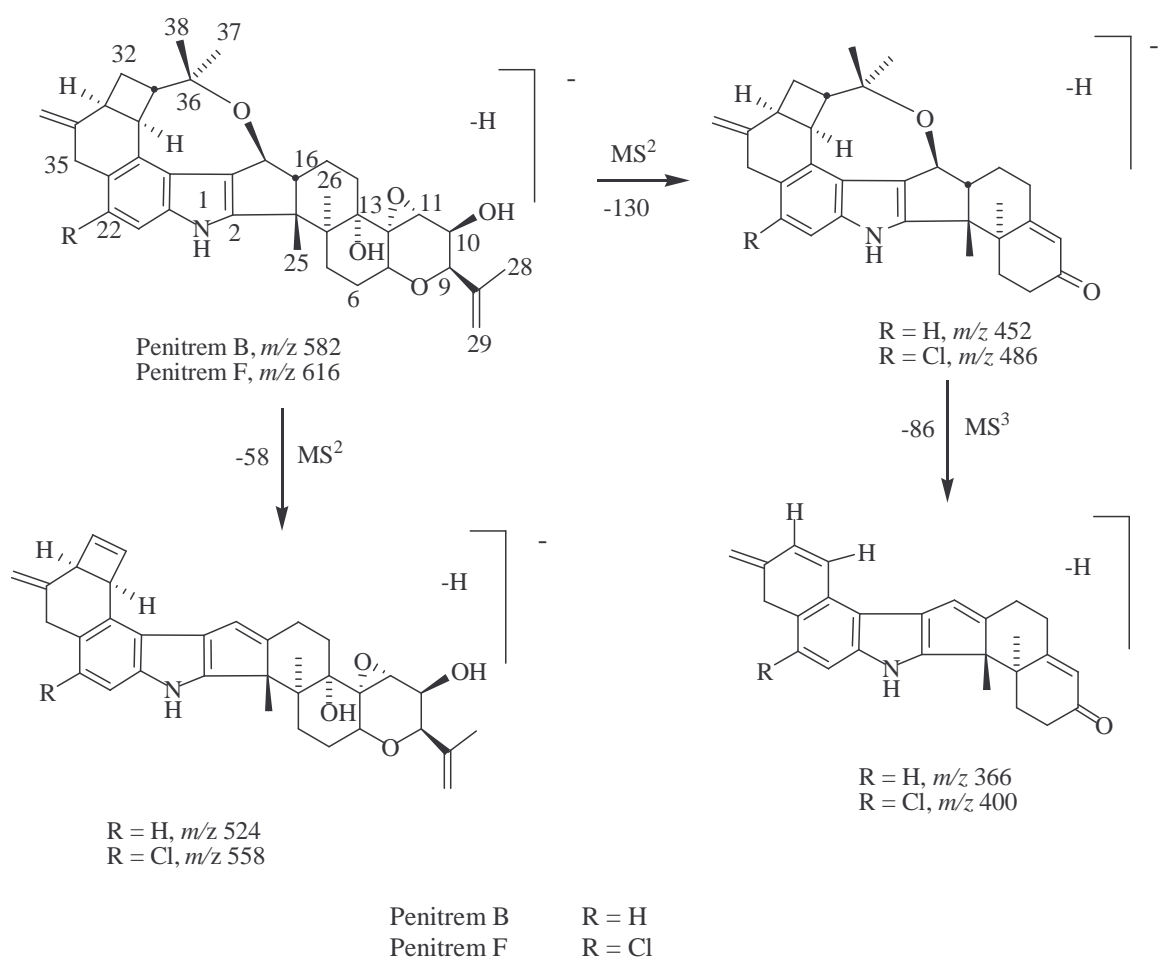


Figure 4.55. Fragmentation of penitrems B and F in negative ion MS^2 and MS^3 spectra.

A loss of 86 *amu* was observed for penitrems B and F under MS^3 conditions, following the loss of the 130 *amu* fragment (Figure 4.55). The 86 *amu* fragment loss is believed to be analogous with that observed under MS^2 conditions for penitrems A, E, C and D and equates to the loss of a $C_5H_{10}O$ molecule.

4.5.3 Fragmentation of Lolitrem B

Lolitrem B, under negative ion MS² conditions using an APCI source, showed losses of both 214 *amu* (dominant fragment) and 244 *amu* to afford *m/z* 470 and 440 ions (Figures 4.56, 4.57 and 4.58). The loss of 214 *amu* is believed to be analogous to the 130 *amu* losses exhibited by penitremes A, E, B and F and janthitrem D. The greater loss in lolitrem B (214 *amu* compared to 130 *amu*) can be attributed to its additional hemi-acetal side chain. This loss appears to be correlated with (i.e. diagnostic for) the presence of an 11,12-epoxy group. The 214 *amu* loss appears to arise by loss of a C₁₁H₁₈O₄ residue. The loss of 214 *amu* could result in a number of possible ion structures, two of which are shown in Figure 4.59.

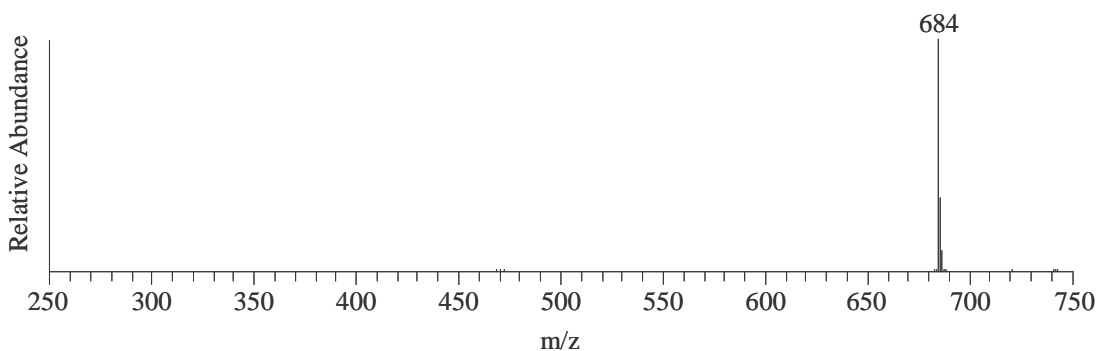


Figure 4.56. Lolitrem B full scan negative ion mass spectrum.

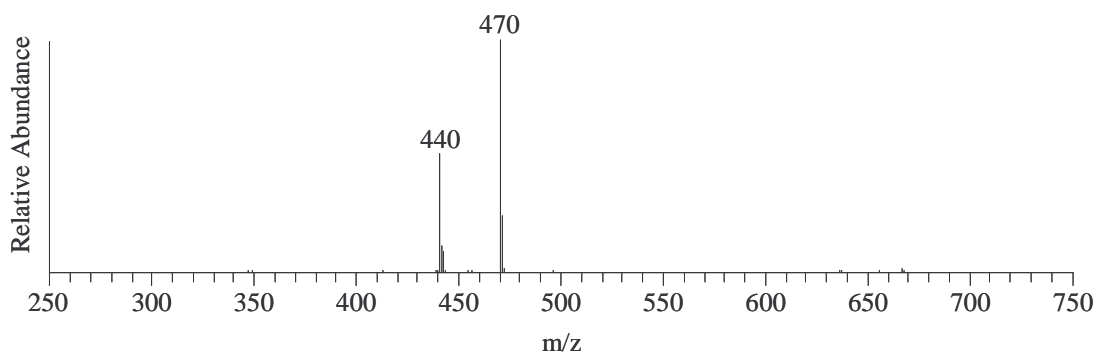


Figure 4.57. Lolitrem B negative ion MS² spectrum (*m/z* 684).

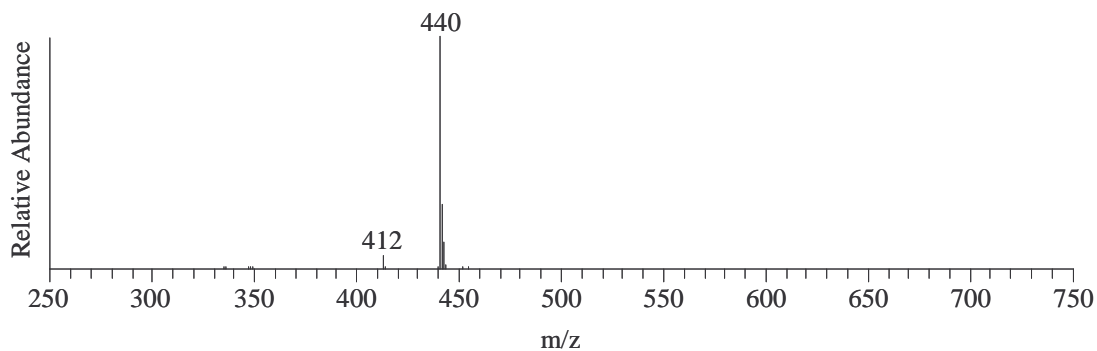


Figure 4.58. Lolitrem B negative ion MS³ spectrum (m/z 684 \rightarrow m/z 470).

Further fragmentation of the m/z 470 (214 *amu* loss) ion under MS³ conditions afforded two significant fragment ions, the more dominant of which occurred at m/z 440 (30 *amu* loss) while the lesser of the two ions occurred at m/z 412 (58 *amu* loss). The 244 *amu* loss observed under MS² conditions for lolitrem B equates to the combined loss of 214 *amu* and 30 *amu*. The 58 *amu* loss can be attributed to the loss of acetone from the left-hand end portion of the molecule (Figure 4.59).

The origin of the loss of 30 *amu* is more difficult to envisage. Generally the loss of 30 *amu* can be attributed to the loss of either ethane (CH₃–CH₃) or formaldehyde (H₂C=O). It is possible that the loss of 30 *amu* arises from elimination of H₂CO from the right-hand end of the structure to give a structure with a 5-membered cyclopentadiene structure (Figure 4.59).

However, the right-hand end of lolitrem B is similar to that of janthitrem D and the penitremes A, E, B and F, yet, none of the latter groups of molecules show the loss of 30 *amu* in their MS² or MS³ spectra. It can therefore be reasoned that the loss of 30 *amu* in the MS³ spectrum of lolitrem B arises from the structurally modified left-hand end of the molecule. Possibly the 30 *amu* loss arises by loss of the 30-keto group with transfer of the H-35 and H-31 protons to the carbonyl carbon with consequential contraction of ring B to afford a cyclopentene ring as depicted in Figure 4.59.

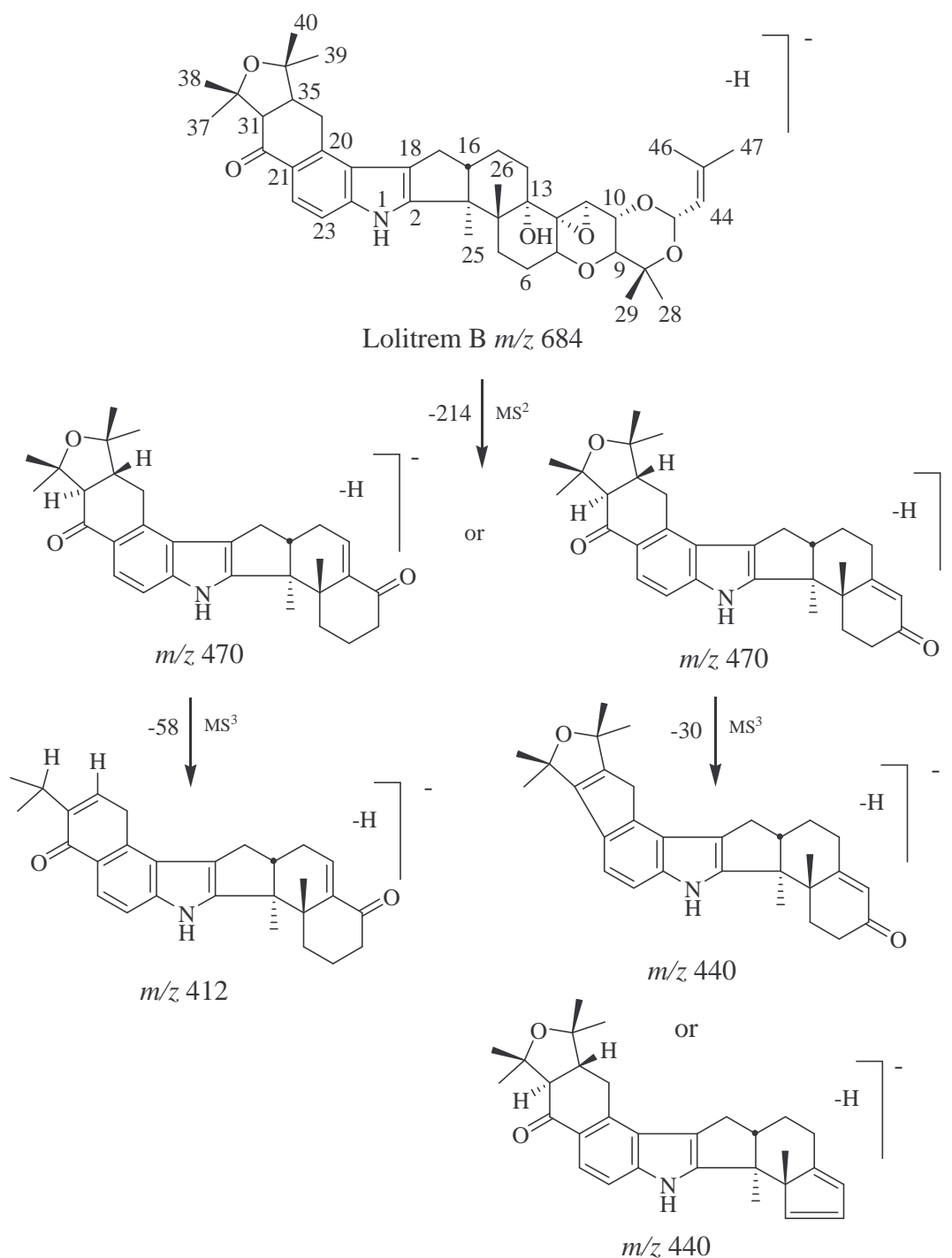


Figure 4.59. Fragmentation of lolitrem B in negative ion MS^2 and MS^3 spectra.

4.5.4 Fragmentation of Paxilline

Fragmentation of the m/z 434 $[M-H]^-$ ion of paxilline under negative ion MS^2 conditions afforded a dominant m/z 376 ion arising from the loss of 58 amu (Figure 4.60). This loss can be attributable to the loss of acetone from the C-9

hydroxyisopropyl group [$-\text{C}(\text{CH}_3)_2\text{OH}$]. Acetone losses are also seen in the MS^2 spectra of janthitrems A, B, C and D, penitrems B and F and lolitrem B (although from different portions of the respective molecules).

Further fragmentation of the m/z 376 ion under MS^3 conditions afforded m/z 358 (-18 amu) and m/z 332 (-44 amu) ions. The loss of 18 amu can be attributed to the loss of water from the hydroxyl group at C-13. The loss of 44 amu is more difficult to envisage. It can be hypothesised that the 44 amu loss arises from the loss of either a CO_2 molecule or an acetaldehyde (CH_3CHO) molecule. A plausible structure for the m/z 332 ion has not, as yet, been identified.

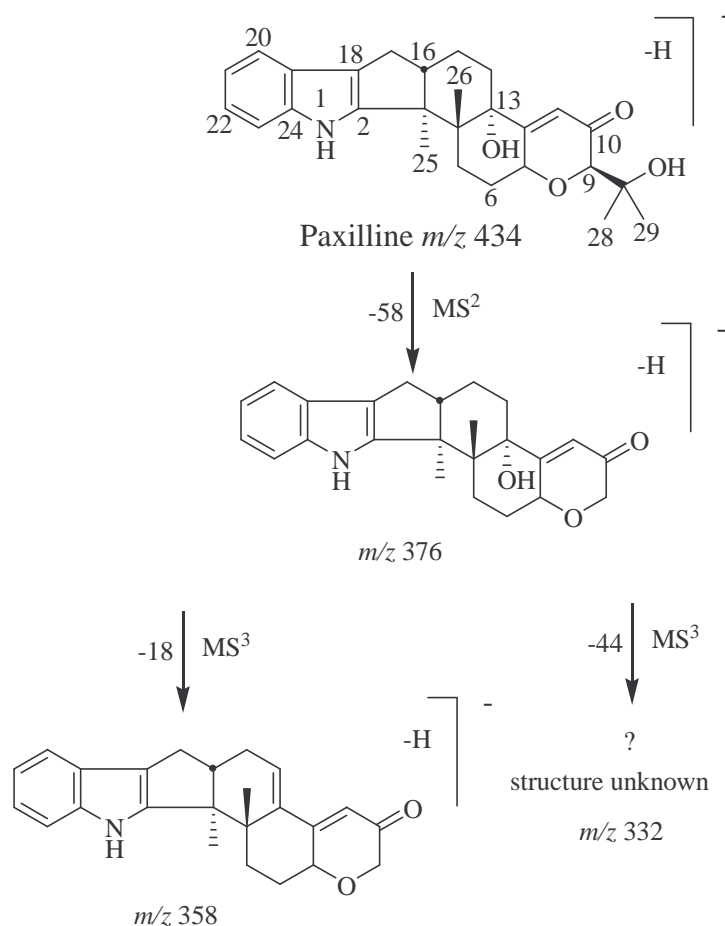


Figure 4.60. Fragmentation of paxilline in negative ion MS^2 and MS^3 spectra.

4.5.5 Fragmentation of Terpendole C

The MS² fragmentation of terpendole C under negative ion conditions paralleled that determined for lolitrem B and janthitrem D, in that the m/z 518 [M-H]⁻ ion of terpendole C showed a loss of 214 *amu* to afford an m/z 304 ion (Figure 4.61). The structure proposed for this ion is analogous to those of the m/z 396 and 470 ions seen in the MS³ of janthitrem D and MS² of lolitrem B respectively. The mass variations of these ions reflect their differing left-hand ring structures. The loss of 214 *amu* can be ascribed to the loss of a C₁₁H₁₈O₄ residue.

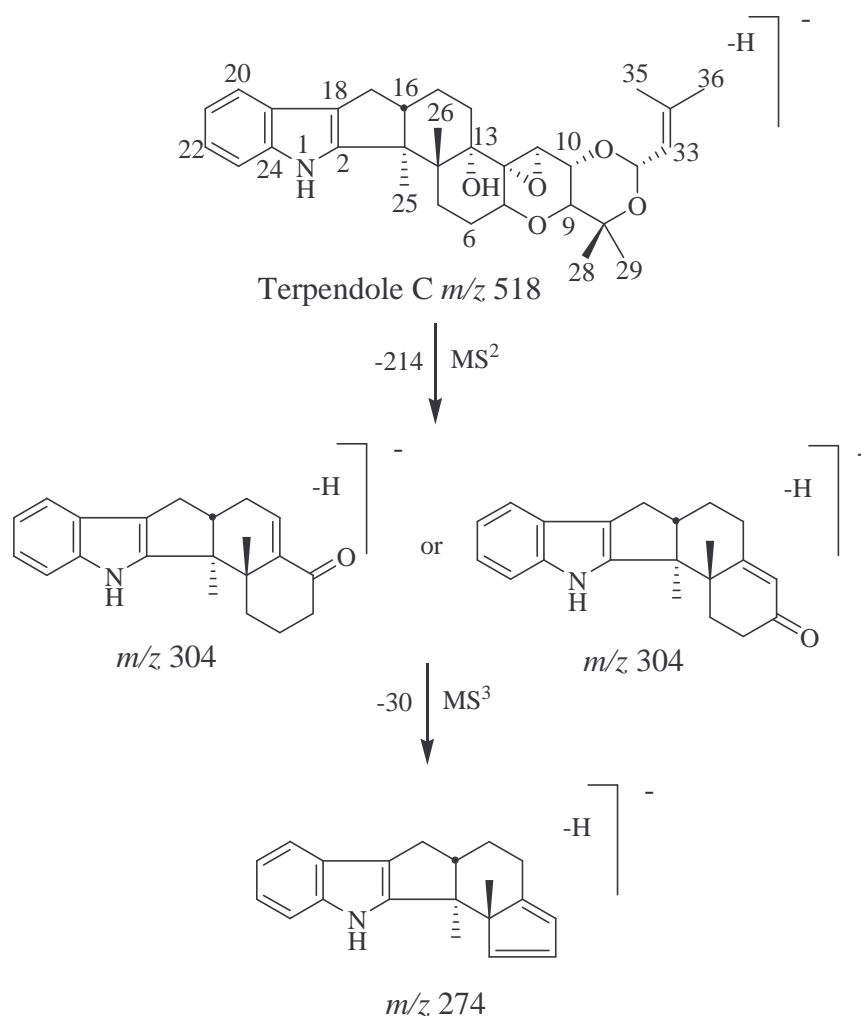


Figure 4.61. Fragmentation of terpendole C in negative ion MS² and MS³ spectra.

Terpendole C also exhibited a 30 *amu* loss following further fragmentation of the m/z 304 ion (-214 *amu*) under MS³ conditions to afford an m/z 274 ion. A loss of

30 *amu* may be due to the loss of ethane or formaldehyde. Of these two possibilities, the loss of formaldehyde is believed to be the more likely. It is possible that the loss of 30 *amu* arises from elimination of H₂CO from the right-hand end of the structure to give a structure with a 5-membered cyclopentadiene structure instead of a cyclohexenone structure (as per the *m/z* 304 ion) (Figure 4.61). A comparable 30 *amu* loss was also observed for lolitrem B (Figure 4.59).

4.5.6 Fragmentation of Paspalinine

Fragmentation of the [M-H]⁻ ion, which occurred at *m/z* 432 under negative ion MS² conditions, afforded a dominant *m/z* 414 ion. This ion corresponds to a loss of 18 *amu* from the [M-H]⁻ ion, most likely by loss of water from the 13-OH group.

Further fragmentation of the *m/z* 414 ion under MS³ conditions afforded two dominant ions at *m/z* 356 (-58 *amu*) and *m/z* 342 (-72 *amu*). The 58 *amu* loss (a frequently encountered loss throughout this investigation in both the negative and positive ion modes), can be attributed to the loss of acetone from the 7,27-oxido linkage (Figure 4.62). The loss of 72 *amu* can be accounted for by loss of a C₄H₈O residue from the right-hand side of the molecule to afford an *m/z* 342 ion (Figure 4.62). Since the loss of 72 *amu* is only observed in paspalinine and not in analogues possessing a C-9 isopropenyl or hydroxyisopropyl group, this loss appears diagnostic for the presence of a 7,27-ether linkage.

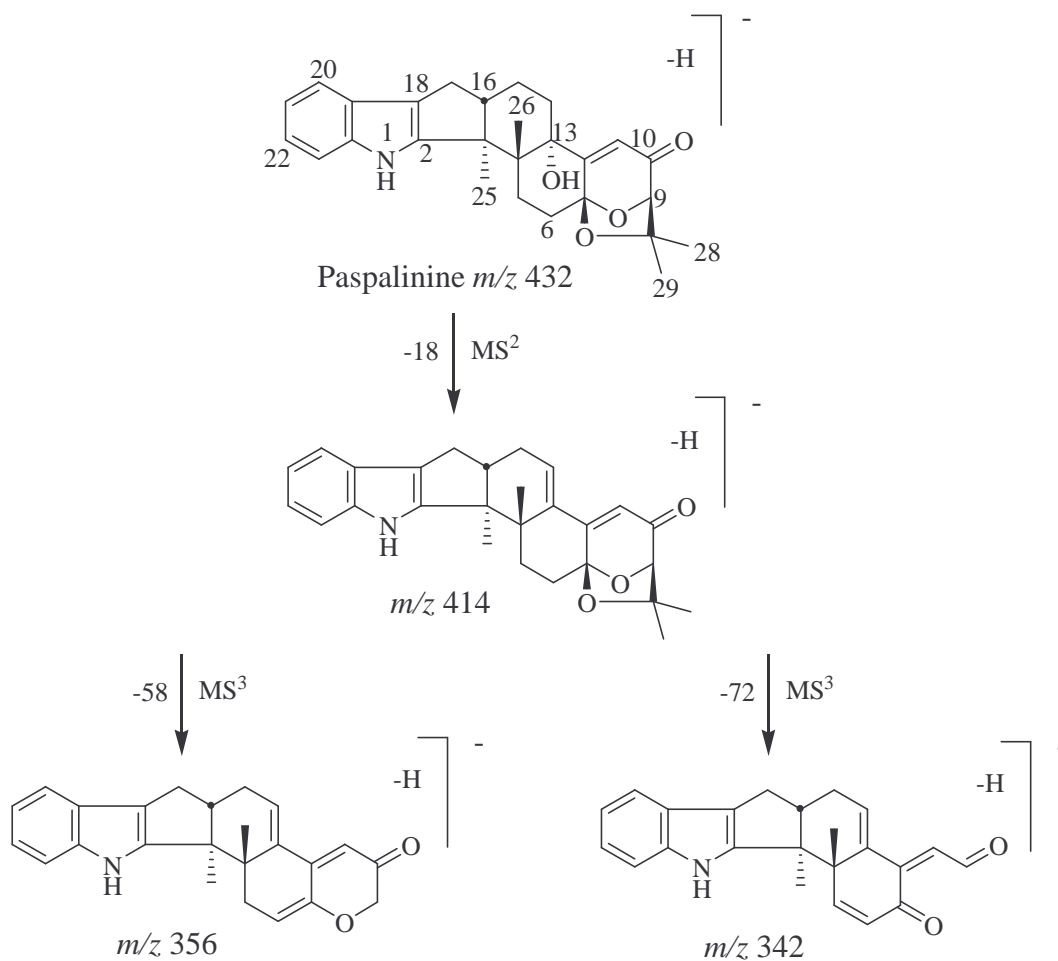


Figure 4.62. Fragmentation of paspalinine in negative ion MS^2 and MS^3 spectra.

4.5.7 Summary of Findings

Negative ion mode APCI LC–UV–MS analyses of indole–diterpenoid compounds affords two dominant peaks in full scan mode, namely an $[M-H]^-$ ion and an acetate adduct ion, $[M+OAc]^-$. Attempts to obtain MS^2 and MS^3 data from the acetate adduct ion peak were unsuccessful, even at both low (20%) and high (60%) collision energy. SID (25–30 V) was introduced along with high collision energy (60%) into the negative ion method, resulting in suppression of the acetate adduct peak and the exclusive formation of $[M-H]^-$ ions, which could successfully be fragmented to provide acceptable MS^2 and MS^3 data.

Negative ion MSⁿ spectra were characterised by the presence of a series of structurally informative ions. Generally the fragmentations under positive ion conditions involved losses relating to acetone and either water or oxygen. In contrast, losses observed under negative ion conditions seemed dependent on the presence of either an 11(12)-double bond (affording a loss of 70 *amu*) or an 11,12-epoxide (affording a loss of 130 *amu*).

The results from the negative ion investigations allow the identification of compounds based on the fragmentation patterns observed and hence is a new and valuable tool in identifying unknown compounds and structural properties of known compounds.

CHAPTER FIVE

In vivo Effects of the Isolated Indole– Diterpenoid Compounds

5.1 Assessment of Tremorgenicity, Heart Rate, Blood Pressure and Motor Control of Mice Dosed with Janthitrems A and B

5.1.1 Introduction

The indole–diterpenoids, janthitrem A and janthitrem B (isolated during the course of this research), were tested on mice to assess their tremorgenicity and their effects on blood pressure, heart rate and motor control. Motor control was measured using an accelerating rotarod instrument (Figure 5.1) and blood pressure and heart rate measured with a blood pressure and heart rate analysis system which utilised a non-invasive tail-cuff system (Figure 5.2). Full experimental details are described in Section 8.6.3. The tremorgenicity was assessed by a procedure developed at Ruakura, New Zealand. This method has been used extensively to test the tremorgenicity of a large number of indole–diterpenoid neurotoxins (Miles et al., 1992; Munday-Finch et al., 1995; Munday-Finch et al., 1996b; Munday-Finch et al., 1997).

The assessment of *in vivo* effects induced by indole–diterpenoid compounds was carried out in mice as testing on cattle or sheep would require a large amount of the test compound, which is not feasible.

Janthitrem A and janthitrem B were investigated in this study. While toxins such as lolitrem B and paxilline have been shown to have effects on smooth muscle and electrophysiological preparations (such as BK channels by patch-clamping)

(Dalziel et al., 2005; Knaus et al., 1994; Sanchez and McManus, 1996), there is currently no other method to determine tremorgenicity in the living animal, which is the objective of these experiments.

Ethics approval was obtained from the Ruakura Animal Ethics Committee established under the Animal Protection (code of ethical conduct) Regulations Act, 1987 (New Zealand) and The University of Waikato Animal Ethics Committee. The mice employed in the experiment were female Swiss mice (25 ± 3 grams).

The significance of the results were assessed using the Student's t-test and are expressed as a *p*-value. The error bars on Figures 5.3–5.8 and Figure 5.10 represent the standard error of the mean of the respective data.



Figure 5.1. The rotamex 4 rotarod.



Figure 5.2. The BP-2000 blood pressure and heart rate measurement instrument.

5.1.2 Tremorgen Bioassay

The symptoms of ryegrass staggers have been experimentally reproduced in mice by the intraperitoneal administration of the tremorgen lolitrem B (Gallagher and Hawkes, 1985). This method has been successfully used to test indole–diterpenoids for tremorgenicity. Experimental details of the tremorgen bioassay are outlined in Sections 8.6.1 and 8.6.2.

Mice were dosed with janthitrem B (6 mg kg^{-1}) and compared to a control group dosed vehicle alone (DMSO–water 9:1). Due to the structural similarity between janthitrem A and janthitrem B, the same dose rate was initially used (6 mg kg^{-1}) for janthitrem A. However, injection into the first mouse resulted in severe tremoring. This indicated the dose rate was too high and no more mice were dosed at this level. A lower dose of 4 mg kg^{-1} was subsequently used, yielding tremor activity similar to that observed in the janthitrem B experiment (Figure 5.3). The control animals for both the janthitrem A and janthitrem B experiments showed no signs of tremorgenic activity.

These results showed that janthitrem A induced more severe tremors in comparison to janthitrem B since a lower dose rate of janthitrem A was used. A comparison of the time course of action also showed a difference with the tremors induced by janthitrem A peaking slightly more quickly compared to that of janthitrem B (15 minutes compared to 30 minutes) and lasting considerably longer. At 6 hours post-dosing, mice dosed with janthitrem B had completely recovered whereas those dosed with janthitrem A still showed a significant tremor (score of approximately 1).

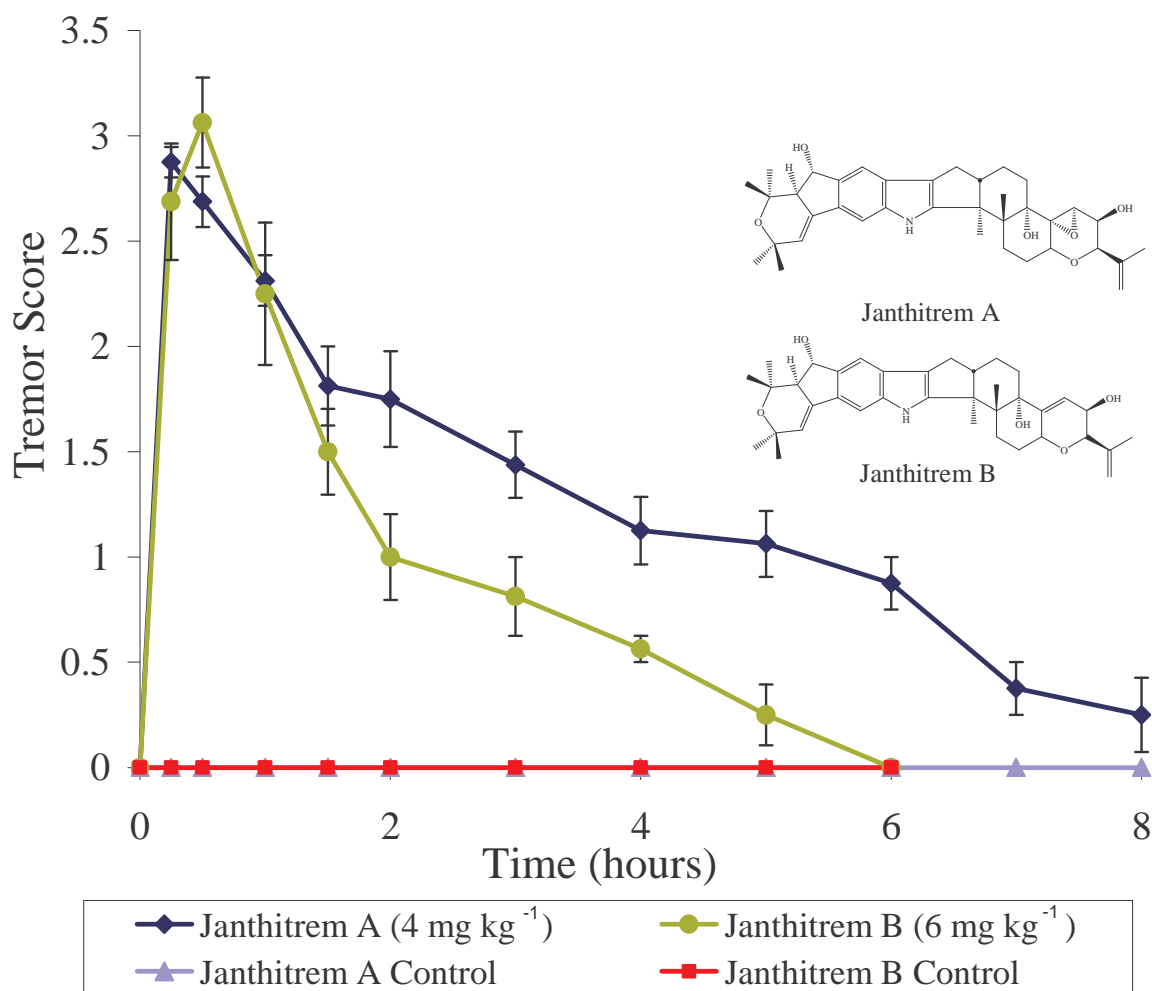


Figure 5.3. Mean tremor score vs time post-injection for mice dosed i.p. with janthitrem A (n = 4), janthitrem B (n = 4) and their respective controls (n = 4).

5.1.3 Effect of the Test Compounds on the Heart Rate of the Mice

In addition to tremorgenicity, the blood pressure and heart rate were measured periodically during the experiment using a computerised, non-invasive tail-cuff system, the BP-2000 (Figure 5.2). Janthitrem A and janthitrem B both caused a rapid dramatic decrease in heart rate (Figure 5.4). Within 30 minutes post-injection the heart rate of the janthitrem dosed mice had decreased by approximately 40% ($p > 0.01$). This slowly returned to normal within 7 hours and at that time there was no significant difference between the test janthitrem and its respective control ($p > 0.1$). Although the effect on heart rate between janthitrem A and B was similar, janthitrem A was dosed at a lower dose rate and can therefore be considered to have a greater effect on heart rate compared to that induced by janthitrem B.

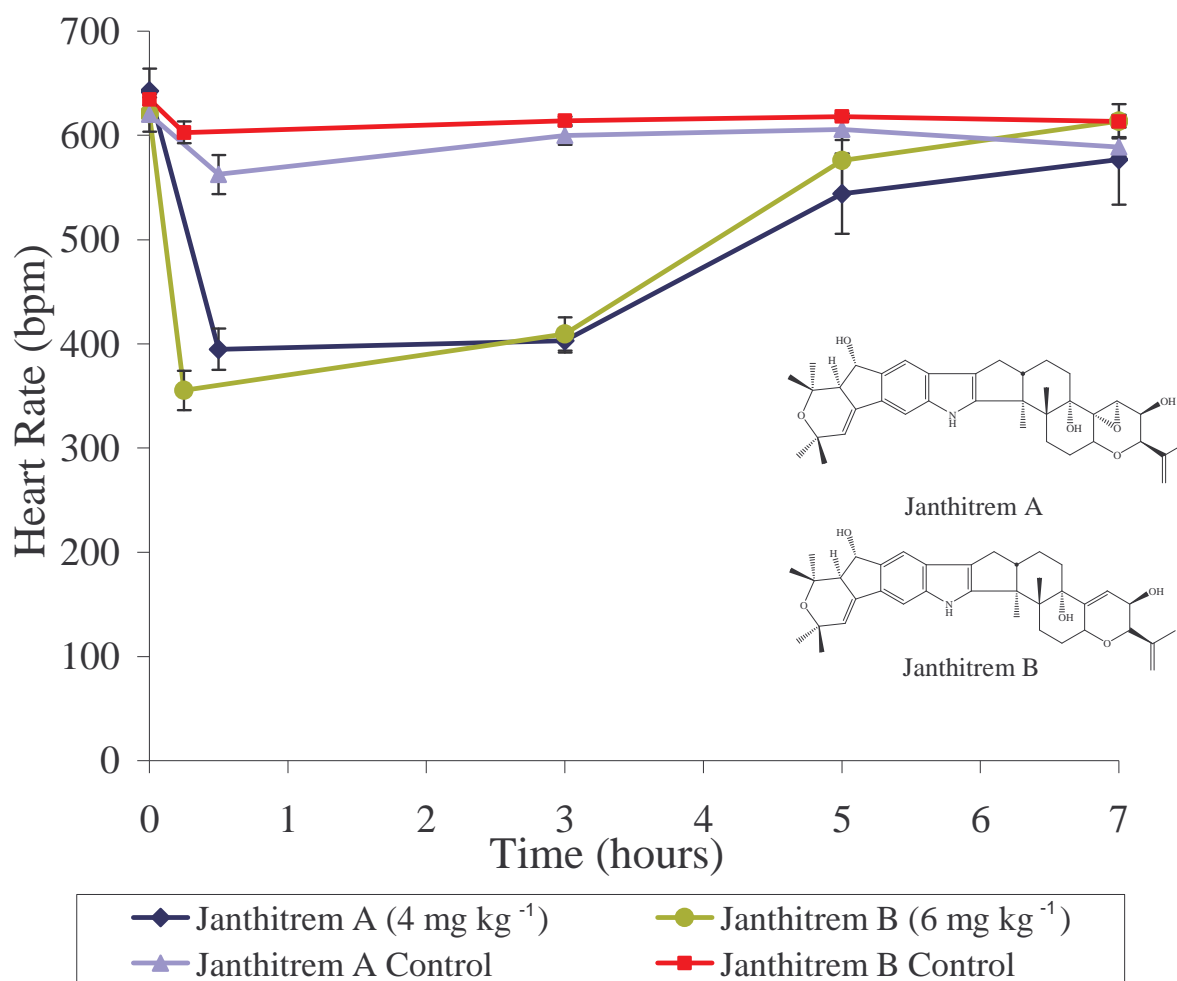


Figure 5.4. Mean heart rate vs time post-injection time for mice dosed i.p. with janthitrem A (n = 4), janthitrem B (n = 4) and their respective controls (n = 4).

5.1.4 Effect of the Test Compounds on the Systolic Pressure of the Mice

A less dramatic drop in systolic pressure was observed in mice dosed janthitrems in comparison to heart rate. This drop was only significant for the first recording period following administration of both janthitrems in comparison to their controls ($p < 0.1$) (Figure 5.5).

Due to the observed fluctuation of the systolic pressure over time for the controls, conclusions regarding the effect of janthitrems A and B on the systolic pressure cannot be made.

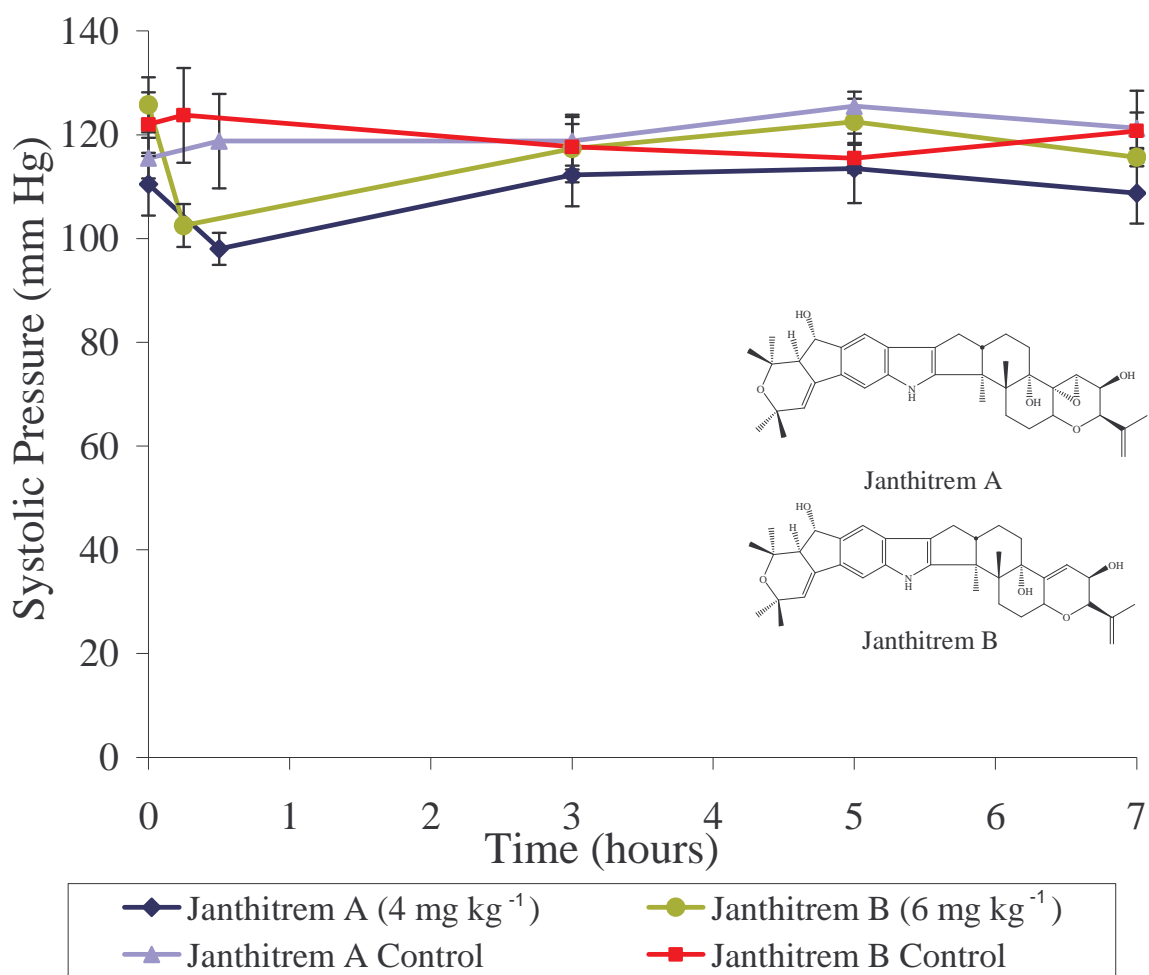


Figure 5.5. Mean systolic pressure vs time post-injection for mice dosed i.p. with janthitrem A (n = 4), janthitrem B (n = 4) and their respective controls (n = 4).

5.1.5 Effect of the Test Compounds on the Diastolic Pressure of the Mice

No significant differences were observed in the diastolic pressure of the mice administered janthitrems (Figure 5.6). Janthitrem A seemed to cause a drop following administration but considering the observed fluctuations throughout the experiment and the fact that janthitrem B appeared to have no effect on diastolic pressure, no conclusions can be drawn.

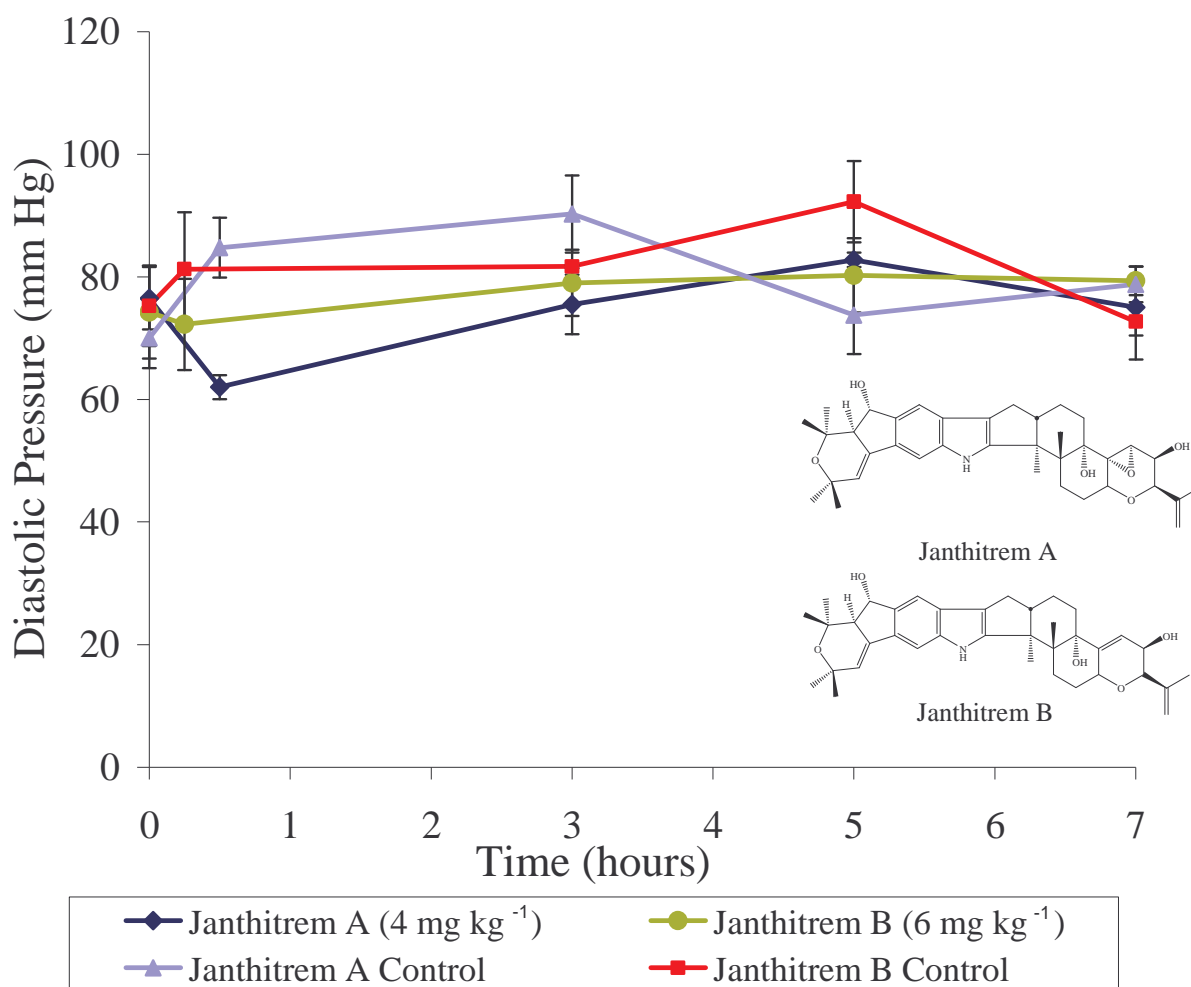


Figure 5.6. Mean diastolic pressure vs time post-injection for mice dosed i.p. with janthitrem A (n = 4), janthitrem B (n = 4) and their respective controls (n = 4).

5.1.6 Effect of the Test Compounds on the Motor Control of the Mice

The rotarod instrument was used to evaluate the effect of janthitrems A and B on the motor control of mice. The rotarod measures the ability of mice to balance and walk around a moving rod (refer to Section 8.6.4 for full experimental

details). Our initial experiment used an injection volume of 100 μL 9:1 DMSO–water, but in this case control mice showed a significant decrease in their ability to perform the rotarod task due to the effect of DMSO. DMSO can cause mice to become unresponsive, placid and docile and consequently the mice can experience difficulty staying on the rotarod. Reducing the injection volume to 50 μL caused only a minimal effect on control mice, so this volume was used for all subsequent experiments.

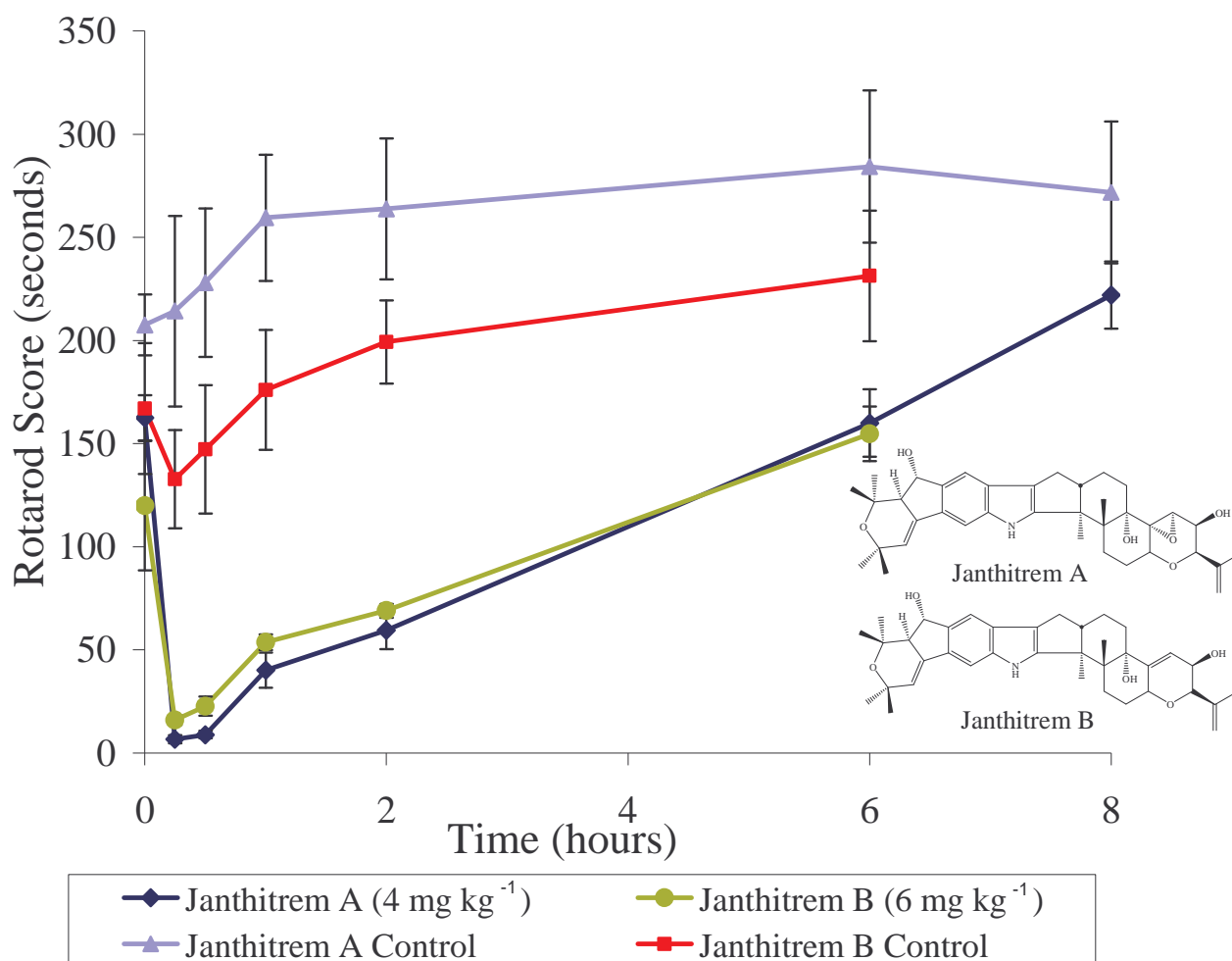


Figure 5.7. Mean rotarod score vs time post-injection for mice dosed i.p. with janthitrem A ($n = 4$), janthitrem B ($n = 4$) and their respective controls ($n = 4$).

As indicated by the high error bars (Figure 5.7), the rotarod test is associated with a high variability among animals. This fact is also shown by the high degree of variability encountered for the time zero measurements of the different groups of

animals (Figure 5.7) despite an analogous training regimen. To allow an easier interpretation of results, the rotarod scores at each measurement time were also compared as a percentage of their initial score (at $t = 0$) (Figure 5.8).

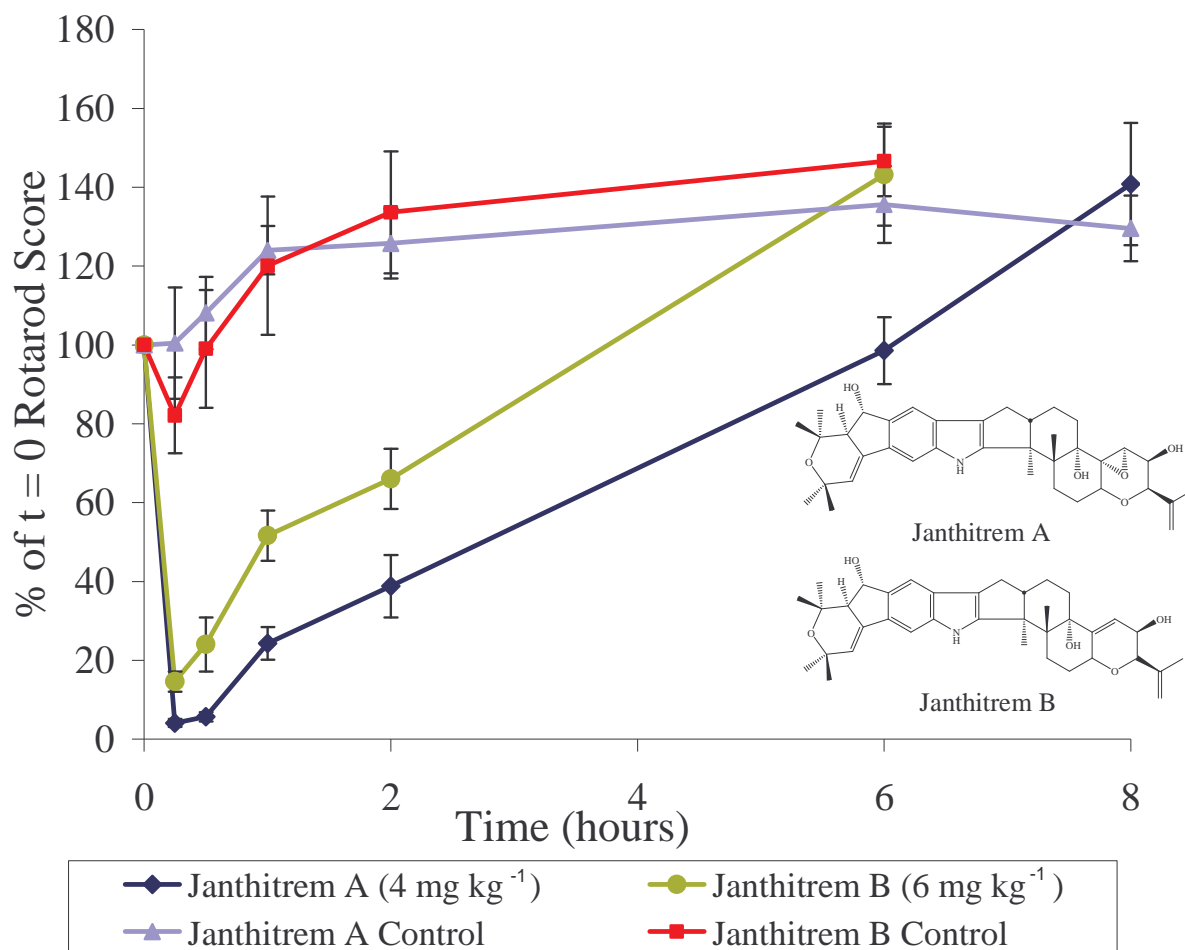


Figure 5.8. Mean rotarod scores expressed as a percentage of the score at $t = 0$ vs time post-injection for mice dosed i.p. with janthitrem A ($n=4$), janthitrem B ($n=4$) and their respective controls ($n=4$).

Both janthitrem A and janthitrem B had an immediate and dramatic effect on the motor control of mice. The effect induced by janthitrem A, when considering the lower dose rate administered, was more severe than that induced by janthitrem B. The time course was also longer for the effect induced by janthitrem A as indicated by the fact that mice dosed with janthitrem B returned to their normal rotarod scores within 6 hours. In contrast, however, janthitrem A dosed mice still had significant motor impairment ($p < 0.05$).

5.1.7 Summary of Findings

This is the first time an epoxyjanthitrem (janthitrem A) has been tested on mice, and it was shown to induce tremors which were slightly more intense and longer acting than those induced by the more common janthitrem, janthitrem B (Table 5.1). This difference in tremorigenicity must be due to the epoxide at C-11–C-12, as structurally, this is the only difference between the two compounds. Both janthitrem A and janthitrem B also caused a dramatic effect on the heart rate and motor control of mice.

Table 5.1. Tremorigenic activity of the tested janthitrem.

Compound	Dose (mg kg ⁻¹)	Time of Maximum Tremor (Hours)	Maximum Tremor Score	Duration of Tremors (Hours)
Janthitrem A	6	Dosage too high – therefore dosage was reduced to 4 mg kg ⁻¹		
	4	0.25	2.69	8
Janthitrem B	6	0.5	3.06	5–6

The staggers observed by animals grazing on AR37 endophyte-infected pastures are believed to be caused by janthitrem produced by this novel endophyte. The janthitrem in this case are epoxyjanthitrem, making the results of janthitrem A (an epoxyjanthitrem) compared to the results of janthitrem B (not an epoxyjanthitrem) commercially important.

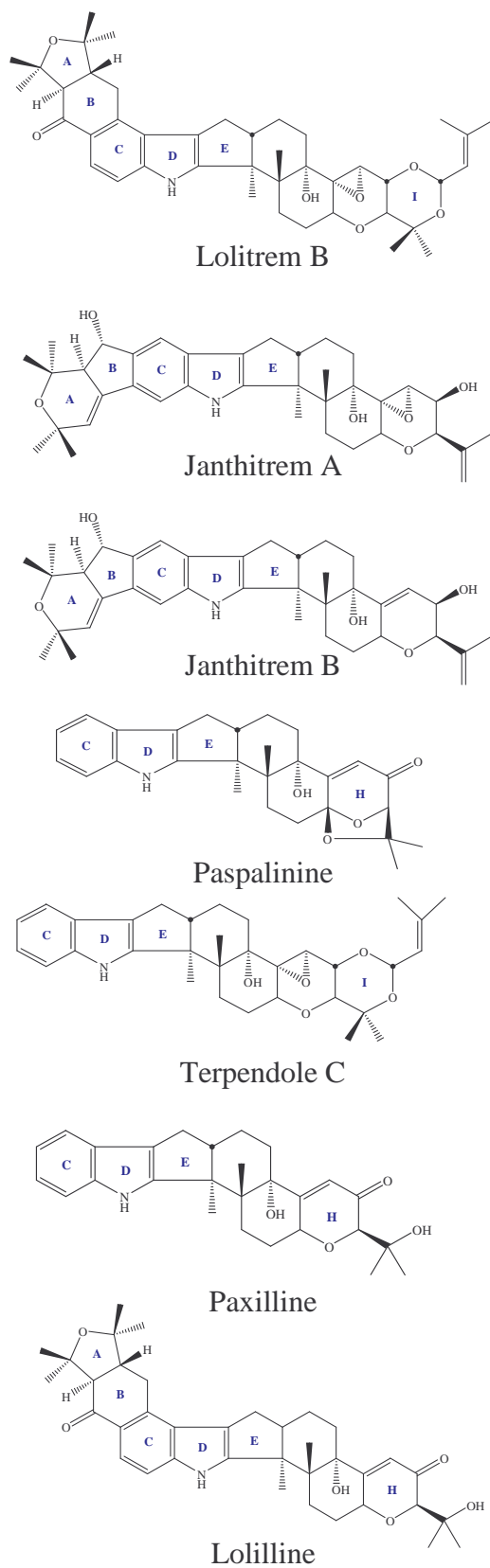


Figure 5.9. Structures of lolitrem B, janthitrem A, janthitrem B, paspalinine, terpendole C, paxilline and lolilline.

The tremorigenic activity induced by janthitrem A and janthitrem B were compared to that published for other indole–diterpenoids such as lolitrem B and paxilline (Figure 5.9) (Munday-Finch, 1997).

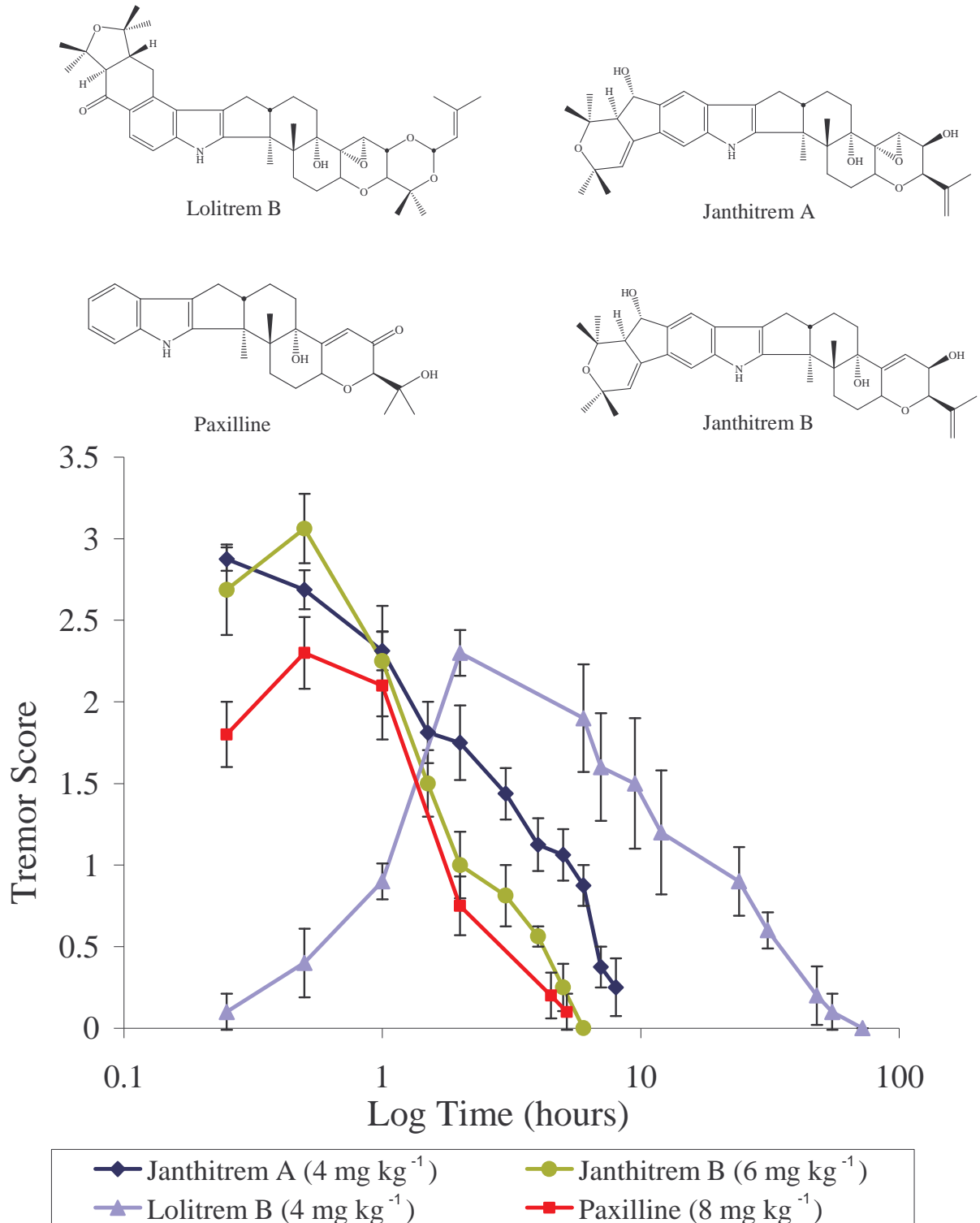


Figure 5.10. Comparison of mean tremor scores vs time post-injection for mice dosed i.p. with janthitrem A (n = 4), janthitrem B (n = 4), lolitrem B (Munday-Finch, 1997) and paxilline (Munday-Finch, 1997).

As evident in Figure 5.10, the janthitrems were more potent in comparison to paxilline but produced similar fast onset but short duration tremors. In contrast, lolitrem B gave slow onset but long duration tremors. Since lolitrem B is unique in its ability to induce long duration tremors, and those which induce short duration tremors such as paxilline, paspalinine and terpendole C lack the A/B rings of lolitrem B (Figure 5.9), it has been previously suggested (Munday-Finch, 1997) that these rings are essential for the generation of a sustained tremor effect. The janthitrems do contain additional rings in comparison to paxilline, paspalinine and terpendole C but these rings are different to those found with the lolitrems and are not sufficient to give long duration tremors.

The effect of the janthitrems on heart rate, blood pressure and motor control are consistent with that previously observed for paxilline and lolitrem B (S.C. Finch, AgResearch Ruakura, Hamilton, New Zealand, personal communication, June 2008).

The structure–activity relationships of indole–diterpenoids are very complex making it impossible to predict biological effects on the basis of structure. This is consistent with the hypothesis that indole–diterpenes act upon specific receptor sites to generate tremors. It has previously been suggested (Munday-Finch et al., 1997) that indole–diterpenes could act upon more than one receptor site. Terpendole C and lolilline, structural intermediates of paxilline and lolitrem B, differ in their tremorigenic behaviour when injected intraperitoneally to mice (Munday-Finch et al., 1997). Terpendole C gave fast acting tremors which were more intense than an equivalent dose of paxilline but were of shorter duration than the tremors induced by lolitrem B. In contrast, lolilline gave no detectable tremors at 8 mg kg^{-1} , making it much less active than paxilline, terpendole C and lolitrem B. These observations by Munday-Finch et al. (1997) highlight the unlikelihood of a single receptor site model for tremorigenic activity. Our new results with the janthitrems are consistent with this hypothesis as the tremorigenic

activity of the janthitrems could not be predicted based on the structure–activity relationships of other indole–diterpenoids such as lolitrem B.

This investigation has shown that janthitrem A and janthitrem B are tremorgenic to mice. The novel endophyte AR37 (Chapter 1, Section 1.7 and 1.8) produces janthitrems, and these tremorgenicity results strengthens the hypothesis that these compounds are responsible for the observed cases of ryegrass staggers on pastures infected with this endophyte.

5.2 Insect Testing of Janthitrem A and Janthitrem B

5.2.1 Introduction

Fungal metabolites such as tremorgenic mycotoxins are believed to act as chemical defence systems for the fungi which produce them, and subsequently protect the host from consumption by other organisms such as insects (Dowd et al., 1988). The mechanism of toxicity is not known.

Many mycotoxins, such as penitrems A–D and F, (Gonzalez et al., 2003), 10-oxo-11,33-dihydropenitrem B (Laakso et al., 1993), 6-bromopenitrem A (Hayashi, 1998; Hayashi et al., 1993) and sulphinines (Laakso et al., 1992) have been shown to have anti-insect properties. Endophyte-infected ryegrasses have also been shown to have anti-insect activity (Ball et al., 2006; Breen, 1994; Goldson et al., 2000; Jensen and Popay, 2004; Latch, 1993; Pennell et al., 2005; Popay and Mainland, 1991; Popay and Wyatt, 1995). For perennial ryegrass in New Zealand infected with the wild-type endophyte, peramine has been shown to be the major compound responsible for activity against Argentine stem weevil (*Listronotus bonariensis*) (Rowan and Gaynor, 1986) while ergovaline affects black beetle (Ball et al., 1997). For other insects such as pasture mealybug (*Balanococcus poae*), the alkaloid responsible for endophyte-mediated resistance is unknown.

Ryegrass containing the novel endophyte, AR37, although it produces neither peramine nor ergovaline, is as active against Argentine stem weevil (Popay and Wyatt, 1995), black beetle and pasture mealybug as ryegrass with the wild-type endophyte. It has also been shown to have very effective resistance to insect pests not normally affected by the wild-type endophyte, such as porina (*Wiseana cervinata*) (Jensen and Popay, 2004) and the root aphid (*Aploneura lentisci*) (Popay and Gerard, 2007) but the compounds responsible for this resistance are unknown. Since janthitrems are unique to AR37 it is possible that these compounds are involved with this anti-insect activity.

The anti-insect activities of janthitrem A, janthitrem B and paxilline were assessed along with endophyte-free ryegrass and ryegrass infected with AR37. The janthitrems were sourced during extraction and isolation of a *P. janthinellum* culture, strain E1 (Chapter 2, Section 2.2), whilst the paxilline was available from previous work conducted at AgResearch, Ruakura (Munday-Finch et al., 1996a). Insect testing was carried out on the insect porina (*Wiseana cervinata*) (Figure 5.11) which is a major pest of New Zealand pastures.



Figure 5.11. Porina (*Wiseana cervinata*) larva. Photo courtesy of AgResearch, Ruakura.

5.2.2 Stability of the Test Mycotoxins Janthitrem A, Janthitrem B and Paxilline in the Diets Prepared for the Insect Bioassay

For a test compound to be effectively evaluated it must survive the diet-making process and be stable long enough to determine its activity against the test insect. Due to the unstable nature of the janthitrems, experiments had to be carried out to ensure that these requirements were met.

Diets were prepared containing janthitrems A and B and paxilline using established methods (see Section 8.7.2). Sub-samples of the diets were taken immediately after preparation and then again after 24 hours at 15°C. All samples were frozen until they could be analysed. The frozen diet samples were freeze-dried to remove water and accurate dry-weights measured. The samples were then extracted and analysed by analytical HPLC using PDA detection at 247 nm. This wavelength was chosen as prior experience during stability trials (Chapter 2, Section 2.4) showed that janthitrems A and B and paxilline were all detectable at this wavelength. Details of the extraction procedure and HPLC method are outlined in the Experimental Chapter (Section 8.7.1).

Table 5.2. Mycotoxin recovered (as a percentage of that added) from diets at time zero and after 24 hours.

Mycotoxin	Mycotoxin in Diet (%) t = 0	Mycotoxin Remaining in Diet (%) t = 24
Janthitrem A	96.5	93.2
Janthitrem B	97.2	96.2
Paxilline	96.7	95.8

Results showed that janthitrem A, janthitrem B and paxilline survived the diet-making process and remained close to 100% over the 24 hour stability period (Table 5.2). The small observed differences of *ca.* 4–7% may in part be due to factors such as the compounds not being fully extracted during the extraction procedure or sample loss during transfer stages of the extraction. This experiment

proved that if diets were made daily, janthitrems A and B and paxilline were stable under the conditions of the insect trial.

The diets containing the ryegrass were not analysed since, as the pure janthitrems were found to be stable, it was believed that there would not be an issue with the ryegrass diets.

5.2.3 Preparation of the Diets for the Insect Bioassay

Diets were prepared for each of the nine treatments (Table 5.3) involving addition of either the test mycotoxin (Figure 5.12), AR37-infected ryegrass or endophyte-free ryegrass (details of the diet preparation are presented in Sections 8.7.2 and 8.7.3).

Treatments B–G involved addition of the test mycotoxin (janthitrem A, janthitrem B or paxilline) at two concentrations of 20 and 50 $\mu\text{g g}^{-1}$ (wet weight concentrations). The control diet (treatment A) was prepared by the addition of the carrier used for mycotoxin addition (100 μL DMSO).

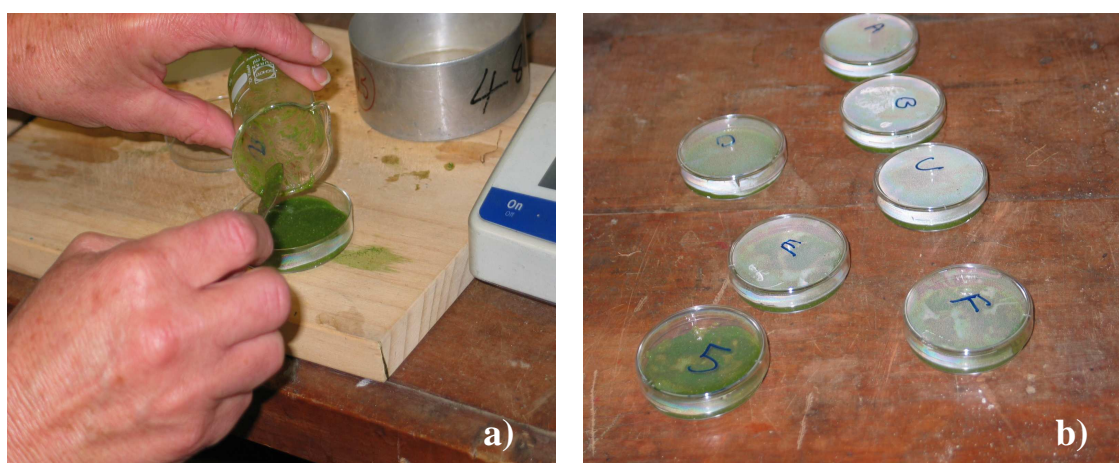


Figure 5.12. a) Transfer of the prepared diet with the test mycotoxin into a petri dish and b) allowing the prepared diets for each treatment to cool.

Table 5.3. Prepared bioassay diets with the test mycotoxin/ryegrass.

Insect Diet		Treatment Name	Concentration ($\mu\text{g g}^{-1}$)
Test Mycotoxin Included in Diet	No Mycotoxin (Control)	A	–
	Janthitrem A	B	20
		C	50
	Janthitrem B	D	20
		E	50
	Paxilline	F	20
		G	50
Ryegrass Included in Diet	Endophyte-free Ryegrass	H	–
	AR37 Infected Ryegrass	I	–

Over the treatment period (5 days), the mycotoxin diets were prepared fresh daily.

Two further treatments were also tested involving endophyte-free ryegrass or ryegrass infected with AR37 (Table 5.3). The diet was prepared in the same way as the mycotoxin diets, with the carrot and clover plant material in the latter replaced by the same weight of ryegrass. During the diet preparation, the ryegrass was blended with additional water (to ensure adequate mixing), some of which was later removed so that the same quantity of liquid was added to both diets. A previous experiment showed that this discarded solution had no bioactivity against porina (A.J. Popay, AgResearch Ruakura Ltd, Hamilton, New Zealand, personal communication, June 2008).

5.2.4 *Insect Bioassay*

The bioassay trial (performed by A.J. Popay, AgResearch Ruakura Ltd, Hamilton, New Zealand) was carried out using porina larvae. Porina were obtained from a

colony held in controlled environment rooms that had been reared from eggs. The porina larvae were all approximately four and a half months old but their weights at the commencement of the trial ranged between 75 and 637 mg. The larvae selected for each treatment were representative of the range of weights so that the average weight of the 12 larvae used in each treatment was similar (mean 250 mg; range 215 – 265 mg). Details of the bioassay trial are described in Section 8.7.4. The trial was carried out in a controlled environment room at 15°C, 16:8 light:dark regimen (Figure 5.13).



Figure 5.13. Specimen containers placed in a controlled environment room.

Larvae survival was 100% for the control, janthitrem B $50 \mu\text{g g}^{-1}$, paxilline $20 \mu\text{g g}^{-1}$ and in the AR37-infected ryegrass treatments. Two of the twelve larvae died in the janthitrem B $20 \mu\text{g g}^{-1}$ treatment (84% survival), while the remaining treatments (janthitrem A $20 \mu\text{g g}^{-1}$, $50 \mu\text{g g}^{-1}$, paxilline $50 \mu\text{g g}^{-1}$, endophyte-free ryegrass) had one larva die in each of them (92% survival).

Table 5.4 . Results of the insect bioassay.

Treatment	Porina Weight change (mg)	Percentage of Diet Eaten				
		Day 1	Day 2	Day 3	Day 4	Day 5
Control	13	81.3	80.9	75.4	66.6	76
Janthitrem A (20 $\mu\text{g g}^{-1}$)	-20.2	43.9	35.2	32.5	29.8	27.9
Janthitrem A (50 $\mu\text{g g}^{-1}$)	-17.6	41.1	30.7	29.5	23.5	26.4
Janthitrem B (20 $\mu\text{g g}^{-1}$)	5.6	70.8	60.7	60.4	49.1	32.9
Janthitrem B (50 $\mu\text{g g}^{-1}$)	-17.9	43.6	33.4	32.1	25.6	29.5
Paxilline (20 $\mu\text{g g}^{-1}$)	-11.8	48.9	35.4	37.5	31.8	35.9
Paxilline (50 $\mu\text{g g}^{-1}$)	-8.7	42.2	36.5	36.0	28.1	28.7
Endophyte-free Ryegrass (Control)	27.3	51.2	43.5	42.3	40.4	37.6
AR37-infected Ryegrass	1.2	20.4	19.7	12.4	9.9	8.7
<i>p</i>	<0.001	<0.001	<0.001	<0.001	<0.001	<0.001

With the exception of janthitrem B at 20 $\mu\text{g g}^{-1}$, all the mycotoxin treatments significantly reduced the weight of the porina in comparison to the control (Table 5.4, the *p* values represent the probability of a significant difference between the different treatments). Consistent with this change in weight was the reduction in diet consumption observed for the mycotoxin treatments (again with the exception of janthitrem B at 20 $\mu\text{g g}^{-1}$) compared to the control. For the janthitrem B treatment at 20 $\mu\text{g g}^{-1}$, it was not until day 5 that a significant reduction in diet consumption was observed. Statistical analysis was performed by A.J. Popay, AgResearch Ruakura Ltd, Hamilton, New Zealand.

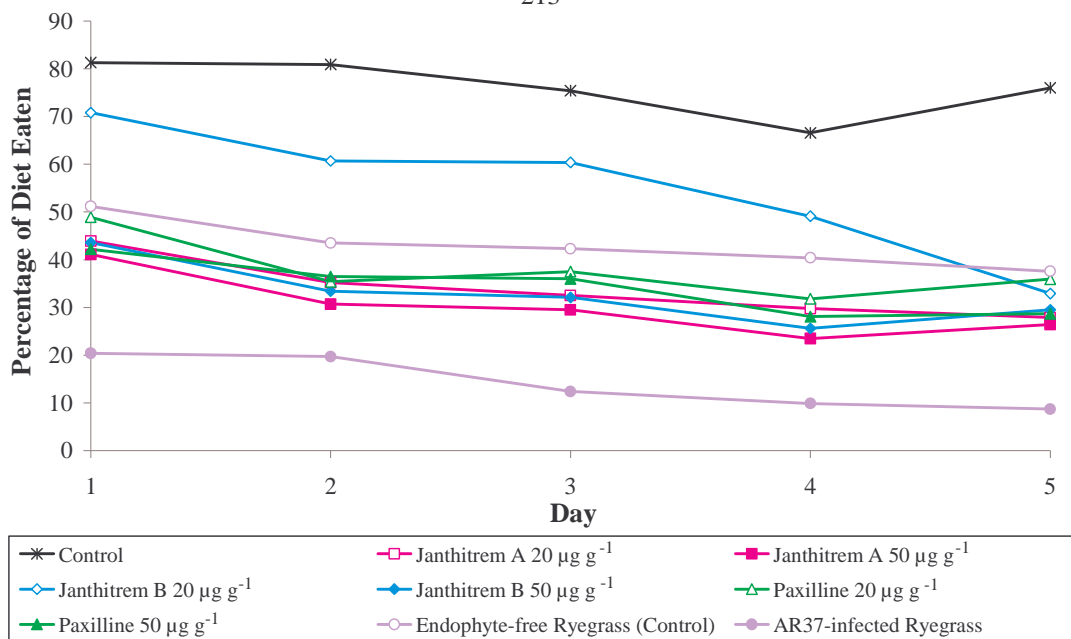


Figure 5.14. Percentage of diet eaten by the porina for each treatment.

Janthitrem A and paxilline had a similar effect on the weight of the porina and the percentage of diet eaten. For janthitrem B however, while the higher concentration gave a similar response to that observed for janthitrem A and paxilline, the lower concentration was less effective. This difference was reflected both in the lower weight loss of the porina and the fact that it took 4–5 days before a reduction in diet consumption was noted (Figure 5.14). Since the presence of an epoxide (janthitrem A) rather than a double bond (janthitrem B) is the only structural difference between these two compounds, the presence of this epoxide may promote greater anti-insect activity. Such a difference was also observed during the mouse bioassay investigation, where janthitrem A displayed greater tremorgenicity in comparison to janthitrem B. These results take on greater significance since the janthitremes present in the AR37 endophyte-infected grass are also 11,12-epoxides (like janthitrem A).

The AR37 ryegrass diet resulted in a significantly reduced weight gain and diet consumption of the larvae compared to the endophyte-free ryegrass (Table 5.4 and Figure 5.14), suggesting the endophyte has deterrent properties. Complete deterrence was not observed as some consumption of AR37-infected ryegrass did occur. These findings were in accordance with a study carried out by Jensen and

Popay (2004) which showed fewer tillers damaged by porina larvae in the AR37-infected ryegrass and decreased growth and survival on AR37-infected ryegrass. In a 6 week experimental trial carried out by Jensen and Popay (2004), only 5% of porina survived on AR37-infected ryegrass compared to 95% for the endophyte-free ryegrass (this trial was 5 weeks longer in duration than our present study). Therefore the effect on insects of AR37-infected ryegrass may be due to both toxicity and deterrence, as decreased growth and decreased survival of porina larvae were observed as well as a reduction in the consumption of the grass.

A direct comparison of the effects of AR37 ryegrass with the mycotoxins is not possible because of the differences in diet composition. However, relative to their respective controls, the weight change of larvae on AR37 diet (26.1 mg) was similar to that on the mycotoxin diets (averages of 31.9, 19.2 and 23.3 mg for janthitrem A, janthitrem B and paxilline respectively). In addition, the percent reduction in diet consumption compared with controls was also comparable (average of 58, 43, 53 and 66% for janthitrem A, janthitrem B, paxilline and AR37 ryegrass respectively). Thus, effects of the mycotoxins on porina were similar to the effects of the AR37 ryegrass on porina. This suggests that the janthitrems in AR37 may be responsible for the detrimental activity of this endophyte on porina.

5.2.5 Summary of Findings

The mycotoxins janthitrem A, janthitrem B and paxilline were found to be deterrent to porina feeding, with janthitrem B being less deterrent at the lower concentration compared to janthitrem A and paxilline. The change in weight of the larvae is most likely due to deterrence, but could also indicate toxicity, particularly as there was substantial weight loss of larvae despite some consumption of diet. Further testing of some structurally related non-tremorgenic compounds could be carried out to determine whether tremorgenicity and anti-insect activity are linked.

CHAPTER SIX

Analysis of Mouldy Walnuts

6.1 Introduction

The presence of tremorgenic mycotoxins in mouldy walnuts was investigated after a dog was found to exhibit tremors upon consumption of the walnuts. A one year old Labrador-cross dog was observed to vomit three hours after ingestion of the aforementioned walnuts. Over the following hour the dog became progressively incoordinated and developed marked tremors. Upon examination by the veterinarian, the dog was observed to have severe generalised tremors, elevated temperature, marked ataxia, hyperaesthesia and mild hypersalivation. The dog was treated by inducing vomiting, administering an IV of lactated Ringer's solution (to reduce temperature), administering an IV injection of diazepam and administering activated charcoal orally. Diazepam initially controlled the muscle tremors, but after six hours, tremors were again detectable and after a further four hours, an additional dose of diazepam was administered. Eighteen hours after examination by the veterinarian and eight hours after receiving the last diazepam treatment, tremors were no longer observed.

The veterinarian tentatively diagnosed the dog's condition as tremorgenic mycotoxicosis. Intoxication of dogs by tremorgenic mycotoxins has been previously reported (Arp and Richard, 1979; Boysen et al., 2002; Hocking et al., 1988; Naude et al., 2002; Richard et al., 1981; Walter, 2002; Young et al., 2003). The majority of these cases were from North America (Arp and Richard, 1979; Richard et al., 1981; Boysen et al., 2002; Walter, 2002; Young et al., 2003) with

one case reported in Australia (Hocking et al., 1988) and one in South Africa (Naude et al., 2002).

The first reported case of canine tremorgenic mycotoxicosis involved intoxication of a dog after ingestion of mouldy cream cheese (Arp and Richard, 1979). The fungus *P. crustosum* and the mycotoxin penitrem A were isolated from the cream cheese. A few years later, intoxication of two dogs after consumption of mouldy walnuts was reported (Richard et al., 1981). *P. crustosum* and penitrem A were isolated from the mouldy walnuts. In 1988, a dog developed severe muscle tremors after consumption of a mouldy hamburger bun (Hocking et al., 1988). Analysis of the remaining portion of the hamburger bun led to the subsequent isolation of *P. crustosum* and penitrem A as well as trace amounts of other penitrem compounds.

The remaining four accounts of canine tremorgenic mycotoxicosis were reported over a decade later. These cases involved nine dogs which were observed to develop clinical symptoms after ingestion of unspecified garbage (Walter, 2002), compost (Boysen et al., 2002), mouldy cream cheese (Young et al., 2003) and rice (Naude et al., 2002). In all of the other cases, the mycotoxins penitrem A and roquefortine C were identified in the contaminated source, with the exception of the case reported by Naude et al. (2002) where the fungus and mycotoxin were isolated from the rice vomitus.

In this investigation, the walnuts the dog had consumed (which had fallen from a tree on the owner's property) were mouldy and had been lying on the ground for approximately five months. The dog also had access to a compost bin in the garden. The source of the tremorgenic mycotoxins was therefore believed to be either the walnuts or the compost.

Although canine tremorgenic mycotoxicosis has been previously reported due to consumption of mouldy compost (Boysen et al., 2002), this was considered less likely to be the cause in the present case because there was no evidence of compost in the vomit. In contrast, examination of the vomit by the owner revealed an unidentified brown material, suggestive of walnuts. Therefore the clinical symptoms and history in this case were considered by the veterinarian as most suggestive of intoxication, most likely with tremorgenic mycotoxins from the mouldy walnuts. To allow the source to be confirmed, the walnuts were analysed for the presence of mycotoxins. Fungi were also isolated from the walnuts, grown in culture, and analysed for mycotoxins.

6.2 Identification of the Fungus from the Mouldy Walnuts

The fallen mouldy walnuts (Figure 6.1) were collected by the dog's owner from the ground in areas that the dog had access to.



Figure 6.1. The collected mouldy walnuts.

The walnuts had fragile or broken shells, and kernels coated with amorphous brown material. The walnuts were visibly mouldy as fragments of fungal hyphae and numerous subglobose hyaline spores approximately 3 μm in diameter were observed on direct examination. The fungi from fragments of the mouldy walnuts were cultured by a mycologist (as described in Section 8.8.1). The fungus, *P. crustosum* (strain 21143), was isolated and deposited in the International Collection of Micro-organisms from Plants, Landcare Research, Auckland. A culture of this *P. crustosum* strain 21143 was prepared for chemical examination (Figure 6.2). Experimental details of the extraction of toxins from the culture and mouldy walnuts are presented in Section 8.8.2.

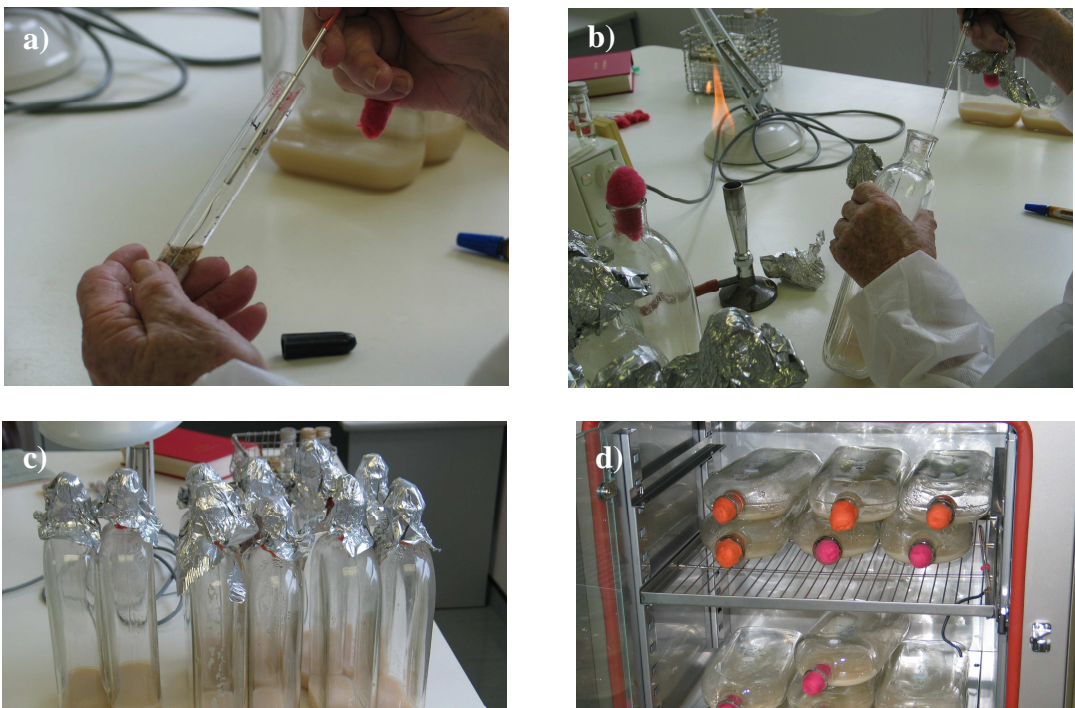


Figure 6.2. a) Extraction of the fungus. b) Inoculation of the media with the fungus. c) The inoculated culture flasks. d) Incubation of the cultures.

The resulting heavy growth of blue–green fungal colonies was identified by a mycologist to be *P. crustosum* Thom (Pitt, 1979). This fungal species has also been reported as *Penicillium cyclopium* and *Penicillium palitans* (as described in Chapter 1, Section 1.4.1). *P. crustosum* is a food-bourne fungal species that has been isolated from foods such as nuts, meat, cheese and vegetables (Sonjak et al.,

2005). Virtually all isolates of *P. crustosum* produce penitrems (Pitt, 1979). As mentioned earlier in this section, canine tremorgenic mycotoxicosis has been previously reported. However, this condition is rare with only 13 dogs known to have suffered from this intoxication (Arp and Richard, 1979; Boysen et al., 2002; Hocking et al., 1988; Naude et al., 2002; Richard et al., 1981; Walter, 2002; Young et al., 2003). In each of these cases where fungal cultures were isolated, *P. crustosum* was identified.

6.3 LC–UV–MS Analysis of the Mouldy Walnuts and *P. crustosum* Extracts

LC–UV–MS analysis was performed with an LCQ Advantage mass spectrometer fitted with an APCI source. Quantitation was performed by integration of peaks in the UV absorbance chromatograms obtained from the PDA at 296 nm. Results from sequential extractions were combined to determine total concentrations. The samples were quantitated against standards prepared from an accurately weighed specimen of penitrem A. Details of the LC–UV–MS method are described in Section 8.8.3.

6.3.1 LC–UV–MS Method Validation

The LC–UV–MS method was validated by evaluating the parameters of linearity, accuracy and precision (refer to Section 8.8.4 for experimental details). The data was analysed to determine whether a linear relationship existed between the concentration of penitrem A and peak area over a range of concentrations. Concentrations were used which could feasibly be present in actual samples. A straight line relationship was found for five concentrations of penitrem A (2, 5, 10, 20 and 50 $\mu\text{g mL}^{-1}$), indicating that the peak area was proportional to the concentration (Figures 6.3 and 6.4).

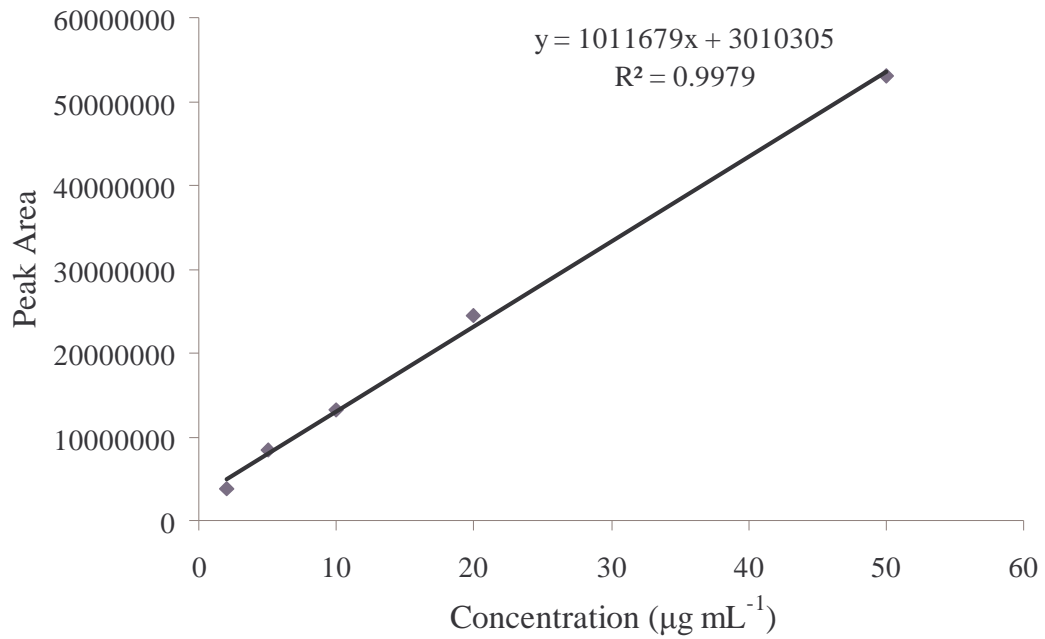


Figure 6.3. Calibration curve for five penitrem A standards obtained from the mass spectrometer (using an APCI source). The error bars representing the relative standard deviation are too small to be visible.

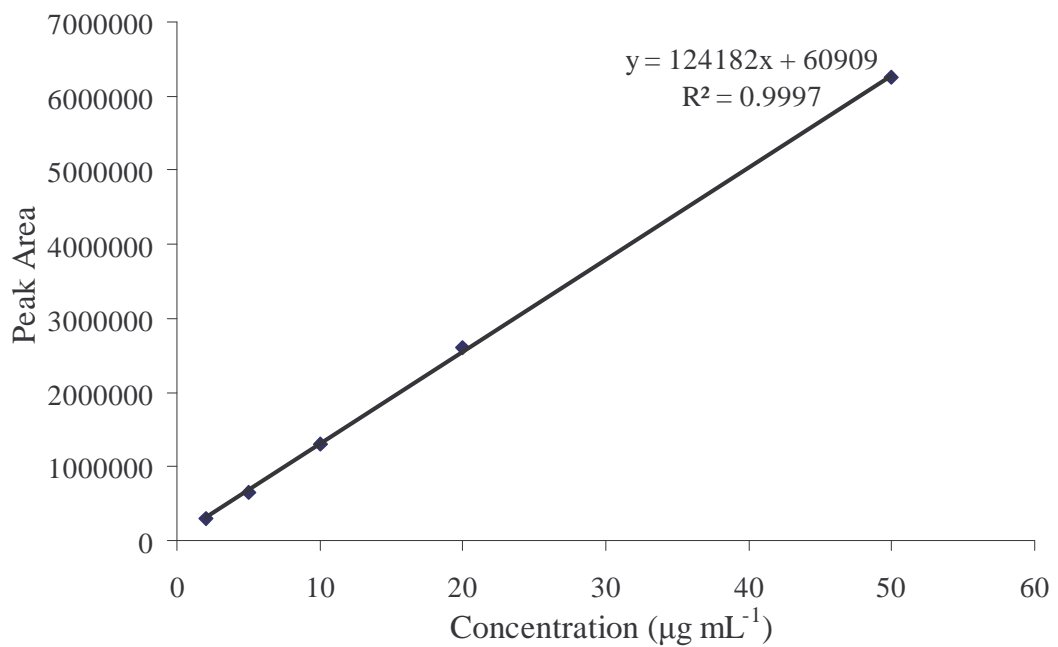


Figure 6.4. Calibration curve for five penitrem A standards obtained from the PDA (at 296 nm). The error bars representing the relative standard deviation are too small to be visible.

In order for the calibration curve to be acceptable, the R^2 value should be greater than or equal to 0.995 (Delmulle et al., 2006). The mass spectrometer and PDA calibration curves for penitrem A gave R^2 values of 0.9979 (Figure 6.3) and 0.9997 (Figure 6.4) respectively, both of which are above the required 0.995, and therefore acceptable calibration curves.

The PDA (at 296 nm) was chosen for quantification of penitrem A in this study, since the R^2 value was closer to 1, indicating a more linear relationship. Furthermore, when using mass spectrometry for quantitative analysis, the effect of ionisation suppression by matrix components must be considered. It has been reported that LC–MS or MS analysis of penitrem standards needs to be carried out in the same matrix as that used for samples since this has an effect on the peak area and peak height. For example a 40% reduction in peak height and area was observed by Rundberget and Wilkins (2002b) when MS analysis of penitrem A standards was carried out in the matrix as opposed to the mobile phase. This was attributed to suppression of ionisation by components in the matrix (Rundberget and Wilkins, 2002b). In addition to matrix effects, the tendency of compounds to produce fragment ions, can also reduce the sensitivity of the method, thus giving a higher detection limit.

To further validate the developed analytical method, the reproducibility of the calibration curve was assessed on three different days. This showed that the analytical method was reliable since the three calibration curves agreed within error. The method was also shown to be accurate and precise since the concentration obtained from the calibration curve (the graph plotted when testing the linearity, Figure 6.4) corresponded to the actual concentrations tested (4, 15 and 34 $\mu\text{g mL}^{-1}$) with a low percentage relative standard deviation (Table 6.1).

Table 6.1. Comparison of the reference concentration and the average experimental concentration for penitrem A.

Reference Concentration ($\mu\text{g mL}^{-1}$)	Average Concentration ($\mu\text{g mL}^{-1}$) (Determined from the Calibration Curve)	% Relative Standard Deviation
4	4.06	0.40
15	15.10	0.46
34	33.66	0.34

6.3.2 LC–UV–MS Identification of the Penitrems and Roquefortine C in the Mouldy Walnuts and *P. crustosum* Extracts

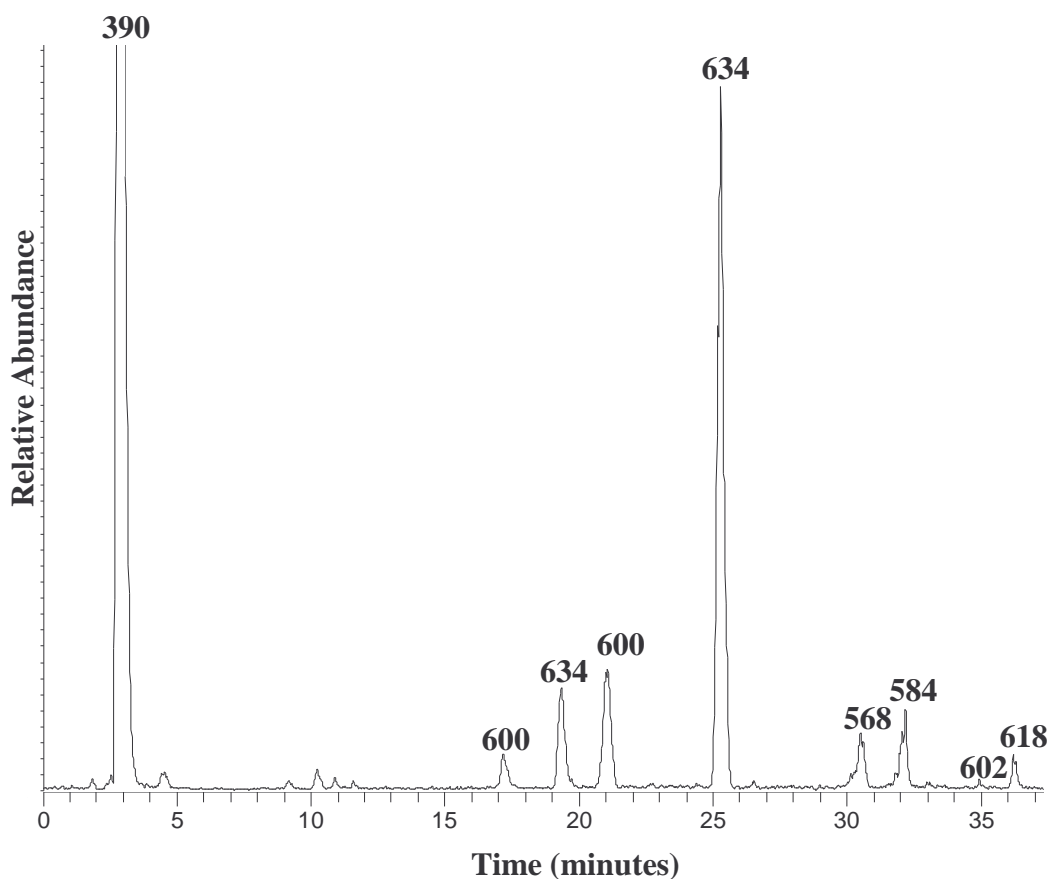


Figure 6.5. LC–MS chromatogram of *P. crustosum*. Values of m/z for $[M+H]^+$ are given above their corresponding peaks.

LC–UV–MS analysis of the extracts of both the *P. crustosum* culture, strain 21143 (Figure 6.5), and the mouldy walnuts (Figure 6.6) revealed the presence of

a number of peaks in each chromatogram. Similar peaks were observed in both the walnuts and culture, although differences were also evident, with the walnuts giving rise to more compounds than the culture, as discussed later in this section.

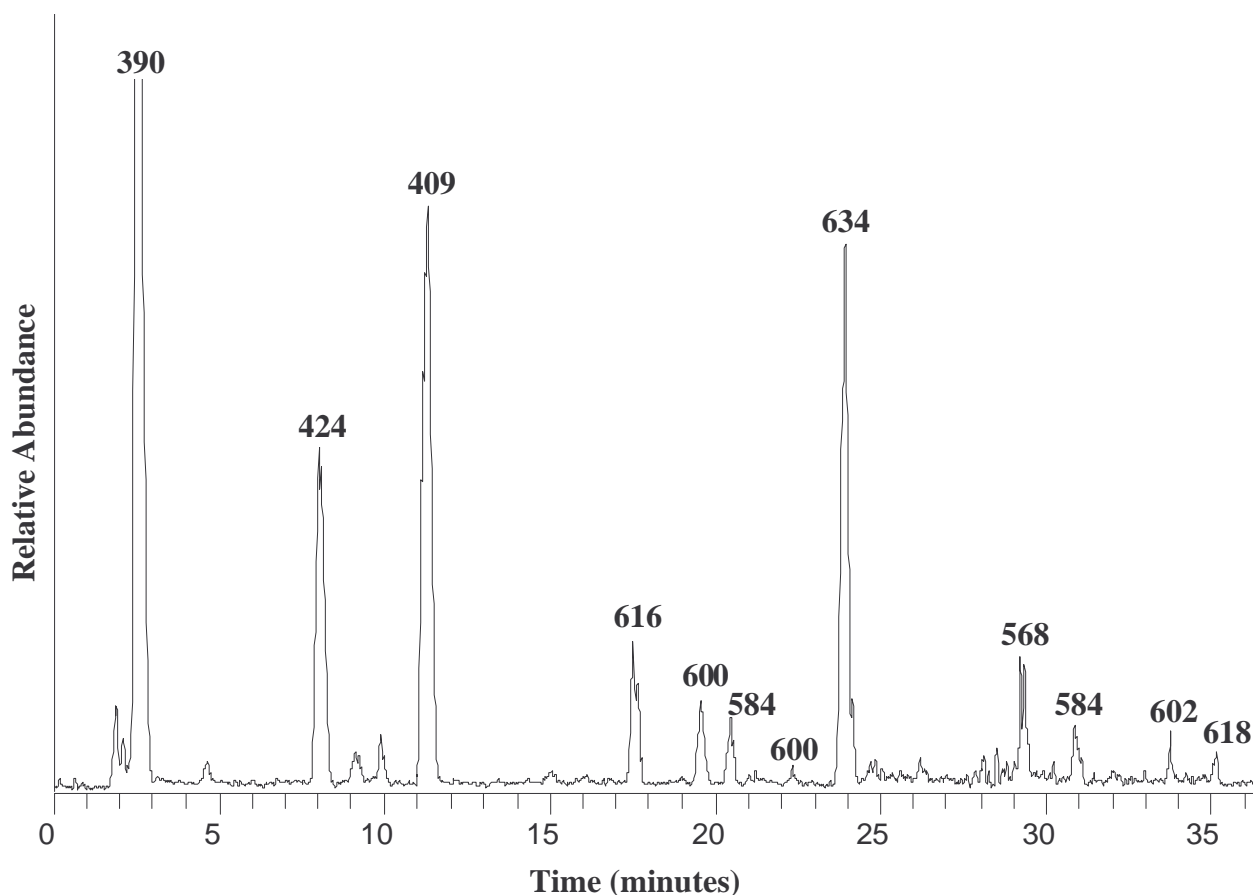


Figure 6.6. LC-MS chromatogram of the mouldy walnut extract. Values of m/z for $[M+H]^+$ are given above their corresponding peaks.

The peak giving an m/z value of 634, eluting at approximately 24 minutes (Figure 6.6), is attributable to penitrem A based on comparison of its retention time, mass spectrum, mass spectral fragmentation (Figures 6.7, 6.8 and 6.9), and UV spectrum (Figure 6.10) with those of an authentic specimen of penitrem A.

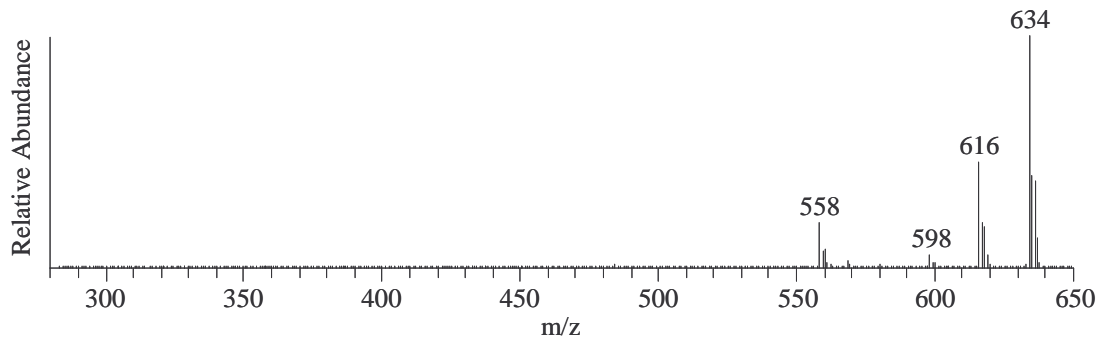


Figure 6.7. Full scan of penitrem A peak from *P. crustosum*. Values of m/z for major ions observed are given.

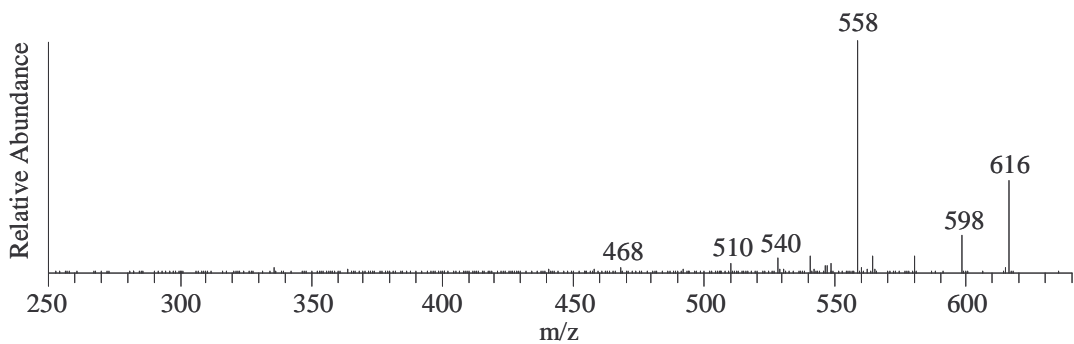


Figure 6.8. MS^2 (m/z 634) spectrum of penitrem A peak from *P. crustosum*. Values of m/z for major ions observed are given.

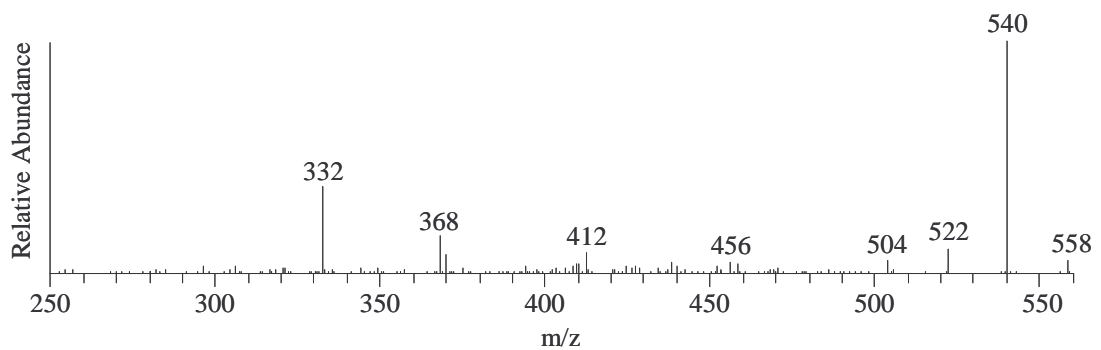


Figure 6.9. MS^3 (m/z 634 \rightarrow 558) spectrum of penitrem A peak from *P. crustosum*. Values of m/z for major ions observed are given.

The UV spectrum of penitrem A exhibits UV absorption maxima at 235 and 296 nm (Figure 6.10). The absorption maximum at 235 nm is much greater in magnitude than the absorption maximum at 296 nm, which if used as the detecting wavelength would allow greater sensitivity. Despite this, 296 nm was chosen as the detecting wavelength to quantify the penitrems as fewer compounds interfere at this wavelength. Although the sensitivity is lower at this wavelength, it still allows sufficient sensitivity to detect small quantities of penitrems.

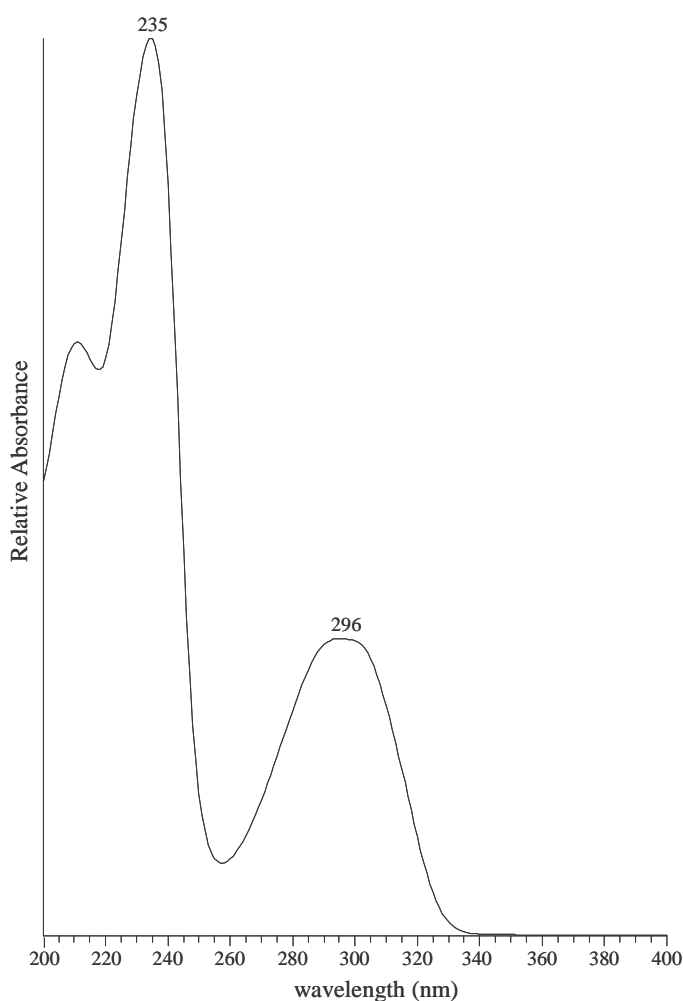


Figure 6.10. UV absorbance spectrum of penitrem A.

Peaks with mass and UV spectral properties consistent with penitrems B–F and roquefortine C were also observed in chromatograms of extracts of *P. crustosum* strain 21143 and the mouldy walnuts. The retention times and spectral properties of these peaks were found to be identical to those observed for penitrems B–F and

roquefortine C in an extract of a well characterised strain of *P. crustosum* (Rundberget et al., 2004a), and are in accord with chromatographic analysis for penitrems (Maes et al., 1982) and for roquefortine C (Tor et al., 2006).

6.3.3 LC–UV–MS Quantitation of Penitrems in Mouldy Walnuts and *P. crustosum* Extracts

The penitrem levels in the mouldy walnuts and the culture were quantitated by LC–UV–MS against the calibration curve at 296 nm (Figure 6.4). Penitrem A was the major penitrem in both the fungal culture (138 mg L⁻¹) and the mouldy walnuts (26.5 mg kg⁻¹). Assuming the response factors for penitrems B–F were the same as that of the penitrem A standard, the total amount of penitrems A–F in the walnuts and *P. crustosum* strain 21143 were estimated to be 36.4 mg kg⁻¹ and 171 mg L⁻¹, respectively. The concentration of roquefortine C, which has been described as a paralytic agent but has no definitive reported tremorgenic activity (Naude et al., 2002), was not determined.

Penitrem A is the most commonly identified canine tremorgenic mycotoxin and this toxin is produced by *P. crustosum* (Arp and Richard, 1979; Hocking et al., 1988; Naude et al., 2002; Richard et al., 1981; Walter, 2002; Young et al., 2003). For both the culture and the mouldy walnuts, penitrem A was the major penitrem present, followed by penitrem F (Table 6.2). Some differences in penitrem abundancies were evident. For example, penitrem C was the least abundant penitrem in the fungal culture compared to penitrem B in the mouldy walnuts. The variation in production of metabolites may be influenced by factors such as the substrate involved, water activity (a measure of how pure the water is for microbial growth), temperature and pH (di Menna et al., 1986; Hou et al., 1971; Rundberget et al., 2004b). Water activity is believed to influence penitrem production, where a decrease in water activity leads to a decrease in penitrem A production (ICMSF, 1996; Rundberget et al., 2004b). The mouldy walnuts and

culture had differing substrates, therefore the medium the culture was grown on may give conditions which favour production of penitrems which differ from that observed with the walnuts. In addition, the variation in abundance may also be due to different extraction efficiencies of the penitrems from the two different substrates.

Table 6.2. Comparison of penitrem production in the mouldy walnuts and *P. crustosum* extracts.

	Penitrems Detected in Descending Order of Abundance					
Culture	A	F	E	D	B	C
Walnuts	A	F	C	D	E	B

The production of penitrems (in culture and as contaminants in food such as walnuts) reported in the literature is mainly in accordance with the results obtained in this study, where penitrem A was predominately the major penitrem (Hocking et al., 1988; Rundberget et al., 2004b).

Of all other reported cases of canine tremorgenic mycotoxicosis, the report by Hocking et al. (1988) is the only one in which penitrem A is quantified in the contaminated source. In this case a Siberian husky dog developed severe muscle tremors after ingestion of a mouldy hamburger bun (Hocking et al., 1988). *P. crustosum* was isolated from the hamburger bun and penitrems were found to be produced. The amount of penitrem A in the hamburger bun was found to be 35 mg kg⁻¹ (the remaining penitrem compounds were not quantified) compared to the 26.5 mg kg⁻¹ found in the walnuts. The greater level of penitrem A in the hamburger bun may explain the greater severity of symptoms in the dog which consumed the hamburger bun. The dog which had consumed the mouldy hamburger bun did not fully recover until after 2 weeks compared to 18 hours for the dog investigated in this study which had consumed the mouldy walnuts (both dogs were treated for their symptoms). However, the absolute quantities of penitrems consumed by the dogs cannot be compared. Furthermore, direct

comparison is impossible due to the different breeds of dog, possible difference in size between the dogs, and the different duration and methods of treatments.

6.3.4 LC–UV–MS Identification of Additional Metabolites Detected in the Mouldy Walnuts and *P. crustosum* Extracts

In addition to the peaks correlating to penitrems A–F, further peaks with m/z values of 600, 584, 616, 409 and 424 were observed in the walnut extracts but not the *P. crustosum* culture.

The ions at m/z 600, 584 and 616 are consistent with the $[M+H]^+$ for penitremones A, B and C, respectively. The penitremones (10-keto-11,33-dihydro-variants of the penitrem indole–diterpenoid skeleton) were identified by Naik et al. (1995) from a *P. crustosum* species that readily produces penitrem A. The UV spectra of the walnut compounds were slightly different to those reported for the penitremones. Penitremones A–C have UV absorption maxima at 260 and 280 nm (Naik et al., 1995) compared to the 255 and 280 nm absorption maxima which were observed in this study. These compounds were not observed in the culture extracts investigated in this research. The reason why these compounds were detected in the walnuts but not the culture is not known.

The compounds which afforded $[M+H]^+$ ions at m/z 409 and 424 remain unidentified. The relative intensity of the peaks of these compounds was quite high. These compounds were not detected in the culture of *P. crustosum* and the molecular weights did not correlate to any other reported metabolites produced by *P. crustosum*. These compounds may therefore originate from the walnut matrix. To investigate this further, walnuts uninfected by *P. crustosum* could be extracted and analysed.

In the culture extract, additional peaks corresponding to m/z 634 and 600 (at retention times differing to those observed in the walnuts) were observed. These peaks were tentatively assigned as thomitrem A and E, respectively, based on comparison of the observed molecular weights and UV spectra with those reported by Rundberget and Wilkins (2002a). These compounds were not detected in the walnut extract, which suggests that the culture growth conditions may have favoured the production of these compounds.

6.4 Summary of Findings

A definitive diagnosis of tremorgenic mycotoxicosis requires identification of mycotoxins in the serum, urine or vomit from the affected dog. Methods for identifying penitrem A in food (Braselton and Johnson, 2003), vomit (Braselton and Johnson, 2003), serum (Tor et al., 2006) and urine (Tor et al., 2006) have been published. However, these tests are not routinely available in New Zealand and due to the delay and expense which would be involved, are not readily an option for New Zealand veterinarians in clinical situations.

In conclusion, the findings of this research support the diagnosis of tremorgenic mycotoxicosis made by the veterinarian, as the tremorgenic mycotoxins, penitrem A–F, were found in mouldy walnuts from the same location as those the dog had consumed. This is the first reported case of tremorgenic canine mycotoxicosis in New Zealand. A full account of this investigation has been published in the New Zealand Veterinary Journal (refer to Appendix 1).

CHAPTER SEVEN

Summary and Conclusions

7.1 Screening of Cultures

Analysis of a series of extracted *P. janthinellum* cultures (obtained from three different sources as described in Section 2.1) by LC–UV–MS showed the presence of janthitrems in the majority of the strains. Strains E1 and 5674 contained the highest quantities of janthitrem B and other janthitrem-related compounds. Instead of janthitrems, LC–UV–MS analysis revealed the presence of penitrem A in two of the *P. janthinellum* strains, E2 and E3. In addition, the E2 strain also produced penitrems B–F and roquefortine C. The production of penitrems by some *P. janthinellum* strains has previously been tentatively identified by di Menna et al. (1986) on the basis of HPLC. This tentative report, however, can now be confirmed on the basis of comprehensive LC–UV–MS analysis.

7.2 Isolation and Structure Elucidation of Janthitrems A and B

A reliable, rapid and efficient method for the extraction and isolation of janthitrem B from a *P. janthinellum* culture (strain E1) on a preparative scale has now been developed. The extraction and isolation processes were optimised to obtain the compounds of interest in a relatively short period of time – approximately 6 mg of janthitrem B from 900 mL of fungal culture in 2 days. This method can now be

conducted routinely, allowing the ready availability of janthitrem B whenever necessary.

Detailed analyses of the isolated compound by one- and two-dimensional NMR (^1H , ^{13}C , DEPT-135, COSY, TOCSY, HSQC, HMBC and NOESY) and HRMS showed it to be consistent with the structure of janthitrem B. Signal assignments for janthitrem B were compared to those previously reported for this compound (Wilkins et al., 1992) which showed that some revisions of the original assignments (H-14, H-16, H-39 and H-40) were necessary.

During the isolation of janthitrem B, a further janthitrem was also isolated. One- and two-dimensional NMR experiments (including ^1H , ^{13}C , DEPT-135, COSY, TOCSY, NOESY, HSQC, and HMBC spectra), HRMS, UV and fluorescence data and LC–UV–MS fragmentation patterns (in negative ion) led to the identification of this compound, revealing it to be 11,12-epoxyjanthitrem B.

11,12-Epoxyjanthitrem B appears to correspond to the partially characterised janthitrem A (identical molecular weights and characteristic UV absorbance spectra) previously detected in extracts of the same strain of *P. janthinellum* culture (Gallagher et al., 1980a). At the time however, Gallagher et al. (1980a) were not able to determine the structure of the compound they designated as janthitrem A and since no further information regarding janthitrem A has been reported, it is impossible to definitively associate a subsequently obtained structure with their compound. Consequently it was proposed that the trivial name janthitrem A be given to the 11,12-epoxyjanthitrem B based on the belief that Gallagher et al.'s (1980a) janthitrem A is likely to have been 11,12-epoxyjanthitrem B.

NMR data for janthitrem A was consistent with the proposed NMR assignment revisions for janthitrem B. Previously no structure has been reported for

janthitrem A, and due to its structural similarity with the commercially important epoxyjanthitrem, the isolation of this compound is important for use as a model compound.

7.3 Isolation and Structure Elucidation of Janthitrem C and D

LC–UV–MS analysis of E1 fungal culture extracts also showed the presence of a further two unknown janthitrem compounds. These compounds were targeted using an additional preparative scale culture that was extracted and isolated using a method based on that utilised during the purification of janthitrem A and B, leading to the isolation of janthitrem C and D. Initial NMR analysis indicated that the isolated janthitrem C and janthitrem D samples were not completely pure. However, due to the stability issues surrounding janthitrem, further NMR analysis was performed on these impure samples to enable their structures to be determined prior to any additional purification attempts which would risk decomposition of the compounds.

One- and two-dimensional NMR spectroscopy (including ^1H , ^{13}C , DEPT-135, COSY, TOCSY, NOESY, HSQC, and HMBC spectra), HRMS, UV and fluorescence data and LC–UV–MS fragmentation patterns (in negative ion) led to the elucidation of the structures of janthitrem C and 11,12-epoxyjanthitrem C. NMR assignments were made on the basis of comparison with data already attained for janthitrem A and B and with that already published for janthitrem C (Penn et al., 1993). NMR data attained for janthitrem C showed that some revisions of the original assignments (C-25, C-37, C-38, C-40, H-5, H-14, H-15, H-16, H-25, H-26, H-35, H-37 and H-38) were necessary.

Janthitrem D was proposed as the trivial name for the janthitrem C epoxide (11,12-epoxyjanthitrem C). Janthitrem D was originally named in the literature

based on its characteristic janthitrem-like UV absorbance spectrum, however, a structure for the compound was not reported (Lauren and Gallagher, 1982) and since there is no further information regarding janthitrem D it is impossible to definitively associate a subsequently obtained structure with their compound. Therefore it was proposed that the janthitrem C epoxide be given the trivial name, janthitrem D.

As with janthitrem A, no structure had previously been reported for janthitrem D. The structure proposed for janthitrem D was also similar in structure to the commercially important epoxyjanthitremes. The isolation of compounds similar to the epoxyjanthitremes is important for use as model compounds.

7.4 Janthitremes Structural Inter-Relationship

On the basis of the structures elucidated for janthitremes A and D, a diagram depicting the inter-relationships between the janthitrem structures can be proposed (Figure 7.1). The two distinct janthitrem groups (janthitremes E–G and janthitremes A–D) differ by a dehydrated terminal isoprene unit (Figure 7.2).

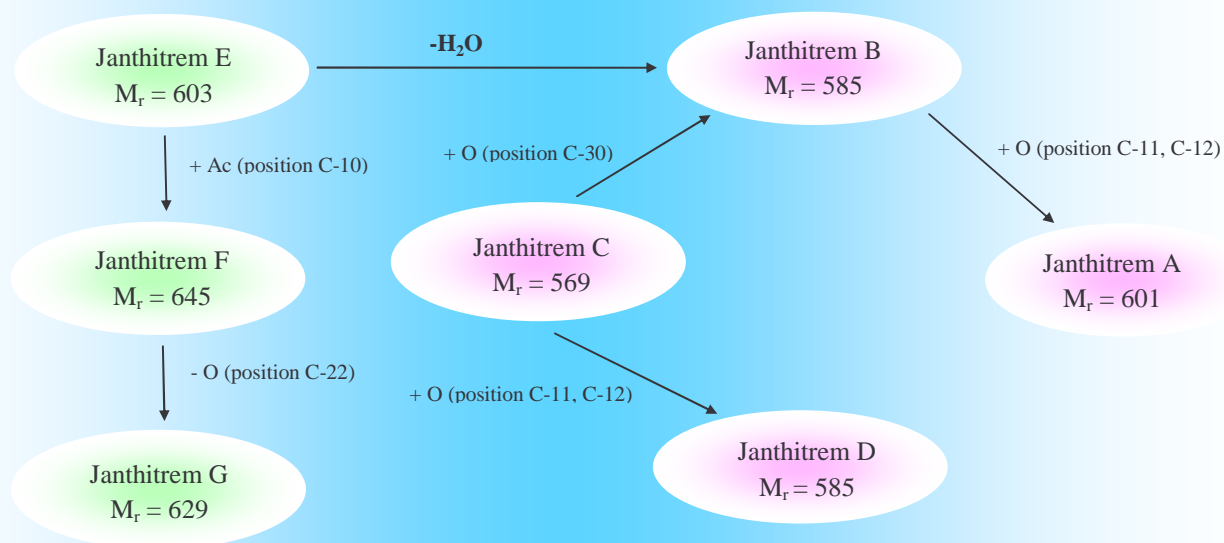
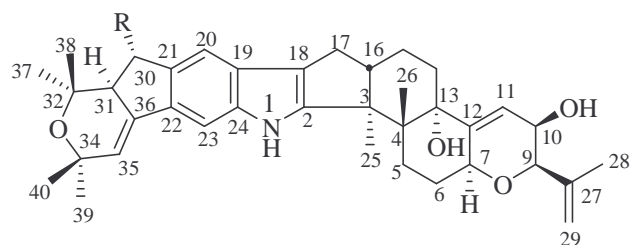
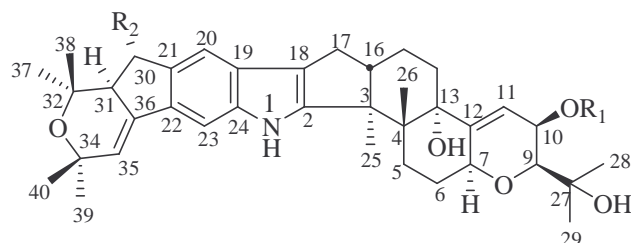
P. janthinellum (type Jan E-G)*P. janthinellum* (type Jan A-D)

Figure 7.1. The structural inter-relationship between the janthitrems.



Janthitrem A	R = OH	C-11,12-epoxide
Janthitrem B	R = OH	
Janthitrem C	R = H	
Janthitrem D	R = H	C-11,12-epoxide



Janthitrem E	R ₁ = H	R ₂ = OH
Janthitrem F	R ₁ = COCH ₃	R ₂ = OH
Janthitrem G	R ₁ = COCH ₃	R ₂ = H

Figure 7.2. Structure of janthitrems A–G.

7.5 Stability of Janthitrem B

Stability testing on janthitrem B identified conditions which would provide a lower risk of janthitrem degradation. Janthitrem B samples were stored using eight different conditions, which allowed the effect of solvent, storage temperature and light to be assessed. The extent of degradation observed varied widely between the different conditions, from as high as 29% degradation to as low as 7% degradation. The least favourable storage condition was that in methanol at room temperature, which lost approximately 29% of janthitrem B over 300 days. The optimum condition for the storage of janthitrem B was dry at -80°C , which only lost approximately 7% over 300 days. Janthitrem B exhibited greater stability in acetone (15% degradation) compared to methanol (29% degradation), therefore all subsequent handling of janthitrem B was carried out using acetone wherever possible.

Details from this experiment provided practical information on how to handle janthitrem B and minimise loss of sample. The information from these trials will be invaluable for future experiments involving janthitrem B, particularly for extractions from endophyte-infected grasses since previous isolation attempts of janthitrem B from herbage and seed have been severely hindered by instability and decomposition.

7.6 Bioactivity of Janthitrem B

7.6.1 Mice Testing

Two of the isolated janthitrem B, janthitrem A and janthitrem B, were assessed for bioactivity using mice. The compounds were administered to mice intraperitoneally and their tremorgenicity and effect on blood pressure, heart rate and motor control/balance monitored over 24 hours. While the tremorgenicity of janthitrem B has been previously assessed, this is the first time an

epoxyjanthitrem (janthitrem A) has been assessed, and it is the first time that blood pressure, heart rate and motor control have been included in the study of janthitrem. This investigation revealed that both janthitrem A and janthitrem B are tremorgenic to mice. The results showed that janthitrem A induced more severe tremors in comparison to janthitrem B and had a slightly longer time-course of action.

Janthitrem A and janthitrem B also induced a marked and immediate drop in the heart rate of mice. This effect showed a similar time course of action to that observed for tremor, with the heart rate of mice returning to normal within 7 hours. Although the effect on heart rate induced by janthitrem A and B was similar, janthitrem A was more potent than janthitrem B since it was administered at a lower dose rate. No significant effect of janthitrem on the blood pressure of mice was observed.

Janthitrem A and B also induced a significant effect on the motor control of mice which was especially pronounced within the first hour post-injection. The mice dosed with janthitrem B returned to their normal rotarod scores within 6 hours. In contrast, however, the mice given janthitrem A were not observed to return normal measurements until after 8 hours. Consequently it can be concluded that janthitrem A has a longer lasting effect on motor control than janthitrem B.

The novel endophyte AR37, (Chapter 1, Section 1.7 and 1.8) is known to produce janthitrem, and sporadic cases of staggers have been observed in animals grazing pastures containing this endophyte type. These studies conclusively show that janthitrem is tremorgenic and furthermore, that those containing a C-11, C-12 epoxide (such as those associated with AR37) appear to be of higher potency. This suggests that the cases of ryegrass staggers observed with ryegrass pastures infected with the endophyte AR37 may very well be due to the presence of epoxyjanthitrem.

7.6.2 *Insect Testing*

Insect testing was carried out using porina larvae (*Wiseana cervinata*). Three compounds were tested on the insects: janthitrem A, janthitrem B and paxilline, in conjunction with a control. Two further treatments were also tested: endophyte-free ryegrass and AR37 endophyte-infected ryegrass. The results from this trial indicate that the diets treated with janthitrem A, janthitrem B and paxilline displayed anti-insect activity, as the porina exhibited a reluctance to consume any diets treated with these compounds. This is the first time pure janthitrems have been tested on insects.

The results from the insect trial also confirmed that AR37 shows very promising insect resistance, and that the insect resistance displayed by AR37 may be related to the presence of janthitrems. The AR37-infected ryegrass resulted in reduced consumption by porina, in comparison to the endophyte-free ryegrass. This indicated that the endophyte may have deterrent properties and since decreased growth and survival of the porina larvae were also observed, inferences can be made that the anti-insect effects of AR37-infected ryegrass may be caused by toxicity as well. These findings were in agreement with the study carried out by Jensen and Popay (2004) where they showed that in a 6 week trial only 5% of porina survived on AR37-infected ryegrass compared to 95% for the endophyte-free ryegrass.

7.7 LC–UV–MS Investigations

7.7.1 *APCI vs. ESI*

Analysis of penitrems using an ESI source and an APCI source confirmed the observations made by Rundberget and Wilkins (2002b), that penitrems were more sensitive by analysis in APCI mode compared to ESI mode by a factor of *ca.* 10. This was also the case for the majority of the other indole–diterpenoids tested in

this investigation (janthitrems A–D, lolitrem B, paspalinine, paxilline, penitrem A and terpendole C). The only exception was paspaline.

7.7.2 *Positive Ion Analysis*

The behaviour of indole–diterpenoid compounds (i.e. their ability to fragment and the type of fragmentation observed) was explored through the use of LC–UV–MS with both an ESI source and an APCI source. A range of indole–diterpenoid compounds were analysed: janthitrems A–D, penitrems A–F, lolitrem B, terpendole C, paxilline and paspalinine. Under APCI conditions an increased number of water losses were observed, whereas under ESI conditions losses of oxygen were more common. The loss of water under APCI conditions may primarily arise from thermal dehydration of the vapourising analyte (Rundberget and Wilkins, 2002b). No structurally significant fragments were observed under the positive ion conditions, particularly when using an ESI source.

7.7.3 *Negative Ion Analysis*

The indole–diterpenoid compounds run in negative ion mode on the LC–UV–MS using an APCI source provided significant results. To date, no data has been reported for such analyses of indole–diterpenoids. Initial attempts to obtain negative ion MS data afforded a mixture of the anticipated $[M-H]^-$ ion plus an acetate adduct ion, which originated from the acetic acid in the eluent. The adduct peak was unable to be fragmented using the standard conditions and therefore MS^2 and MS^3 data could not be obtained. However, after the introduction of source-induced dissociation in combination with an increase in the collision energy, the adduct peak was able to be suppressed and an $[M-H]^-$ ion observed as the dominant ion, allowing high quality full scan, MS^2 and MS^3 data to be attained.

In contrast to the fragments observed under positive ion conditions (where losses of acetone and water or oxygen were dominant) more informative fragments were observed using these conditions. Negative ion results showed common fragments between compounds with certain functional groups, i.e. structures with an epoxide at C-11 and C-12 were observed to fragment across this epoxide and, as a result, indole–diterpenoids will now be more easily identified by their fragmentation patterns. The development of improved and more sensitive LC–UV–MS methods for the analysis of indole–diterpenoids (in particular through the use of negative ion APCI methods) will allow future endophyte products to be more thoroughly screened for different classes of secondary metabolites. The knowledge gained from the negative ion analysis of indole–diterpenoids is to be put to use in other laboratories, in particular at the National Veterinary Institute in Oslo, Norway.

7.8 Mouldy Walnuts Investigation

The presence of tremorgenic mycotoxins in mouldy walnuts was investigated after a dog was found to exhibit tremors upon consumption of the walnuts. Detailed qualitative and quantitative LC–UV–MS analyses were performed on extracts of the mouldy walnuts and the fungal culture isolated from the walnuts. Peaks attributable to penitrem A in both the fungal culture and walnut sample were confirmed based on comparison of its retention time, mass spectrum, mass spectral fragmentation, and UV spectrum with those of an authentic specimen of penitrem A. In addition, peaks with mass and UV spectral properties consistent with penitrems B–F and roquefortine C were also observed in chromatograms of extracts of the fungal culture and the mouldy walnuts.

Quantitation of the samples (by UV at 296 nm) revealed penitrem A to be the major penitrem in both the fungal culture (138 mg L⁻¹) and the mouldy walnuts (26.5 mg kg⁻¹). The total amount of penitrems A–F in the walnuts and *P.*

crustosum strain 21143 were estimated to be 36.4 mg kg⁻¹ and 171 mg L⁻¹, respectively (assuming similar absorbance to penitrem A at 296 nm).

The identification of the tremorgenic mycotoxins, penitrems A–F, in the mouldy walnuts the dog had consumed supported the tentative diagnosis of tremorgenic mycotoxicosis by the veterinarian. This is the first case of tremorgenic canine mycotoxicosis reported in New Zealand. The analysis of the mouldy walnuts was carried out prior to the development of the negative ion methods on the LC–UV–MS system. Analysis of these samples through negative ion LC–UV–MS would have helped with the identification of penitrems B–F.

7.9 Conclusion

The results from the experiments run during the course of this research will help further progress the work AgResearch performs in developing commercial novel endophytes to be utilised in establishing safe pastures. In particular, the results from the insect and mouse testing gives an insight into possible compounds which have the ability to deter insect attack and those which are responsible for the staggers-like symptoms observed with AR37 endophyte-infected pastures.

LC–UV–MS methods have been improved significantly for not only the analysis of janthitrems, but also other indole–diterpenoids. This will allow future endophyte products to be more thoroughly screened for different classes of secondary metabolites. In particular, the development of the negative ion method has been successful in identifying diagnostic fragments from certain indole–diterpenoids. The success of the negative ion methods are such that they are to be employed in various other laboratories.

7.10 Future Work

Following on from the janthitrem B stability investigations, janthitrem C and D should also be investigated to confirm that the stability issues associated with these janthitrem is consistent with that found for janthitrem B. The janthitrem present in the endophyte are very similar to janthitrem D (in terms of structure) as they both have an epoxide at C-11, C-12 and no hydroxyl group at C-30, so it is important that the issues surrounding the stability of these compounds is fully understood.

Due to the commercial potential of AR37, further work is required to better understand the compounds responsible for the insect bioactivity and livestock effects. The current study indicates that the epoxyjanthitrem may be involved in these effects. Using the knowledge gained during the isolation of janthitrem from culture, further attempts will be made to isolate epoxyjanthitrem from AR37-infected plant material.

Important information can also be gained by testing janthitrem C and D, isolated during the present study, for effects on mice and insects. This may allow structural features which are required for bioactivity to be identified for this class of compound. The shearinines would also be of interest since they are closely related to the janthitrem.

It has recently been proposed that tremorgenicity is induced by interactions with the BK channel. This theory was developed using lolitrem and paxilline, but now that janthitrem are available in sufficient quantities, further studies using BK channels and another class of tremorgen are possible. This would allow the relationship between tremorgens and BK channels to be better understood.

CHAPTER EIGHT

Experimental

8.1 Screening of Cultures

8.1.1 *Culturing*

A total of 31 isolates were cultured. The isolates were inoculated in potato–milk–sucrose broth (50 mL per 150 mL conical flask), incubated at 20°C for 6 weeks in the dark, and then stored at –20°C until required for extraction. Culturing was performed by Dr M. E. di Menna, AgResearch Ruakura Ltd, Hamilton, New Zealand.

8.1.2 *Extraction*

The cultures were thawed immediately prior to extraction and the mycelium separated from the culture medium by filtration (Qualitative 1, 18.5 cm, Whatman International Limited, Kent, UK), under gravity. The mycelium was transferred from the filter with distilled water (approximately 10 mL) and the mycelium homogenised in a 1-litre Waring blender (Torrington, CT, USA) with acetone (BDH Laboratory Supplies, England) (150 mL) for 3 min (22 000 rpm). The acetone extract was then filtered (as described above) and the blender and residue were rinsed with acetone (50 mL). The residual mycelium was re-extracted in the same manner with methanol (Mallinckrodt Baker, Inc. NJ, USA) (100 mL) for 3 min (22 000 rpm). The acetone and methanol extracts were evaporated to dryness under vacuum and stored at –20°C until required for analysis.

8.1.3 LC–UV–MS

ESI

All fungal extracts were initially analysed by LC–UV–MS using an LTQ Linear Ion Trap mass spectrometer fitted with an ESI interface (ThermoFinnigan, San Jose, CA, USA) and coupled to a SurveyorTM HPLC, autosampler, MS pump and PDA detector. The column used was a Phenomenex Luna 5 μ C18 (2) 100 Å (Phenomenex, Torrance CA, USA), 150 \times 2 mm. Elution was with a linear gradient (200 μ L min⁻¹) of acetonitrile–water (2:3) containing 0.1% (v/v) acetic acid (solvent A) and acetonitrile containing 0.1% (v/v) acetic acid (solvent B), from 100 to 0% solvent A over 40 min, 20 min hold, followed by a return to 100% A over 5 min and then held at 100% A for 10 min to re-equilibrate the column. Injection volume was 10 μ L, the PDA detector was scanned over the range 200–400 nm and the MS was scanned in positive ion mode from 200–800 mass units. The sheath gas flow rate, auxiliary gas flow rate, probe voltage, capillary temperature, capillary voltage and tube lens offset were set at 20, 5, 4.5 kV, 275°C, 35 V and 85 V, respectively. Each extract was made up in 1 mL of 50:50 acetonitrile–water for analysis.

APCI

The fungal culture extracts were also run on an LCQ Advantage mass spectrometer fitted with an APCI source. The run conditions were the same as the ESI experiment (described above). The MS was scanned in positive ion mode from 300–1600 mass units. The vaporiser temperature, sheath gas flow rate, auxiliary gas flow rate, discharge current, capillary temperature, capillary voltage and tube lens offset were set at 350°C, 30, 5, 5 μ A, 200°C, 39 V and 15 V, respectively (Rundberget and Wilkins, 2002b).

8.2 Isolation of Janthitrem A and Janthitrem B

8.2.1 *Culturing*

The *P. janthinellum* strain E1 was inoculated on 900 mL of potato–milk–sucrose broth and split among 6, 1 L Roux flasks. The E1 strain was grown from freeze-dried preparations made on October 1979 of *P. janthinellum* strains 1–4 of di Menna et al. (1986). The culture was incubated at 20°C for 6 weeks in the dark.

8.2.2 *Extraction*

The mycelium was harvested and separated from the culture medium by filtration (Qualitative 1, 18.5 cm), under gravity. The mycelium was rinsed on the filter with distilled water (approximately 10 mL) and the mycelium homogenised in a 1-litre Waring blender with acetone (300 mL) for 3 min (22 000 rpm). The acetone extract was filtered under gravity, and the blender and residue were rinsed with acetone (50 mL).

8.2.3 *Flash Column Chromatography*

Flash column chromatography was carried out according to Still et al., (1978) and performed on a 160 × 20 mm column of 40–63 µm silica gel 60 (Merck KGaA, Darmstadt, Germany). To pack the column, the silica and eluent were mixed together to make a ‘slurry’ to ensure no air bubbles were present in the column. The sample was applied and eluted with 200 mL of toluene (Mallinckrodt Chemicals, NJ, USA)–acetone (7:3) with a linear flow of *ca.* 2 cm min⁻¹. Fractions from the flash columns were collected in test tubes (*ca.* 10 mL per test tube). All fractions collected from the flash columns were kept for analysis. All flash columns were flushed with acetone upon completion to ensure all compounds of interest had been collected off the column. These fractions were combined to give an “acetone flush” fraction.

8.2.4 *TLC*

The fractions which came off the column were analysed by TLC. As each fraction was collected, *ca.* 5 μL was taken from each and transferred to a silica TLC plate (E. Merck 5554) and analysed under short wave (254 nm) and long wave (366 nm) ultra-violet light (Ultra-Violet Products Inc., Ca, USA) after development with 3:2 toluene–acetone as the eluent.

8.2.5 *Analytical HPLC*

HPLC was performed using a Phenomenex Prodigy 5 μ ODS(3) 100 \AA (Phenomenex, Torrance CA, USA), 250 \times 4.60 mm fitted with a 4 \times 3 mm Phenomenex Security Guard containing two C₁₈ cartridges (Torrance, CA, USA). Elution was with an isocratic system of acetonitrile–water (23:2), with a flow rate of 1 mL min⁻¹. The injection volume was 10 μL . The column was equilibrated with the solvent system for 15 min prior to the first injection to equilibrate the column. Detection was by UV, with the PDA detector being scanned from 190–400 nm.

8.2.6 *De-fatting of Samples*

To a separating funnel, 100 mL of 95% (v/v) *n*-hexane (Mallinckrodt Chemicals, NJ, USA) was added, along with 100 mL of 80% (v/v) methanol which contained the sample. The separating funnel was up-ended several times to ensure adequate mixing before being stored at 4°C overnight. The lower layer (80% (v/v) methanol) was collected and dried down on the rotary evaporator. A further 100 mL of 80% (v/v) methanol was added to the separating funnel, shaken and left to stand in the fridge for 4 hours. The lower layer was then run off, combined with the first extract and dried down under vacuum on the rotary evaporator.

8.2.7 *Flash Column Chromatography 2*

Flash column chromatography was performed on a 240 × 10 mm Merck LiChroprep Si 60 (40–63 μm) glass column (Merck KGaA, Darmstadt, Germany) eluted with toluene–acetone (17:3) at 5 mL min⁻¹. Eluting compounds were detected with a 1040M diode array UV detector (Hewlett-Packard, California, USA) at a wavelength of 330 nm. The sample was made up in 500 μL toluene and injected onto the column in 100 μL aliquots. The compounds of interest, collected based on absorbance at 330 nm, were combined and evaporated to dryness *in vacuo*.

8.2.8 *Solid Phase Extraction*

The sample was applied to a Strata-X column (33 μm, 500 mg/6 mL, 8B-S100-HCH) (Phenomenex, Torrance, CA, USA) in 60% (v/v) methanol (2 mL). The column was then eluted successively with 10 mL of 30, 40, 50, 60, 70, 80, 90 and 100% (v/v) methanol, and each fraction was analysed by HPLC. The 80 and 90% (v/v) methanol fractions, which contained the compounds of interest, were combined and evaporated to dryness under a stream of dry nitrogen.

8.2.9 *Semi-preparative HPLC*

Semi-preparative HPLC was performed on a 250 × 10 mm Phenomenex Prodigy 5 μ ODS(3) 100 Å column (Phenomenex, Torrance CA, USA) fitted with a 4 × 3 mm Phenomenex Security Guard column containing two C₁₈ cartridges (Torrance, CA, USA). Elution was with acetonitrile–water (3:2) at 5 mL min⁻¹, with detection at 330 nm by a PDA detector. The samples were made up in 1 mL of 1:1 methanol–water and the column was pumped with the solvent system for 15 min prior to the first injection to equilibrate the column. Peaks of interest were collected and evaporated to dryness *in vacuo*.

8.2.10 HRMS

HRMS was performed in positive ion mode on a Bruker Daltonics MicroTOF mass spectrometer. The samples were dissolved in MeOH and infused via a syringe pump at $4 \mu\text{L min}^{-1}$. Cluster ions from sodium formate (2 mM) were used for mass calibration. Mass spectra were acquired with a time-of-flight analyser over m/z 500–1500. Capillary voltage and skimmer cone voltage were set at 120 V and 40 V, respectively.

8.2.11 NMR

NMR spectra were obtained from solutions of purified janthitrems A and B in acetone- D_6 ($(\text{CD}_3)_2\text{CO}$) (99.9 atom % D; Sigma Aldrich, USA) using a Bruker Avance DRX 400 MHz spectrometer fitted with a 5 mm dual inverse-probe. NMR data was acquired and processed using Topspin V1.3 software (©Bruker Biospin 2005). Chemical shifts were determined at 30°C and spectra calibrated relative to internal $\text{CHD}_2\text{COCD}_3$ (2.04 ppm, ^1H NMR) and $(\text{CD}_3)_2\text{CO}$ (29.9 ppm, ^{13}C NMR). Assignments were obtained from examination of ^1H , ^{13}C , DEPT-135, COSY, TOCSY, g-HSQC, g-HMBC and NOESY NMR spectra. ^{13}C NMR signal multiplicities (s, d, t or q) were determined using the DEPT-135 sequence. Two-dimensional COSY and inverse-mode g-HMBC were obtained in absolute value mode. TOCSY, g-HSQC and NOESY spectra were obtained in phase-sensitive mode.

8.2.12 Molecular Modelling

The energy minimised three-dimensional structures presented in Chapter 3 were generated using both Chem3D Ultra 8.0 (CambridgeSoft Corporation, Cambridge, MA, USA) using the supplied MM2 constants and energy minimisations and the PyMOL Molecular Graphics System, Version 0.97 (DeLano Scientific LLC, Ca, USA).

8.3 Isolation of Janthitrem C and Janthitrem D

8.3.1 *De-fatting of Samples*

After extraction of the fungal culture the extract was dried down (rotary evaporator) until only water remained. This solution (75 mL) was transferred to a separating funnel and a volume of acetonitrile (300 mL) was added so that the solution was now 80% (v/v) acetonitrile. An equal amount of 95% (v/v) *n*-hexane (375 mL) was then added to the separating funnel and the separating funnel was up-ended several times to ensure adequate mixing before being left to stand for 2 hours in a refrigerator at 4°C. The lower layer (80% (v/v) acetonitrile) was collected and dried down on the rotary evaporator. A further 100 mL of 80% (v/v) acetonitrile was added to the separating funnel, shaken and left to stand in the refrigerator for 1 hour before the lower layer was run off, combined with the previous acetonitrile layer and dried using a rotary evaporator.

8.3.2 *Flash Column Chromatography*

The fungal extract was fractionated by flash column chromatography as described in Section 8.2.3. The fungal extract was introduced to the flash column using 9:1 toluene–acetone. Toluene (100 mL) was then passed through the column followed by 100 mL of 9:1, 200 mL of 17:3 and 100 mL of 4:1 toluene–acetone, before finally flushing the column with 100 mL of acetone.

8.3.3 *TLC*

Fractions (10 mL) were collected and analysed by TLC. As each fraction was collected, *ca.* 5 µL was transferred to a silica TLC plate (E. Merck 5554) and analysed under short wave (254 nm) and long wave (366 nm) ultra-violet light (Ultra-Violet Products Inc., Ca, USA) in conjunction with a janthitrem B standard. TLC plates were developed with 3:2 toluene–acetone as the eluent.

8.3.4 NMR

To confirm the identity of the samples as janthitrem C and janthitrem D a series of NMR experiments were run including ^1H , COSY, TOCSY, g-HSQC and g-HMBC NMR spectra for janthitrem C and ^1H , ^{13}C , DEPT-135, COSY, TOCSY, g-HSQC, g-HMBC and NOESY NMR spectra for janthitrem D. NMR acquisition and processing parameters are reported in Section 8.2.11.

8.4 Stability Trial

Eight test conditions were trialled (Table 8.1) and the rate of degradation (if any) of janthitrem B over time was monitored. Janthitrem B samples were mixed with equal amounts of paxilline, as a reference standard, in each of the trial environments.

Table 8.1. Conditions used to monitor the stability of janthitrem B.

Test Condition
1) Acetone at room temperature.
2) Methanol at room temperature.
3) DMSO at room temperature.
4) Dry sample at room temperature.
5) Dry sample wrapped in tinfoil at room temperature.
6) Dry sample at 4°C.
7) Dry sample at -20°C.
8) Dry sample at -80°C.

Each of the test samples were analysed after 0, 3, 10, 24, 60, 120, 200 and 300 days. Test solutions 1–3 were prepared by dissolving 15 μg of janthitrem B and 15 μg of paxilline in 500 μL of the chosen solvent to give a concentration of 0.03 $\mu\text{g mL}^{-1}$ of both janthitrem B and paxilline.

Dry samples (test conditions 4–8, see Table 8.1) were prepared by dissolving 200 μg of janthitrem B and 200 μg of paxilline in 5 mL of acetone in a 20 mL scintillation vial giving a $0.04 \mu\text{g } \mu\text{L}^{-1}$ concentration of both janthitrem B and paxilline. Aliquots of the stock solution (ten aliquots per test condition) were transferred to individual vials and dried under a steady stream of nitrogen and stored for up to 300 days. At $t = 0$, and after 3, 10, 24, 60, 120, 200 and 300 days, 100 μL of acetone was added to the vials and 10 μL of the acetone solution was analysed by HPLC as described below. The injected 10 μL sample contained 0.3 μg (per injection) of paxilline and janthitrem B.

Analytical HPLC was performed as described in Section 8.2.5. Elution was with an isocratic system of acetonitrile–water (7:3), with a flow rate of 1 mL min^{-1} . The column was flushed with the mobile phase for 15 min prior to the first injection to equilibrate the column. Trial samples showed a wavelength of 248 nm was suitable for analysis since paxilline and janthitrem B showed similar but not identical responses at this wavelength. The ratio of 248 nm UV responses for the $t = 0$ reference 1:1 mixture of janthitrem B and paxilline based on a 10 μL sample that contained 0.3 μg of each compound was 0.70. The % degradation of janthitrem B was calculated by dividing the ratio of the paxilline and janthitrem B response at each time point by the ratio of the paxilline and janthitrem B response at $t = 0$. The value was expressed as a percent, as shown in the following equation:

$$\begin{aligned} \% &= 100 \times \frac{(\text{area janthitrem B (248 nm, n days)} / \text{area paxilline (248 nm, n days)})}{(\text{area janthitrem B (234 nm, } t = 0) / \text{area paxilline (234 nm, } t = 0))} \\ &= 100 \times \frac{(\text{area janthitrem B (248 nm, n days)} / \text{area paxilline (248 nm, n days)})}{0.70} \end{aligned}$$

8.5 LC–UV–MS Analysis

8.5.1 APCI vs. ESI

The University of Waikato LC–UV–MS system was an LCQ Advantage mass spectrometer fitted with either an ESI source or an APCI interface (as described in Section 8.1.3). A series of indole–diterpenoid standards (janthitrems A–D, penitrem A, lolitrem B, paxilline, paspaline, paspalinine and terpendole C) were analysed using both the APCI and ESI source. The janthitrems were isolated during the course of this research, penitrem A was purchased as a standard (Sigma–Aldrich, USA), lolitrem B, paxilline, paspaline and paspalinine were isolated from previous work at AgResearch and terpendole C from a previous sample provided to AgResearch by S. Omura and H. Tomada (Tomoda et al., 1995). Each standard solution (10 μL , at a concentration of 50 $\mu\text{g mL}^{-1}$) was injected on to the LC–UV–MS system.

The APCI and ESI experiments were run consecutively so that the samples were exposed to the same conditions and instrument settings for the purpose of direct comparison between the results generated from the APCI source and the ESI source. In order to directly compare the ability of the APCI source against the ESI source, the UV and mass area of the base peak generated by each indole–diterpenoid standard was measured and given as a percentage for the ratio of UV area over the mass area. The janthitrems were determined at 260 nm, the penitrems were determined at 233 nm, lolitrem B was determined at 268 nm, paxilline determined at 235 nm and paspalinine and terpendole C determined at 230 nm.

An opportunity was also afforded for the penitrem containing samples to be run on an LTQ LC–UV–MS system at the National Veterinary Institute in Oslo, Norway as opposed to the LCQ Advantage system available at The University of Waikato. The Oslo LTQ Linear Ion Trap system (run by Professor A. L. Wilkins, The University of Waikato, Hamilton, New Zealand) was fitted with an APCI

source (Finnigan MAT, San Jose, CA, USA) coupled to a SurveyorTM HPLC, autosampler and MS pump and scanned in positive ion mode from 300–1600 mass units. The vaporiser temperature, sheath gas flow rate, auxiliary gas flow rate, discharge current, capillary temperature, capillary voltage and tube lens offset were set at 375°C, 60, 5, 5 μA , 220°C, 39 V and 15 V, respectively.

8.5.2 APCI Vapouriser Temperatures

The janthitrem B standard was run using an LCQ Advantage mass spectrometer fitted with an APCI interface as described in Section 8.1.3. The MS was scanned in positive ion mode from m/z 400 to m/z 900. Five vapourisation temperatures were evaluated; namely 250, 300, 350, 400 and 450°C. 10 μL of a 50 $\mu\text{g mL}^{-1}$ janthitrem B reference solution was injected in each run.

8.5.3 Positive Ion Analyses

The LC–UV–MS system employed was an LCQ Advantage mass spectrometer fitted with either an ESI or APCI interface with conditions as described in Section 8.1.3.

8.5.4 Negative Ion Analyses

The indole–diterpenoid compounds analysed included janthitrems A, B, C and D, penitrems A, B, C, D, E and F, lolitrem B, paxilline, terpendole C and paspalinine. LC–UV–MS analysis was performed with an LCQ Advantage mass spectrometer fitted with an APCI interface in negative ion mode as described in Section 8.1.3. Source-induced dissociation was set at 20 V and collision energy at 35%.

8.6 Assessment of Tremorgenicity, Heart Rate, Blood Pressure and Motor Control on Mice Dosed with Janthitrems A and B

8.6.1 Mouse Bioassay

Prior to administration of the toxin, each mouse was weighed and labelled by marking a coloured band on the tail with a marker pen. A different coloured band was used for each treatment group.

The dose of test compound given was based on our previous knowledge of the class of tremorgen. Dose rates were chosen to prevent any unnecessary discomfort to the animal and a tremor score of 3 was the maximum desired response. For compounds of unknown potency, some range finding concentrations were needed. In this case, only small numbers of mice were dosed. This minimised the number of animals used and prevented unnecessary manipulations. Once the appropriate dose rates were determined, groups of four mice were used in each assay to ensure the accuracy of results, whilst also trying to minimise the number of mice tested. Groups of animals receiving the test compound were paired with those receiving the solvent vehicle alone (9:1 DMSO–water controls).

To prepare the dose, the test compound was dissolved in the appropriate volume of DMSO. The solution was then sonicated to ensure complete dissolution of the toxin. Water was added to the solution to give a final composition of 9:1 DMSO–water. Each mouse was injected intraperitoneally (into the abdominal cavity) with the appropriate dosage. Dose volumes of 50–100 μL were used.

After dosing, the mice were observed closely and tremors assessed after 15, 30 and 60 minutes. The tremors were then measured hourly for 8 hours, after which time the tremors had ceased. They were then observed for a further 2 weeks (after the 72 hour period) to ensure no delayed toxic effects occurred. At the end of this 2 week period the mice were killed by carbon dioxide inhalation.

8.6.2 Tremor Score

Tremor was assessed on an arbitrary scale, both in terms of spontaneous tremor and that induced by exercise/handling. The mouse was firstly observed in the cage for spontaneous tremor then gently placed in the palm of the hand to feel for subtle tremors and finally placed on an outstretched finger and gently spun around forcing the mouse to rebalance. This shows tremors enforced by exercise/handling. The extent of tremor was rated on a scale of 1–5 as described by Gallagher and Hawkes (1985; 1986) (Table 8.2).

Table 8.2. The visual rating scale for tremor assessment.

Score	Clinical Signs
0	No tremor, animal behaviour normal.
1	No resting tremor. A short duration, low intensity, single burst, whole body tremor elicited by exercise/handling.
2	No resting tremor. Several moderate intensity, whole body tremor bursts elicited on exercise/handling.
3	Spontaneous, continuous, low intensity resting tremor may be present. Repeated moderate to severe intensity tremor bursts elicited on exercise/handling.
4	Pronounced, protracted, spontaneous resting tremor. Movement, exercise or handling may induce convulsive episodes in addition to severe tremor.
5	Severe spontaneous tremor, usually accompanied by convulsive episodes, and eventually culminating in death.

8.6.3 Blood Pressure and Heart Rate

The blood pressure and heart rate was measured periodically during the experiment using a computerised, non-invasive tail-cuff system, the BP-2000 (Visitech Systems Inc., NC, USA). To determine blood pressure, the mouse was placed in a holder on a warmed plate which kept the animal in a warm and dark environment, minimising stress and keeping it calm for the length of the measurement period. The mouse's tail was threaded through a tail-cuff which inflated to measure blood pressure and heart rate. For each heart rate/blood

pressure determination, 30 separate readings were made and the results averaged. To ensure that the blood pressure cuff was not overly inflated causing discomfort to the animal, the instrument automatically stopped inflating at 240 mm Hg, even if the blood pressure of the animal had not been determined.

Before the test compound was injected, the blood pressure and heart rate of the mice at time zero was recorded. It was then recorded at 0.25, 0.5, 3, 5 and 7 hours post-injection.

8.6.4 Motor Control

Motor control and balance of the mice was measured using a rotamex 4 rotarod (Columbus Instruments, Ohio). Mice were placed on a drum which rotated, forcing the mice to walk around it. The rotating speed of the drum was then gradually increased until the mice lost their balance and fell onto a padded surface below (approximately a 40 cm drop). Infra-red sensors detected the movement of the mice and digitally recorded the speed of the drum and the time taken for the mice to fall. The drum had 4 lanes to enable the simultaneous testing of four mice. The rotational speed was increased from 13 to 79 rpm over 12 minutes. Once all four mice had fallen, the drum automatically stopped, allowing the animals to be removed.

Each mouse was given two attempts at the test with a resting period of at least 2 minutes between attempts. The results of the two trials were averaged. Since the mice needed to learn the ability to perform this task, it was necessary to pre-train the animals prior to the experiment. Previous work using the rotarod has shown that training for 3 days prior to the experiment was sufficient (S.C. Finch, AgResearch Ruakura Ltd, Hamilton, New Zealand, unpublished observations).

Before the compound was injected, the rotarod scores of the mice at time zero were recorded. The scores were then recorded at 0.25, 0.5, 1, 2 and 6 hours post-injection. An extra measurement at 8 hours was also taken for janthitrem A as the rotarod score at 6 hours had not reached the $t = 0$ reading. A further reading for both janthitrems A and B was also taken at 24 hours to ensure no delayed effects had occurred.

8.7 Insect Testing

8.7.1 Stability of the Test Mycotoxins

The diets were extracted by placing freeze-dried samples of the diet (*ca.* 500 μg) into 2 mL Eppendorf tubes, adding 500 μL acetone, shaking (up-ending several times), centrifuging at 8 000 rpm for 5 min (Centrifuge 5415C, Eppendorf, Germany) extracting on a mini labroller (Labnet International, Inc. NJ, USA) for 2 hours and finally centrifuging again (8 000 rpm for 5 min). A sample of the supernatant was taken and analysed on an analytical HPLC system.

Analytical HPLC, for analysis of the insect diets, was performed using a Phenomenex Prodigy 5 μ ODS(3) 100Å (Phenomenex, Torrance CA, USA), 250 \times 4.6 mm fitted with a 4 \times 3 mm Phenomenex Security GuardTM containing two C₁₈ cartridges (Torrance, CA, USA). Elution was with an isocratic system of acetonitrile–water (7:3), with a flow rate of 1 mL min⁻¹. The injection volume was 10 μL . The column was eluted with solvent for 15 min prior to the first sample injection to allow the column to equilibrate. Quantitation was by UV, with a PDA detector at 247 nm.

Standards of janthitrems A and B and paxilline (10 μL injection of a 30 $\mu\text{g mL}^{-1}$ solution) were run for quantitation. The amount of test mycotoxin in the diet was

calculated by measuring the area of the standard peaks and comparing to the area of the insect diet sample peaks.

8.7.2 Diets Prepared with the Inclusion of the Test Mycotoxins

The diet for the insects was prepared by blending 50 g of fresh clover and 50 g of fresh carrot in 100 mL deionised water. Agar (1.2 g) was mixed with 30 mL water and boiled in the microwave. The agar and water mixture was cooled to 70°C and 1.6 g yeast and 40 g of the clover/carrot mixture (warmed to 60°C) added. The diet mixture was then cooled to below 40°C. The diet mixture (5 g) was weighed into a beaker and the test mycotoxin, dissolved in 100 µL DMSO, was added as appropriate to give final wet weight concentrations of 20 (low) and 50 (high) µg g⁻¹. The mixture was mixed thoroughly and transferred into a plastic Petri dish (6 cm diameter) and allowed to cool.

A total of 7 treatments were prepared which represented 3 mycotoxins (janthitrem A, janthitrem B and paxilline) and 1 control. Each mycotoxin was tested at 2 concentrations of 20 and 50 µg g⁻¹ (wet weight concentrations). A control diet was also prepared by addition of 100 µL DMSO, the solvent used as the carrier for the mycotoxin. Diets were prepared fresh daily.

8.7.3. Diets Prepared with the Inclusion of Endophyte-Free and AR37-Infected Ryegrass

Two further treatments were also tested — endophyte-free ryegrass and ryegrass infected with AR37. The ryegrass (cv. Samson) tillers for these diets were cut approximately 10 mm from the base of the plant and the dead material removed and leaf blades trimmed by approximately 2 cm. The ryegrass diets were prepared one day after the preparation of the mycotoxin diets by blending either 50 g of endophyte-free grass (treatment H) or 50 g ryegrass infected with AR37

(treatment I) in 150 mL of water. A volume of water (100 mL) was then drained from the blended mixture and discarded.

Agar (3 g) was boiled in 75 mL of water and once the mixture had cooled to 70°C, the blended ryegrass was added (the diet for each treatment was prepared separately). These diets were stored in the fridge (4°C) and used for the 5 days of the trial.

8.7.4 *Insect Bioassay Trial*

The bioassay trial (performed by A.J. Popay, AgResearch Ruakura Ltd, Hamilton, New Zealand) was carried out using porina larvae. Porina were obtained from a colony held in controlled environment rooms at 15°C, 16:8 (hours) light:dark regime. The porina larvae were approximately four and a half months old and of a range of weights. The larvae for each treatment were selected so that they were representative of the range of weights.

The selected larvae were weighed and transferred individually into a 70 mL specimen container filled two thirds with moist bark chips. Each treatment consisted of 15 replicate specimen containers — 12 with porina and the remaining 3 without porina. The three diets without porina were set up in case the diets were required for subsequent analysis of the mycotoxins in the samples.

The diets for each treatment were cut with a 10 mm core-borer, weighed and added to the appropriate container. Lids were placed on the containers and the trial carried out in a controlled environment room at 15°C, 16:8 light:dark regime.

A fresh batch of diet was prepared each day for the mycotoxin treatments. Uneaten diet remaining in each container was removed, weighed and replaced with a fresh piece of weighed diet. In the case of treatments where ryegrass was

added, the diet was not made up daily, but the diet was renewed each day. Each time a new diet was supplied, samples of the diet were frozen for stability analysis (as described in Section 8.7.1). At the conclusion of the trial, all porina were weighed.

The percentage of diet consumed for each day of the trial was calculated and this data as well as the data on weight change of larvae were analysed by analysis of variance in Genstat Release 10.2 (Lawes Agricultural Trust; Rothamstead Experimental Station, 2007). Untransformed data was used after residual data had been examined for homogeneity and normality. Statistical analysis was performed by A.J. Popay, AgResearch Ruakura Ltd, Hamilton, New Zealand.

8.8 Analysis of Mouldy Walnuts

8.8.1 Culturing and Isolation of Fungus from the Mouldy Walnuts

The fungi from fragments of the mouldy walnuts were cultured by a mycologist on potato–glucose–chloramphenicol agar for 4 days at 25°C. The fungus *Penicillium crustosum* (strain 21143) was isolated and deposited in the International Collection of Micro-organisms from Plants, Landcare Research, Auckland. A culture of this *P. crustosum*, strain 21143, was prepared for chemical examination. The culture was prepared by inoculating one litre of Czapek–Dox yeast extract broth, dispensing the broth into conical flasks to a depth of 3 cm, and finally static incubation at 25°C for 3 weeks. The cultures were stored at –20°C until extraction. The culturing, isolation and identification of the fungus were performed by M.E. di Menna, (AgResearch Ruakura Ltd, Hamilton, New Zealand), a mycologist.

8.8.2 *Toxin Extraction*

The culture was thawed immediately prior to extraction. The combined mycelium from each culture was firstly separated from the culture medium by filtration under gravity. The mycelium was then rinsed on the filter with distilled water (approximately 10 mL) and the mycelium (57.22 g) homogenised in a 1-litre Waring blender with acetone (300 mL) for 3 min (22 000 rpm). The acetone extract was filtered, and the blender and solid residue rinsed with acetone (50 mL). The solid residue from the first extraction was then recovered and re-extracted with acetone (200 mL for 3 min) and filtered as above. Finally, the residual mycelium was extracted with methanol (200 mL, 3 min) and the extract filtered. Extracts were dried and stored at -20°C until analysis.

Five randomly selected mouldy walnuts (shell and meat) (31.88 g) were homogenised in the Waring blender with acetone (200 mL) for 3 min. The resulting suspension was left to stand for 1 hour and the extract filtered based on the method reported by Richard et al. (1981). Filtered extracts were immediately evaporated to dryness *in vacuo* and stored at -20°C until required for analysis.

8.8.3 *LC–UV–MS Analysis*

LC–UV–MS analysis was performed with an LCQ Advantage mass spectrometer fitted with an APCI as per Section 8.1.3.

Quantitation was performed by integration of peaks in the UV absorbance chromatograms obtained from the PDA at 296 nm. Results from sequential extractions were combined to determine total concentrations. The samples were quantitated against standards prepared from an accurately weighed specimen of penitrem A (Sigma–Aldrich, USA). Where necessary, extracts were diluted to bring them into the concentration range for linear response covered by the

standards (2–50 $\mu\text{g mL}^{-1}$). Standards and extracts were prepared in methanol for LC–UV–MS analysis.

8.8.4 LC–UV–MS Method Validation

Penitrem A standards were prepared by dissolution in methanol to give concentrations of 2, 5, 10, 20 and 50 $\mu\text{g mL}^{-1}$. 10 μL of each standard was injected into the LC–UV–MS. The peak area of penitrem A was measured and plotted against the corresponding concentration of each penitrem A standard to give a calibration curve. The precision was assessed by preparing the calibration curve on three different days.

To assess the accuracy of the method, three samples of 4 $\mu\text{g mL}^{-1}$, 15 $\mu\text{g mL}^{-1}$ and 34 $\mu\text{g mL}^{-1}$ penitrem A dissolved in methanol were introduced to the LC–UV–MS to determine whether the concentrations from the calibration curve matched the actual concentration of the prepared samples. The precision was once more assessed by measuring the relative standard deviation (RSD) of each of the three samples (4 $\mu\text{g mL}^{-1}$, 15 $\mu\text{g mL}^{-1}$ and 34 $\mu\text{g mL}^{-1}$ penitrem A) three times.

References

- Aasen, A.J., Culvenor, C.C.J., Finnie, E.P., Kellock, A.W., Smith, L.W., 1969. Alkaloids as a possible cause of ryegrass staggers in grazing livestock. *Australian Journal of Agricultural Research* 20, 71–86.
- Acklin, W., Weibel, F., Arigoni, D., 1977. Zur biosynthese von paspalin und verwanten metaboliten aus *Claviceps paspali*. *Chimia* 31, 63.
- AgResearch, 2005. Your Paddock is Our Lab – Annual Report 2005, pp. 1–15.
- Armstrong, M.C., 1956. Ryegrass staggers prevalent in autumn after dry summer. *New Zealand Journal of Agriculture* 93, 56.
- Arp, L.H., Richard, J.L., 1979. Intoxication of dogs with the mycotoxin penitrem A. *Journal of the American Veterinary Medical Association* 175, 565–566.
- Ball, O.J.-P., Prestidge, R.A., Sprosen, J.M., 1993. Effect of plant age and endophyte viability on peramine and lolitrem B concentration in perennial ryegrass seedlings. In: Hume, D.E., Latch, G.C., Easton, H.S. (Eds.), *Proceedings of the Second International Symposium on Acremonium/Grass Interactions*. AgResearch, Palmerston North, New Zealand, pp. 63–65.
- Ball, O.J.-P., Miles, C.O., Prestidge, R.A., 1997. Ergopeptine alkaloids and *Neotyphodium lolii*-mediated resistance in perennial ryegrass against adult *Heteronychus arator* (Coleoptera: Scarabaeidae). *Journal of Economic Entomology* 90, 1382–1391.
- Ball, O.J.-P., Coudron, T.A., Tapper, B.A., Davies, E., Trently, D., Bush, L.P., Gwinn, K.D., Popay, A.J., 2006. Importance of host plant species, *Neotyphodium* endophyte isolate, and alkaloids on feeding by *Spodoptera frugiperda* (Lepidoptera: Noctuidae) larvae. *Journal of Economic Entomology* 99, 1462–1473.
- Belofsky, G.N., Gloer, J.B., Wicklow, D.T., Dowd, P.F., 1995. Antiinsectan alkaloids: shearinines A–C and a new paxilline derivative from the ascostromata of *Eupenicillium shearii*. *Tetrahedron* 51, 3959–3968.
- Berny, P., Jaussaud, P., Durix, A., Ravel, C., Bony, S., 1997. Rapid determination of the mycotoxin lolitrem B in endophyte-infected perennial ryegrass by high-performance thin-layer chromatography: a validated assay. *Journal of Chromatography A* 769, 343–348.
- Bills, G.F., Giacobbe, R.A., Lee, S.H., Pelaez, F., Tkacz, J.S., 1992. Tremorgenic mycotoxins, paspalitrem A and C, from a tropical *Phomopsis*. *Mycological Research* 96, 977–983.
- Blackwood, J.E., Gladys, C.L., Loening, K.L., Petrarca, A.E., Rush, J.E., 1968. Unambiguous specification of stereoisomerism about a double bond. *Journal of the American Chemical Society* 90, 509–510.
- Blodgett, D.J., 2001. Fescue toxicosis. *The Veterinary Clinics of North America: Equine Practice* 17, 567–577.

- Boysen, S.R., Rozanski, E.A., Chan, D.L., Grobe, T.L., Fallon, M.J., Rush, J.E., 2002. Tremorgenic mycotoxicosis in four dogs from a single household. *Journal of the American Veterinary Medical Association* 221, 1441–1444.
- Braselton, W.E., Johnson, M., 2003. Thin layer chromatography convulsant screen extended by gas chromatography-mass spectrometry. *Journal of Veterinary Diagnostic Investigation* 15, 42–45.
- Breen, J.P., 1994. *Acremonium* endophyte interactions with enhanced plant resistance to insects. *Annual Reviews Entomology* 39, 401–423.
- Bruehl, G.W., Kaiser, W.J., Klein, R.E., 1994. An endophyte of *Achnatherum inebrians*, an intoxicating grass of northwest China. *Mycologia* 86, 773–776.
- Bush, L.P., Fannin, F.F., Siegel, M.R., Dahlman, D.L., Burton, H.R., 1993. Chemistry, occurrence and biological effects of saturated pyrrolizidine alkaloids associated with endophyte–grass interactions. *Agriculture, Ecosystems & Environment* 44, 81–102.
- Campbell, A.G., 1986. Selection strategies for animal disease resistance. *New Zealand Agricultural Science* 20, 169–171.
- Cheeke, P.R., 1995. Endogenous toxins and mycotoxins in forage grasses and their effects on livestock. *Journal of Animal Science* 73, 909–918.
- Ciegler, A., 1969. Tremorgenic toxin from *Penicillium palitans*. *Applied Microbiology* 18, 128–129.
- Clegg, F.G., Watson, W.A., 1960. Ryegrass staggers in sheep. *Veterinary Record* 72, 731–733.
- Cole, R.J., Kirksey, J.W., Wells, J.M., 1974. A new tremorgenic metabolite from *Penicillium paxilli*. *Canadian Journal of Microbiology* 20, 1159–1162.
- Cole, R.J., Dorner, J.W., Lansden, J.A., Cox, R.H., Pape, C., Cunfer, B., Nicholson, S.S., Bedell, D.M., 1977. Paspalum staggers: isolation and identification of tremorgenic metabolites from sclerotia of *Claviceps paspali*. *Journal of Agricultural and Food Chemistry* 25, 1197–1201.
- Cole, R.J., Dorner, J.W., Springer, J.P., Cox, R.H., 1981. Indole metabolites from a strain of *Aspergillus flavus*. *Journal of Agricultural and Food Chemistry* 29, 293–295.
- Cunningham, I.J., 1958. Non-toxicity to animals of ryegrass endophyte and other endophytic fungi of New Zealand grasses. *New Zealand Journal of Agricultural Research* 1, 489–497.
- Cunningham, I.J., Hartley, W.J., 1959. Ryegrass staggers. *New Zealand Veterinary Journal* 7, 1–7.
- Dalziel, J.E., Finch, S.C., Dunlop, J., 2005. The fungal neurotoxin lolitrem B inhibits the function of human large conductance calcium-activated potassium channels. *Toxicology Letters* 155, 421–426.

de Jesus, A.E., Steyn, P.S., van Heerden, F.R., Vlegaar, R., Wessels, P.L., Hull, W.E., 1981. Structure and biosynthesis of the penitremes A–F, six novel tremorgenic mycotoxins from *Penicillium crustosum*. *Journal of the Chemical Society, Chemical Communications*, 289–291.

de Jesus, A.E., Steyn, P.S., van Heerden, F.R., Vlegaar, R., Wessels, P.L., Hull, W.E., 1983a. Tremorgenic mycotoxins from *Penicillium crustosum*: isolation of penitremes A–F and the structure elucidation and absolute configuration of penitrem A. *Journal of the Chemical Society, Perkin Transactions 1*, 1847–1856.

de Jesus, A.E., Steyn, P.S., van Heerden, F.R., Vlegaar, R., Wessels, P.L., Hull, W.E., 1983b. Tremorgenic mycotoxins from *Penicillium crustosum*. Structure elucidation and absolute configuration of penitremes B–F. *Journal of the Chemical Society, Perkin Transactions 1*, 1857–1861.

de Jesus, A.E., Gorst-Allman, C.P., Steyn, P.S., van Heerden, F.R., Vlegaar, R., Wessels, P.L., Hull, W.E., 1983c. Tremorgenic mycotoxins from *Penicillium crustosum*. Biosynthesis of penitrem A. *Journal of the Chemical Society, Perkin Transactions 1*, 1863–1868.

de Jesus, A.E., Steyn, P.S., van Heerden, F.R., Vlegaar, R., 1984. Structure elucidation of the janthitrems, novel tremorgenic mycotoxins from *Penicillium janthinellum*. *Journal of the Chemical Society, Perkin Transactions 1*, 697–701.

Delmulle, B., De Saeger, S., Adams, A., De Kimpe, N., Van Peteghem, C., 2006. Development of a liquid chromatography/tandem mass spectrometry method for the simultaneous determination of 16 mycotoxins on cellulose filters and in fungal cultures. *Rapid Communications in Mass Spectrometry* 20, 771–776.

di Menna, M.E., Mantle, P.G., Mortimer, P.H., 1976. Experimental production of a staggers syndrome in ruminants by a tremorgenic *Penicillium* from soil. *New Zealand Veterinary Journal* 24, 45–46.

di Menna, M.E., Mantle, P.G., 1978. The role of *Penicillia* in ryegrass staggers. *Research in Veterinary Science* 24, 347–351.

di Menna, M.E., Lauren, D.E., Wyatt, P.A., 1986. Effect of culture conditions on tremorgen production by some *Penicillium* species. *Applied and Environmental Microbiology* 51, 821–824.

Dorner, J.W., Cole, R., Cox, R.H., Cunfer, B.M., 1984. Paspalitrem C, a new metabolite from sclerotia of *Claviceps paspali*. *Journal of Agricultural and Food Chemistry* 32, 1069–1071.

Dowd, P.F., Cole, R., Vesonder, R.F., 1988. Toxicity of selected tremorgenic mycotoxins and related compounds to *Spodoptera frugiperda* and *Heliothis zea*. *The Journal of Antibiotics* 41, 1868–1872.

Easton, H.S., Lane, G.A., Tapper, B.A., Keogh, R.G., Cooper, B.M., Blackwell, M., Anderson, M., Fletcher, L.R., 1996. Ryegrass endophyte-related heat stress in cattle. *Proceedings of the New Zealand Grassland Association* 57, 37–41.

- Ede, R.M., Miles, C.O., Meagher, L.P., Munday, S.C., Wilkins, A.L., 1994. Relative stereochemistry of the A/B rings of the tremorgenic mycotoxin lolitrem B. *Journal of Agricultural and Food Chemistry* 42, 231–233.
- Epstein, W., Gerber, K., Karler, R., 1964. The hypnotic constituent of *Stipa vaseyl*, sleepy grass. *Experientia* 20, 390.
- Erental, A., Dickman, M.B., Yarden, O., 2008. Sclerotial development in *Sclerotinia sclerotiorum*: awakening molecular analysis of a "Dormant" structure. *Fungal Biology Reviews* 22, 6–16.
- Faulkner, J.R., Hussaini, S.R., Blankenship, J.D., Pal, S., Branan, B.M., Grossman, R.B., Schardl, C., 2006. On the sequence of bond formation in loline alkaloid biosynthesis. *ChemBioChem* 7, 1078–1088.
- Fehr, T., Acklin, W., 1966. Die isolierung zweier neuartiger indol-derivate aus dem mycel von *Claviceps paspali* STEVENS *et* HALL. *Helvetica Chimica Acta* 49, 1907–1910.
- Finch, S.C., Imlach, W.L., Dunlop, J., Meredith, A.L., Aldrich, R.W., Dalziel, J.E., 2006. Mode of Action of Tremorgens. In: Popay, A.J., Thom, E.R. (Eds.), *Proceedings of the 6th International Symposium on Fungal Endophytes of Grasses*. New Zealand Grassland Association, Dunedin, New Zealand, pp. 363–364.
- Fink-Gremmels, J., Blom, M., 1994. Ryegrass staggers linked to lolitrem B: a case report. *Proceedings, 6th EAVPT International Congress*.
- Fletcher, L.R., Harvey, I.C., 1981. An association of a *Lolium* endophyte with ryegrass staggers. *New Zealand Veterinary Journal* 29, 185–186.
- Fletcher, L.R., Barrell, G.K., 1984. Reduced liveweight gains and serum prolactin levels in hoggets grazing ryegrasses containing *Lolium* endophyte. *New Zealand Veterinary Journal* 32, 139–140.
- Fletcher, L.R., Easton, H.S., 1997. The evaluation and use of endophytes for pasture improvement. In: Bacon, C.W., Hill, N.S. (Eds.), *Neotyphodium/Grass Interactions*. Plenum Press, New York, pp. 209–227.
- Galey, F.D., Tracy, M.L., Craigmill, A.L., Barr, B.C., Markegard, G., Peterson, R., O'Connor, M., 1991. Staggers induced by consumption of perennial ryegrass in cattle and sheep from northern California. *Journal of the American Veterinary Medical Association* 199, 466–470.
- Gallagher, R.T., Keogh, R.G., Latch, G.C.M., Reid, C.S.W., 1977. The role of fungal tremorgens in ryegrass staggers. *New Zealand Journal of Agricultural Research* 20, 431–440.
- Gallagher, R.T., Latch, G.C., Keogh, R.G., 1980a. The janthitrems: fluorescent tremorgenic toxins produced by *Penicillium janthinellum* isolates from ryegrass pastures. *Applied and Environmental Microbiology* 39, 272–273.

Gallagher, R.T., Finer, J., Clardy, J., Leutwiler, A., Weibull, F., Acklin, W., Arigoni, D., 1980b. Paspalinine a tremorgenic metabolite from *Claviceps paspali* Stevens et Hall. Tetrahedron Letters 21, 235–238.

Gallagher, R.T., White, E.P., Mortimer, P.H., 1981. Ryegrass staggers: isolation of potent neurotoxins lolitrem A and lolitrem B from staggers-producing pastures. New Zealand Veterinary Journal 29, 189–190.

Gallagher, R.T., Campbell, A.G., Hawkes, A.D., Holland, P.T., McGaveston, D.A., Pansier, E.A., Harvey, I.C., 1982a. Ryegrass staggers: the presence of lolitrem neurotoxins in perennial ryegrass seed. New Zealand Veterinary Journal 30, 183–184.

Gallagher, R.T., Smith, G.S., di Menna, M.E., Young, P.W., 1982b. Some observations on neurotoxin production in perennial ryegrass. New Zealand Veterinary Journal 30, 203–204.

Gallagher, R.T., Hawkes, A.D., Steyn, P.S., Vleggaar, R., 1984. Tremorgenic neurotoxins from perennial ryegrass causing ryegrass staggers disorder of livestock: structure elucidation of lolitrem B. Journal of the Chemical Society, Chemical Communications, 614–616.

Gallagher, R.T., Hawkes, A.D., 1985. Estimation of neurotoxin levels in perennial ryegrass by mouse bioassay. New Zealand Journal of Agricultural Research 28, 427–431.

Gallagher, R.T., Hawkes, A.D., 1986. The potent tremorgenic neurotoxins lolitrem B and aflatrem: a comparison of the tremor response in mice. Experientia 42, 823–825.

Gatenby, W.A., Munday-Finch, S.C., Wilkins, A.L., Miles, C.O., 1999. Terpendole M, a novel indole–diterpenoid isolated from *Lolium perenne* infected with the endophytic fungus *Neotyphodium lolii*. Journal of Agricultural and Food Chemistry 47, 1092–1097.

Gilruth, J.A., 1906. Meningo-encephalitis (stomach staggers) in horses, cattle and sheep. Annual Report of the New Zealand Department of Agriculture 14, 293–297.

Goldson, S.L., Proffitt, J.R., Fletcher, L.R., Baird, D.B., 2000. Multitrophic interaction between the ryegrass *Lolium perenne*, its endophyte *Neotyphodium lolii*, the weevil pest *Listronotus bonariensis*, and its parasitoid *Microctonus hyperodae*. New Zealand Journal of Agricultural Research 43, 227–233.

Gonzalez, M., Lull, C., Moya, P., Ayala, I., Primo, J., Yufera, E., 2003. Insecticidal activity of penitrems, including penitrem G, a new member of the family isolated from *Penicillium crustosum*. Journal of Agricultural and Food Chemistry 51, 2156–2160.

Hayashi, H., Asabu, Y., Murao, S., Nakayama, M., Arai, M., 1993. A new congener of penitrems, 6-bromopenitrem E, from *Penicillium simplicissimum* AK-40. Chemistry Express 8, 233–236.

- Hayashi, H., 1998. Fungal metabolites with bioactivity to insects. *Recent Research Developments in Agricultural and Biological Chemistry* 2, 511–525.
- Hemken, R.W., Bull, L.S., Boling, J.A., Kane, E., Bush, L.P., Buckner, R.C., 1979. Summer fescue toxicosis in lactating dairy cows and sheep fed experimental strains of ryegrass–tall fescue hybrids. *Journal of Animal Science* 49, 641–646.
- Hemken, R.W., Jackson, J.A., Boling, J.A., 1984. Toxic factors in tall fescue. *Journal of Animal Science* 58, 1011–1016.
- Hemken, R.W., Bush, L.P., 1989. Toxic alkaloids associated with tall fescue toxicosis. In: Cheeke, P.R. (Ed.), *Toxicants of Plant Origin*, Vol. 1: Alkaloids. CRC Press, Boca Raton, pp. 281–289.
- Hocking, A.D., Holds, K., Tobin, N.F., 1988. Intoxication by tremorgenic mycotoxin (penitrem A) in a dog. *Australian Veterinary Journal* 65, 82–85.
- Hosoe, T., Nozawa, K., Udagawa, S., Nakajima, S., Kawai, K., 1990. Structures of new indoloditerpenes, possible biosynthetic precursors of the tremorgenic mycotoxins, penitrems, from *Penicillium crustosum*. *Chemical and Pharmaceutical Bulletin* 38, 3473–3475.
- Hosoe, T., Itabashi, T., Kobayashi, N., Udagawa, S., Kawai, K., 2006. Three new types of indoloditerpenes, emindole PA–PC, from *Emericella purpurea*. Revision of the structure of emindole PA. *Chemical and Pharmaceutical Bulletin* 54, 185–187.
- Hou, C.T., Ciegler, A., Hesseltine, C.W., 1970. Tremorgenic toxins from *Penicillia* : I. Colorimetric determination of tremortins A and B. *Analytical Biochemistry* 37, 422–428.
- Hou, C.T., Ciegler, A., Hesseltine, C.W., 1971. Tremorgenic toxins from *Penicillia*. III. Tremortin production by *Penicillium* species on various agricultural commodities. *Applied Microbiology* 21, 1101–1103.
- Hoveland, C.S., 1993. Importance and economic significance of the *Acremonium* endophytes to performance of animals and grass plant. *Agriculture, Ecosystems and Environment* 44, 3–12.
- Huang, X., Tomoda, H., Nishida, H., Masuma, R., Omura, S., 1995a. Terpendoles, novel ACAT inhibitors produced by *Albophoma yamanashiensis*. I. Production, isolation and biological properties. *The Journal of Antibiotics* 48, 1–4.
- Huang, X., Nishida, H., Tomoda, H., Tabata, N., Shiomi, K., Yang, D., Takayanagi, H., Omura, S., 1995b. Terpendoles, novel ACAT inhibitors produced by *Albophoma yamanashiensis* II. Structure elucidation of terpendoles A, B, C and D. *The Journal of Antibiotics* 48, 5–11.
- Hunt, L.D., Blythe, L., Holtan, D.W., 1983. Ryegrass staggers in ponies fed processed ryegrass straw. *Journal of the American Veterinary Medical Association* 182, 285–286.

- ICMSF (International Commission on Microbiological Specifications for Foods), 1996. Toxigenic fungi: *Penicillium*. In: Microorganisms in Foods 5. Blackie Academic & Professional, London, pp. 397–413.
- Jackson, J.A., Varney, D.R., Petroski, R.J., Powell, R.G., Bush, L.P., Siegel, M.R., Hemken, R.W., Zavos, P.M., 1996. Physiological responses of rats fed loline and ergot alkaloids from endophyte-infected tall fescue. *Drug and Chemical Toxicology* 19, 85–96.
- Jensen, J.G., Popay, A.J., 2004. Perennial ryegrass infected with AR37 endophyte reduces survival of porina larvae. *New Zealand Plant Protection* 57: 323–328.
- Kawai, K., Nozawa, K., 1988. Novel biologically active compounds from *Emericella* species. In: Natori, S., Hashimoto, K., Ueno, Y. (Eds.), *Mycotoxins and Phycotoxins '88. A Collection of Invited Papers Presented at the Seventh International IUPAC Symposium on Mycotoxins and Phycotoxins*, Tokyo, Japan, 16-19 August, 1988. Elsevier Science Publishers B.V., Amsterdam, pp. 205–212.
- Keogh, R., 1973. Induction and prevention of ryegrass staggers in grazing sheep. *New Zealand Journal of Experimental Agriculture* 1, 55–57.
- Keogh, R.G., Tapper, B.A., Fletcher, R.H., 1996. Distributions of the fungal endophyte *Acremonium lolii*, and of the alkaloids lolitrem B and peramine, within perennial ryegrass. *New Zealand Journal of Agricultural Research* 39, 121–127.
- Kimura, Y., Nishibe, M., Nakajima, H., Hamasaki, T., Shigemitsu, N., Sugawara, F., Stout, T.J., Clardy, J., 1992. Emeniveol; A new pollen growth inhibitor from the fungus, *Emericella nivea*. *Tetrahedron Letters* 33, 6987–6990.
- Knaus, H.G., McManus, O.B., Lee, S.H., Schamalhafer, W.A., Garcio-Calvo, M., Helms, L.M., Sanchez, M., Giangiacomo, K., Reuben, J.P., Smith, A.B., Kaczorowski, G.J., Garcia, M.L., 1994. Tremorgenic indole alkaloids potently inhibit smooth muscle high-conductance calcium-activated potassium channels. *Biochemistry* 33, 5819–5828.
- Laakso, J., Gloer, J.B., Wicklow, D.T., Dowd, P.F., 1992. Sulpinines A–C and secopenitrem B: new antiinsectan metabolites from the sclerotia of *Aspergillus sulphureus*. *Journal of Organic Chemistry* 57, 2066–2071.
- Laakso, J.A., Gloer, J.B., Wicklow, D.T., Dowd, P.F., 1993. A new penitrem analog with antiinsectan activity from the sclerotia of *Aspergillus sulphureus*. *Journal of Agricultural and Food Chemistry* 41, 973–975.
- Latch, G.C.M., Christensen, M.J., 1985. Artificial infection of grasses with endophytes. *Annual Applied Biology* 107, 17–24.
- Latch, G.C.M., 1993. Physiological interactions of endophytic fungi and their hosts. Biotic stress tolerance imparted to grasses by endophytes. *Agriculture, Ecosystems and Environment* 44, 143–156.

- Lauren, D.R., Gallagher, R.T., 1982. High-performance liquid chromatography of the janthitrems: fluorescent tremorgenic mycotoxins produced by *Penicillium janthinellum*. *Journal of Chromatography* 248, 150–154.
- Laws, I., Mantle, P.G., 1989. Experimental constraints in the study of the biosynthesis of indole alkaloids in fungi. *Journal of General Microbiology* 135, 2679–2692.
- Li, C., Nan, Z., Paul, V.H., Dapprich, P.D., Liu, Y., 2004. A new *Neotyphodium* species symbiotic with drunken horse grass (*Achnatherum inebrians*) in China. *Mycotaxon* 90, 141–147.
- Li, C., Nan, Z., Li, F., 2008. Biological and physiological characteristics of *Neotyphodium gansuense* symbiotic with *Achnatherum inebrians*. *Microbiological Research*, 163, 431–440.
- Mackintosh, C.G., Orr, M.B., Gallagher, R.T., Harvey, I.C., 1982. Ryegrass staggers in Canadian Wapiti deer. *New Zealand Veterinary Journal* 30, 106–107.
- Maes, C.M., Steyn, P.S., Van Heerden, F.R., 1982. High-performance liquid chromatography and thin-layer chromatography of penitrems A–F, tremorgenic mycotoxins from *Penicillium crustosum*. *Journal of Chromatography A* 234, 489–493.
- Mantle, P.G., Mortimer, P.H., White, E.P., 1977. Mycotoxic tremorgens of *Claviceps paspali* and *Penicillium cyclopium*: a comparative study of effects on sheep and cattle in relation to natural staggers syndromes. *Research in Veterinary Science* 24, 49–56.
- Mantle, P.G., Day, J.B., Haigh, C.R., Penny, R.H.C., 1978. Tremorgenic mycotoxins and incoordination syndromes. *Veterinary Record* 103, 403.
- Mantle, P.G., Penn, J., 1989. A role for paxilline in the biosynthesis of indole-diterpenoid penitrem mycotoxins. *Journal of the Chemical Society, Perkin Transactions 1*, 1539–1540.
- Mantle, P.G., Burt, S.J., MacGeorge, K.M., Bilton, J.N., Sheppard, R.N., 1990. Oxidative transformation of paxilline in sheep bile. *Xenobiotica* 20, 809–821.
- McMillan, L.K., Carr, R.L., Young, C.A., Astin, J.W., Lowe, R.G.T., Parker, E.J., Jameson, G.B., Finch, S.C., Miles, C.O., McManus, O.B., Schmalhofer, W.A., Garcia, M.L., Kaczorowski, G.J., Goetz, M., Tkacz, J.S., Scott, B., 2003. Molecular analysis of two cytochrome P450 monooxygenase genes required for paxilline biosynthesis in *Penicillium paxilli*, and effects of paxilline intermediates on mammalian maxi-K ion channels. *Molecular Genetics and Genomics* 270, 9–23.
- Meerdink, G.L., 2002. Mycotoxins. *Clinical Techniques in Equine Practice* 1, 89–93.
- Miles, C.O., Wilkins, A.L., Gallagher, R.T., Hawkes, A.D., Munday, S.C., Towers, N.R., 1992. Synthesis and tremorgenicity of paxitriols and lolitriol:

possible biosynthetic precursors of lolitrem B. *Journal of Agricultural and Food Chemistry* 40, 234–238.

Miles, C.O., Munday, S.C., Wilkins, A.L., Ede, R.M., Towers, N.R., 1994. Large-scale isolation of lolitrem B and structure determination of lolitrem E. *Journal of Agricultural and Food Chemistry* 42, 1488–1492.

Miles, C.O., Lane, G.A., di Menna, M.E., Garthwaite, I., Piper, E.L., Ball, O.J.-P., Latch, G.C.M., Bush, L.P., Feng, K.M., Fletcher, I., Harris, P.S., Smith, B.L., 1995a. *Achnatherum inebrians*. *Toxinology & Food Safety Research Report*. AgResearch, p. 20.

Miles, C.O., Wilkins, A.L., Garthwaite, I., Ede, R.M., Munday-Finch, S.C., 1995b. Immunochemical techniques in natural products chemistry: isolation and structure determination of a novel indole–diterpenoid aided by TLC–ELISAgram. *Journal of Organic Chemistry* 60, 6067–6069.

Miles, C.O., Lane, G.A., di Menna, M.E., Garthwaite, I., Piper, E.L., Ball, O.J.-P., Latch, G.C.M., Allen, J.M., Hunt, M.B., Bush, L.P., Ke Min, F., Fletcher, I., Harris, P.S., 1996. High levels of ergonovine and lysergic acid amide in toxic *Achnatherum inebrians*. *Journal of Agricultural and Food Chemistry* 44, 1285–1290.

Mitchell, P.J., McCaughan, C.J., 1992. Perennial ryegrass staggers in fallow deer (*Dama dama*). *Australian Veterinary Journal* 69, 258–259.

Mortimer, P.H., Fletcher, L.R., di Menna, M.E., Harvey, I.C., Smith, G.S., Barker, G.M., Gallagher, R.T., White, E.P., 1982. Recent advances in ryegrass staggers. *Proceedings of the Ruakura Farmers' Conference* 34, 71–74.

Mortimer, P.H., di Menna, M.E., 1983. Ryegrass staggers: further substantiation of a lolium endophyte aetiology and the discovery of weevil resistance of ryegrass pastures infected with lolium endophyte. *Proceedings of the New Zealand Grassland Association* 44, 240–243.

Munday-Finch, S.C., Miles, C.O., Wilkins, A.L., Hawkes, A.D., 1995. Isolation and structure elucidation of lolitrem A, a tremorgenic mycotoxin from perennial ryegrass infected with *Acremonium lolii*. *Journal of Agricultural and Food Chemistry* 43, 1283–1288.

Munday-Finch, S.C., Wilkins, A.L., Miles, C.O., 1996a. Isolation of paspaline B, an indole–diterpenoid from *Penicillium paxilli*. *Phytochemistry* 41, 327–332.

Munday-Finch, S.C., Wilkins, A.L., Miles, C.O., Ede, R.M., Thomson, R.A., 1996b. Structure elucidation of lolitrem F, a naturally occurring stereoisomer of the tremorgenic mycotoxin lolitrem B, isolated from *Lolium perenne* infected with *Acremonium lolii*. *Journal of Agricultural and Food Chemistry* 44, 2782–2788.

Munday-Finch, S.C., 1997. Aspects of the Chemistry and Toxicology of Indole–Diterpenoid Mycotoxins Involved in Tremorgenic Disorders of Livestock, PhD Thesis, Department of Chemistry, The University of Waikato, Hamilton, New Zealand. pp. 334.

- Munday-Finch, S.C., Wilkins, A.L., Miles, C.O., Tomoda, H., Omura, S., 1997. Isolation and structure elucidation of lolilline, a possible biosynthetic precursor of the lolitrem family of tremorgenic mycotoxins. *Journal of Agricultural and Food Chemistry* 45, 199–204.
- Munday-Finch, S.C., Wilkins, A.L., Miles, C.O., 1998. Isolation of lolicine A, lolicine B, lolitriol and lolitrem N from *Lolium perenne* infected with *Neotyphodium lolii* and evidence for the natural occurrence of 31-epilolitrem N and 31-epilolitrem F. *Journal of Agricultural and Food Chemistry* 46, 590–598.
- Munday, B.L., Monkhouse, I.M., Gallagher, R.T., 1985. Intoxication of horses by lolitrem B in ryegrass seed cleanings. *Australian Veterinary Journal* 62, 207.
- Naik, J.T., Mantle, P.G., Sheppard, R.N., Waight, E.S., 1995. Penitremones A–C, *Penicillium* metabolites containing an oxidised penitrem carbon skeleton giving insight into structure-tremorgenic relationships. *Journal of the Chemical Society Perkin Transactions 1*, 1121–1125.
- Naude, T.W., O'Brien, O.M., Rundberget, T., McGregor, A.D.G., Roux, C., Flåøyen, A., 2002. Tremorgenic neuromycotoxicosis in 2 dogs ascribed to the ingestion of penitrem A and possibly roquefortine in rice contaminated with *Penicillium crustosum*. *Journal of the South African Veterinary Association* 73, 211–215.
- Neill, J.C., 1941. The endophytes of *Lolium* and *Festuca*. *The New Zealand Journal of Science and Technology* 23A, 185–193.
- Norris, P.J., Smith, C.C.T., De Bellerocche, J., Bradford, H.F., Mantle, P.G., Thomas, A.J., Penny, R.H.C., 1980. Actions of tremorgenic fungal toxins on neurotransmitter release. *Journal of Neurochemistry* 34, 33–42.
- Nozawa, K., Nakajima, S., Kawai, K., 1988a. Isolation and structures of indoloditerpenes, possible biosynthetic intermediates to the tremorgenic mycotoxin, paxilline, from *Emericella striata*. *Journal of the Chemical Society, Perkin Transactions 1*, 2607–2610.
- Nozawa, K., Yuyama, M., Nakajima, S., Kawai, K., Udagawa, S., 1988b. Studies on fungal products. Part 19. Isolation and structure of a novel indoloditerpene, emindole SA, from *Emericella striata*. *Journal of the Chemical Society, Perkin Transactions 1*, 2155–2160.
- Odriozola, E., Lopez, T., Campero, C., Placeres, C.G., 1993. Ryegrass staggers in heifers: a new mycotoxicosis in Argentina. *Veterinary and Human Toxicology* 35, 144–146.
- Parker, E.J., Scott, B., 2004. Indole–diterpene biosynthesis in ascomycetous fungi. In: An, Z. (Ed.), *Handbook of Industrial Mycology*. Marcel Dekker, New York, pp. 405–426.
- Penn, J., Biddle, J.R., Mantle, P.G., Bilton, J.N., Sheppard, R.N., 1992. Pennigritrem, a naturally-occurring penitrem A analogue with novel cyclisation in

the diterpenoid moiety. *Journal of the Chemical Society, Perkin Transactions* 1, 23–26.

Penn, J., Swift, R., Wigley, L.J., Mantle, P.G., Bilton, J.N., Sheppard, R.N., 1993. Janthitrems B and C, two principal indole–diterpenoids produced by *Penicillium janthinellum*. *Phytochemistry* 32, 1431–1434.

Penn, J., Mantle, P.G., 1994. Biosynthetic intermediates of indole–diterpenoid mycotoxins from selected transformations at C-10 of paxilline. *Phytochemistry* 35, 921–926.

Pennell, C.G.L., Popay, A.J., Ball, O.J.-P., Hume, D.E., Baird, D.B., 2005. Occurrence and impact of pasture mealybug (*Balanococcus poae*) and root aphid (*Aploneura lentisci*) on ryegrass (*Lolium* spp.) with and without infection by *Neotyphodium* fungal endophytes. *New Zealand Journal of Agricultural Research* 48, 329–337.

Petriz, D.C., Lechtenburg, V.L., Smith, W.H., 1980. Performance and economic returns of beef cows and calves grazing grass–legume herbage. *Agronomy Journal* 72, 581–584.

Petroski, R.J., Powell, R.G., Clay, K., 1992. Alkaloids of *Stipa robusta* (Sleepygrass) infected with an *Acremonium* endophyte. *Natural Toxins* 1, 84–88.

Petroski, R.J., Powell, R.G., Ratnayake, S., McLaughlin, J.L., 1994. Cytotoxic activities of *N*-acyllolines. *International Journal of Pharmacognosy* 32, 409–412.

Pitt, J.I., 1979. *Penicillium crustosum* and *P. simplicissimum*, the correct names for two common species producing tremorgenic mycotoxins. *Mycologia* 71, 1166–1177.

Popay, A.J., Mainland, R.A., 1991. Seasonal damage by Argentine stem weevil to perennial ryegrass pastures with different levels of *Acremonium lolii*. *Proceedings of the New Zealand Weed and Pest Control Conference* 44, 171–175.

Popay, A.J., Wyatt, R.T., 1995. Resistance to Argentine stem weevil in perennial ryegrass infected with endophytes producing different alkaloids. *Proceedings of the New Zealand Plant Protection Conference* 48, 229–236.

Popay, A.J., Gerard, P.J., 2007. Cultivar and endophyte effects on a root aphid, *Aploneura lentisci*, in perennial ryegrass. *New Zealand Plant Protection* 60, 223–227.

Powell, R.G., Petroski, R.J., 1992. The loline group of pyrrolizidine alkaloids. In: Pelletier, S.W. (Ed.), *The Alkaloids: Chemical and Biological Perspectives*, Vol. 8. Springer, Berlin, pp. 320–338.

Prestidge, R.A., Pottinger, R.P., Barker, G.M., 1982. An association of *Lolium* Endophyte with ryegrass resistance to Argentine stem weevil. *Proceedings of the New Zealand Weed and Pest Control Conference* 35, 119–122.

- Prestidge, R.A., Barker, G.M., Pottinger, R.P., 1991. The economic cost of Argentine stem weevil in pastures in New Zealand. *Proceedings of the New Zealand Weed and Pest Control Conference* 44, 165–170.
- Prestidge, R.A., Ball, O.J.-P., 1993. The role of endophytes in alleviating plant biotic stress in New Zealand. In: Hume, D.E., Latch, G.C.M., Easton, H.S. (Eds.), *Second International Symposium on Acremonium/Grass Interactions: Plenary Papers*. AgResearch, Palmerston North, New Zealand, pp. 141–151.
- Richard, J.L., Bacchetti, P., Arp, L.H., 1981. Moldy walnut toxicosis in a dog, caused by the mycotoxin, penitrem A. *Mycopathologia* 76, 55–58.
- Rowan, D.D., Gaynor, D.L., 1986. Isolation of feeding deterrents against Argentine stem weevil from ryegrass infected with the endophyte *Acremonium loliae*. *Journal of Chemical Ecology* 12, 647–658.
- Rowan, D.D., Shaw, G.J., 1987. Detection of ergopeptine alkaloids in endophyte-infected perennial ryegrass by tandem mass spectrometry. *New Zealand Veterinary Journal* 35, 197–198.
- Rowan, D.D., 1993. Lolitrems, peramine and paxilline: mycotoxins of the ryegrass/endophyte interaction. *Agriculture, Ecosystems and Environment* 44, 103–122.
- Rundberget, T., Wilkins, A.L., 2002a. Thomitrems A and E, two indole-alkaloid isoprenoids from *Penicillium crustosum* Thom. *Phytochemistry* 61, 979–985.
- Rundberget, T., Wilkins, A.L., 2002b. Determination of *Penicillium* mycotoxins in foods and feeds using liquid chromatography–mass spectrometry. *Journal of Chromatography A* 964, 189–197.
- Rundberget, T., Skaar, I., Flåøyen, A., 2004a. The presence of *Penicillium* and *Penicillium* mycotoxins in food wastes. *International Journal of Food Microbiology* 90, 181–188.
- Rundberget, T., Skaar, I., O'Brien, O., Flåøyen, A., 2004b. Penitrem and thomitrem formation by *Penicillium crustosum*. *Mycopathologia* 157, 349–357.
- Sanchez, M., McManus, O.B., 1996. Paxilline inhibition of the alpha-subunit of the high-conductance calcium-activated potassium channel. *Neuropharmacology* 35, 963–968.
- Schardl, C.L., Grossman, R.B., Nagabhyru, P., Faulkner, J.R., Mallik, U.P., 2007. Loline alkaloids: currencies of mutualism. *Phytochemistry* 68, 980–996.
- Schmidt, S.P., 1986. Alabama report, *Proceedings Tall Fescue Toxicosis Workshop*, Southern Region Information Exchange Group 37, Atlanta, Georgia, USA.
- Scott, B., Schardl, C., 1993. Fungal symbionts of grasses: evolutionary insights and agricultural potential. *Trends in Microbiology* 1, 196–200.

- Seath, D.M., Lassiter, C.A., Rust, J.W., Cole, M., Bastin, G.M., 1956. Comparative value of kentucky bluegrass, kentucky 31 fescue, orcard grass, and brome grass as pastures for milk cows. I. How kind of grass affected persistence of milk production, TDN yield, and body weight. *Journal of Dairy Science* 39, 574–580.
- Shreeve, B.J., Patterson, D.S.P., Roberts, B.A., Macdonald, S.M., Wood, E.N., 1978. Isolation of potentially tremorgenic fungi from pasture associated with a condition resembling ryegrass staggers. *Veterinary Record* 103, 209–210.
- Smith, A., Cui, H., 2003. Indole–diterpene synthetic studies: total synthesis of (–)-21-isopentenylpaxilline. *Helvetica Chimica Acta* 86, 3908–3938.
- Sonjak, S., Frisvad, J.C., Gunde-Cimerman, N., 2005. Comparison of secondary metabolite production by *Penicillium crustosum* strains, isolated from Arctic and other various ecological niches. *FEMS Microbiology Ecology* 53, 51–60.
- Springer, J.P., Clardy, J., Wells, J.M., Cole, R., Kirksey, J.W., 1975. The structure of paxilline, a tremorgenic metabolite of *Penicillium paxilli* Bainier. *Tetrahedron Letters* 16, 2531–2534.
- Springer, J.P., Clardy, J., 1980. Paspaline and paspalicine, two indole–mevalonate metabolites from *Claviceps paspali*. *Tetrahedron Letters* 21, 231–234.
- Staub, G.M., Gloer, K.B., Gloer, J.B., 1993. New paspalinine derivatives with antiinsectan activity from the sclerotia of *Aspergillus Nomius*. *Tetrahedron Letters* 34, 2569–2572.
- Steyn, P.S., Vlegaar, R., 1985. Tremorgenic mycotoxins. In: Herz, W., Grisebach, H., Kirby, G.W., Tamm, C. (Eds.), *Progress in the Chemistry of Organic Natural Products*. Springer-Verlag, New York, pp. 1–80.
- Still, W.C., Kahn, M., Mitra, A., 1978. Rapid chromatographic technique for preparative separations with moderate resolution. *Journal of Organic Chemistry* 43, 2923–2925.
- Sutherland, R.J., 1984. Idiopathic bovine hyperthermia. *Surveillance* 11, 16–17.
- Tapper, B.A., Lane, G.A., 2004. Janthitrems found in a *Neotyphodium* endophyte of perennial ryegrass. In: Kallenbach, R., Rosenkrans, C.J., Lock, T.R. (Eds.), 5th International Symposium on *Neotyphodium/Grass* Interactions, Fayetteville, Arkansas, Abstract Number 301.
- Tomoda, H., Tabata, N., Yang, D., Takayanagi, H., Omura, S., 1995. Terpendoles, novel ACAT inhibitors produced by *Albophoma yamanashiensis*. III. Production, isolation and structure elucidation of new components. *The Journal of Antibiotics* 48, 793–804.
- Tong, D.-W., Wang, J.-Y., Brain, P., Gooneratne, R., 2006. Seasonal change of loline alkaloids in endophyte-infected meadow fescue. *Agricultural Sciences in China* 5, 793–797.

- Tor, E.R., Puschner, B., Filigenzi, M.S., Tiwary, A.K., Poppenga, R.H., 2006. LC–MS/MS screen for penitrem A and roquefortine C in serum and urine samples. *Analytical Chemistry* 78, 4624–4629.
- van Heeswijck, R., McDonald, G., 1992. *Acremonium* endophytes in perennial ryegrass and other pasture grasses in Australia and New Zealand. *Australian Journal of Agricultural Research* 43, 1683–1709.
- van Zijll de Jong, E., Dobrowolski, M.P., Sandford, A., Smith, K.F., Willocks, M.J., Spangenberg, G.C., Forster, J.W., 2008. Detection and characterisation of novel fungal endophyte genotypic variation in cultivars of perennial ryegrass (*Lolium perenne* L.). *Australian Journal of Agricultural Research* 59, 214–221.
- Walter, 2002. Acute penitrem A and roquefortine poisoning in a dog. *Canadian Veterinary Journal* 43, 372–374.
- Weedon, C.M., Mantle, P.G., 1987. Paxilline biosynthesis by *Acremonium loliae*; a step towards defining the origin of lolitrem neurotoxins. *Phytochemistry* 26, 969–971.
- Wei, Y.K., Gao, Y.B., Xu, H., Su, D., Zhang, X., Wang, Y.H., Lin, F., Chen, L., Nie, L.Y., Ren, A.Z., 2006. Occurrence of endophytes in grasses native to northern China. *Grass and Forage Science* 61, 422–429.
- Wells, J.M., Cole, R.J., 1977. Production of penitrem A and of an unidentified toxin by *Penicillium lanoso-coeruleum* isolated from weevil-damaged pecans. *Phytopathology* 67, 779–782.
- White, E.P., Smith, G.S., di Menna, M.E., Mortimer, P.H., 1980. Absorption and translocation of *Penicillium* by ryegrass plants. *New Zealand Veterinary Journal* 28, 123–124.
- Wilkins, A.L., Miles, C.O., Ede, R.M., Gallagher, R.T., Munday, S.C., 1992. Structure elucidation of janthitrem B, a tremorgenic metabolite of *Penicillium janthinellum*, and relative configuration of the A and B rings of janthitrems B, E, and F. *Journal of Agricultural and Food Chemistry* 40, 1307–1309.
- Wilkinson, H.H., Siegel, M.R., Blankenship, J.D., Mallory, A.C., Bush, L.P., Schardl, C.L., 2000. Contribution of fungal loline alkaloids to protection from aphids in a grass–endophyte mutualism. *Molecular Plant – Microbe Interactions* 13, 1027–1033.
- Wilson, B.J., Wilson, C.H., 1964. Toxin from *Aspergillus flavus*: production on food materials of a substance causing tremors in mice. *Science* 144, 177–178.
- Wilson, B.J., Wilson, C.H., Hayes, A.W., 1968. Tremorgenic toxin from *Penicillium cyclopium* grown on food materials. *Nature* 220, 77–78.
- Wrightson Seeds, 5 January 2007. Understanding Endophytes (Farmer Information Sheet), Forage Focus 5, Christchurch, New Zealand.

Xu, M., Gessner, G., Groth, I., Lange, C., Christner, A., Bruhn, T., Deng, Z., Li, X., Heinemann, S.H., Grabley, S., Bringmann, G., Sattler, I., Lin, W., 2007. Shearinines D–K, new indole triterpenoids from an endophytic *Penicillium* sp. (strain HKI0459) with blocking activity on large-conductance calcium-activated potassium channels. *Tetrahedron* 63, 435–444.

Yates, S.G., Petroski, R.J., Powell, R.G., 1990. Analysis of loline alkaloids in endophyte-infected tall fescue by capillary gas chromatography. *Journal of Agricultural and Food Chemistry* 38, 182–185.

Young, K.L., Villar, D., Carson, T.L., Imerman, P.M., Moore, R.A., Bottoff, M.R., 2003. Tremorgenic mycotoxin intoxication with penitrem A and roquefortine in two dogs. *Journal of the American Veterinary Medical Association* 222, 52–53.

Yunusov, S.Y., Akramov, S.T., 1955. Investigation of the alkaloids of the seeds of *Lolium cuneatum* (Nevski). *Journal of General Chemistry (Moscow)* 25, 1765–1771.

APPENDIX

Appendix 1: Published account of mouldy walnuts investigation.

Appendix 2: Poster presented at the 6th International Symposium on Fungal Endophytes of Grasses, 2007.

Clinical Communication

Presumptive tremorogenic mycotoxicosis in a dog in New Zealand, after eating mouldy walnuts

JS Munday*[§], D Thompson[†], SC Finch[‡], JV Babu^{‡#}, AL Wilkins^{#¥}, ME di Menna[‡] and CO Miles^{‡¥}

Abstract

CASE HISTORY: A 1-year-old, intact male Labrador-cross dog vomited after eating walnuts that had been on the ground for 5 months. The dog then developed tremors, ataxia, increased salivation, and hyperaesthesia.

CLINICAL FINDINGS: The dog had marked generalised tremors, ataxia and a temperature of 39.9°C. Both pupils were of normal size and normally responsive to light. Vomiting was induced, and walnut shell was visible in the vomitus.

DIAGNOSIS: Due to the sudden onset of tremors, lack of exposure to other convulsive toxins, and the evidence of ingestion of walnuts, the provisional diagnosis was tremorogenic mycotoxicosis. The dog was treated symptomatically, and made a full recovery over 18 hours. Tremorogenic mycotoxins were detected within walnuts collected from the dog's environment.

CLINICAL RELEVANCE: Fungi that produce tremorogenic mycotoxins are present in New Zealand. Intoxication should be suspected in dogs that suddenly develop muscle tremors, especially if there is a history of ingestion of mouldy food 2–3 hours prior to the development of tremors.

KEYWORDS: Intoxication, dog, penitrem A, tremorogenic mycotoxins, roquefortine

Introduction

A sudden onset of generalised tremors and ataxia in a dog could be due to intoxication; metabolic disorders such as hypocalcaemia or hypoglycaemia; cerebral haemorrhage due to a primary vascular disorder or neoplasm; inflammatory disease such as infectious inflammatory diseases, steroid-responsive suppurative meningitis, or granulomatous meningoencephalitis; epilepsy; or trauma (Nelson and Couto 1998).

Toxins that cause muscle tremors include tremorogenic mycotoxins, organophosphates, organochlorides, permethrin, metaldehyde, carbamates, strychnine, methylxanthines, bromethalin, zinc phosphide, drugs of abuse, and fluoroacetate (Braselton and Johnson 2003; Sherley 2004). To the authors' knowledge, there has been no review of the causes of intoxication in dogs in New Zealand. However, a review of cases in Australia between 1978

and 1990 revealed 20% of fatalities were due to organophosphates, 10% metaldehyde, 8.9% strychnine, 8.2% carbamates, and 0.6% fluoroacetate (Robertson *et al.* 1992).

Intoxication of dogs by tremorogenic mycotoxins has rarely been reported; only 13 dogs have been described in seven reports. Cases of intoxication have been reported in North America (Arp and Richard 1979; Richard *et al.* 1981; Boysen *et al.* 2002; Walter 2002; Young *et al.* 2003), South Africa (Naude *et al.* 2002), and Australia (Hocking *et al.* 1988). Mycotoxins were ingested with compost in four cases (Boysen *et al.* 2002); dairy products in three (Arp and Richard 1979; Young *et al.* 2003); rice in two (Naude *et al.* 2002); and walnuts (*Juglans regia*) (Richard *et al.* 1981), bread (Hocking *et al.* 1988), and unspecified garbage (Walter 2002) in one case each. Penitrem A and roquefortine were the two most common tremorogenic mycotoxins (Walter 2002).

This case report describes the clinical presentation and treatment of a dog suspected of being intoxicated with tremorogenic mycotoxins produced by a fungus growing on walnuts. While cases of suspected tremorogenic mycotoxicosis have been previously reported in New Zealand (Anonymous 2005, non-peer reviewed), this is the first time that the toxins have been identified within food consumed by a dog in New Zealand, that subsequently developed tremors.

Case history

A 1-year-old, intact male Labrador-cross dog was observed vomiting. Examination by the owner of the vomitus revealed walnut shells, lemon peel, and fresh grass. Over the following hour the dog became progressively incoordinated and developed marked tremors. The owner had observed the dog eating walnuts 3 hours before vomiting; the walnuts had been lying on the ground for approximately 5 months. The dog had previously been seen eating walnuts without developing clinical signs. However, approximately 1 week before intoxication occurred there had been 3 days of heavy rain. The intoxication occurred in August (late winter).

Clinical findings

The dog was presented to the veterinarian approximately 1 hour after first being observed vomiting. On presentation, it had severe generalised tremors, marked ataxia, hyperaesthesia, and mild hypersalivation. The dog had a temperature of 39.9 (normal range 38–39)°C and a capillary refill time of 1.5 seconds. Both pupils were of normal size and normally responsive to light. Examination of the oral cavity did not reveal any abnormalities. Due to the muscle tremors, it was not possible to determine heart or respiration rates.

The clinical symptoms and history in this case were consistent with tremorogenic mycotoxicosis. To ensure the stomach was empty, vomiting was induced using 0.8 mg/kg apomorphine S/C

* Department of Pathobiology, Institute of Veterinary, Animal and Biomedical Sciences, Massey University, Private Bag 11222, Palmerston North, New Zealand.

† VetEnt Napier, 120 Taradale Road, Napier, New Zealand.

‡ AgResearch Ltd, Ruakura Research Centre, Private Bag 3123, Hamilton 3240, New Zealand.

Chemistry Department, University of Waikato, Private Bag 3105, Hamilton 3240, New Zealand.

¥ National Veterinary Institute, PB 8156 Dep, NO-0033 Oslo, Norway.

§ Author for correspondence. Email: j.munday@massey.ac.nz

(Apomorphine Hydrochloride Tablets; Jurox Pty Ltd, Rutherford, NSW, Australia). Small pieces of walnut shell were visible in the resultant vomitus. As the dog was hyperthermic, cool (19°C) lactated Ringer's solution (Baxter Healthcare Pty Ltd, Old Toongabbie, NSW, Australia) at twice maintenance rate was given I/V. Muscle tremors were controlled using 1 mg/kg diazepam I/V (Pamlin Injection; Parnell Laboratories NZ Ltd, East Tamaki, NZ).

This initial treatment resulted in cessation of the muscle tremors. One hour after apomorphine was given, 0.5 mg/kg activated charcoal (Red Seal Natural Health, Auckland, NZ) was administered orally. The dog was normothermic one hour after administration of the diazepam. Six hours after administration of the diazepam, the muscle tremors recurred, and progressively increased in severity over the following 4 hours when they were considered severe enough to require a repeat dose of diazepam (1 mg/kg). The temperature of the dog was monitored during this time and did not become elevated. Additional activated charcoal (0.5 mg/kg) and 1 mg/kg epsom salts (Multichem NZ Ltd, Auckland, NZ) were administered orally 10 hours after the initial presentation.

Eighteen hours after initial presentation and 8 hours after last receiving diazepam, no tremors were observed. Although the dog was eating and drinking normally, it was kept under observation for a further 24 hours before being discharged.

Laboratory findings

Walnuts were collected from the ground in areas that the dog had access to. The fallen walnuts had fragile or broken shells and the kernels were visibly mouldy. Microscopic examination revealed fragments of fungal hyphae and numerous subglobose hyaline spores that were approximately 3 µm in diameter. Fragments of walnut cultured on potato-glucose agar (Merck, Darmstadt, Germany) containing 10 mg/L chlortetracycline (Sigma, St Louis MO, USA) for 4 days at 25°C produced a heavy growth of blue-green fungal colonies identified as *Penicillium crustosum* Thom, using the criteria proposed by Pitt (1980). *Penicillium crustosum* designated Strain 21143 was isolated from the walnuts and deposited in the International Collection of Micro-organisms from Plants, Landcare Research, Auckland.

To determine if tremorgenic toxins were present within the walnuts, five visibly mouldy walnuts were collected from the dog's environment. An extract of homogenised walnuts (31.88 g) was prepared using 200 ml acetone, as described previously (Richard et al. 1981). The extract was analysed using liquid chromatography with ultraviolet absorbance and tandem mass spectrometric detection, similar to that described previously (Rundberget and Wilkins 2002). Analysis of the walnut extract revealed peaks consistent with penitrems A–F and roquefortine C (Maes et al. 1982; Rundberget et al. 2004; Tor et al. 2006).

The samples were quantified using ultraviolet detection at 235 nm against standards of penitrem A (Sigma-Aldrich, St Louis MO, USA). Penitrem A was the major penitrem (26.5 mg/kg) in the walnuts, while the concentration of penitrems B–F was estimated to be 9.9 mg/kg. As no standard was available, the concentration of roquefortine C was not quantified.

Discussion

A presumptive diagnosis of tremorgenic mycotoxicosis was made in this case due to the history of ingestion of walnuts, the clinical signs displayed by the dog, and the detection of mycotoxin

in walnuts collected from the dog's environment. Detection of mycotoxins in the vomitus would have supported this diagnosis; however, vomitus was not collected in this case. Definitive diagnosis of tremorgenic mycotoxicosis requires identification of mycotoxins in either serum or urine. Methods for identifying penitrem A in food (Braselton and Johnson 2003), vomitus (Braselton and Johnson 2003), and serum and urine (Tor et al. 2006) have been published, but routine testing is not available at veterinary diagnostic laboratories in New Zealand. Therefore, considering the short clinical course of disease and the delay associated with sending samples to an overseas diagnostic laboratory, mycotoxin assays are not likely to be a valuable diagnostic test.

Penicillium crustosum was isolated from associated materials in all previous cases of mycotoxicosis in which fungal cultures were prepared (Arp and Richard 1979; Richard et al. 1981; Hocking et al. 1988; Naude et al. 2002). This fungus is a common food mould and has been detected in 52% of food-waste samples during summer months (Rundberget et al. 2004). However, the mould only produces toxin when substrate moisture levels are high (Pitt 2002). This moisture requirement probably accounts for the rarity of tremorgenic mycotoxicosis in dogs despite the common presence of *P. crustosum* and lack of dietary discretion typically shown by dogs. The dog in the present report was intoxicated by eating mouldy walnuts. Walnuts have previously caused tremorgenic mycotoxicosis in dogs (Richard et al. 1981). Nuts are a good substrate for the production of toxins, and penitrem A produced by *P. crustosum* is recognised as an important contaminant of many commercially harvested nut species (Overy et al. 2003). In the present case, the walnuts had been previously eaten by the dog without causing clinical signs of intoxication. It is hypothesised that the period of heavy rain reported a week prior to intoxication allowed increased fungal growth or increased production of toxin by the fungi.

Tremorgenic mycotoxicosis in dogs is most often attributable to the ingestion of penitrem A produced by *P. crustosum* (Rundberget et al. 2004). The mechanism by which penitrem A induces tremors is not known. The toxin inhibits high-conductance calcium-activated potassium channels (Cotton et al. 1997), influencing action-potential waveform, neurotransmitter release, and cerebellar function (Dalziel et al. 2005). However, other mycotoxins also block these channels without inducing tremors (Dalziel et al. 2005). Penitrem A may also activate γ -aminobutyric acid receptors (Selala et al. 1989). Roquefortine is also produced by *P. crustosum*, and both penitrem A and roquefortine are often present in cases of tremorgenic mycotoxicosis in dogs. It is currently uncertain whether or not roquefortine C induces tremors (Naude et al. 2002), and its mechanism of toxicity is unknown.

Previous cases of tremorgenic mycotoxicosis in dogs demonstrated that clinical signs developed 2–3 hours after ingestion of the toxin. Ingestion of small quantities of mycotoxin resulted in vomiting, salivation, anxiety, and the development of fine tremors (Boysen et al. 2002; Naude et al. 2002). In cases where greater quantities of toxin had been ingested, the symptoms progressed to whole-body tremors, agitation, and seizures (Boysen et al. 2002). The symptoms observed in the case described here, vomiting followed by a sudden onset of generalised, progressively severe tremors, ataxia, excessive salivation, and hyperaesthesia, are consistent with those previously reported.

Penitrem A has been experimentally administered to rats and dogs. Rats given 3 mg/kg penitrem A intraperitoneally developed generalised tremors and ataxia that persisted for 48 hours (Cavanagh et al. 1998). Euthanasia and necropsy revealed widespread necrosis of cerebellar granular cells and Purkinje cells. However, intraperitoneal doses between 0.5 and 1.5 mg/kg penitrem A resulted in tremors, but no cell necrosis. Intraperitoneal administra-

tion of 0.5 mg/kg penitrem A to dogs resulted in convulsions and death (Hayes *et al.* 1976). Necropsy examination of those animals did not reveal necrosis of Purkinje cells. Death probably occurred due to respiratory impairment and seizures, as anaesthetised dogs consistently survived.

Other toxins which may induce tremors and convulsions in dogs include metaldehyde and organophosphates. Metaldehyde intoxication was considered unlikely in the present case because there was no known exposure to the toxin and no slug-bait dye nor acetaldehyde odour in the vomitus. Organophosphate toxicity was also considered unlikely as there was no history of exposure, and no additional clinical signs such as lacrimation or myosis. Strychnine, zinc phosphide, and bromethalin are extremely uncommon causes of intoxication in New Zealand. Mycotoxic intoxication was considered the most likely cause of the tremors in this case, although a sudden onset of epilepsy, encephalitis, or a metabolic disease, although unlikely, could not be excluded clinically.

As there is no antidote for tremorgenic mycotoxicosis, treatment can be divided into two phases. Firstly, further absorption of the toxin from the intestine should be prevented. As in the present case, this can include emetics, activated charcoal to bind the toxin, and cathartics. Unfortunately, experimental studies of penitrem A intoxication used intraperitoneal (Hayes *et al.* 1976) or I/V (Peterson *et al.* 1982) routes of administration, so the rate of intestinal absorption of this toxin is unknown. Therefore, it is uncertain how quickly the initial treatment has to be given to be beneficial. The second phase of treatment is control of muscle tremors. Prolonged muscle contraction causes death due to respiratory failure, hyperthermia, or hypoglycaemia. Mild tremors, as in the present case, can be controlled using diazepam; however, general anaesthesia can be required in more severe cases (Boysen *et al.* 2002). Severely intoxicated dogs can become apnoeic and require forced ventilation (Boysen *et al.* 2002). Cooled I/V fluids are indicated if the dog is hyperthermic. Preventing tremors may be required for up to 36 hours after ingestion of the toxin (Boysen *et al.* 2002). However, most dogs make a full clinical recovery within 4 days of ingestion of toxin (Richard *et al.* 1981; Boysen *et al.* 2002; Naude *et al.* 2002; Young *et al.* 2003).

In conclusion, this is the first time a tremorgenic mycotoxin has been identified in a case of suspected tremorgenic mycotoxicosis in a dog in New Zealand. Due to the range of substrates on which *P. crustosum* is able to proliferate and produce toxins, it is possible that tremorgenic mycotoxicosis is under-reported in dogs in New Zealand. Currently in New Zealand, there is no commercially available test for tremorgenic mycotoxins. Initial treatment of an intoxicated animal should reduce absorption of the toxin from the gastrointestinal tract. Supportive care, possibly including anaesthesia and forced ventilation, may be necessary once clinical signs of disease develop. The prognosis for tremorgenic mycotoxicosis is excellent, and most dogs make a full clinical recovery within 4 days.

Acknowledgement

We would like to thank T Rundberget and A Moldes-Anaya of the National Veterinary Institute, Oslo, Norway, for helpful advice on toxin analyses and providing an extract of *P. crustosum* with a characterised toxin profile.

References

Anonymous. Quarterly review of diagnostic cases – July to Sept 2005. *Surveillance* 32 (4), 15, 2005

- Arp LH, Richard JL.** Intoxication of dogs with the mycotoxin penitrem A. *Journal of the American Veterinary Medical Association* 175, 565–6, 1979
- Boysen SR, Rozanski EA, Chan DL, Grobe TL, Fallon MJ, Rush JE.** Tremorgenic mycotoxicosis in four dogs from a single household. *Journal of the American Veterinary Medical Association* 221, 1441–4, 2002
- Braselton WE, Johnson M.** Thin layer chromatography convulsant screen extended by gas chromatography-mass spectrometry. *Journal of Veterinary Diagnostic Investigation* 15, 42–5, 2003
- Cavanagh JB, Holton JL, Nolan CC, Ray DE, Naik JT, Mantle PG.** The effects of the tremorgenic mycotoxin penitrem A on the rat cerebellum. *Veterinary Pathology* 35, 53–63, 1998
- Cotton KD, Hollywood MA, McHale NG, Thornbury KD.** Outward currents in smooth muscle cells isolated from sheep mesenteric lymphatics. *Journal of Physiology* 503, 1–11, 1997
- Dalziel JE, Finch SC, Dunlop J.** The fungal neurotoxin lolitrem B inhibits the function of human large conductance calcium-activated potassium channels. *Toxicology Letters* 155, 421–6, 2005
- Hayes AW, Presley DB, Neville JA.** Acute toxicity of penitrem A in dogs. *Toxicology and Applied Pharmacology* 35, 311–20, 1976
- Hocking AD, Holds K, Tobin NE.** Intoxication by tremorgenic mycotoxin (penitrem A) in a dog. *Australian Veterinary Journal* 65, 82–5, 1988
- Maes CM, Steyn PS, Van Heerden FR.** High-performance liquid chromatography and thin-layer chromatography of penitrems A–F, tremorgenic mycotoxins from *Penicillium crustosum*. *Journal of Chromatography A* 234, 489–93, 1982
- Naude TW, O'Brien OM, Rundberget T, McGregor AD, Roux C, Flaoyen A.** Tremorgenic neuromycotoxicosis in 2 dogs ascribed to the ingestion of penitrem A and possibly roquefortine in rice contaminated with *Penicillium crustosum*. *Journal of the South African Veterinary Association* 73, 211–5, 2002
- Nelson RW, Couto CG.** Seizures. In: Nelson RW, Couto CG (eds). *Small Animal Internal Medicine*. Pp 988–1001. Mosby Inc, St Louis MO, USA, 1998
- Overy DP, Seifert KA, Savard ME, Frisvad JC.** Spoilage fungi and their mycotoxins in commercially marketed chestnuts. *International Journal of Food Microbiology* 88, 69–77, 2003
- Peterson DW, Penny RH, Day JB, Mantle PG.** A comparative study of sheep and pigs given the tremorgenic mycotoxins verruculogen and penitrem A. *Research in Veterinary Science* 33, 183–7, 1982
- Pitt JI.** Subgenus *Penicillium*. *The Genus Penicillium and its Teleomorphic States Eupenicillium and Talaromyces*. Pp 339–44. Academic Press, London, UK, 1980
- Pitt JI.** Biology and ecology of toxigenic *Penicillium* species. *Advances in Experimental Medicine and Biology* 504, 29–41, 2002
- Richard JL, Bacchetti P, Arp LH.** Moldy walnut toxicosis in a dog, caused by the mycotoxin, penitrem A. *Mycopathologia* 76, 55–8, 1981
- Robertson ID, Leggoe M, Dorling PR, Shaw SE, Clark WT.** A retrospective study of poisoning cases in dogs and cats: comparisons between a rural and an urban practice. *Australian Veterinary Journal* 69, 194–5, 1992
- Rundberget T, Wilkins AL.** Determination of *Penicillium* mycotoxins in foods and feeds using liquid chromatography-mass spectrometry. *Journal of Chromatography A* 964, 189–97, 2002
- Rundberget T, Skaar I, Flaoyen A.** The presence of *Penicillium* and *Penicillium* mycotoxins in food wastes. *International Journal of Food Microbiology* 90, 181–8, 2004
- Selala MI, Daelemans F, Schepens PJ.** Fungal tremorgens: the mechanism of action of single nitrogen containing toxins – a hypothesis. *Drug and Chemical Toxicology* 12, 237–57, 1989
- Sherley M.** The traditional categories of fluoroacetate poisoning signs and symptoms belie substantial underlying similarities. *Toxicology Letters* 151, 399–406, 2004
- Tor ER, Puschner B, Filigenzi MS, Tiwary AK, Poppenga RH.** LC-MS/MS screen for penitrem A and roquefortine C in serum and urine samples. *Analytical Chemistry* 78, 4624–9, 2006
- Walter SL.** Acute penitrem A and roquefortine poisoning in a dog. *Canadian Veterinary Journal* 43, 372–4, 2002
- Young KL, Villar D, Carson TL, Ierman PM, Moore RA, Bottoff MR.** Tremorgenic mycotoxin intoxication with penitrem A and roquefortine in two dogs. *Journal of the American Veterinary Medical Association* 222, 52–3, 2003

Submitted 12 November 2007

Accepted for publication 17 April 2008

Structure Elucidation of 11,12-Epoxyjanthitrem B and Isolation of Janthitrem B from *Penicillium janthinellum* Cultures



Jacob V. Babu,^{1,2} Alistair L. Wilkins,² Christopher O. Miles,¹ Sarah C. Finch¹
¹AgResearch Ltd, Ruakura Research Centre, PB 3123, Hamilton, New Zealand, ²The University of Waikato, Hamilton, New Zealand
 jacob.babu@agresearch.co.nz



Sheep suffering from severe ryegrass staggers.

Janthitrem B and '11,12-epoxyjanthitrem B', a new janthitrem analogue closely related to janthitrem B, were isolated from a *Penicillium janthinellum* fungal culture. The novel compound differs from janthitrem B at carbons 11 and 12 with the presence of an epoxide rather than a double bond. Janthitrem B and the novel janthitrem compound will be used as an analytical standard for investigations into the stability of janthitrems and for bioactivity work, i.e. insect and mice testing.



Endophyte-free ryegrass on the left and endophyte-infected ryegrass on the right.

Why of Interest?

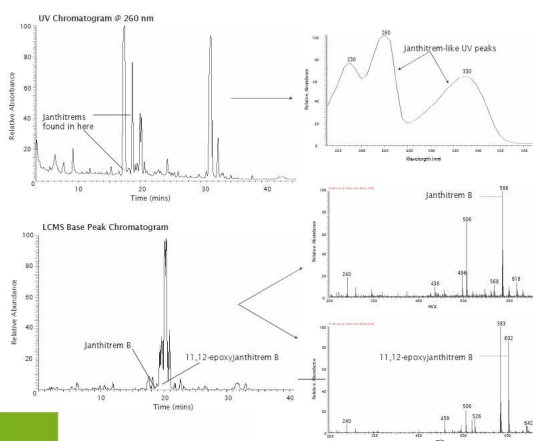
Early investigations into ryegrass staggers were directed towards the characterisation of tremorgen-producing *Penicillium* species (Gallagher *et al.* 1977). Work in the 1980s identified a number of *Penicillium janthinellum* strains isolated from pastures where there had been outbreaks of staggers (Gallagher *et al.* 1980).

While the janthitrems were found not to be the cause of ryegrass staggers, interest in these compounds has recently been rekindled due to the fact that janthitrems are present in perennial ryegrass infected with the novel endophyte AR37. The janthitrems present in pasture however, are very unstable and difficult to isolate. Janthitrems from a fungal source will therefore be used as model compounds. Of particular importance is the novel compound, 11,12-epoxyjanthitrem B, since this compound contains the same epoxide group present in the janthitrem compounds produced by the AR37 endophyte in perennial ryegrass (e.g. 11,12-epoxyjanthitrem G). This compound will be an excellent model compound for use in chemical and biological assays.

Isolation of 11,12-Epoxyjanthitrem B:

A janthitrem-producing isolate of *Penicillium janthinellum* was extracted using acetone. Flash column chromatography was then performed on the extract using toluene:acetone (70:30) as the eluent. Thin layer chromatography identified the presence of janthitrems. The extract was then subjected to solvent partitioning, solid phase extraction and separation through first a normal phase and then a reverse phase column on a high performance liquid chromatography system. The peaks of interest were collected and analysed by NMR and LCMS.

LCMS Analysis of *P. janthinellum* Extract



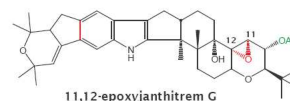
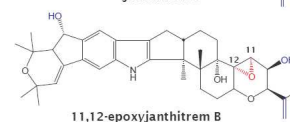
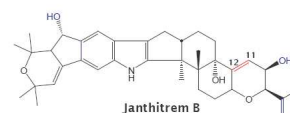
agresearch Farming, Food and Health. First
 Te Ahuwhenua, Te Kai me te Whai Ora. Tuatahi

NMR Identification:

The structure of 11,12-epoxyjanthitrem B was elucidated using 1-D and 2-D NMR spectroscopy (including ¹H, ¹³C, DEPT135, COSY, TOCSY, NOESY, HSQC, and HMBG spectra).

Main points of interest were:

- Full structural assignment of the epoxyjanthitrem confirmed its close structural relationship to janthitrem B (the difference between the two structures has been highlighted in different colours).
- 11,12-epoxyjanthitrem has one more oxygen than janthitrem B.
- Shift of H-11 proton signal.



HR-MS Confirmation:

High Resolution Mass Spectrometry using direct infusion electrospray was performed on the 11,12-epoxyjanthitrem B. This confirmed the atomic composition of the sample.

HR-MS m/z 624.3296 [M+Na]⁺
 calculated C₃₇H₄₇O₆NNa = 624.76199

Conclusions:

- Janthitrem B was isolated from *P. janthinellum*.
- A novel analogue, 11,12-epoxyjanthitrem B, was also isolated from *P. janthinellum*.
- Janthitrems from *Penicillium* are excellent surrogates for endophyte janthitrems in chemical and biological assays.
- Can now investigate structure-activity e.g. tremorgenic activity, insect toxicity.

References:
 Gallagher, R. T.; Keogh, R.G.; Latch, G.C.M.; Reid, C.S.W. 1977. 'The role of fungal tremorgens in ryegrass staggers.' *N.Z. Journal of Agricultural Research* 20: 431-440.
 Gallagher, R. T.; Latch, G.C.M.; Keogh, R.G. 1980. 'The janthitrems: fluorescent tremorgenic toxins produced by *Penicillium janthinellum* isolates from ryegrass pastures.' *Applied and Environmental Microbiology* 39(1): 372-373.

Acknowledgements:
 AgResearch Grasslands, Palmerston North, New Zealand; Karl Fraser, LCMS, The University of Waikato, Hamilton, New Zealand.
 The Foundation for Research, Science and Technology, Technology for Industry Fellowships (TIF), (contract no. AGRN0506).